University of Alberta

Heavy Oil-in-Water Emulsion Flow and Blocking Mechanism in Porous Media

by

Khalil Zeidani 

A thesis submitted to the Faculty of Graduate Studies and Research
in partial fulfillment of the requirements for the degree of

Doctor of Philosophy
in
Petroleum Engineering

Department of Civil and Environmental Engineering

Edmonton, Alberta
Fall 2007

Your file Votre référence
ISBN: 978-0-494-33096-8
Our file Notre référence
ISBN: 978-0-494-33096-8

Abstract

The application of heavy oil-in-water emulsion as a novel sealant in the near wellbore region is proposed in this research. The process in mind is one where a created emulsion will be injected, break and seal the porous matrix in the vicinity of the wellbore or at some pre-determined distance from it, thereby reducing water (and/or gas) coning or eliminating the leakage in abandoned wells. Laboratory experiments at micro- and macro-scale levels were performed to: a) provide a detailed understanding of emulsion flow and blocking mechanisms and, b) set criteria with which to control emulsion penetration depth before it breaks down and seals a porous medium.

In these experiments, well-characterized oil-in-water emulsions were injected into etched-glass micro-models and micro-models packed with glass beads. The effect of droplet-to-pore size ratio, droplet stability, oil and surfactant type and concentration were studied through visualization experiments. It was concluded that blockage occurred because of the size of the oil droplets was larger than the pore throat constrictions. The blockage was accelerated due to droplets coalescence as a result of a high shear rate or surfactant adsorption onto the porous medium. Furthermore, emulsion droplet size distribution, emulsion viscosity and oil droplets-to-water interfacial tensions increased as the surfactant content decreased, resulting in high capillary pressure across the trapped oil droplet.

The effects of oil type, rock permeability, injection velocity, and wettability alteration were also studied. The results indicated that a heavy oil-in-water emulsion sealed unconsolidated cores for long periods of time, and that emulsions carrying more viscous oils could resist higher pressures. Moreover, by conditioning the medium with surfactant and alkaline based pre-flush solutions, the emulsion penetration depth enhanced significantly. However, the emulsion may break down and emplace at a desired depth as a result of using low pH pre-flush solutions.

A novel sealant that uses a heavy oil-in-water emulsion to block the near wellbore matrix has been developed. Stable reduction in permeability to other fluids was observed as the plug withstood 42,500 kPa/m (about 1,800 psi/ft) pressure gradients. Criteria are defined for the field application of this blockage phenomenon.

Acknowledgments

I am thankful to Dr. M. Polikar for his supervision, guidance and encouragement over the course of this research. I would also like to thank Dr. J. H. Masliyah for his input and recommendations during my Candidacy Examination and follow-up meetings.

In addition, a sincere thank you to Dr. H. Huang for helping to provide the laboratory equipment at the Alberta Research Council (ARC) and the ARC employees who assisted me in conducting the experiments in particular Gerard Korpany, Eddie Jossy, Brian Wiwchar, Brad Wasylyk, Gerald Kissel and Linda Coates.

I am grateful for many valuable discussions with Dr. I. Y. Akkutlu and Dr. T. Cyr.

I would like to acknowledge the AERI Core University Research in Sustainable Energy for their financial support.

Finally, I would like to express my sincere appreciation to my family and friends for their ongoing encouragement and support. This dissertation is dedicated to them.

Table of Contents

List of Tables

List of Figures

Nomenclature

CMC	=	critical micelle concentration
DP_1	=	two-parallel plate micro-model front section pressure drop
DP_2	=	two-parallel plate micro-model rear section pressure drop
HLB	=	hydrophilic-lipophilic balance
IPA	=	isopropyl alcohol
k	=	permeability to injected emulsion
$k_{original}$	=	absolute permeability
L	=	length
L_1	=	two-parallel plate micro-model front section length
L_2	=	two-parallel plate micro-model rear section length
L_F	=	front position
LMO	=	Lloydminster oil
L_T	=	two-parallel plate micro-model total length
MO	=	mineral oil
O/W	=	oil-in-water emulsion
P_c	=	capillary pressure
P_{inj}	=	injection pressure
PV	=	pore volume of injected fluid
R_d	=	pore diameter
R_f	=	radius of curvature at the ganglion's flowing head
R_t	=	radius of curvature at the ganglion's tail
R_{th}	=	throat diameter
rpm	=	revolutions per minute
s	=	second
v	=	injection velocity
v/v	=	volume/volume ratio
WCO	=	Western Canadian oil
W/O	=	water-in-oil emulsion

X = emulsion quality

Greek Letters

μ = *viscosity*

Subscripts

E = emulsion

inj = injection

Chapter 1. Introduction

Emulsion systems have been studied extensively in different fields of science and engineering. Most of the scientific studies address the ex situ production of emulsions, their life span and stability. Emulsions formulation has been studied more extensively in the food industry, biochemistry, biomedicine and pharmaceutical science. Extensive efforts have been put forth to characterize these emulsion systems and enhance their stability. Much progress has been achieved in this regard since the components constituting these emulsion systems are relatively known and their properties are identified. Therefore, the resulting emulsion systems can be studied and characterized more scientifically.

Although the scientific advancements can be applied to most emulsions, they do not explain the inclusive complexity of petroleum emulsions. The primary problem is related to the composition of the petroleum fluids and the properties of the underground reservoir rocks that obscure stability and flow behavior predictions.

From the early 60's to the late 70's, two petroleum emulsion-related problems arose that still continue to be the top priorities in the petroleum industry. The depletion of mature light oil reservoirs across the world and the use of emulsions to enhance the oil recovery mechanism were major concerns. Many researchers investigated the use of emulsions as blocking agents in secondary recovery to improve the sweep efficiency of waterflooding in layered reservoirs or under bottom-water conditions. This included reuse of native emulsions, ex situ production and injection of emulsions, and more importantly, the in situ emulsification of oil by alkali and surfactant solutions as a form of viscous oil recovery. Nevertheless, the use of sodium hydroxide and alkaline salts in the waterflood recovery of crude oils dates back to 1917. Exhaustive research continued in the 1930's and beyond. The core mechanisms proposed by different authors were as follow: the effect of alkaline

solutions on the reduction of oil-water interfacial tension, wettability reversal, and in situ emulsification and entrainment/entrapment of oil droplets.

The second matter was related to the production of viscous heavy or bituminous oils like those in Western Canada and Venezuela. The production of these extra heavy oils through the conventional techniques of surface mining or steam-assisted gravity drainage (SAGD), and combination with other chemical processes, occurs in the form of an emulsion. While many researchers have investigated the mobilization and flow mechanics of emulsions in underground media, others have focused on the surface separation or transportation of the produced emulsions.

All things considered, this research study introduces new concepts to the use of heavy oil-in-water (O/W) emulsions as a novel sealant in the near wellbore region. The main objective is to eliminate the water and gas leakage from abandoned wells. The 2002 survey of the Alberta Energy and Utilities Board indicates more than 3000 orphan wells, many of which are leaking to the surface or underground formations. Leakage causes pollution of subsurface waters, loss of petroleum resources and expulsion of green house gases into the atmosphere. Companies have reported hundreds of leaking producing wells, some of which are "wells from hell". For instance, two companies spent more than $1.4 million in their unsuccessful attempt to seal a leaky well.

Common practice is to use cement to block the formation from which leaks to the surface. This process is expensive, damages the formation, and in many cases, as in abandoned wells, this practice has failed. This could be due to either poor completion jobs or the nature of the formation and its fluids. The new approach appears to be more applicable compared to past investigations in which emulsions are applied as blocking agents to improve secondary oil recovery. Contrary to the complexity that might be involved to deliver the emulsion further into the reservoir, it would be more realistic to use the emulsion as a blocking agent in the near wellbore region.

As illustrated in Figure 1.1, this process consists of injecting a carefully-designed heavy oil-in-water emulsion through the well casing so that the injected emulsion will fix or break near the wellbore or at some pre-determined distance from it. As such, it will be an effective, stable plug against, for instance, water or gas coning. A detailed understanding of the physics of emulsion flow during the displacement process and the main factors controlling the emulsion propagation depth into the porous medium are required to perform an effective sealing.

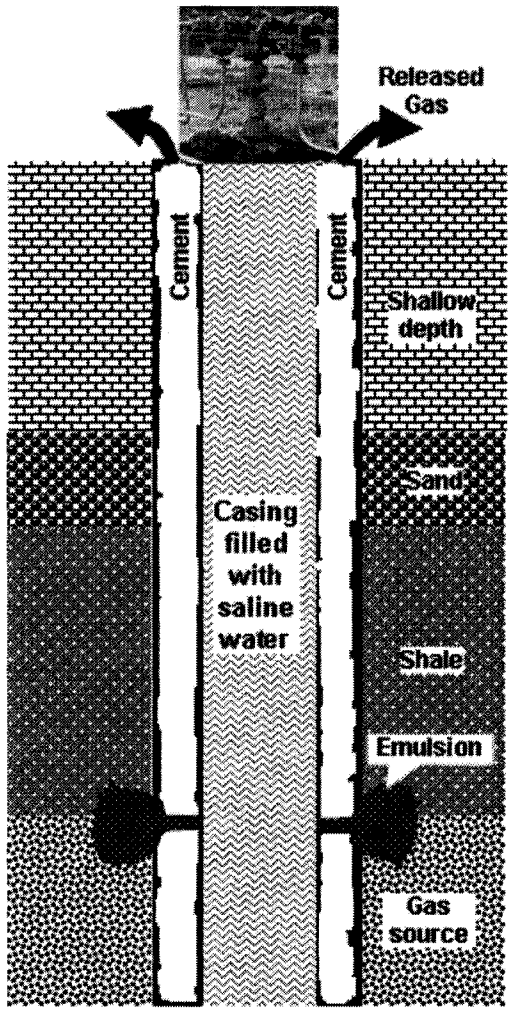

Figure 1.1 Schematic of the near wellbore region

There are a number of fundamental questions that require answers before such a process can be examined in the field. More specifically, further research must be

performed in using a stable emulsion to block a porous medium and therefore create a stable plug against the flowing fluids. As a result, the scope of this study aims to demonstrate the effectiveness and applicability of a novel sealant, identify the key factors in the blocking mechanism, and offer applicable methods with which to control and fix an emulsion within a porous medium.

As a preliminary step, the emulsion properties, past experimental work, mathematical modelling and field tests that were performed on testing of emulsions as blocking agents in underground media are critically reviewed. The results are presented in Chapter 2. The theory of emulsion flow and blocking mechanisms are discussed according to the recent observations and advancements published in the literature. Chapter 3 presents the objectives of the experiments. The results of the experiments are presented in Chapters 4 through 6 according to the type of experiments. In Chapter 4, methods used for emulsion formulation and characterization are presented. Following this are qualitative descriptions of the emulsion blocking and droplets capture mechanisms at the micro-scale level. Chapter 5 includes a detailed quantitative description of emulsion flow in porous media at the macro-scale level. Chapter 6 demonstrates the effectiveness of the novel sealant in blocking a porous medium and provides criteria for blocking a variety of porous media. Finally, observations on the blocking phenomena and critical factors affecting the emulsion flow behaviour and sealing principles are discussed and compared with the relevant published works in the literature. This work concludes with recommendations proposed for further research and field applications.

Chapter 2. Literature Review

2.1 *Emulsions Formation and Properties*

An emulsion is a thermodynamically unstable dispersion of two mutually insoluble liquids, such as water and oil. One of these two components is present in the form of finely dispersed spherical droplets in the second, continuous phase. If oil is dispersed in water, the emulsion is referred to as an oil-in-water (O/W) emulsion; the reverse case is a water-in-oil emulsion (W/O). It can be classified as a macro-emulsion if the droplet size is larger than 0.1 μm or as a micro-emulsion if the droplet size is smaller than 0.1 μm. Generally, droplet diameters in macro-emulsions are greater than 1 μm, the same magnitude as the pore constrictions.

Compared with a macroscopically extended system, the free energy of a dispersed system is greater by the amount of surface energy. Therefore, collisions between droplets in pure emulsions result in their coalescence and, eventually, in the separation of the emulsion into separate phases, a state of lower energy. Such technical emulsions are short-lived. In order to produce a resilient technical emulsion, a third component is required, namely, an emulsifier. The emulsifier must accumulate at the interface and form a protective layer in the form of a tough, elastic film that remains unbroken when droplets collide. To optimize these properties in practice, different mixtures of emulsifiers are often used.

Droplets are said to coalesce when they unite irreversibly. The cause of coalescence is the tendency to minimize surface area while maximizing volume. A drop formed in this manner will have a smaller surface area than that of its two parent droplets combined.

Emulsion instability may occur in the form of coalescence, creaming or sedimentation. The stability of an emulsion with respect to coalescence has greater practical significance than in sedimentation, since droplets may coexist for long periods of time without actually coalescing. A stable barrier, consisting of a thin layer of the outer phase separating the droplets, maintains such aggregates. Only when this barrier has been destroyed may the droplets coalesce.

Emulsions can be formed in almost every phase of oil production and processing. Field emulsions, for example, can be generated within oil reservoirs, in the wellbore during production or in the pipelines during transportation.

The majority of the world's crude oil is produced in emulsion form because natural emulsifiers exist in petroleum reservoirs. These natural emulsifiers, found in (heavy) crude oil, can be formed from asphaltenes, asphaltic and resinous materials, oil-soluble organic acids, such as naphthenic acids, fatty acids or aromatic acids, or cyclic compounds (cyclic aromatics), such as toluene, benzene, decalin, methylcyclohexane and cyclo-octane.

King[1] proposed three hypothetical emulsions:

(1) Viscous crudes containing high concentrations of asphaltenes and resinous acids generally will not form emulsions at room temperature because of their high viscosity.
(2) Moderately viscous crudes with intermediate concentrations of asphaltenes and resinous acids will readily form stable emulsions.
(3) Low viscosity crudes with low concentrations of asphaltenes and/or resinous acids will not form emulsions because of low natural surfactant content.

Crude oil emulsions are generally of the water-in-oil type, which are more viscous than either of their constituents. The production of this type of emulsions has been increased recently because many oil reservoirs throughout the world are being watered out. The produced emulsions must be treated: salty water droplets need to

be removed in order to meet crude specifications for transportation, storage, and export as well as to avoid catalyst poisoning in the refineries. However, emulsion treating is not a simple task. It requires the application of various thermal, mechanical, chemical and/or electrical processes or a combination of them.[2-5]

On the other hand, oil-in-water emulsions have lower viscosities than the oil constituents. This fact has been considered by many researchers in the development of systems for producing and transporting crude oil as an oil-in-water emulsion.[6-8] A surfactant can be injected with the produced water to form an oil-in-water emulsion down hole, which makes it easier for the oil to be pumped to the surface.

In summary, emulsion banks formed in situ in enhanced oil recovery methods, such as chemical, thermal, and carbon dioxide flooding, seem to improve oil displacement efficiency under certain conditions. Moreover, emulsions may be generated ex situ from any type of oil if a synthesized surfactant is employed. Such emulsions can be injected externally to improve the secondary and tertiary oil recoveries or as a blocking agent in the near wellbore matrix, thereby reducing gas and water coning or eliminating gas leakage to the surface.[9]

2.1.1 Emulsion Formulation

A produced emulsion can be either oil-in-water or water-in-oil depending on the type of emulsifier, the applied mixing procedure, and the dispersed-to-continuous phase ratios. If an appropriate emulsifier is used, the internal phase may be dispersed into the continuous phase up to 45% of the total volume, beyond which the emulsion will be inverted.

The selection of appropriate emulsifiers for preparing a specific emulsion is considered to be one of the most critical factors affecting stability. The most carefully constructed system is that of Griffin, based on the concept of hydrophile-lipophile balance (HLB). The practical significance of the HLB concept lies in the

fact that every substance that is to be emulsified has its own "required HLB value" and each emulsifier is assigned a dimensionless number between zero and twenty. Emulsifiers with HLB values between zero and nine are considered to be oil-soluble hydrophobic emulsifiers and those with HLB values between eleven and twenty are water-soluble hydrophilic. To emulsify a particular substance, an emulsifier or a mixture of emulsifiers with the same HLB value must therefore be used. The following summarizes the HLB required for different applications:

I. HLB values from three to eight create W/O emulsions;

II. HLB values from eight to eighteen create O/W emulsions; and

III. HLB values from seven to nine are considered to be wetting agents.

2.1.2 Emulsification Technique

A common technique to disperse a liquid in another immiscible liquid is to divide large drops into smaller ones by means of mechanical energy. This can be achieved with the use of a simple mixer, a homogenizer, or an ultrasonic device. The order and method of mixing the components impacts the course of emulsification and its results. There are four standard techniques for addition of components[10]:

I. *Agent in water*

The emulsifier is dissolved directly in water and the oil is then added while the mixer is stirred vigorously. This method requires a large input of energy and creates O/W emulsions directly.

II. *Agent in oil*

The emulsifier is dissolved in the oil phase. The emulsion can be formed in two ways: direct addition of the mixture to the water creates an O/W emulsion usually with a consistent size. Addition of the water to the mixture, slowly and in small quantities, creates a W/O emulsion.

III. *Nascent soap method*

Only suitable for sulfonated oils that can be emulsified and stabilized by in situ soap formation. This permits formation of both O/W and W/O emulsions.

IV. *Alternating addition*

Water and oil are added alternately and in small quantities to the emulsifier.

2.2 *Experimental Studies of Emulsion Flow in Porous Media*

A number of laboratory studies have been conducted to understand both the qualitative and quantitative behavior of emulsions and their flow mechanisms through porous media. Most of these studies were carried out to determine how to improve oil recovery by in situ emulsification or by injecting emulsions externally. Although most of these studies suggest that oil-in-water emulsions can be used to obtain a deeper formation plugging and better sweep efficiency, they reveal limited information about the blocking mechanism itself, which has the potential to recover oil more efficiently. A review of the most important experimental work conducted on emulsion flow in porous media is given below.

The use of sodium hydroxide and alkaline salts for in situ emulsification of crude oils during waterflooding recovery dates back to 1917. At that time, Squires[11] found that the displacement of oil from sand was improved by introducing an alkali into the water.

Beckstrom and Van Tuyl[12] published the results of a series of waterflooding experiments on oil sands in 1926. In these studies, they found that diluted solutions of sodium hydroxide, at a concentration nearing 1%, was more effective than a highly concentrated solution in increasing the yield of oil. Higher oil recovery resulted from an increase in experimental temperature.

Uren and Fahmy[13] carried out further investigations on the effects of chemicals on oil recovery during 1927. They concluded that sodium hydroxide might be the most useful of all the reagents used. They found that the interfacial tension between the oil and the mineral that the sand is composed of must be greater than the sum of the

interfacial tensions between the water and the mineral and between the flood water and the oil for release of adherent oil from oil wet sand grains.

In 1927, Atkinson[14] obtained the first patent on flooding oil-bearing sands with water containing caustic alkalis. He recognized that the capillarity and adhesive property of the oil would cause it to wet and adhere as films to sand grains. As such, the viscosity of the oil would enhance this trapping of it. A secondary recovery method, such as a waterflood, could not overcome these factors. By adding caustic alkali, Atkinson realized that the tension at the oil water interface would change, bringing about the displacement of oil by the water more readily.

Since the 1930's, when Haines[15] published his classic paper on the capillarity effect associated with the mobilization of non-wetting oil droplets in underground media, a great deal of work on the in situ emulsification of underground oils has been carried out. Cartmill,[16, 17] aiming to investigate the mechanism of oil migration through reservoir sandstones, focused on the flow of stable crude oil-in-water emulsions that were prepared without the use of wetting agents, through packed beads each with differing permeability zones in series. He found that 80% of the oil droplets were retained at the junction of different permeability zones. The amount removed depended on the contrast in grain size, the nature, and the preferential wettability of the porous media, with maximum retention at the front portion of the low permeability zone. Consequently, permeability of the porous media was reduced. He also emphasized that the screening did not occur as a result of capillary effects because the pores were many times the diameter of the droplets. He hypothesized that electrostatic forces might be more important than the capillary forces in causing permeability reduction.

The flow behavior of emulsions through tubes as well as unconsolidated synthetic porous media was studied experimentally by Marsden and Uzoigwe.[18] They observed no retention of droplets within the porous media during the flow of oil-in-water emulsions though glass bead packs.

According to the literature, McAuliffe[19] was first to use an oil-in-water emulsion as a blocking agent. He conducted laboratory studies to illustrate that oil-in-water emulsions can be used as a selective plugging agent to improve oil recovery in water floods. By injecting caustic oil-in-water emulsions with various drop sizes into Berea sandstone under a constant pressure, McAuliffe noted a larger reduction in water permeability of sandstone with larger drop-size to initial permeability ratio. Furthermore, permanent permeability reduction was observed even when many pore volumes of water followed the emulsion. He also observed that the rate and amount of permeability reduction decreased with increasing injection pressure. He called this flow behavior pseudo non-Newtonian, regardless of the oil content of the emulsion. For parallel cores of different permeabilities, an oil-in-water emulsion was found to proportionally reduce the permeability in high permeability cores more than in low permeability cores.

Finally, McAuliffe observed that oil-in-water emulsions displaced oil more efficiently than water. He postulated that the injected emulsion entered the most permeable zones first, restricting the flow, and thereby causing the fluid to flow in the less permeable zones, resulting in improved sweep efficiency. He also suggested that for an emulsion to be the most effective, the droplets of oil in the emulsion should be slightly larger than the pore-throat constrictions in the porous medium. Once oil droplets plug the pores, they can only be forced through the constrictions if the applied pressure can overcome the capillary retarding force. Field tests substantiated the laboratory observations. Oil-in-water emulsions were found to reduce water channeling from injection to production wells, thus increasing oil recovery, lowering water-oil ratios, and considerably increasing the volumetric sweep efficiency.

Cooke et al.[20] flooded with alkaline water a watered-out oil porous medium containing organic acids. Their results revealed an additional recovery of around 50% of the residual oil left in the watered-out model. High recovery efficiency

resulted from the formation of a bank of viscous water-in-oil emulsion as surface active agents (soaps) were created by the combination of base in the water and organic acids in the oil. The type and amount of organic acids in the oil, the pH and salt content of the water, and the amount of fines in the porous medium were the primary factors that determined the amount of additional oil recovered by this method.

Johnson,[21] in reviewing the several proposed mechanisms by which caustic water flooding may improve oil recovery, suggested that either emulsions formed in situ or those injected externally were useful in recovering viscous oils and oils in heterogeneous reservoirs where sweep efficiency is poor.

Radke and Somerton[22] studied the improved recovery efficiencies of acidic crude oils with alkaline agents. They focused on the displacement dynamics, chemical transport, emulsion flow, and interfacial tensions of the process. Displacement tests of Wilmington oil-field cores with alkali at reservoir temperature and rate showed tertiary oil recoveries of 10 to 40% of the residual oil. Recovered oil was produced at low oil-to-water ratios after alkali was observed at the core exit. They also suggested the alternative of using dilute emulsions, instead of polymer, to improve mobility control in caustic flooding. The advantage of using emulsion is that its effectiveness is quite insensitive to temperature and alkalinity. Also, emulsion is less expensive than polymers because they can be easily prepared using acidic crude oils.

Foster[23] summarized a field test observation that was conducted in South Texas on a sandstone reservoir with the aim of developing an economic low-tension waterflooding process. The objective of the field test was to examine certain aspects of surfactant behavior and a later polymer injection study at the same site at a later date. The results of field tests led to the conclusion that a tertiary oil bank can be formed in a reservoir using low-tension surfactants. Foster also concluded that it was essential to control the mobility immediately behind the bank to ensure that a significant fraction of the mobilized oil would be driven to the producing wells.

Finally, he found that the compositional requirements that must be met in order to achieve and maintain a condition of very low tension are different than those required in the miscible flood process (zero interfacial tension).

Soo and Radke[24, 25] studied the flow mechanism of dilute, stable oil-in-water emulsions in porous media by first determining the transient permeabilities, the pore size distribution of the porous medium, and the inlet and effluent drop concentrations and size distributions. The oil droplet migration in the porous medium was also observed by means of a visual micro-model. They argued that dilute, stable oil-in-water emulsions did not flow in porous media as continuous, viscous liquids or by being squeezed through pore constrictions but that they flowed by the capture of the dispersed phase with a subsequent reduction of permeability to the continuous phase. This droplet capture mechanism was found to be similar to a filtration process. Soo and Radke discovered that during the transient permeability reduction caused by droplet retention in pores, the drops not only blocked pores with throat sizes smaller than their own (straining), but also were captured on the surface of and in crevices or pockets formed by the sand grains (interception). The capture of these small droplets on the rock surface depends on the surface chemistry of the drops and the porous matrix, especially the pH and ionic strength of the aqueous phase. A steady state is reached once all capture sites are occupied because liquid droplets cannot be captured on top of one another.

Soo and Radke concluded that the overall permeability reduction is controlled by two factors: the volume of droplets retained, and the droplets' ability to restrict flow. As the drop size of the emulsion increased, the drop retention also increased because of the high probability of capture. However, at identical volume retentions, smaller-sized drops were more effective in restricting flow during the transient state. Once steady state flow was obtained, the larger droplets caused a greater reduction in permeability than the smaller ones because of the combination of these two factors. Finally, they observed that the viscosity of the oil phase had little impact on both effluent concentration and transient permeability histories.

Schmidt,[26] in collaboration with Soo and Radke, proposed that for continuous, linear, secondary oil displacement by an oil-in-water emulsion, the displacement was improved by microscopic mobility control through entrapment or local permeability reduction, but not through viscosity ratio improvement. For parallel core flooding, displacement was improved through macroscopic mobility control by diverting flow to the lower permeability core.

French et al.[27] performed laboratory work on the development of an emulsion blocking technique for mobility control during steamflooding. Coreflood experiments demonstrated the effectiveness of emulsion blocking at temperatures ranging from ambient to 194°C. The permeability reduction of various types of cores, using externally produced and in situ generated emulsions, was measured for light and heavy crude oils. Externally produced emulsions injected into oil-free cores reduced the permeability by 86% at 110°C and 77% at 160°C. Injection of externally produced emulsions into cores containing residual oil, where some of the pores are already blocked, netted a 30 to 91% reduction in permeability. Generally, their observations support the emulsion flow mechanism proposed by Soo and Radke, and their results indicated that emulsions formed in situ did not perform as well as those prepared externally.

Yeung[28] and Yeung and Farouq Ali[29] suggested three different displacement processes with which to improve vertical sweep efficiency during the water flooding of bottom-water formations: the Emulsion Slug Process (ESP), the Alternating Water Emulsion Process (AWE), and the Dynamic Blocking Procedure (DBF). For low surfactant emulsions (0.016 to 0.04%), the DBF and AWE processes resulted in higher oil recoveries than the ESP process under bottom-water conditions. The reverse was true for emulsions with higher surfactant concentrations (0.4%). Yeung and Farouq Ali also found that a high surfactant concentration did not guarantee a higher oil recovery for both homogeneous and bottom-water conditions.

Fiori and Farouq Ali[30] proposed the use of solvents in adjusting the emulsion characteristics for increased oil displacement efficiency. Emulsion slugs were then injected into partially water-flooded cores, resulting in incremental recoveries of up to 70%. They concluded that carefully designed crude oil emulsions (water-in-oil) can be used as oil recovery agents for heavy oil reservoirs with low primary conductivity, poor response to water flooding, and low potential for thermal recovery applications.

Khambharatana et al.[31] performed experimental work to observe the physical mechanisms that occur when a stable emulsion flows in a porous medium (for a system of comparable drop and pore sizes). They investigated emulsion rheologies and droplet capture for both caustic and surfactant emulsions flowing through Berea sandstone and Ottawa sand packs. Their results indicated that the change in emulsion rheology in a porous medium follows an overall trend similar to what occurs in a viscometer for the shear rates of interest. Furthermore, the emulsion droplets were found to be captured according to a filtration process proposed by Soo and Radke.

Mendez,[32] on the other hand, investigated the mechanisms of permeability impairment caused by the flow of oil-in-water emulsions in porous media. She injected well-characterized oil-in-water emulsions into cores containing residual saturation. The permeability of different sections of the cores as well as the droplet concentration and size distribution were measured as a function of time and position. Prudhoe Bay and North Sea oils were used in Berea sandstone and Aloxite cores. The experimental results indicated that the presence of residual oil profoundly affected the measured permeability decline. Droplets were generated from the residual oil present at the pore throats after a critical capillary number was exceeded.

Mendez found that high injection rates and low permeabilities enhanced droplet formation, and observed that the permeability decline occurred in two stages: one associated with the injected droplets followed by the second stage, during which

generation of droplets played a pivotal role. Finally, she emphasized that the permeability of the porous medium, droplet concentrations, concentration of emulsifier present, flow rate, and the properties of crude oil all play equally integral roles in determining the extent and rate of permeability impairment.

Woo et al.[33] conducted an experimental study to examine the effect of emulsion system stability on the flow of water-in-oil emulsions through porous media. Emulsion flow experiments were conducted in a sand pack to determine flow characteristics and phase interactions. In addition, the pore level phenomena occurring during the flow processes were visualized in a high pressure etched glass micro-model. The results indicate that emulsion stability dramatically affected the mobility of water-in-oil emulsions in porous media. They observed that the mobility of stable water-in-oil emulsions increased with water concentration. In general, they found that the mobility of the emulsion decreased with increasing emulsion stability, although the type of emulsifier used influenced mobility.

Collins et al.[34] used water-in-oil emulsions to deploy scale inhibitors in porous media. Their use of slowly degrading emulsion systems provided a means with which to the scale inhibitor and the subsequent controlled release of the chemical within the porous media. Core flood experiments indicated that this extended the inhibitor's lifetime up to four times compared to the base case, non-emulsified product. In addition, they performed a field trial on the Forties field in the U.K. sector of the North Sea using the emulsion system. The field data confirmed that the use of an emulsion system allowed the potential ingress of the scale inhibitor into parts of the reservoir that were typically inaccessible to an aqueous-based formulation. This improved contact between the scale inhibitor and the produced reservoir fluids.

Romero et al.[35] investigated the use of an emulsion to plug highly permeable, fractured zones. Their investigation included the use of a heavy oil-in-water emulsion, formulated using alkaline solutions as emulsifier agents, laboratory

evaluation of the emulsion's ability to plug and the development of a field pilot test. Parameters such as emulsifier types and concentrations, oil/water ratios and shear rate were adjusted to produce a desirable, stable emulsion. Various types of cores, including those with a longitudinal fracture, were used. Romero et al. observed an undesirable breakdown of the emulsion that generated plugging at the core injection inlet. By flushing the core with an alkaline conditioner, they minimized the breaking of the emulsion before it entered the cores. In addition, injection of externally-produced emulsions into the cores after the pre-flush with the alkaline conditioner reduced the permeability up to 80%. Finally, they observed zero time degradation on the emulsion plug, even after 27 PV of water was injected.

Wang et al.[36] analyzed the mechanisms of emulsion displacement and its characteristics in porous media by conducting experiments of emulsion flow in micro-models. Their results indicated that the different types of residual oil, formed by waterflooding, are reduced after the emulsion flooding. They recognized two reactions in the mechanism for emulsion flooding: (l) the residual oil, caused by bypassing flow, is reduced by the diffluence effects produced by the plugging of large channels; (2) efficient displacement of residual oil on the edges and corners of the pores is obtained by the actions of extrusion, pull and draught when the emulsion flows into the throats. Wang et al.'s results indicate that oil displacement efficiency increases by approximately 6% after emulsion flooding.

2.3 *Predicting the Flow of Emulsion through Porous Media*

Flow of oil-in-water emulsion in porous media and its application as a blocking agent are inherently complex processes because of the presence and motion of oil droplets in a solid matrix characterized by pore microstructure heterogeneities. Generally, oil droplets trapped in a porous medium by capillary forces are displaced by the flow of aqueous liquids through the medium, which forces the trapped oil to a potentially lower side of the medium. The presence of liquid-liquid and liquid-solid interfaces strongly affects the emulsion flow in a porous matrix. The challenge is to

relate pore-scale hydrodynamics and related physicochemical phenomena to a bulk fluid movement on a macro-scale.

In the next section, the entrapment mechanisms of a non-wetting oil droplet in porous media are discussed first. Subsequent is an overview of the available models that predict the emulsion flow in porous media. Finally, the parameters that may affect the equilibrium forces at interfaces are discussed and the relevant reviewed literature is presented.

2.3.1 Entrapment Mechanism

In quantifying the motion of a dispersed oil droplet flowing through a series of pores, at least two scenarios should be considered: 1) with a low aspect-ratio of pore body-to-throat size, the wetting water phase can displace the non-wetting oil droplets in a piston-like fashion as illustrated in Figure 2.1.

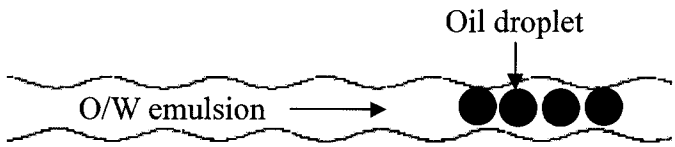

Figure 2.1 Piston-like flow in low aspect-ratio channel

2) for a higher aspect-ratio channel, there is a higher gradient of capillary pressure in the non-wetting phase than in the (continuous) wetting phase, so the non-wetting phase tends to flow backwards locally and the collar of the wetting phase "snaps off" as illustrated in Figure 2.2.

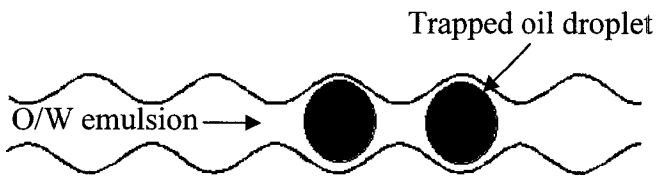

Figure 2.2 Droplets snap-off in high aspect-ratio channel

The flow behavior of a dilute stable oil-in-water emulsion can be categorized as the first scenario if the emulsion is carrying droplets that are much smaller than the pore throat openings. Under such circumstances, an emulsion flows as a homogeneous phase. Consequently, the flow behavior could be predicted reasonably from Darcy's law:

$$v = \frac{k\Delta P}{\mu L} \tag{2.1}$$

where:

v = linear flow velocity, [m/s]

k = absolute permeability, [m^2]

ΔP = pressure drop, [Pa]

μ = viscosity, [Pa.s]

L = length, [m]

Equation 2.1 predicts the flow behavior of laminar Newtonian flow. However, most emulsions exhibit a non-Newtonian behavior, which means their viscosity varies with shear rates. Therefore, using the Darcy's law to predict the flow behavior of these homogeneous emulsion systems requires the application of correct viscosity to the given shear rate. In other words, a homogeneous emulsion should be considered as a single phase fluid that exhibits an average viscosity when it flows through a porous medium.

On the other hand, with the increase of the droplet diameter relative to the pore throat diameter, the movement of a droplet should decrease markedly at some critical limit, which is a function of the internal pressure of the droplet relative to that of the water phase. For oil droplets that are dispersed in the water phase, the pressure equilibrium at the oil-water interface can be calculated by applying the Young-Laplace equation[37]:

$$P_c = P_n - P_w = 2\sigma\cos\theta/R_d \qquad (2.2)$$

P_c = capillary pressure [Pa]

P_n = non-wetting phase pressure [Pa]

P_w = wetting phase pressure [Pa]

σ = oil-to-water interfacial tension [mN/m]

θ = porous medium wettability [dimensionless]

R_d = droplet radius or radius of curvature [m]

The capillary pressure is a function of interfacial tension and radius of curvature. Any deformation in the droplet shape would affect the radius of curvature and the interfacial forces. The interfacial forces arise from the need to expend work in order to create new surface area at the interface.

Figure 2.3 shows a trapped non-wetting oil droplet (or an oil ganglion) in the pore throat. For a trapped droplet, if P is the pressure in the wetting phase at the upstream point, then the non-wetting phase pressure is given by:

$$P_1 = P + 2\sigma/R_t \qquad (2.3)$$

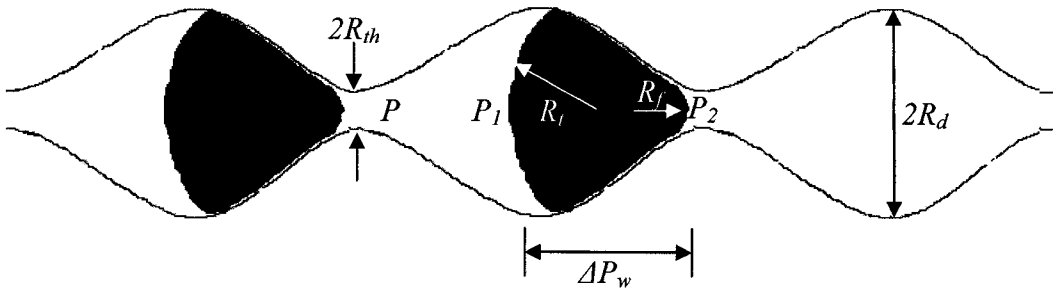

Figure 2.3 Pressures around a trapped non-wetting oil droplet

The pressure in the droplet at the downstream end is as follows:

$$P_2 = P - \Delta P_w + 2\sigma/R_f \qquad (2.4)$$

The oil droplet can only move downstream if $P_1 > P_2$. Consequently, a droplet becomes trapped unless the following occurs:

$$\Delta P_w > 2\sigma\left(\frac{1}{R_f} - \frac{1}{R_t}\right) \approx 2\sigma\left(\frac{1}{R_{th}} - \frac{1}{R_d}\right) \qquad (2.5)$$

In the second scenario, where a droplet larger than the pore throat constrictions flows through a porous medium, there are four main mechanisms proposed by Devereux,[38, 39] and later by Alvarado and Marsden,[40] McAuliffe,[41] and Soo et al.,[42-44] that describe emulsion flow behavior. A purely theoretical model was also developed by Sahimi and Imdakm.[45] Following this is a review of the mathematical models formulated for the hypothesized mechanisms.

Devereux[38, 39] proposed a droplet retardation model, based on the mechanism put forth by McAuliffe,[41] for describing the flow of stable oil-in-water emulsions in porous media, that includes capillary effects but neglects gravitation and compression. Devereux considered the flow of two phases, dispersed and continuous, in porous solids with the capillary effect included. He proposed that the emulsion drops flowed slower than the continuous phase because they encountered capillary resistance during their flow through smaller pore throats. Therefore, this capillary retarding force, which depends on the drop size distribution, was included in the pressure driving force of the dispersed oil phase in this model.

The model derived for the case of constant velocity flow can properly predict transient permeability reduction. That is, the model predicts a greater reduction in permeability with a lower flow rate and a higher drop-to-pore size ratio. However, this retardation model could not predict the permanent permeability reduction observed in the laboratory when many pore volumes of water followed an emulsion flood. Instead, the permeability prior to the emulsion flood was predicted.

Alvarado and Marsden[40] developed a bulk viscosity model in which emulsion is viewed as a homogeneous, single-phase fluid. They derived a simple correlation with which to describe the flow of non-Newtonian oil-in-water macroemulsions through porous media for the range of shear rates investigated, 10^3 to 10^4 s^{-1}. This correlation can be reduced to Darcy's law for oil-in-water Newtonian macroemulsions, including permeability reduction caused by partial plugging. In conclusion, this model considered an emulsion as a homogeneous, non-Newtonian fluid that does not follow Darcy's law because of the change in bulk viscosity with shear rate. The viscosity model was limited to a description of the flow of high-concentration emulsions with small drop-size to pore-size ratios.

Abou-Kassem and Farouq Ali[46] modified the viscosity model, making it practical for use in numerical simulations of EOR processes. For non-Newtonian emulsions, the correlation was presented as a modified Darcy's law. The correlation provides for a quantitative description of the effect of pore size distribution and tortuosity of porous media on flow. The proposed model is recommended for use in the one-dimensional, isothermal, single-phase flow of non-Newtonian fluids in porous media.

Soo et al.[42-44] proposed a flow model that describes the flow of stable, dilute emulsions in unconsolidated porous media based on deep-bed filtration concepts. This model accounts for the interactions between the flowing droplets and the pore constrictions, which helps to predict how emulsions are transported in porous media. In this model, emulsion droplets can be captured in pores by straining and interception, causing permeability reduction. Transient flow behavior is characterized by three parameters: a filter coefficient, a flow-redistribution parameter, and a flow-restriction parameter. The filter coefficient controls the sharpness of the emulsion front. The flow-redistribution parameter dictates the steady-state retention and the flow redistribution phenomenon. The flow-restriction parameter describes the effectiveness of retained drops in reducing permeability. Comparisons to the filtration model and the previously-developed emulsion flow

models indicate that only the filtration model successfully represented all of the experimental observations, such as permanent permeability reduction. This model accurately represents the underlying physical mechanisms but neglects the effects of the chemistry of solid and liquid phases.

In summary, all of the above-mentioned models are developed based on the equilibrium of hydrodynamic forces but ultimately fail to consider the effect of other forces, such as intermolecular and electrostatic forces. Moreover, while some of the models ignore the effect of capillary pressure across a single pore, others simply assume it is constant. Such assumption could be reasonably justified for a highly stable dilute emulsion, but could be potentially misleading for predicting the flow behavior of highly concentrated emulsions, especially those carrying less concentrated surfactants. The neglected considerations are primarily related to the emulsion stability and its quality, which is associated with the transition from Newtonian to non-Newtonian rheological behavior. The latter is mainly dependent on the surfactant (emulsifier) concentration and the local applied shear rates.

Sahimi and Imdakm[45] developed a general model for the flow of suspended particles in a porous medium. The model accounts for the effects of the morphology of the porous medium, including pore surface roughness and fractality, the chemistry of the flowing fluid, and the important forces between the particles and the pore surface. Their approach combines a network model of a porous medium with molecular dynamics-like simulations to determine the exact paths of the particles in the pore space. The porous medium was represented by a simple-cubic network in which each bond, assumed to be a cylindrical tube of a fixed length, represents a pore of the medium. In conclusion, this model only predicts the permeability reduction due to the migration of fine stable emulsion droplets in a porous medium but fails to recognize the effect of droplet size exclusion.

2.3.2 Parameters affecting the Equilibrium Forces at the Interface

Careful investigation of the Young-Laplace equation reveals that oil droplets-to-water interfacial tensions, the droplets' radii, and the wettability of a porous medium cannot be assumed to be constant during an emulsion flow into a porous medium. In fact, they are strong functions of the surfactant type and concentration present in the aqueous phase as well as the chemistry of both solid and liquid phases.[47, 48] The factors affecting the properties of liquid-liquid interfaces are discussed in the following section. Following this, the factors influencing the equilibrium forces at the solid-liquid interface are presented.

Oil droplets-water interface

During a flow of an oil-in-water emulsion though a porous medium, the oil droplets are separated by the protective layer of surfactant. The droplets then will not coalesce unless the local body forces exceed the interfacial forces at the droplets' surface. It is believed that as the emulsion propagates into a porous medium, more surfactant will be adsorbed onto the surface of the sand grains, resulting in the reduction of surfactant concentration within the emulsion.[49, 50] Therefore, droplets may coalesce more easily and produce larger droplets when the surfactant concentration in the solution is below the minimum limit. Droplets may coalesce because of the application of high shear forces rupturing the interface film while they are being forced toward each other.[51, 52] In addition, the droplets may coalesce because of the change in chemistry of the continuous water phase. In particular, changes in solution pH and salinity can affect the properties of the interfacial film and, consequently, droplets' stability.[53-56] In the case of emulsions with a high oil content, in which the droplet-droplet interactions are significant, the effects of these parameters may be more pronounced. Any decrease in surfactant concentration or in the chemistry of the mobile phases may eventually cause droplets to coalesce while they percolate in the porous medium. Because of coalescence, such an increase in droplets' radii will affect the local capillary pressure, the viscosity of the emulsion, and generally, the emulsion flow behavior.

Oil droplets-porous medium interface

The wettability of a porous medium ($cos\theta$ in the Laplace equation) contributes dramatically to the magnitude of the local capillary pressure across a trapped oil droplet in a porous medium. Further study of the interception mechanism, in terms of the capture and release of an oil droplet on the sand surface, revealed a strong interplay of wettability as well as various hydrodynamic, intermolecular and electrostatic forces.[57, 58] Consider that the hydrodynamic forces (gravitational, inertial and drag forces, Brownian motion and molecular dispersion) influence the droplet such that it is now closely spaced to the pore surface. The movement of such droplets is highly constrained by the wettability of the solid porous medium. If the solid surface and the droplet have opposite charges, then the droplet will be attached to the pore surface. Otherwise, the repulsive forces create a certain separation distance and the droplet remains deposited on the sand surface only when the intermolecular attraction forces between the droplet and the sand grain overpower the hydrodynamic and repulsive forces. Nevertheless, the surface potential of the droplet is influenced by the type (i.e., nonionic, cationic and anionic) and concentration of the surfactant in the solution, the composition of the oil, and the chemistry of the continuous phase.

The wettability of the porous medium is a function of solution pH and the adsorption of the surfactant on the pore surface. Figure 2.4 displays the zeta potential or the charge density, at the surface of shear (calculated from electrophoretic mobility data) relating to hydrocarbon oil droplets plotted as a function of pH in acetate-veronal buffer at a constant ionic strength of 0.05 mol dm^{-3}. It indicates that the point of zero charge for the hydrocarbon droplets occurs in the lower ranges of solution pH. As the pH increases, the surface charge density of the oil droplets also increases.

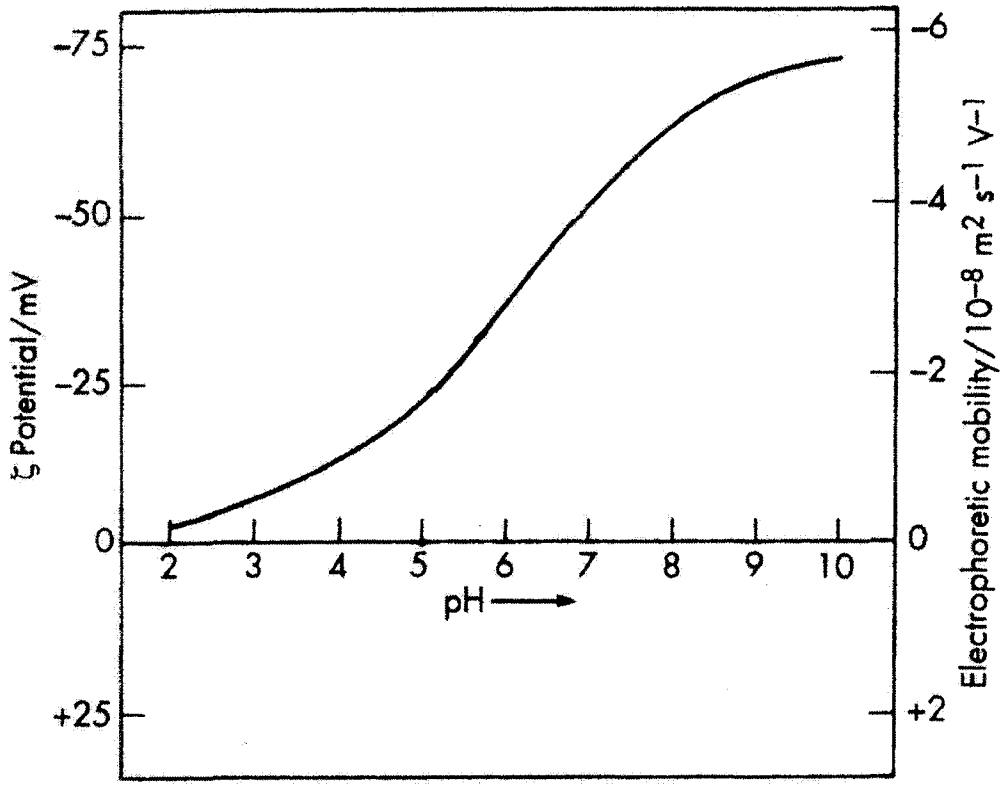

Figure 2.4 Effect of pH on zeta potential of hydrocarbon oil droplets [modified figure, after Shaw[59]]

In addition, the wettability of the porous medium can be altered by adsorption of surfactant on the pore surface. Surfactant adsorption is an important phenomenon in many processes, such as tertiary oil recovery using micellar flooding and in mineral froth flotation. Research in mineral processing during the last eighty years has yielded valuable information on the adsorption characteristics of minerals and mechanisms governing the adsorption. Past studies on adsorption in various systems have been discussed in many publications.[60-63] Most of these, however, represent the surfactant adsorption in binary systems. In other words, they only deal with the surfactant adsorption at the interface of gas-liquid, gas-solid, liquid-liquid, or liquid-solid systems. The literature rarely evaluates the surfactant adsorption on the porous medium when the flowing fluid is an oil-in-water emulsion. The following literature provides more details of the physico-chemical aspects of surfactant adsorption

related to flat surfaces. The effects of relevant factors, such as solution pH, temperature and ionic strength on the emulsion stability will also be discussed.

Lawson[64] studied the stability of water-in-oil-in-water (w1/o/w2) double emulsions by using the capillary video microscopy. Lawson was seeking a better understanding of the role of surfactants in the stability of water-in-oil-in-water double emulsions. Various types and concentrations of surfactants were used to prepare the emulsions. The formation of droplets from the moment of their preparation was observed. Information gathered from the experiments was used to design double emulsions and determine the feasibility of using this type of emulsion for targeted drug delivery. The results indicated that the use of surfactant in the external aqueous phase promoted external coalescence, which is the release of internal w1 droplets to the external w2 phase upon disruption of the oil-surfactant film. Variation of the surfactant concentration in the outer w2 phase enabled control of the rate of release of the internal droplets. Increasing its concentration accelerated the release rate.

Strassner[65] investigated the effect of pH on interfacial films and the stability of crude oil-in-water emulsions. He found that oil field emulsions were stabilized primarily by film-forming, polar asphaltenes and resins containing organic acids and bases. In addition, he observed that the addition of inorganic acids and bases, with subsequent alterations in pH, changed the physical properties of these interfacial films and their ability to stabilize emulsions. In tests with low-gravity Venezuelan crude oil and distilled water, basic pH produced stable oil-in-water emulsions. Moreover, Strassner found that emulsion stability can be decreased by introducing conditions that reduce the film-forming capacity of the crude oil. These films can be minimized or their physical properties altered by treating them with acids and bases alone or in conjunction with inorganic salts, surfactants, heat or electricity. At an optimum pH range, adsorbed film exhibits minimum contracted film properties for most crude oil-brine system. The optimum pH for maximum emulsion instability depends on both crude oil and brine composition.

Further study by Layrisse et al.[66] using two Venezuelan crudes (Cerro Negre CN-36, 8.3°API and Zuaty, 9.5°API) revealed that pH levels influence the natural surfactants present in the crude, and consequently, the interfacial behavior of the crude. Emulsion stability is enhanced by minimum interfacial tension, which was found to be minimized at basic pH. Using acidic pH, the researchers found that the asphaltenes are adsorbed at the interface, whereas the lower interfacial tension found at alkaline pH are due to the more active and lighter resins.

Gillberg and Eriksson[67] investigated the effect of pH on the solubilization capacity of the mixtures of nonionic ampholytic surfactants employed in microemulsions. They found that microemulsions incite minor changes in pH at a constant temperature, due to the variation in the degree of ionization attributable to the ampholytic surfactant with pH. Consequently, this affects the total interaction potential energy by altering the repulsion energy of the surfactant layer.

Levius and Drommond[68] investigated the effect of elevated temperatures as an artificial breakdown stress to evaluate emulsion stability. They found that by increasing the temperature, the mean droplet size and droplet concentration decreased because of a more rapid settling rate.

Harusawa et al.[69] found the hydrophilic/hydrophobic nature of certain nonionic surfactants to be temperature-dependent, which affects the interfacial tension and emulsion stability. Nonionic surfactants containing ethylene oxide chains as hydrophilic groups suffered dehydration of the ethylene oxide moieties as the temperature increased. Surfactants containing less than ten ethylene oxide units experienced an increase in interfacial tension with increasing temperature. A destabilizing influence on an emulsion is thus created with such a surfactant.

Saito and Shinoda[70] investigated the stability of both oil-in-water and water-in-oil type emulsions as a function of temperature. These were cyclohexane-water systems stabilized with the nonionic surfactant polyoxyethylene nonylphenylether. They

found that the mean droplet diameter of either emulsion type diminished as the emulsion temperature approached the phase inversion point (PIT) of the system. This was a result of quick coalescence rates observed for larger droplets near the PIT, and their subsequent creaming out of the solution.

Rosen[71] summarized the effect of temperature change on the stability of emulsions:

1) Thermal agitation of droplets increases the interaction/collision rate through diffusion.
2) The physical properties of the interfacial film are affected by thermal expansion or contraction.
3) The relative solubility of surfactant in either phase is affected.
4) The rheological properties of the liquid constituents are affected.

Yang et al.[72] studied the micron bubble attachment onto a solid surface under varying physicochemical conditions by using a direct microscopic observation method. They conducted bubble attachment experiments on sodium chloride solutions with various concentrations (10^{-1} to 10^{-4} M) and pH values (2.5 to 9.0) under a fixed flow intensity (Reynolds number = 200). In addition, the effect of metal ion valence on the bubble attachment was examined. The results indicated that the bubble attachment flux was dependent on both solution concentration (ionic strength) and pH, suggesting that the electrostatic interaction forces have a strong impact. They reported that the bubble attachment rate was noticeably enhanced in the presence of multivalent metal ions.

Taylor[73] studied the structure of bitumen/water interface and the surface forces that exist between emulsified water droplets. He used the Thin Liquid Film-Pressure Balance Technique to create microscopic water/solvent diluted-bitumen/water films. The films enabled them to study the interaction between two water droplets immersed in a continuous phase of diluted bitumen. Several properties of the film were measured as a function of solvent-to-bitumen ratio, including thickness, drainage rate, and lifetime. Surface force and film structure information was also

obtained from measured disjoining pressure-thickness isotherms. His results indicated that the film was probably stabilized by steric repulsion generated by surface active material from the asphaltene fraction of the bitumen. He also noticed evidence that a change in the solvent-to-bitumen ratio may have caused a change in the surfactant structure within the film.

Stancik[74] attempted to explain that the dominant role in the stabilization mechanism arise due to interfacial particle concentration gradient, and investigated the effects of fundamental flows on the structure and dynamics of mono-disperse spherical polystyrene particles adsorbed to the decane-water interface. He found that a competition between the forces arising from particle interactions and those due to the applied flow field leads to two distinct regimes of particle behavior, governed by interfacial concentration and flow rate. At low concentrations or high flow rates, hydrodynamic forces dominate the system and cause the particles to follow typical streamlines. In contrast, interparticle forces gain importance and lead to collective flow behavior amongst the particles.

Chapter 3. Objectives and Hypotheses

The application of heavy oil-in-water emulsion as a novel sealant in the vicinity of the wellbore is proposed in this research. The prediction of emulsion flow behavior and the blocking mechanism in the near wellbore porous matrix is unclear. The main objectives of this research are as follows:

I. To observe the droplets' capture mechanism in porous media by conducting micro-visualization experiments. The aim is to evaluate the effect of key elements involved in the process of entrapment. Factors that may influence the capture or release of a droplet into a pore are of particular interest, for example, the effect of the physical properties of the mobile phase and the surface chemistry of the solid phase.

II. To study the flow behavior of an oil-in-water emulsion in porous media by macro-visualization experiments. Factors affecting the emulsion propagation rate into the porous medium, in particular, the effect of emulsion stability and porous medium wettability on the blockage phenomenon will be evaluated. In addition, the effect of oil type, porous medium permeability, injection velocity, wettability alteration, and surfactant concentration will be studied.

III. To gauge a heavy oil-in-water emulsion's ability to seal a porous medium by conducting high pressure core flooding experiments. A range of unconsolidated porous media are examined in order to assure the application of the sealing process for further field trial implementation.

Table 3.1 summarizes the objectives and the parameters that will be investigated for each experimental category.

	Experimental category		
	Droplets capture mechanism	**Emulsion flow propagation**	**Blockage demonstration**
Objective	To observe the droplets' capture mechanism in porous media	To evaluate the factors affecting the emulsion propagation rate in porous media	To seal a variety of porous media with different permeabilities
Type of investigation	Low pressure visual micro-scale flow tests	Low pressure visual macro-scale flow tests	High pressure blind flow tests
Flow devices	Etched glass micro-model	Two-parallel plate micro-model packed with glass beads	Core holder packed glass beads
	Two-parallel plate micro-model packed with sand		
Parameters	Oil type	Oil type	Porous medium permeability
	Emulsion quality	Front propagation	Pore throat size distribution
	Droplets stability	Permeability reduction	Droplets size distribution
	Wettability alteration	Droplet-to-pore size ratio	Emulsion penetration depth
	Droplets size distribution	Emulsifier concentration	

Table 3.1 Summary of the objectives and parameters for each set of experimental category

Chapter 4. Microscopic Droplet Capture Mechanism Experiments

A series of experiments at pore scale level were conducted to investigate an emulsion's flow behavior, its blocking mechanism and the methods by which it breaks and attaches itself to a porous medium. The aim was to provide a gross overview of emulsion flow through porous media and its blocking mechanism by using visualization experiments.

Micro-scale investigations were conducted in order to provide a detailed understanding of the emulsion blocking mechanism through porous media. Factors that may influence the capture or release of a droplet into a pore were studied thoroughly. The aim was to observe the movement of the emulsion droplets into the pores and evaluate the effect of key elements involved in the process of droplets entrapment. In particular, the effect of surface chemistry of the solid phase (pore surface) and the physical properties of the mobile phase (the emulsion) were studied. Droplet-droplet and droplet-pore interactions were investigated for emulsions carrying different dispersed phase ratios, viscosities, and droplet size distributions.

The following describes the type of equipment and materials used for the set-up and initiation of the experiments. Following this is a qualitative description of the droplet capture mechanism using two types of micro-models.

4.1 *Experimental Set-up*

Figure 4.1 shows the schematic of the experimental setup. It consists of a positive displacement pump (Beckman/Altex Model 110A), a micro visual cell, a microscope, a light source, three differential pressure transmitters, a CCD camera, an HP data logger and an in-line monitor. A computer is used to record the pressure

data and the captured video images. The injection and differential pressures across different sections of the micro-model are measured by three transmitters, monitored by the HP data logger and stored in the computer. One transmitter measured the pressure drop across the total length of the micro-model, the other measured the upstream (front) section pressure drop, and the third one measured the pressure drop related to the downstream (rear) section.

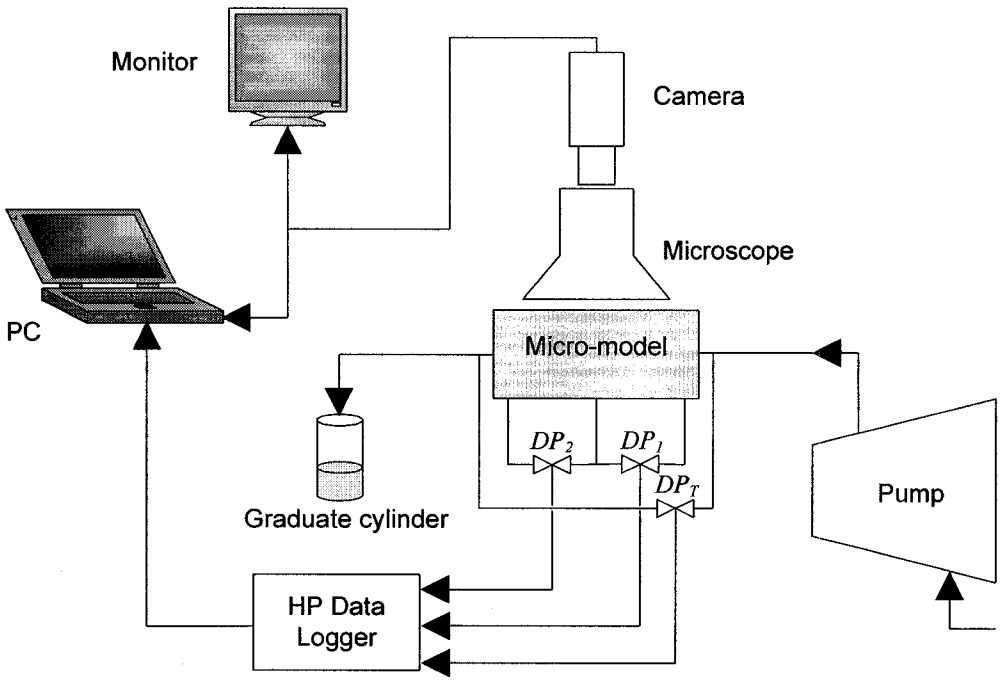

Figure 4.1 Schematic of the experimental setup for micro-scale experiments

The CCD camera is mounted on the dissecting microscope (Leica MZ8 stereo zoom microscope) and its analog output signal is converted to digital signals by Plextrol converter card, then fed into the computer for storage. The container holding the emulsion is placed above a magnetic stirrer to avoid phase segregation because of the density difference between the dispersed oil phase and the continuous water phase. Figure 4.2 is a photograph of the experimental setup.

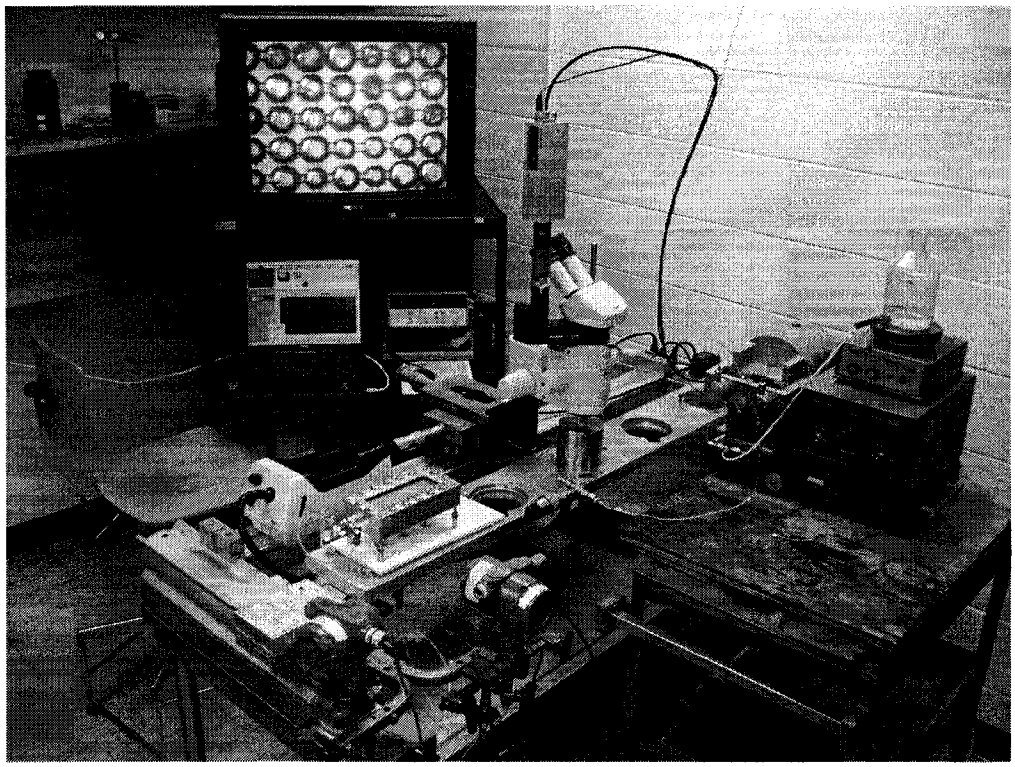

Figure 4.2 Photograph of the experimental setup for micro-scale experiments

4.2 *Micro-models*

Two types of micro-models were used in this study. The first is a dual depth micro-model consisting of two parallel glass plates. A smooth glass sits on top of an etched glass, resembling a highly-ordered pore-throat network. Its actual dimensions are one cm long by one cm wide. Figure 4.3 is an enlarged pore-throat network schematic. Its pores and throats specifications are presented in Table 4.1.

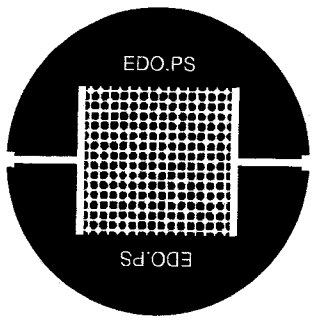

Figure 4.3 Enlarged pore network of etched glass micro-model

pore body depth (μm)		75.0
pore throat depth (μm)		15.0
pore throat average length (μm)		24.4
pore body diameter (μm)	minimum	238.0
	maximum	281.0
	average	263.5
pore throat width (μm)	minimum	73.0
	maximum	122.0
	average	88.0

Table 4.1 Etched glass micro-model specifications

The procedure for etching the glass is presented in Appendix A. Figure 4.4 is three-dimensional (3D) view of the cell holding the etched glass micro-model in place. The confining cell was built by Temco.

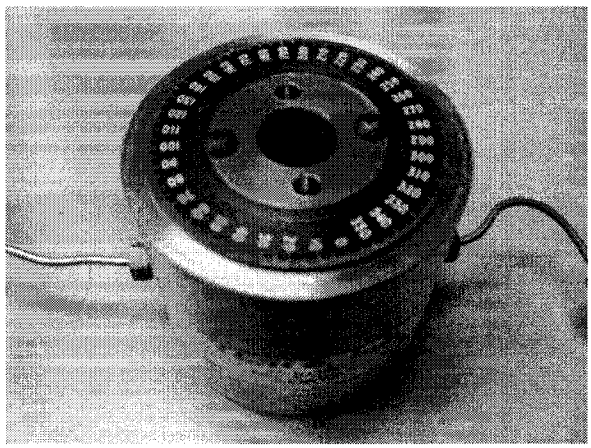

Figure 4.4 Three-dimensional view of etched glass micro-model

The second micro-model is a two-parallel plate model. It consists of a glass plate that sits atop an aluminum plate. A semi-rectangular section (12.5 cm long, 4 cm wide and 0.3 cm deep) was carved inside the aluminum plate, providing space for a synthetic porous medium to be packed. The entrance and exit sections of the carved region were semicircular in shape in order to distribute flow evenly across the cell.

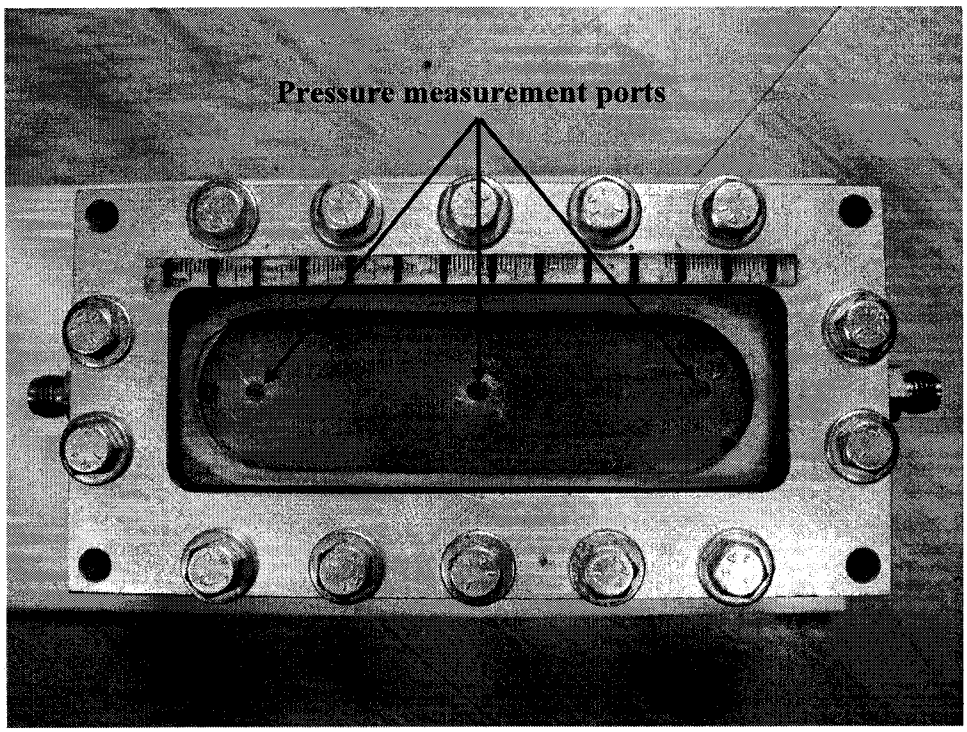

Figure 4.5 Three-dimensional view of two-parallel plate micro-model

Figures 4.5 and 4.6 are three-dimensional views of this micro-model, unpacked and packed with glass beads, respectively. This micro-model was designed by the author and was built by the Alberta Research Council Machine Shop. Its design dimensions are detailed in Appendix B.

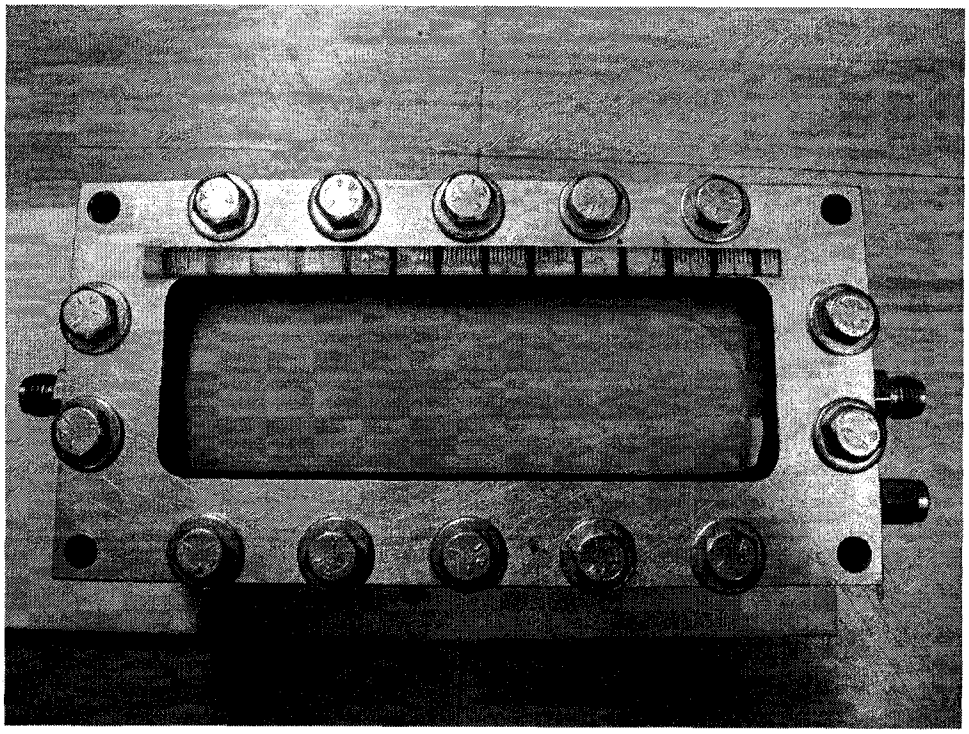

Figure 4.6 Three -dimensional view of two-parallel plate micro-model packed with glass beads

4.3 *Oil Type*

Two types of oil with highly ranging viscosities were used, namely mineral oil (MO) and Lloydminster oil (LMO). The MO was purchased from Fisher Scientific and the LMO was supplied by the Alberta Research Council. The viscosity of the MO at 20°C, (34 mPa·s) is relatively low compared to the other oil. The viscosity for the LMO was measured at two different temperatures by using the CSL-100 Rheometer. Figure 4.7 shows the viscosity of the Lloydminster oil at 20°C and 50°C.

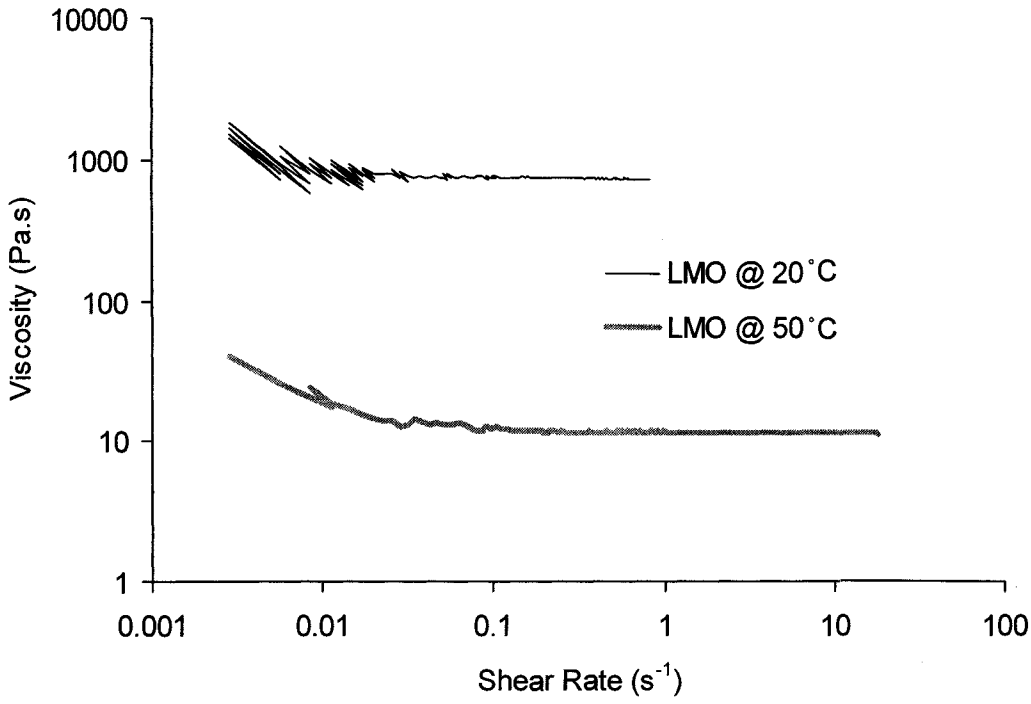

Figure 4.7 Viscosity of Lloydminster oil at different temperatures

4.4 *Emulsions Type and Quality*

The produced emulsion can be either oil-in-water or water-in-oil, depending on the type of emulsifier, the applied mixing procedure, and the dispersed-to-continuous phase ratio. If an appropriate emulsifier is used to produce an emulsion, the internal phase can be dispersed into the continuous phase up to 45% of the total volume beyond which the emulsion will be inverted.

Oil-in-water emulsions were the only types used in the experiments. The emulsion quality, in this case either 5% or 13% by volume, is the percentage of the internal dispersed phase volume relative to the total volume.

4.4.1 Emulsification Technique

Fine emulsions

These types of emulsions were prepared using the agent-in-water method. First, surfactant was added to distilled water and the mixture was homogenized with a Brinkmann homogenizer at 5000 rpm for three minutes. The oil phase was gradually added in known proportions to the aqueous solution as the mixture was homogenized at the same shear rate for approximately 12 minutes. Both nonionic (one brand) and anionic (three brands) surfactants were used. The DOWFAX Triton X-100 nonionic surfactant was purchased from Fisher Scientific. The DOWFAX GR-5M anionic surfactant was provided by Dow Chemical Company. Two more anionic surfactants, PARA-CHEM Stanfax-1012 and PARA-CHEM Stanfax-1045, were supplied by ParaChem.

Among the four surfactants that were used for preparing an emulsion, only the nonionic DOWFAX Triton X-100 surfactant resulted in stable emulsions for long periods of time. It has a hydrophilic-lipophilic balance (HLB) of 13.6 and a critical micelle concentration (CMC) of 130 ppm. The CMC is a measure of the surfactant concentration in a solution which represents the critical value above which the formation of micelles will occur with increasing concentration.[59]

Coarse emulsions

The procedure applied to produce coarse emulsions was similar to that used to produce fine emulsions. Stable emulsions with droplet sizes up to 60 to 70 μm were produced by using the homogenizer. However, the method of mixing the continuous and the dispersed phases was completely different for producing emulsion with larger droplets. Instead of using the Brinkmann homogenizer, the phases were mixed manually. First, the surfactant was added and mixed into distilled water for three minutes. Then the oil phase was added. Finally, the container was closed and manually shaken for four minutes.

4.4.2 Emulsion Stability

Since emulsions are thermodynamically unstable, their lifetime is a primary stability indicator. The rate of coalescence of the droplets is considered to be the only quantitative measure for the stability of the produced emulsions. The stability of the produced emulsions was characterized in terms of their droplet size distributions. A Master Sizer-2000 from the Department of Chemical and Materials Engineering at the University of Alberta was used for measuring the emulsion droplets size distribution over time periods of one and two days, one week, and one month. An emulsion was considered stable if its droplet size distribution did not change drastically over time.

4.5 *Etched Glass Micro-model Experiments*

Before initiating the experiments, the micro-model was flushed with toluene, isopropyl alcohol (IPA), excess amounts of water, and dried at room temperature. The desired emulsion was injected into the micro-model. Then, the microscope was positioned at the top of the micro-model and the pore network geometry was magnified to 325 times its actual size. Once the emulsion injection commenced, the droplets' blocking mechanism was observed. The trapping and coalescence of local droplets, and their squeezing through a single pore, was monitored over time. In addition, the overall pressure profile was recorded over the course of emulsion injection. The effects of oil type, droplet-to-pore size ratio, and wettability alteration were investigated separately.

4.5.1 Experiments to Observe Droplet Capture Mechanism

Three different O/W emulsions, each with different droplet size distributions, were prepared and used in this section to investigate the effects of oil type and droplet-to-pore size ratio. The emulsions' characteristics and the details of each experiment are presented below.

4.5.1.1 Fine mineral oil-in-water emulsion

An emulsion, M/W1, prepared with mineral oil and distilled water by using the homogenizer, consisted of fine droplets with an average size of 5.1 μm. The measured droplet size distribution is presented in Appendix C. The mineral oil was dyed in red BK-50 Unisol liquid for the purpose of detecting and following the flow path of each oil droplet during the emulsion injection. Figure 4.8 shows the dyed mineral oil mixed with distilled water that resulted in the pink colored emulsion.

Figure 4.8 Dyed mineral oil mixed with water to produce a pink colored emulsion

For this emulsion, the phase ratio was 5% oil and 95% water with a surfactant concentration of 0.12% (volume/volume), which corresponds to 0.13 grams of surfactant in 100 cm^3 of water (0.13% weight/volume). The color of the produced emulsion could be close to that of the red-dyed mineral oil, if the produced emulsion had a higher dispersed phase ratio.

Figure 4.9 is a magnified section of the pore-throat network prior to the injection of the emulsion.

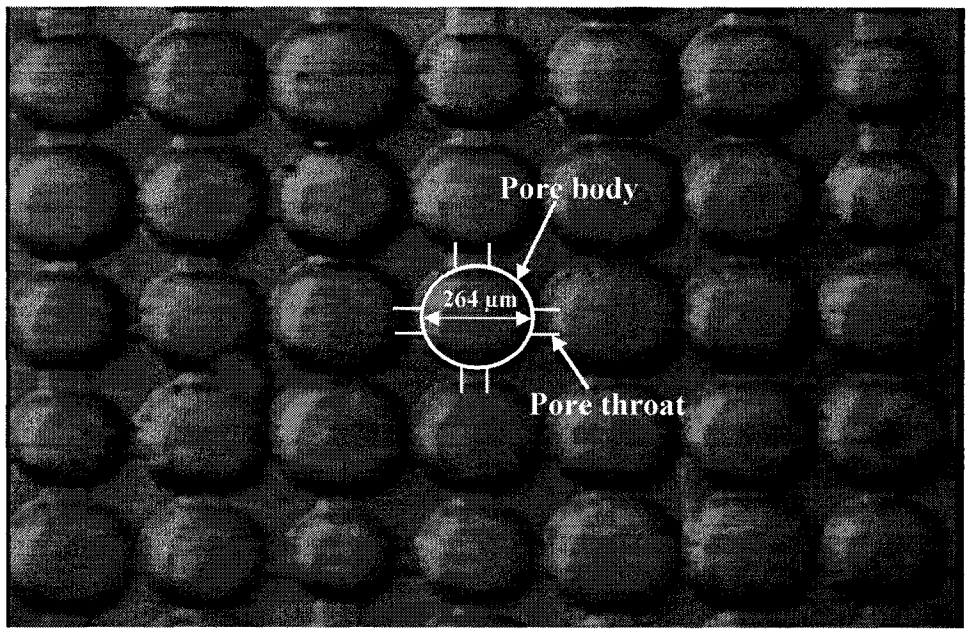

Figure 4.9 Magnified pore-throat network of etched glass micro-model

The emulsion was injected into the micro-model under variable flow rate conditions. Since the emulsion mean droplet size was smaller than the pore throat size by an order of magnitude, there was no sign of straining mechanism. All droplets passed through the pore throat network easily under high flow rate conditions. However, at low flow rates, droplets were deposited in the pore crevices and primarily captured on surfaces close to the pore throat entrances.

Figure 4.10 shows the interception mechanism at the early stages of the injection. Also, it was found that droplets may accumulate on top of each other, coagulate and thereby block the pore throats. Figure 4.11 illustrates such coagulation in the later stages of injection.

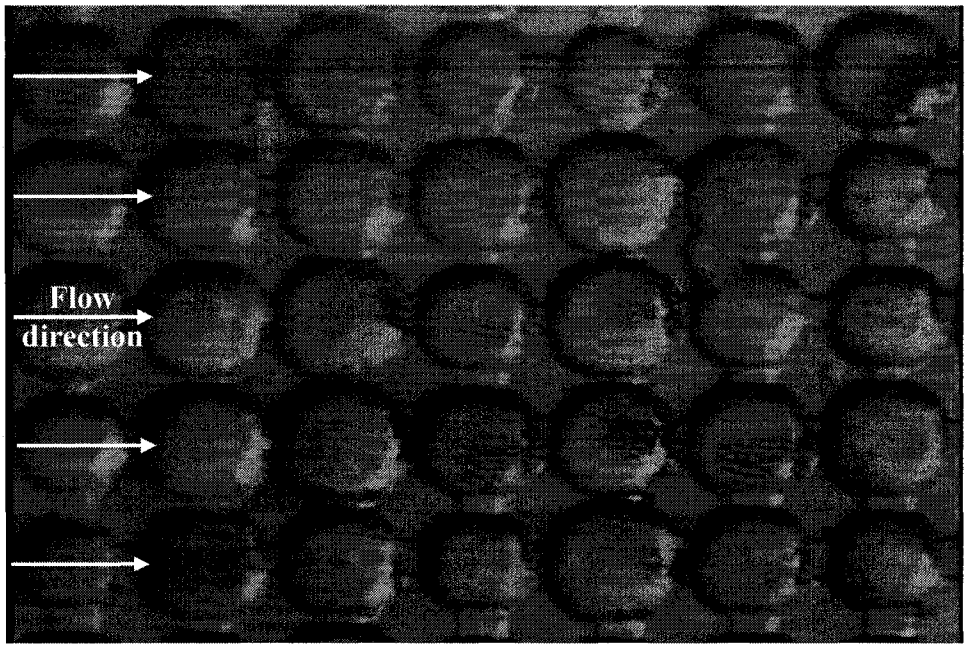

Figure 4.10 Droplets deposition on the pores surface at the early stage of injection

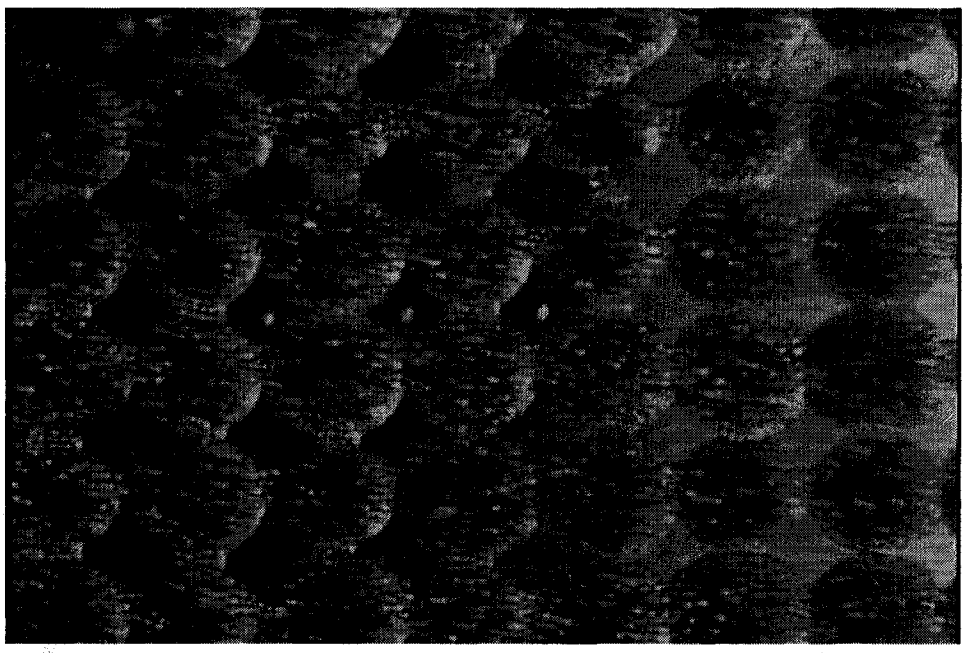

Figure 4.11 Droplets coagulation at the end of injection period

The pressure drop caused by injecting this emulsion was relatively low. Figure 4.12 shows an almost flat trend for the pressure gradient across the micro-model for the injection flow rate of 3 cm^3/min.

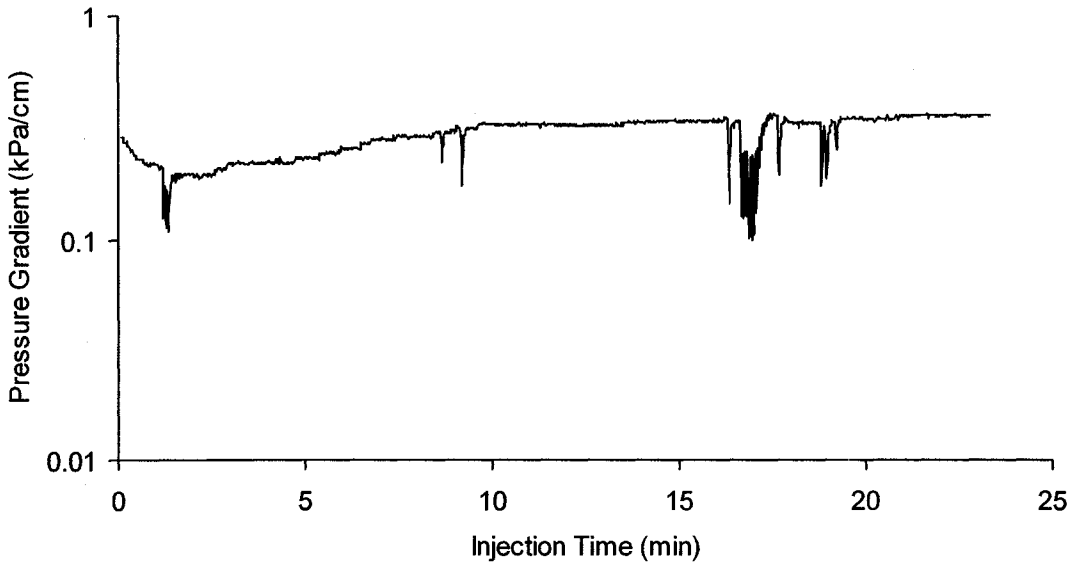

Figure 4.12 Pressure gradient for injecting emulsion M/W1

4.5.1.2 Coarse mineral oil-in-water emulsion

A coarse emulsion, M/W2, was prepared manually from dyed mineral oil and distilled water. The phase ratio was 5% oil and 95% water with a surfactant concentration of 0.12% (volume/volume), corresponding to 0.13 grams of surfactant in 100 cm^3 of water (0.13% weight/volume). Its mean droplet size was measured to be 200 μm. The droplet size distribution is presented in Appendix C.

When this coarse emulsion was injected into the micro-model, most of the droplets were strained into the pore throats which had a smaller diameter compared to the droplets' sizes. Figure 4.13 illustrates the droplets that were filtered out of the continuous phase as they percolated into the downstream pores.

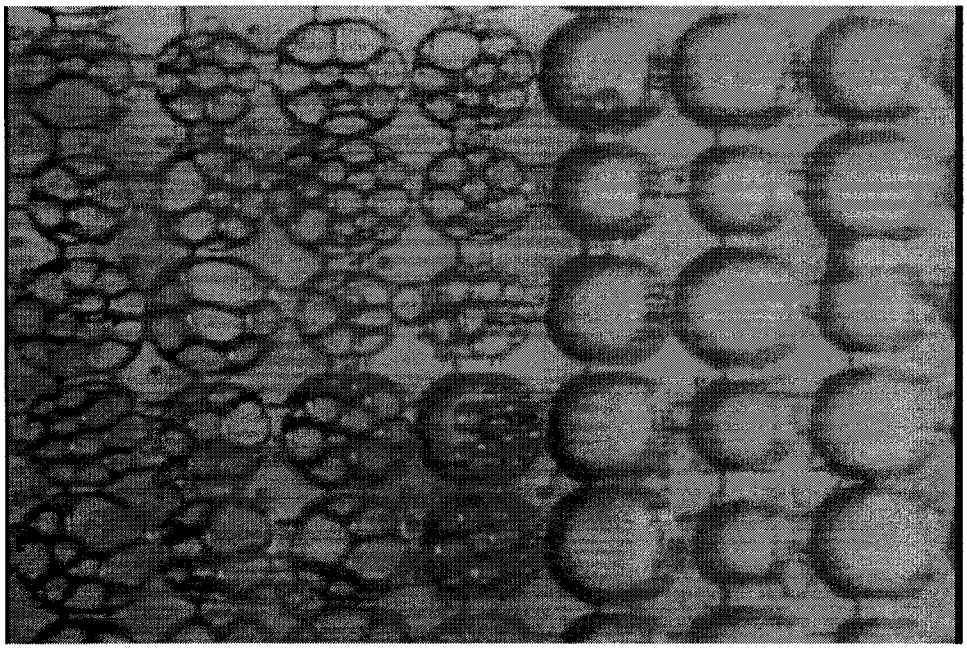

Figure 4.13 Droplets strained into pore throats due to size exclusion

As the emulsion injection continued, more droplets were lodged into the pore entrances. Once the total volume of a pore was occupied by the maximum allowable droplets, they were pushed through the pore throats into the next pores by the incoming injected droplets. This process continued until all capture sites were occupied and the pores filled in series. Meanwhile, the injection pressure built up as more droplets snapped off into the downstream pores.

Figures 4.14 through 4.16 illustrate the process for a strained droplet moving from one pore to another. The emulsion was distributed evenly at the point of injection through a relatively wide channel, perpendicular to the direction of flow. In addition, the emulsion front did not follow a piston-like shape -solid wall plane- although the emulsion was introduced into the entrance pores evenly. Cross-flow was observed and some pores were filled laterally.

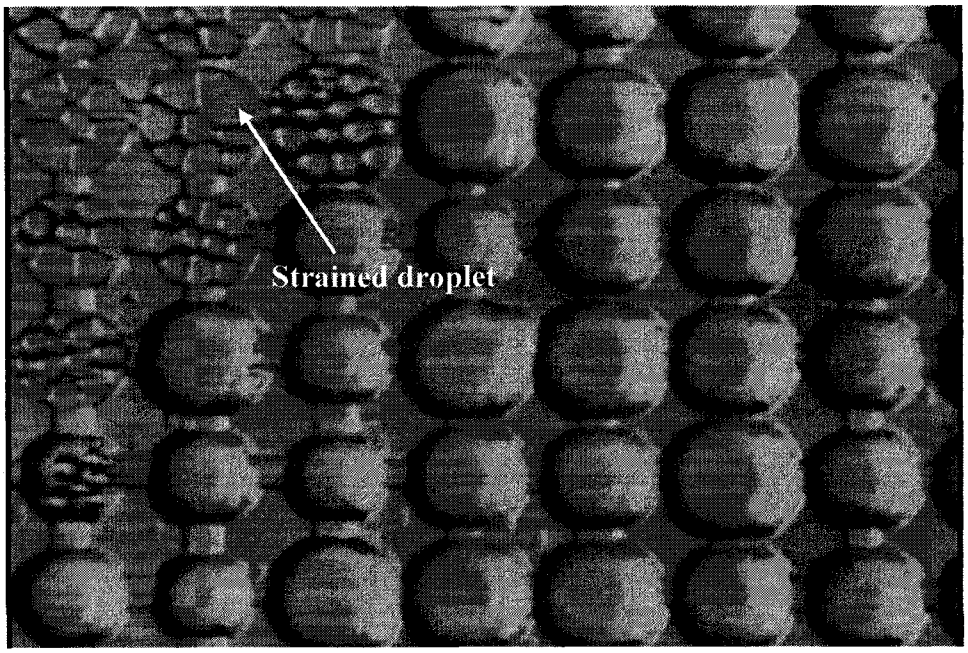

Figure 4.14 A droplet strained at the pore entrance due to size exclusion

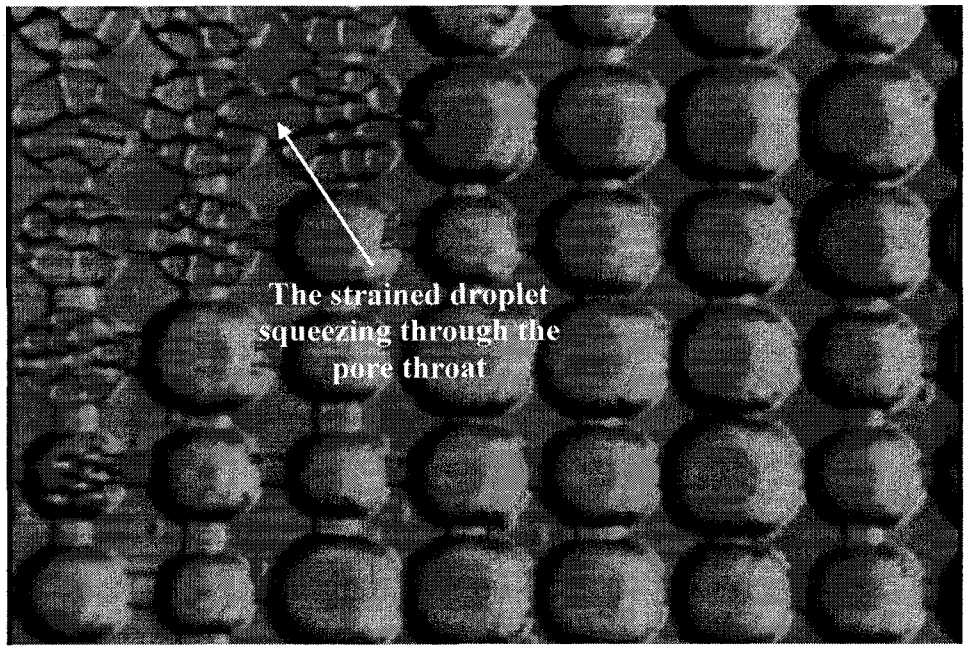

Figure 4.15 The strained droplet squeezing through the pore throat

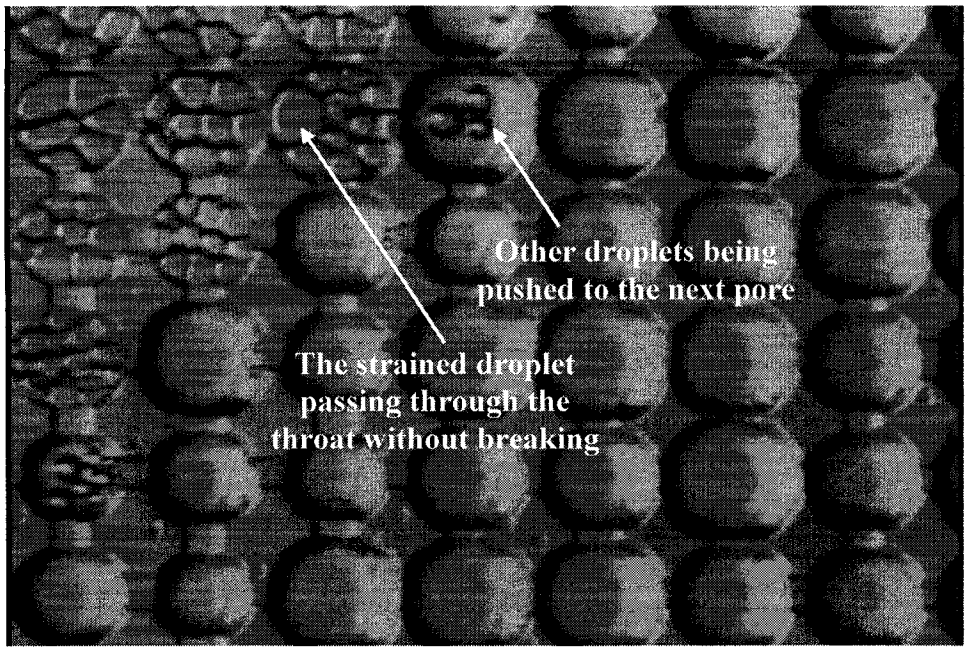

Figure 4.16 The strained droplet passing through the pore throat without breaking

Figure 4.17 indicates that the pressure gradient increased linearly as the pores were filled by droplets with a greater diameter than the pore throats. The pressure gradient trend then flattened, indicating that all pores were filled, and the injection pressure reached a steady state.

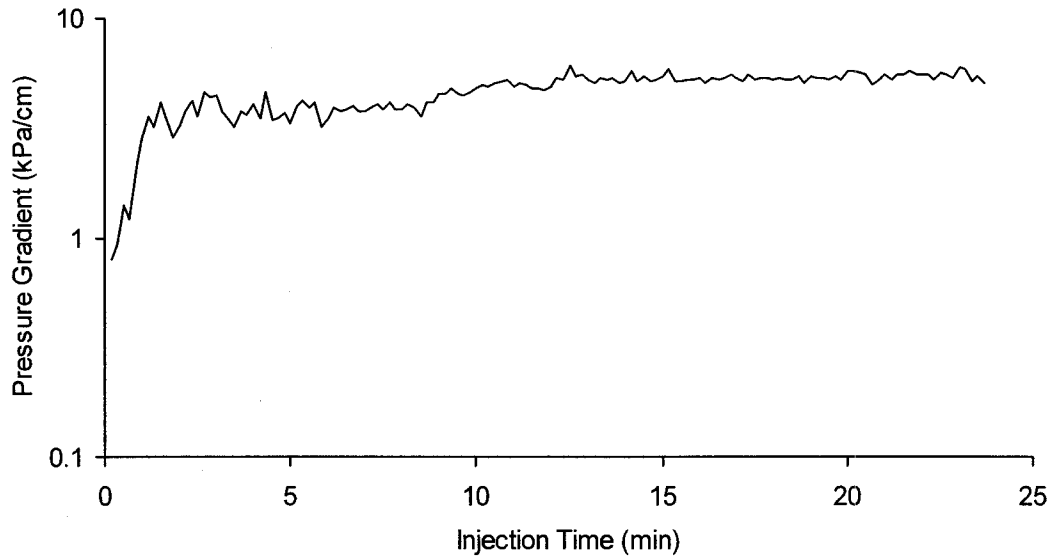

Figure 4.17 Pressure gradient for injecting emulsion M/W2

The emulsion droplets showed high stability. Figure 4.17 illustrates that the droplets were packed closely into a single pore without coalescing with one another.

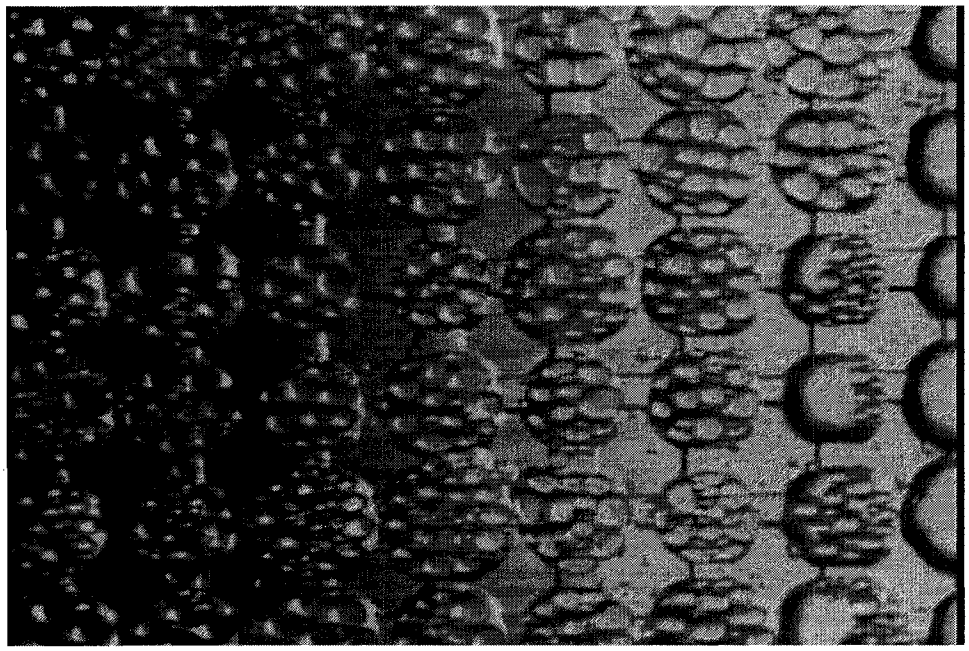

Figure 4.18 Highly stable droplets packed into pores without coalescence

4.5.1.3 Fine Lloydminster oil-in-water emulsion

This emulsion, LM/W1, is comprised of heavy Lloydminster oil and distilled water mixed with the homogenizer. It was impossible to mix the oil into the distilled water at room temperature because of its high viscosity. Therefore, the oil was warmed to 50°C and mixed into preheated distilled water. Different combinations of oil ratios and surfactant concentrations were examined, but only fine emulsions were produced. In an attempt to produce the desired emulsion with larger droplets, two extreme situations were observed in relation to emulsion stability and droplet size distribution. A relatively coarse emulsion was produced when low surfactant content was used in combination with a low applied shear mixing rate. However, the emulsion was not stable enough and the droplets either coalesced with each other immediately or adhered to the container's wall. A fine emulsion was prepared by increasing the surfactant content and the shear mixing rate. Since the transition from

a coarse to a fine emulsion occurs quickly and the range for surfactant content and shear mixing rate is so narrow, it became nearly impossible to produce a coarse Lloydminster O/W emulsion with a droplet size over 25 μm. Therefore, only fine emulsions were examined in this section.

The phase ratio for emulsion LM/W1 was 5% oil and 95% water with a surfactant concentration of 0.12% (volume/volume). Its mean droplet size was 21 μm. The droplet size distribution is given in Appendix C.

Emulsion LM/W1, which carried more viscous droplets compared to the previous two, revealed a relatively different behavior during its injection. These highly viscous droplets were deposited in the pore crevices and captured mainly on the pore surfaces, close to the pore throat entrances. The droplets were deposited because of gravity and the net charge of the forces between the surfaces of the pore bodies and the oil droplets. Figure 4.19 displays the attachment of the droplets on the pore surface and their coalescence.

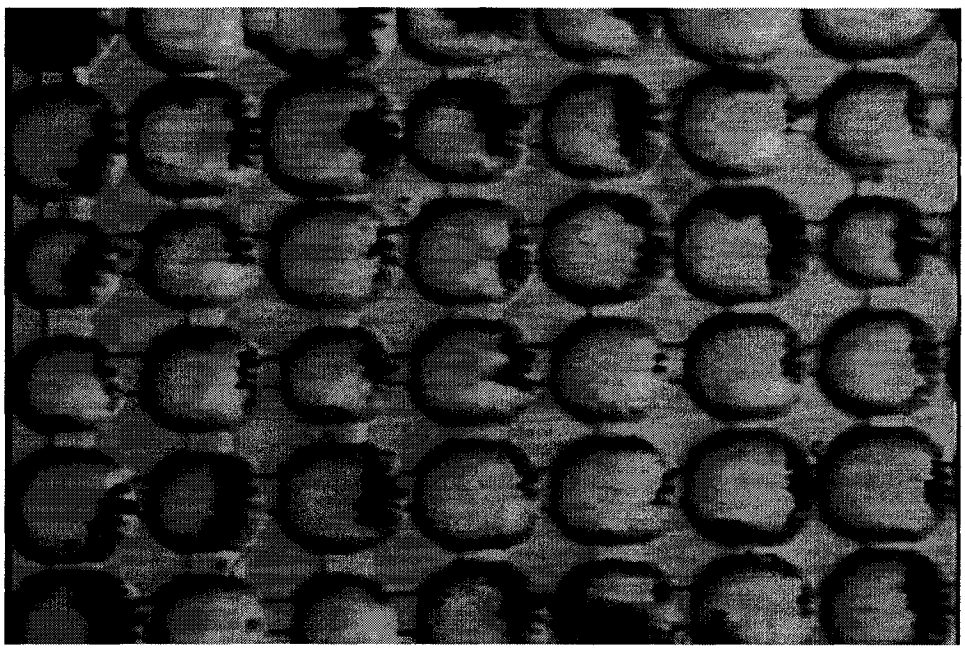

Figure 4.19 Heavy oil droplets attached to pores' surface and their coalescence

Furthermore, droplets that accumulated on top of each other coalesced and produced larger immobile droplets. It seemed that these highly viscous oil droplets were attached to the pore surface strongly enough that they were able to resist the local shear forces and block the pores completely. Although most of the pores were blocked, few other pores were filled partially in series and created a micro-channel flow path. As a result, they facilitated the passage of the injected emulsion to the other end of the micro-model.

Figure 4.20 shows the blocked pores magnified to 325 times their actual size. Also, Figure 4.21 displays a broader region of the blocked pores magnified to 162.5 times their actual size.

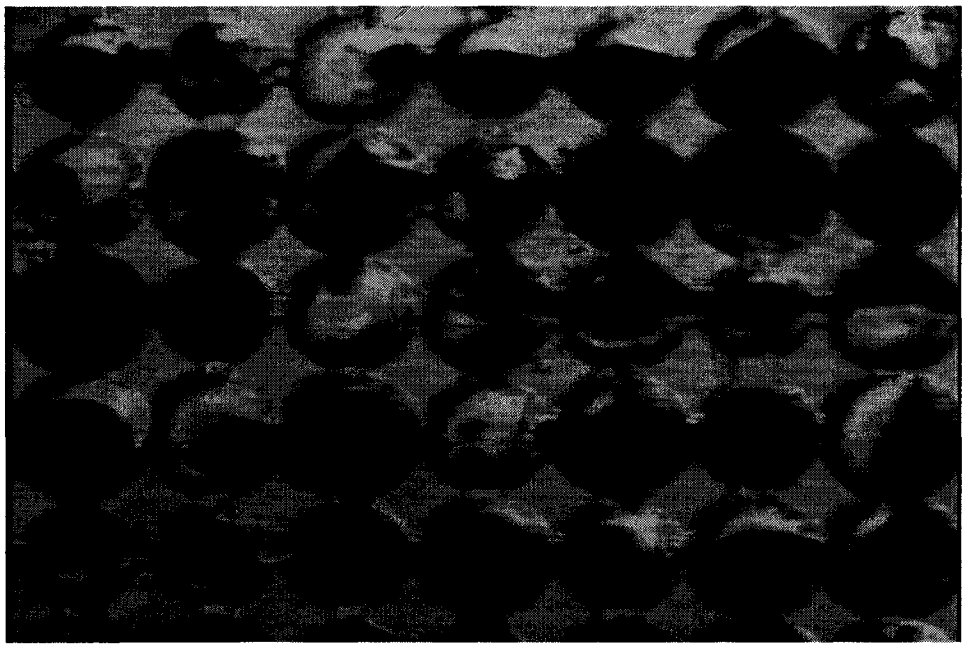

Figure 4.20 Pores filled with coalesced droplets

The pressure profile for this experiment (Figure 4.22) demonstrates that an emulsion, which carried more viscous oil droplets, may resist higher pressures. In addition, the figure indicates that the pressure gradient increased sharply as the pores were filling up with the coalesced droplets. The pressure gradient then reached a

plateau, indicating that the incoming droplets were passing through the micro-channels without blocking them.

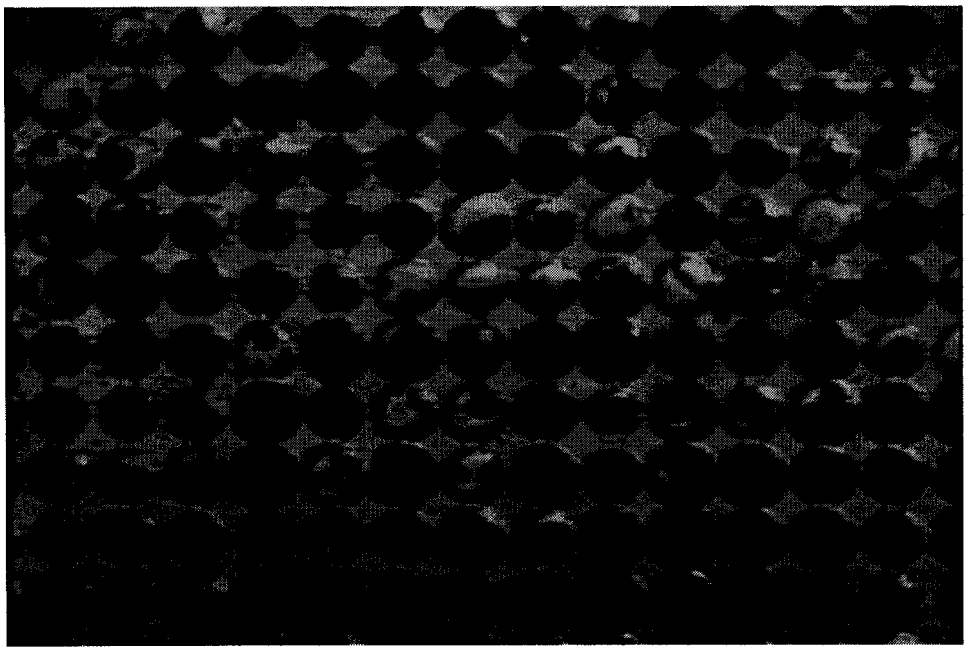

Figure 4.21 Zigzag channel at the centre pores facilitated the passage of droplets

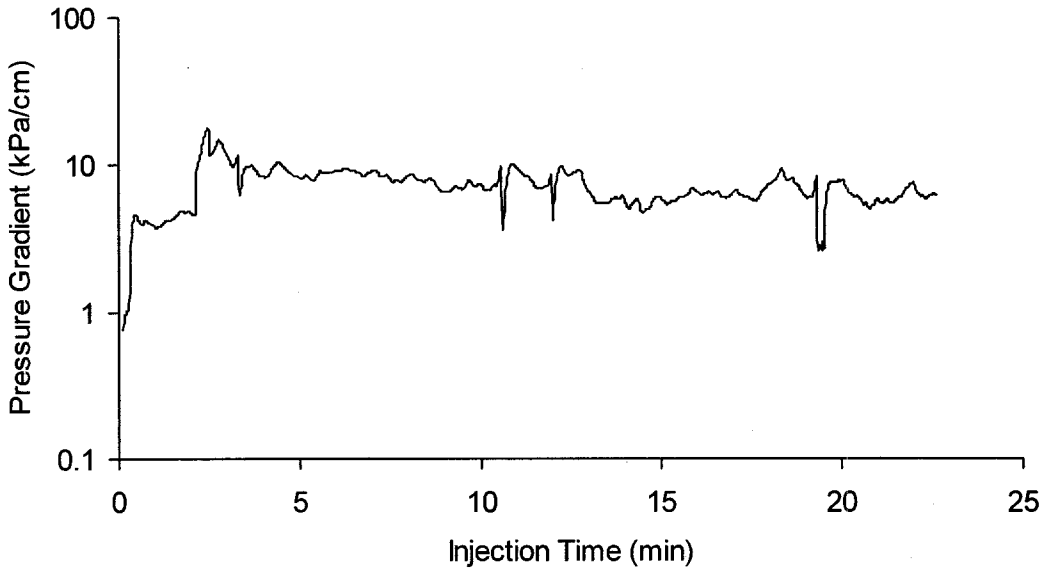

Figure 4.22 Pressure gradient for injecting emulsion LM/W1

4.5.2 Effects of Pre-flush on Wettability and Droplets Stability

Four experiments were conducted to evaluate the effect of different pre-flush solutions on local capillary pressure, which is a function of porous medium wettability and droplet sizes. For the purpose of comparison, all experiments were conducted under identical injection times and flow rates. The injection pressure and the emulsion frontal position were monitored for the duration of each experiment.

4.5.2.1 Base case: Emulsion injection

In this base case experiment, a mineral oil-in-water emulsion (M/W3) with a 13% quality (i.e. 13% oil ratio, volume/volume) and 0.12% surfactant concentration (volume/volume) was injected into the etched glass micro-model. Its mean droplet size was measured to be 225 μm. The droplet size distribution for this emulsion is given in Appendix C.

First, the micro-model was flushed with distilled water and the emulsion injection proceeded at 3 cm^3/min. The droplets equal or smaller in diameter than that of the pore throats passed through toward the downstream pores. However, the larger droplets lodged into the pore throats, which resulted in an injection pressure buildup. These strained droplets also blocked the passage for the incoming droplets, regardless of their size. As the injection continued, more droplets were filtered out of the continuous phase. At the same time, while the pressure increased, the smaller droplets passed between the larger droplets.

The process was then followed by snapping off the larger droplets to the next pores. Since the droplets were larger than the pore throats by an order of magnitude, only sixteen rows of pores were filled after 90 minutes of injection time. The observation was similar to the one presented in Section 4.5.1.2. Figure 4.23 illustrates the emulsion frontal position per number of filled pores. Additionally, Figure 4.24 shows the pressure gradient profile for this experiment.

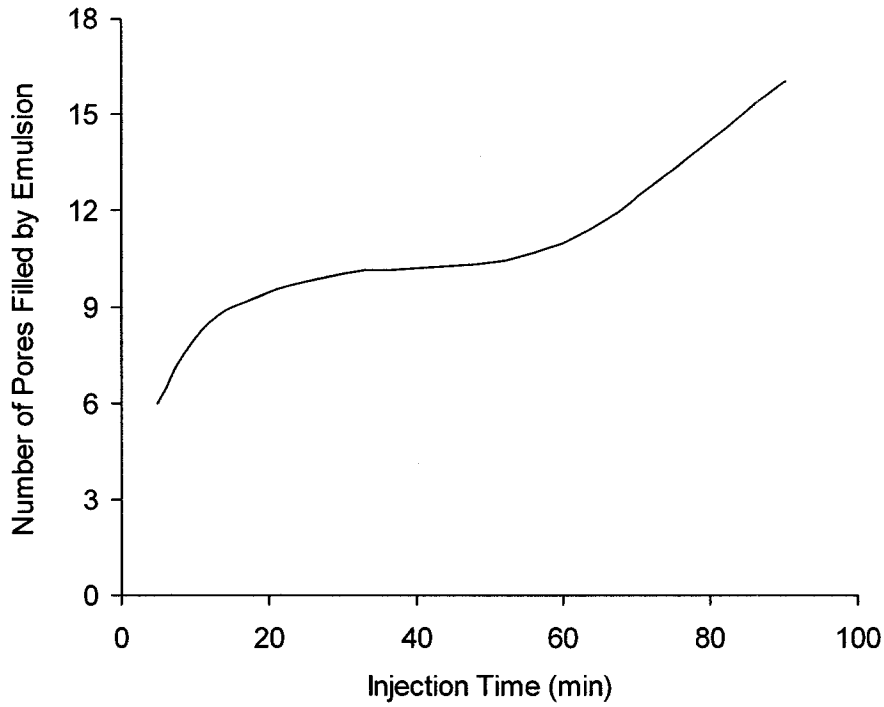

Figure 4.23 Emulsion M/W3 frontal advancement per number of filled pores

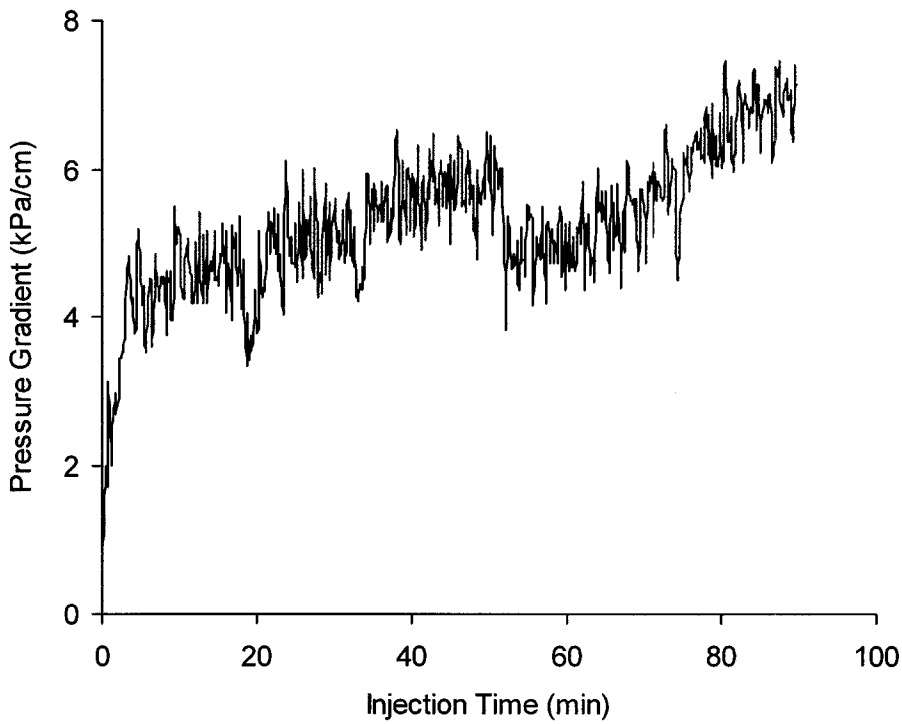

Figure 4.24 Pressure gradient for injecting emulsion M/W3

4.5.2.2 Acidic pre-flush

In this experiment the micro-model was flushed with two pore volumes of acidic solution and two pore volumes of deionized water prior to the emulsion injection. The acidic pre-flush solution was a diluted HCl solution. Its pH was maintained at approximately four to avoid corrosion problems with the equipment. The micro-model then was flushed with two pore volumes of deionized water prior to the injection of emulsion in order to minimize the effect of pre-flush conditioner on the stability of injected oil droplets. Injection of same emulsion (i.e. M/W3) at the same flow rate (3 cm^3/min) was followed.

It was observed that the acidic pre-flush caused some droplets to coalesce and produce larger droplets. Therefore, a higher injection pressure was required to pass these large droplets through the pore throats. Figure 4.25 displays the droplet coalescence at the front section of the etched glass micro-model.

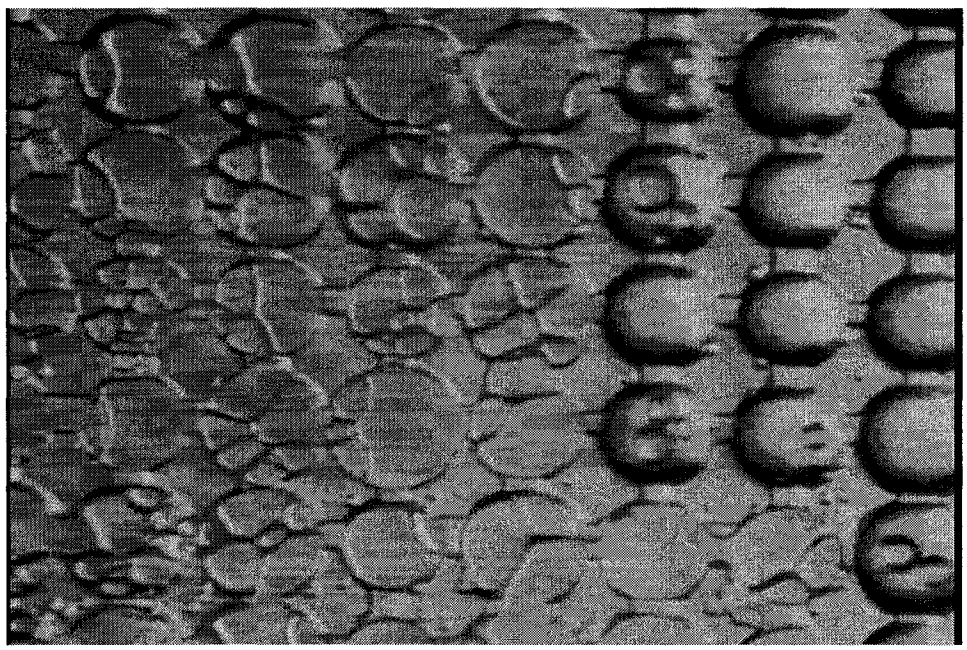

Figure 4.25 Droplets coalescence due to applying acidic pre-flush

Figure 4.26 indicates that the pressure gradient increased steadily at the beginning of the injection and was nearly 50% higher than the base case pressure gradient (Figure 4.27) for the first five minutes.

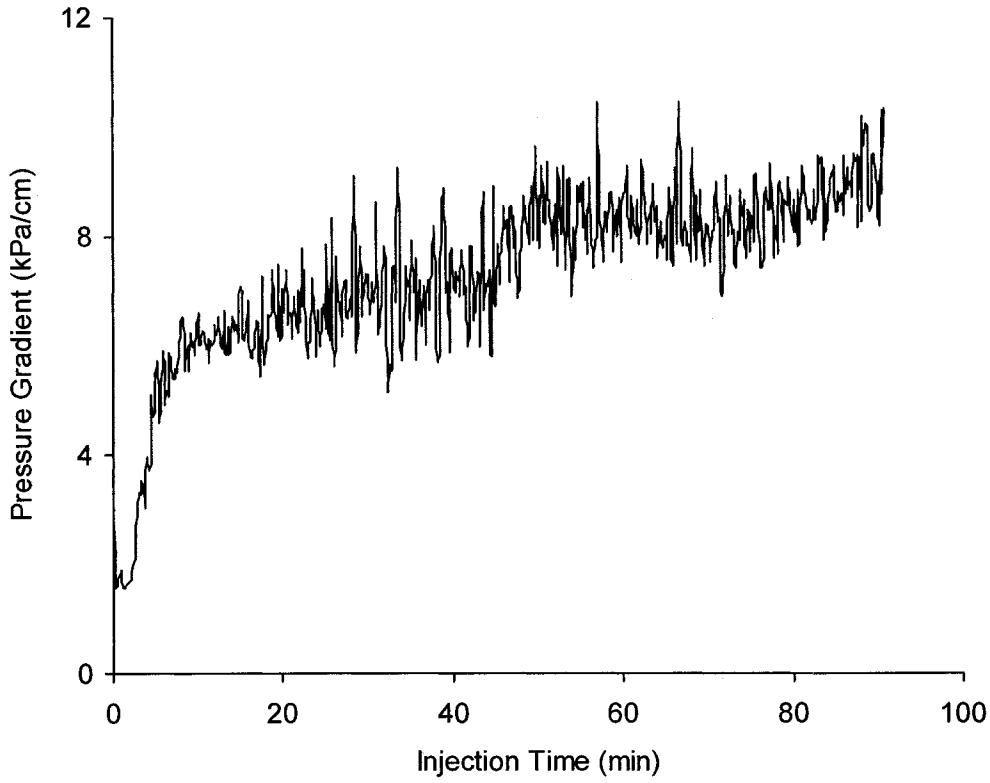

Figure 4.26 Pressure gradient for injecting emulsion M/W3 after acidic pre-flush

In addition, the coalescence of the droplets continued while they were percolating through the porous medium, which resulted in production of oil ganglia. It appeared that the ganglia were squeezed through pore throats easier than the original parental droplets, which were smaller in size. Based on the observed phenomenon, this could be due to the destruction of the interfacial film.

Figure 4.28 indicates that the emulsion frontal advancement into the micro-model was enhanced by 81% for an equal injection time; 29 rows of pores were filled in series for the acidic pre-flush case compared to 16 rows in the base case.

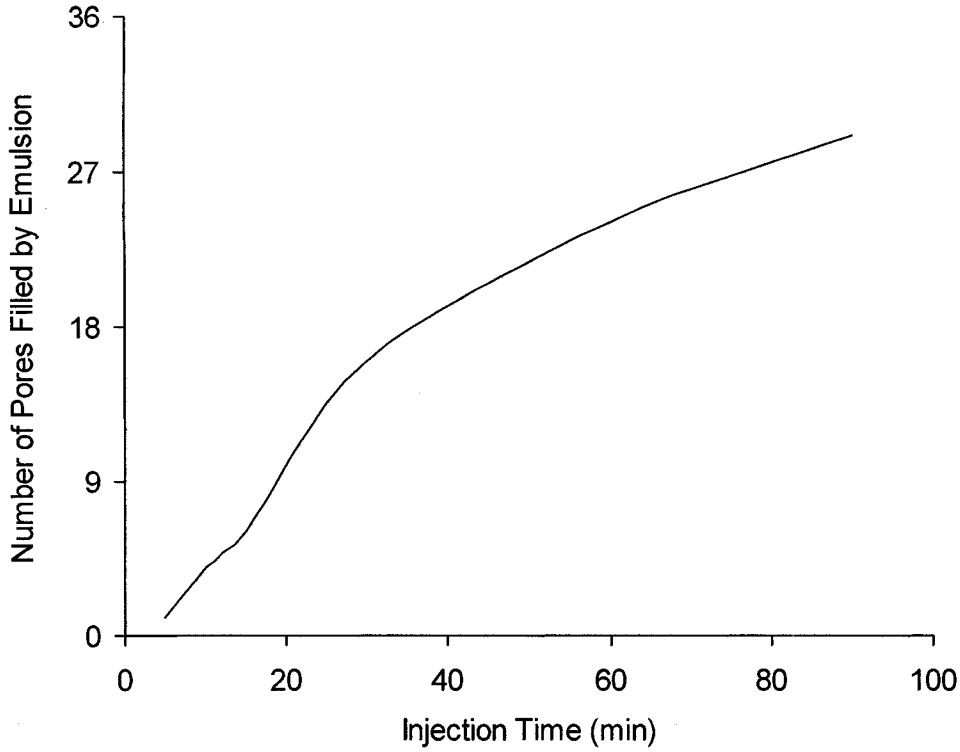

Figure 4.27 Number of pores filled by injecting emulsion M/W3 after acidic pre-flush

By applying the acidic pre-flush solution, the wettability shifted toward an oil-wet system. Although there was no direct method of measuring the wettability changes, the acidic pre-flush solution increased the oil droplets penetration depth by 80% compared to the base case. This contradicted our prediction since the pre-flush solutions affected not only the wettability but also the stability of the interfacial film.

4.5.2.3 Alkaline pre-flush

In this experiment, the micro-model was flushed with two pore volumes of alkaline solution and two pore volumes of deionized water prior to the emulsion injection. The alkaline pre-flush solution was a dilute aqueous sodium hydroxide solution. The solution was maintained at a pH of approximately 10 to avoid corrosion problems with the equipment. The pre-flush conditioner and removing its excess amount by

the deionized water was followed by the injection of the same emulsion (i.e. M/W3) at the same flow rate (3 cm^3/min).

In this case, we observed similar behavior to that of the base case experiment: the droplets equal or smaller in diameter than the pore throats passed through toward the downstream pores; the larger droplets lodged into the pore throats, which resulted in injection pressure buildup; and the strained droplets blocked the passage for the incoming droplets, regardless of their size.

Ordinarily, by applying an alkaline pre-flush solution, the wettability shifts toward a highly water-wet system, easily facilitating the passage of oil droplets into the pores. In addition, depending on the oil type and composition, the alkaline pre-flush solution could result in the generation of extra emulsifier agent upon contact with the oil droplets.

There was no direct method of measuring either the internal surfactant concentration or the wettability changes within the etched glass micro-model, and it was impossible to gauge the effect of pre-flush on these two factors since the droplets were larger than the pore throats by an order of magnitude. The alkaline pre-flush solution caused the droplets to retain their stability. However, it was clear that the droplets' surface was slightly disturbed, not smooth, as in the base case experiment. Visible roughness appeared on the surface of each droplet.

Figure 4.28 indicates that emulsion penetration depth per number of filled rows of pores was nearly identical to that in the base case after 90 minutes of injection time. Figure 4.29 illustrates that the rate of pressure build up for this experiment was lower at the early stages of the injection, and levels off at the end of the injection time like in the base case scenario (Figure 4.24). The later increase in pressure could be due to the consumption of the pre-flush solution that was present in the porous medium. This indicates that, if sufficient amounts of alkaline pre-flush are used, this

may reduce the injection pressure in order to deliver the emulsion to a particular depth.

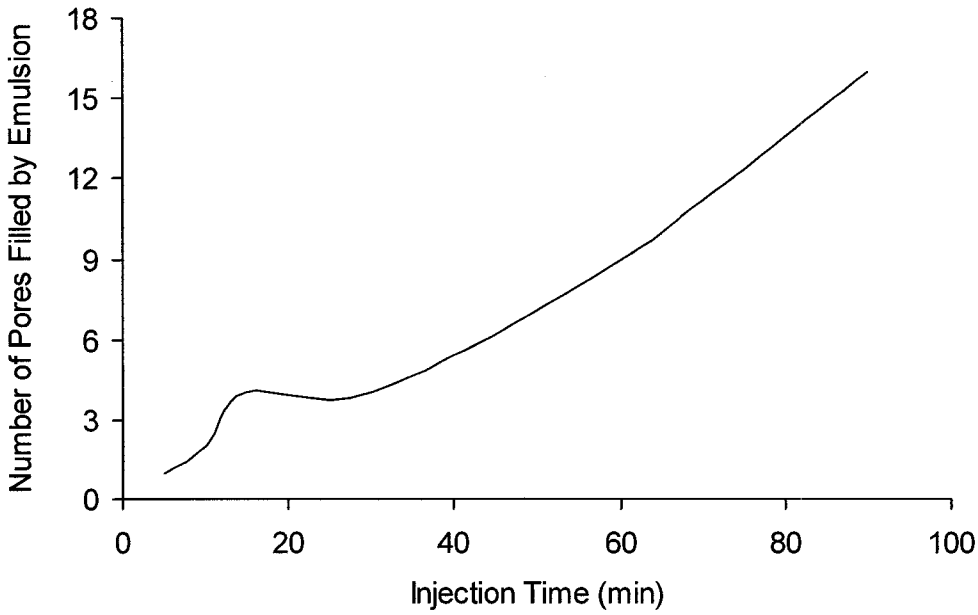

Figure 4.28 Number of filled pores for injecting emulsion M/W3 after alkaline pre-flush

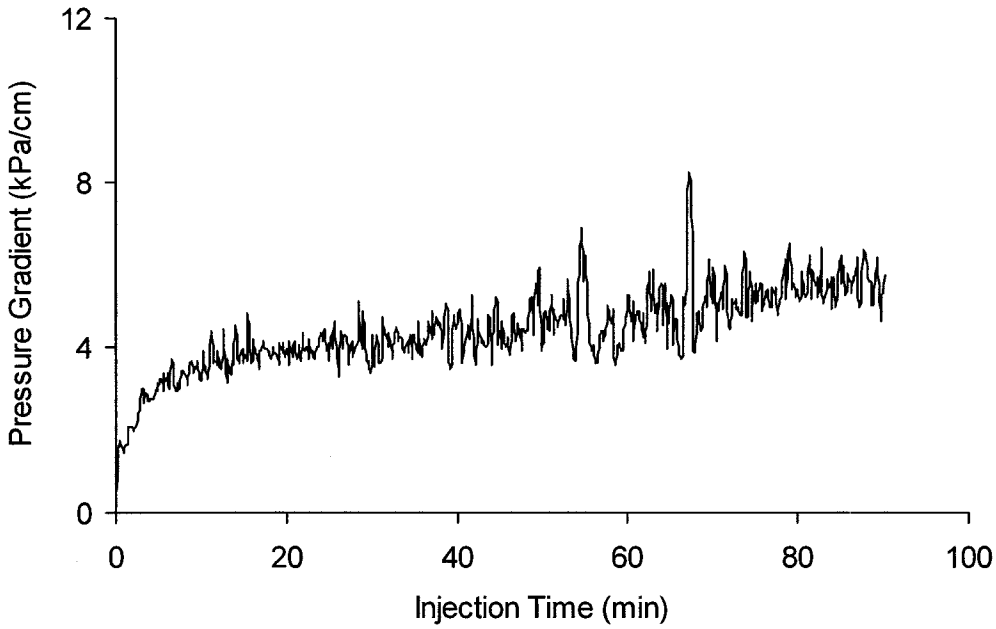

Figure 4.29 Pressure gradient for injecting emulsion M/W3 after alkaline pre-flush

4.5.2.4 Surfactant pre-flush

This experiment was initiated by conditioning the micro-model with excess amounts of surfactant pre-flush, made of TRITON X-100 surfactant and distilled water. Its surfactant concentration was 0.12% (volume/volume), which corresponds to 0.13 grams of surfactant in 100 cm^3 of water (0.13% weight/volume). The experimental procedure was identical to Sections 4.5.2.2 and 4.5.2.3 with the exception of having surfactant pre-flush instead of acidic and alkaline pre-flush solutions.

The oil droplets were squeezed through the pore throats and moved faster into the pore network. Droplets retained their size and shape without coalescing. In addition, their surface seemed smooth, and a sharp distinction between droplet interfaces was apparent even when they were packed too closely into a single pore. Figure 4.30 illustrates that the number of occupied pores per unit length of the micro-model increased by 250% compared to the base case experiment, using the same injection interval.

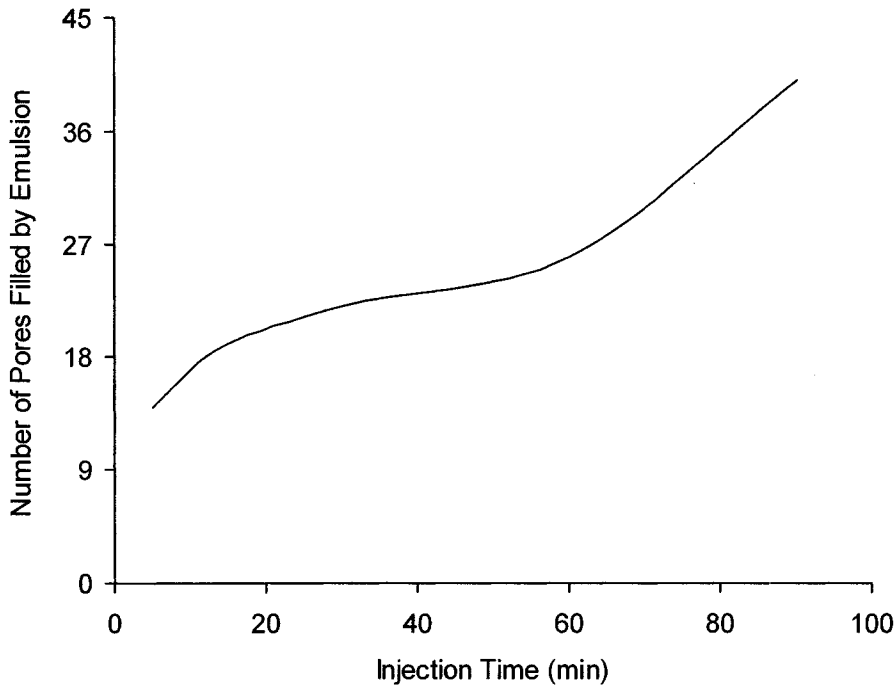

Figure 4.30 Number of filled pores for injecting emulsion M/W3 after surfactant pre-flush

Figure 4.31 illustrates the corresponding pressure gradient across the micro-model for this experiment. Specifically, it indicates that the pressure gradient almost tripled for the surfactant pre-flush case in comparison to the base case during the first 72 minutes of injection time, at which time a technical problem occurred resulting in drastically reduced injection pressure.

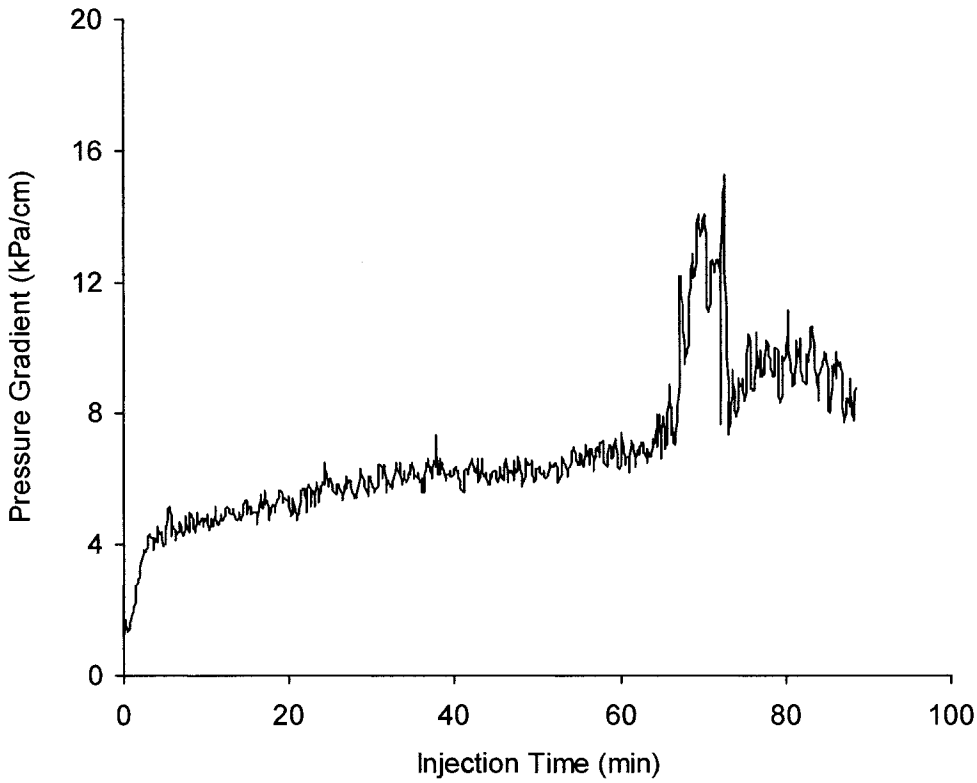

Figure 4.31 Pressure gradient for injecting emulsion M/W3 after surfactant pre-flush

4.5.3 Emulsion Breaking

Emulsion breaking may occur naturally or by means of external forces. The most important factors affecting emulsion stability are the surfactant type and concentration, salinity, solution pH and external applied shear forces. The effects of surfactant concentration and variable shear rates on stability of an emulsion were studied in the previous sections. This portion of the study investigates the effect of solution pH on the breaking of a highly stable emulsion. We observed the change in

solution pH and its effect on the stability of the droplets that were lodged and packed inside a porous medium. For this purpose, two experiments, including the injection of emulsion M/W3 into the etched glass micro-model, were conducted. The procedure for injection was similar to the experiment presented in Section 4.5.2.1.

In the first experiment, the emulsion injection was followed by the injection of one pore volume of alkaline solution (NaOH solution, pH = 11). The alkaline post-flush did not affect the stability of trapped droplets. In the second experiment, the emulsion injection was followed by the injection of one pore volume of acidic solution (HCL solution, pH = 3.5). The trapped droplets began coalescing shortly after the injection of the post-flush acidic solution. Figure 4.32 indicates that each coalesced droplet filled almost the entire volume of each pore. This observation could prove beneficial in predicting the breaking of highly-stable emulsions that are injected into a porous medium once the emulsion has reached the desired depth. If the emulsion is prepared with a highly-viscous oil, such breakage will create a stable plug that requires hundred of thousands of kPa/m to be mobilized.

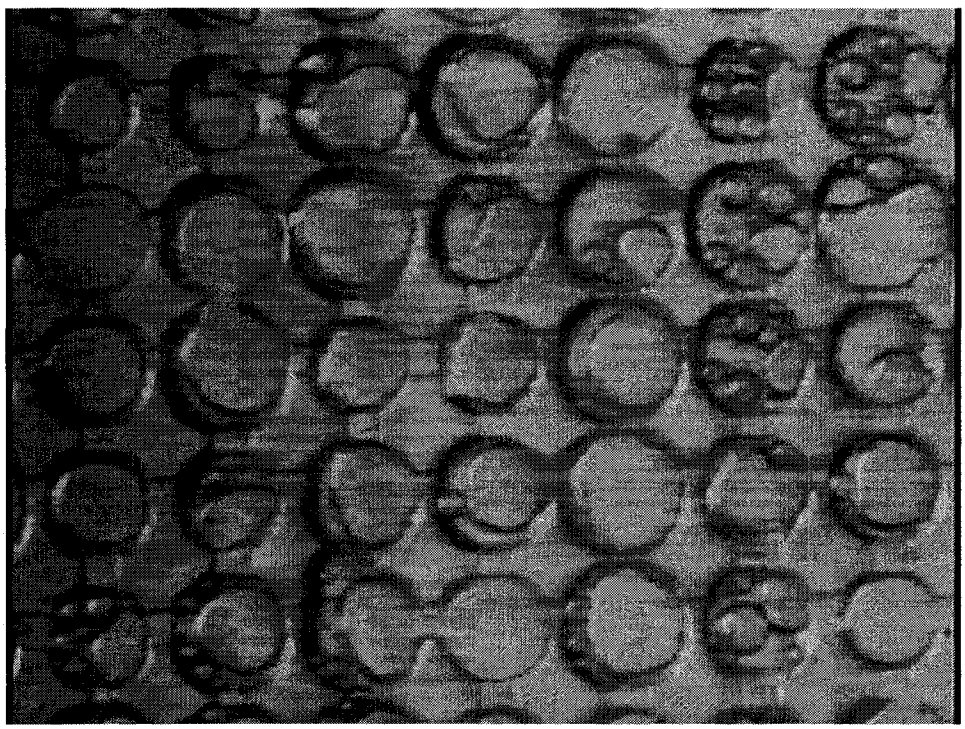

Figure 4.32 Strained droplets coalesced after injecting post-flush acidic solution

4.6 *Two-parallel Plate Micro-model Experiments*

In this part of the experiments, the two-parallel plate micro-model called "visual cell" was packed with Badger field sand with a narrow size between 100 and 120 mesh. The sand has a yellowish color, providing a good contrast when an emulsion flows through the packed medium. This range of grain sizes was the smallest possible size that could be magnified and still produce a sharp image with the available visualization system. For a dry-packed porous medium, even smaller grain sizes could be magnified reasonably with the current system. However, the sharpness of such images vanished as the medium was saturated with water. Moreover, the microscope was only focused on a small section of 2.4 mm^2, since the length and width of the visual cell was too broad for microscopic investigation.

4.6.1 Experimental Procedure

The experimental procedure was identical for all experiments. First, the visual cell was kept in a vertical position so that its exit port was at the top and the injection port was at the bottom. The sand grains were introduced in small portions from a packing port into the gap between the glass and the aluminum plate. The packing port was designed to be beside the flow exit port in order to facilitate full packing of the cell. The visual cell was shaken continuously and vibrated while the sand was introduced. Following this, the dry-packed porous medium was degassed by saturating it in a vertical position and under capillary imbibition forces for a few hours. Once the emulsion injection commenced, the droplets blocking mechanism, which includes the local droplets' trapping, coalescence, and squeezing through a single pore were monitored over time. Also, the overall pressure profile was recorded during the course of emulsion injection. The effect of different oil types and surfactant concentrations on the phenomenon of droplets capture was studied.

4.6.2 Fine Mineral Oil-in-water Emulsion

Mineral oil-in-water emulsion (M/W4), with a relatively high surfactant concentration (0.12%, volume/volume) and 13% quality, was injected under variable injection flow rates into the visual cell. The mean droplet size of this emulsion was 26 μm (details are presented in Appendix C). The droplet sizes were comparable with those of the pore body and throat sizes. Therefore, most of the droplets were captured by size exclusion (i.e. droplets sizes larger than the pore throat sizes). This resulted in an emulsion front that contained a high concentration of droplets. Recognition of the droplets within the highly-concentrated front was relatively impossible through image representation. However, the tip of the emulsion front contained fewer droplets. Figure 4.33 illustrates the droplets that were accumulated and squeezed through the pore throats under higher injection pressure, without coalescence regardless of the injection rate (velocity).

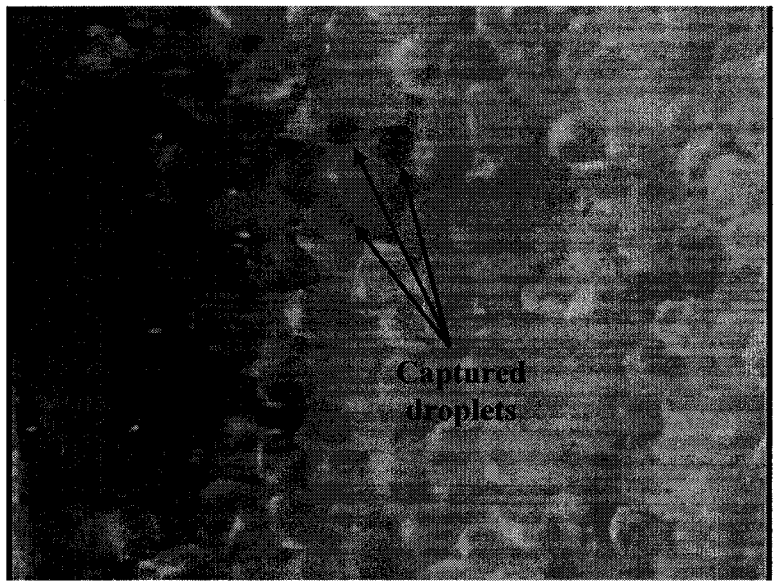

Figure 4.33 Droplets captured due to size exclusion

As the linear flow velocity increased, more droplets with higher penetration rates invaded the porous medium. For any increase in the flow velocity, the pressure gradient increased dramatically and the pressure response was quick (Figure 4.34).

The pressure gradient trend then increased steadily over time for a constant injection rate.

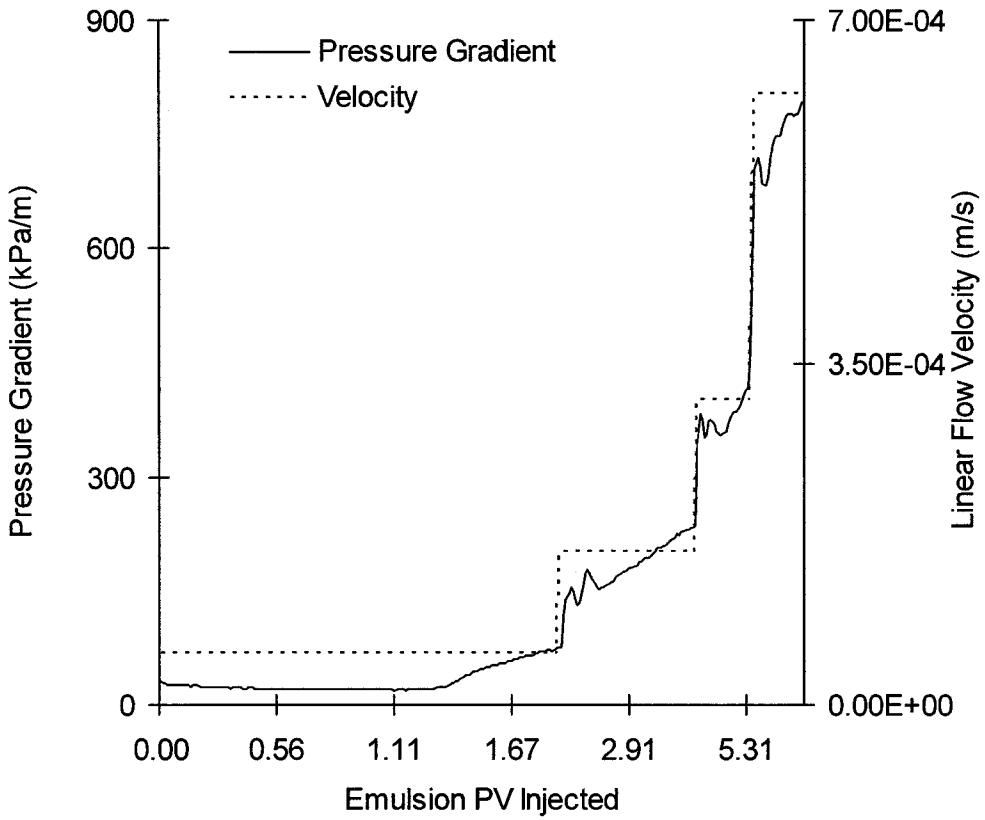

Figure 4.34 Pressure gradient and linear flow velocity profiles for injecting emulsion M/W4

4.6.3 Coarse Mineral Oil-in-water Emulsion

Mineral oil-in-water emulsion (M/W5), with a surfactant concentration of 0.01% (lower than the CMC which is 0.025%, volume/volume) and 13% quality, was injected under variable injection flow rates into the visual cell. The droplets' mean size was 72.2 μm, larger than the pore throats. The emulsion droplet size distribution is presented in Appendix C.

When the emulsion injection began, almost all of the droplets were captured by size exclusion. Also, they coalesced as they percolated into the porous medium. The coalescence of these droplets created an emulsion front that contained a high concentration of the dispersed phase. Although the droplet coalescence phenomenon was recognized during the experiment and throughout the video analysis, it was impossible to identify their interfaces through images. This could be partially because of the photographic quality.

In addition, the droplets that lodged into the pore throats accumulated within them and squeezed through the pore throats under higher injection pressure. The droplets may undergo deformation or in some instances break apart while being squeezed through the pore constrictions.

In addition, it was observed that a smaller number of droplets than expected percolated through the porous medium under higher injection velocity. It seemed that some droplets might have coalesced in the distribution channel rather than inside the porous medium. The other possibility could be a filtration of the incoming droplets in the injection line that was caused by the larger droplets at the sand face.

Figure 4.35 illustrates that the pressure gradient increased due to the sharp increase in the injection velocity. However, the pressure gradient trend for each injection rate period leveled off for the rest of the injection time aside from a few isolated spikes.

After injecting 4.85 pore volumes of the emulsion and with the flow rate increased to 9 cm^3/min (flow velocity of 0.000625 m/s) almost all of the droplets coalesced, resulting in a sharp pressure increase. The sudden increase in pressure occurred because of the generation of immobile oil ganglia as a consequence of dispersed oil droplets' coalescence. With further increase in the injection pressure the ganglia were mobilized downstream. Following this, the pressure gradient dropped to its original value before the coalescence of droplets was initiated.

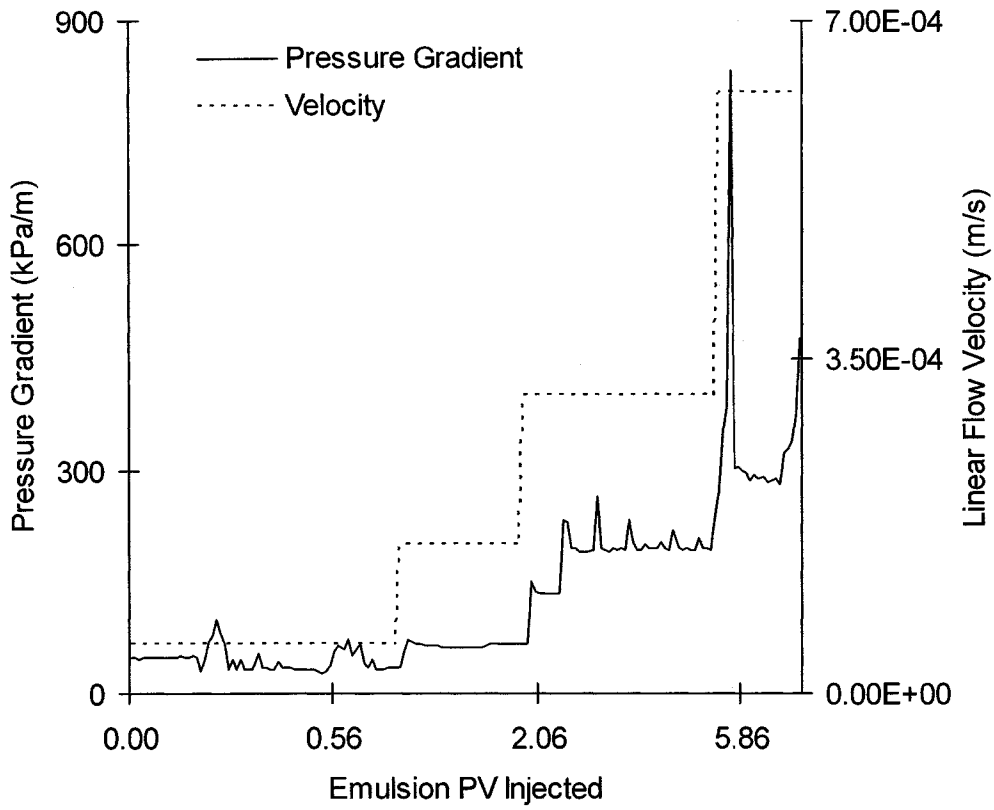

Figure 4.35 Pressure gradient and linear flow velocity profiles for injecting emulsion M/W5

4.6.4 Fine Western Canadian Oil-in-water Emulsion

A fine Western Canadian oil-in-water emulsion, WC/W1, was prepared by mixing the oil and distilled water. The emulsion had a relatively high surfactant concentration (0.12%, volume/volume) and 13% quality. Its mean droplet size was measured to be 15.9 μm. The detail of this droplet size distribution is presented in Appendix C. The droplet sizes were comparable with those of pore throat sizes. Since this emulsion carried black oil droplets it presented a contrast when injected into a porous medium. As the emulsion injection began, the majority of the droplets were captured in the pore throats due to size exclusion. Figure 4.36 shows the captured droplets at the beginning of emulsion injection. The incoming droplets were diverted to the other pores. They moved further inside the porous medium as if

they were of the same size or smaller than the pore throats. As emulsion injection continued, the number of captured droplets within the porous medium increased and the number of captured droplets decreased monotonically from the injection toward the production port.

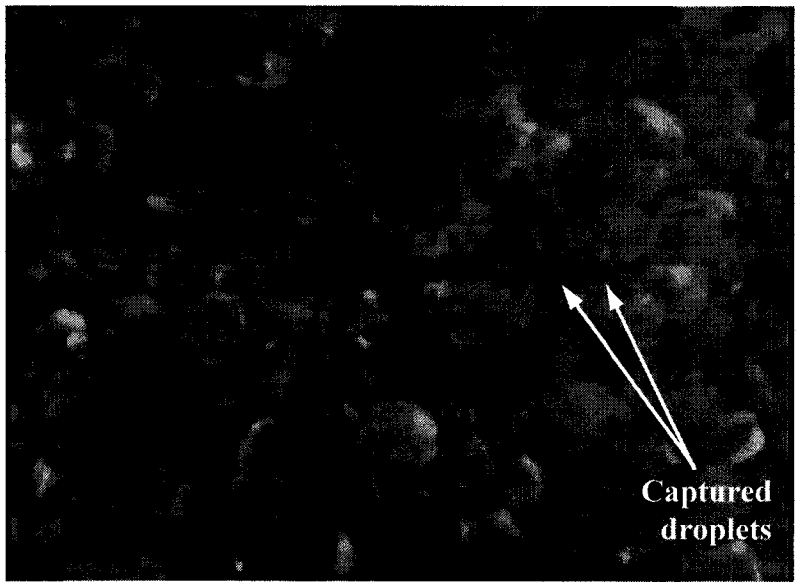

Figure 4.36 Black oil (WCO) droplets captured at the early stage of injecting emulsion WC/W1

While the pressure across the model built up, increasingly, more and more droplets were captured, with many of them sitting behind each other in series. Figure 4.37 illustrates droplets accumulating within the pores. This continued until the pores were completely full. The strained droplets resisted the pressure build up without coalescing with their neighbor droplets. They were pushed ahead and squeezed through the pores by the new injected droplets.

Figure 4.38 illustrates that the pressure gradient increased linearly as the emulsion was injected. Typically, the pressure gradient should level off after all capture sites are filled. However, the experiment ended after injecting only eight pore volumes of emulsion.

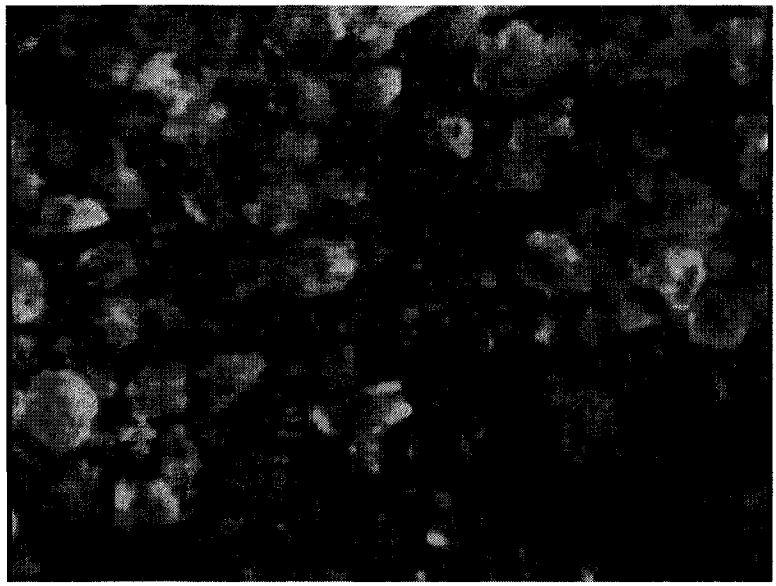

Figure 4.37 Accumulation of highly stable black oil (WCO) droplets at the late stage of injecting emulsion WC/W1

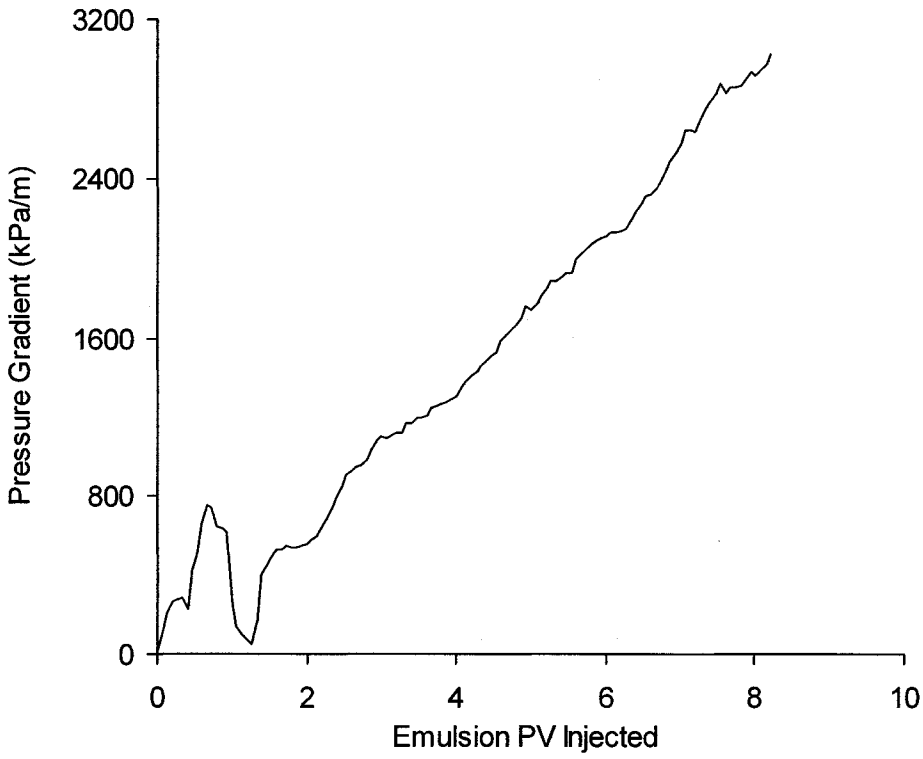

Figure 4.38 Pressure gradient for injecting emulsion WC/W1

4.6.5 Coarse Western Canadian Oil-in-water Emulsion

Western Canadian oil-in-water emulsion (WC/W2), with a relatively low surfactant concentration (0.025%, volume/volume) and 13% quality, was injected at a constant flow rate into the visual cell. The droplet sizes were comparable with those of the pore bodies but were larger in diameter than the pore throats. The mechanism of droplet capture was almost identical to the injection of emulsion M/W5. Almost all of the droplets were captured by size exclusion (Figure 4.39).

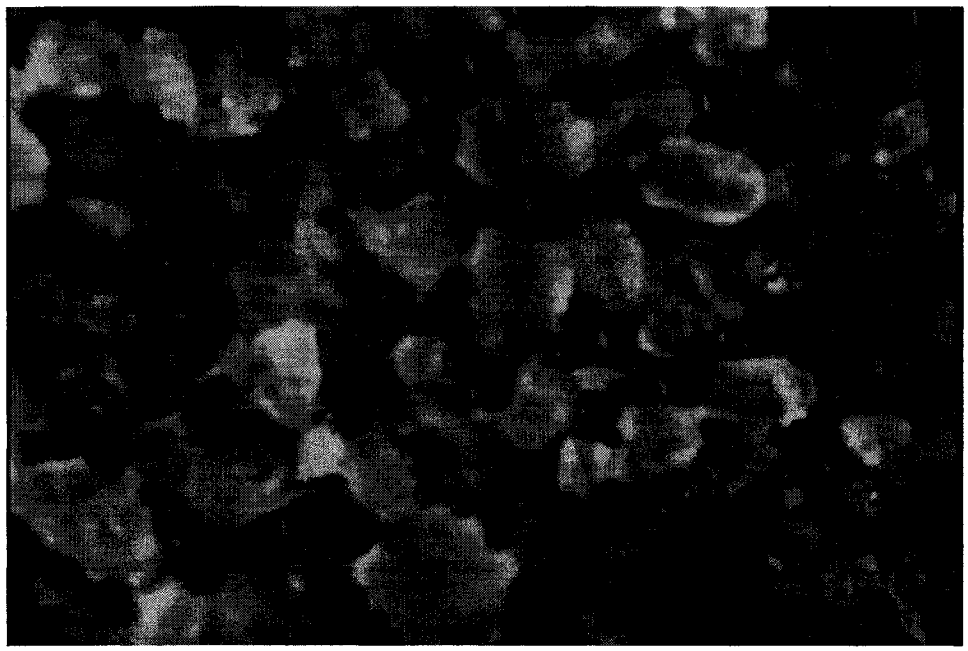

Figure 4.39 Black oil (WCO) droplets captured at the early stage of injecting emulsion WC/W2

With the increased pressure gradient across the cell, droplets were pushed closer together and partially coalesced. The coalesced droplets were squeezed further into the porous medium under even greater pressure.

In addition, the rate of droplet accumulation increased at the entrance of the visual cell. Figure 4.40 displays the pressure gradient increasing up to injecting four pore volumes of the emulsion. At this time a technical problem surfaced; the stirrer was not mixing the emulsion properly and the number of large droplets (mainly migrated

to the upper portion of the fluid due to buoyant force) entering into the pump's inlet reduced. The problem was resolved by injecting two pore volumes of emulsion, and the injection pressure started to increase afterwards. Pores at the entrance section became completely full and the strained droplets became severely clogged at the pore constrictions.

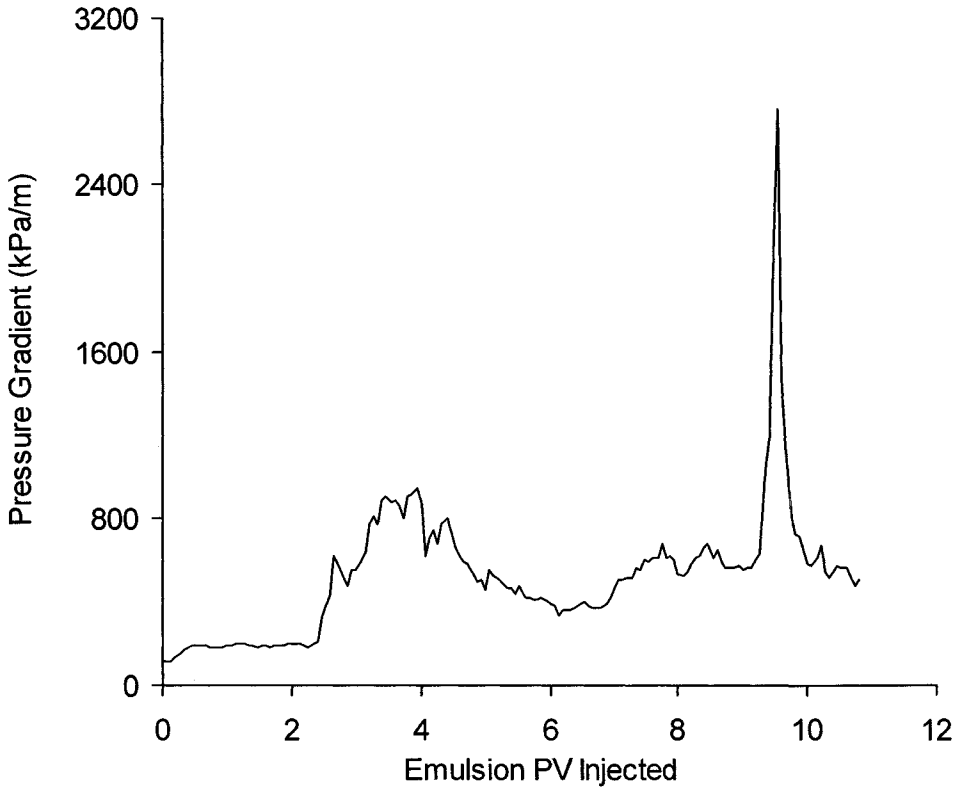

Figure 4.40 Pressure gradient for injecting emulsion WC/W2

As the emulsion injection continued, nearly all of the pores were filled. The rate of droplets coalescence increased after injecting nine pore volumes. This resulted in a sharp increase of the injection pressure.

Figure 4.41 indicates that these highly-packed droplets were pushed too close together, which resulted in the subsequent coalescence and production of highly-

viscous oil ganglia. At a pressure gradient of 2750 kPa/m, the ganglia were pushed further down into the porous medium, which resulted in sudden decrease of the injection pressure.

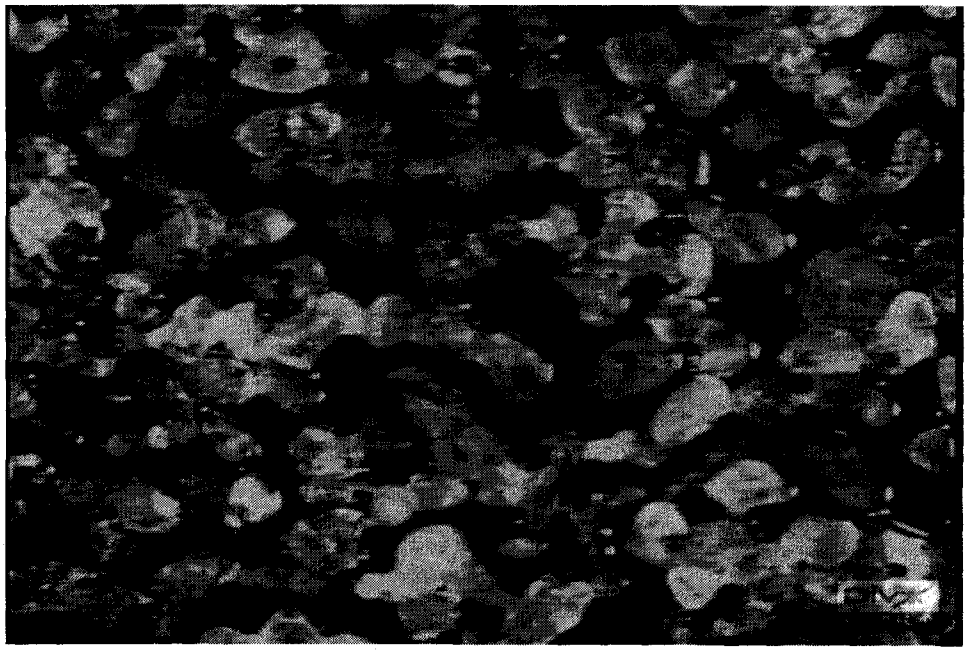

Figure 4.41 Droplets coalescence at the late stage of injecting emulsion WC/W2

Chapter 5. Macroscopic Emulsion Flow Behavior Experiments

Macro-scale investigations were conducted in order to observe the emulsion flow behavior through porous media. Factors affecting an emulsion propagation rate into a porous medium were evaluated, in particular the effect of stability and wettability on the blockage phenomenon.

The macro-scale experiments were conducted on the "visual cell", the two-parallel plate micro-model. It was packed with different glass beads, with each pack yielding a different permeability. In these experiments, we visually monitored an emulsion's frontal propagation rate, and noted the increase in injection pressure and the permeability reduction during the injection process. In essence, the effect of oil type, porous medium permeability, injection velocity, wettability alteration, and surfactant concentration were studied.

5.1 *Experimental Set-up*

Figure 5.1 is a photograph of the experimental setup. The experimental loop was similar to the one utilized for the micro-scale investigation (Chapter 4, Figure 4.1) with the following exceptions: the microscope was removed from the loop and an enlarging lens was mounted at the top of the CCD camera. The CCD camera was located at a distance of approximately 40 cm from the top of the visual cell, enabling a full view of the cell.

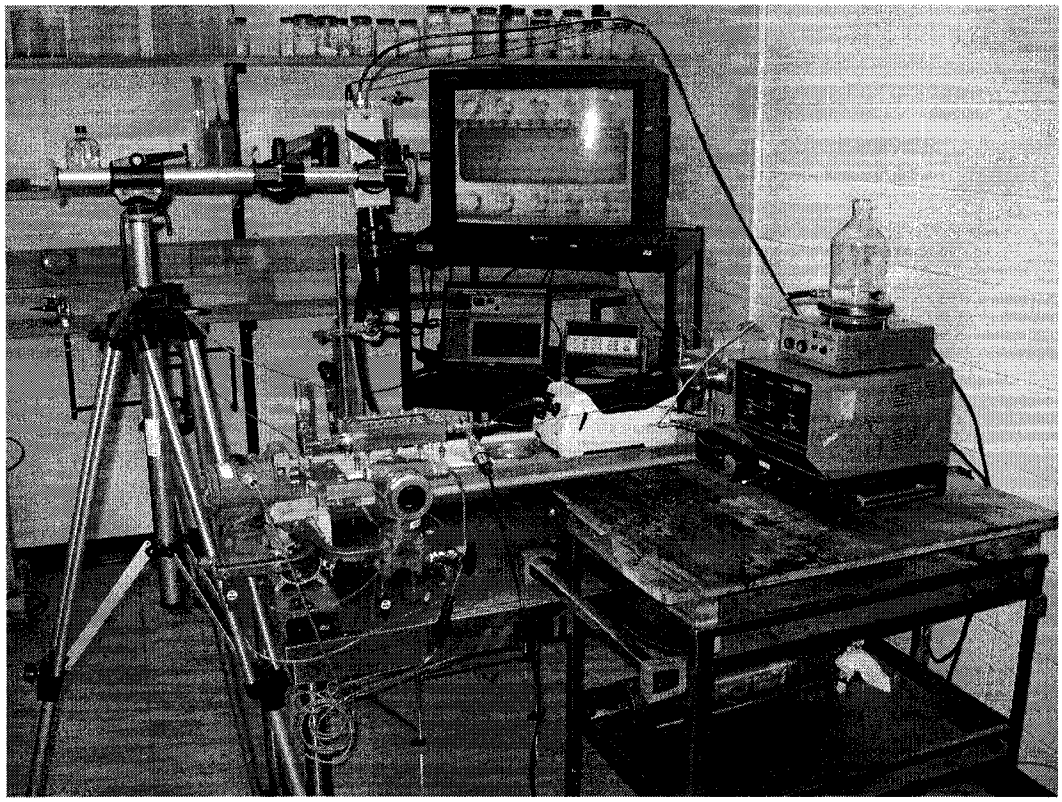

Figure 5.1 Experimental setup for macro-scale experiments

5.2 *Oil Type*

Two types of oil, mineral oil (MO) and Western Canadian oil (WCO) were used in this part of the experiments. The properties of the mineral oil are listed in Section 4.3. The WCO was supplied by the Alberta Research Council. Its viscosity was measured at two different temperatures by using the CSL-100 Rheometer. Figure 5.2 illustrates the viscosity of the Western Canadian oil at 20°C and 50°C.

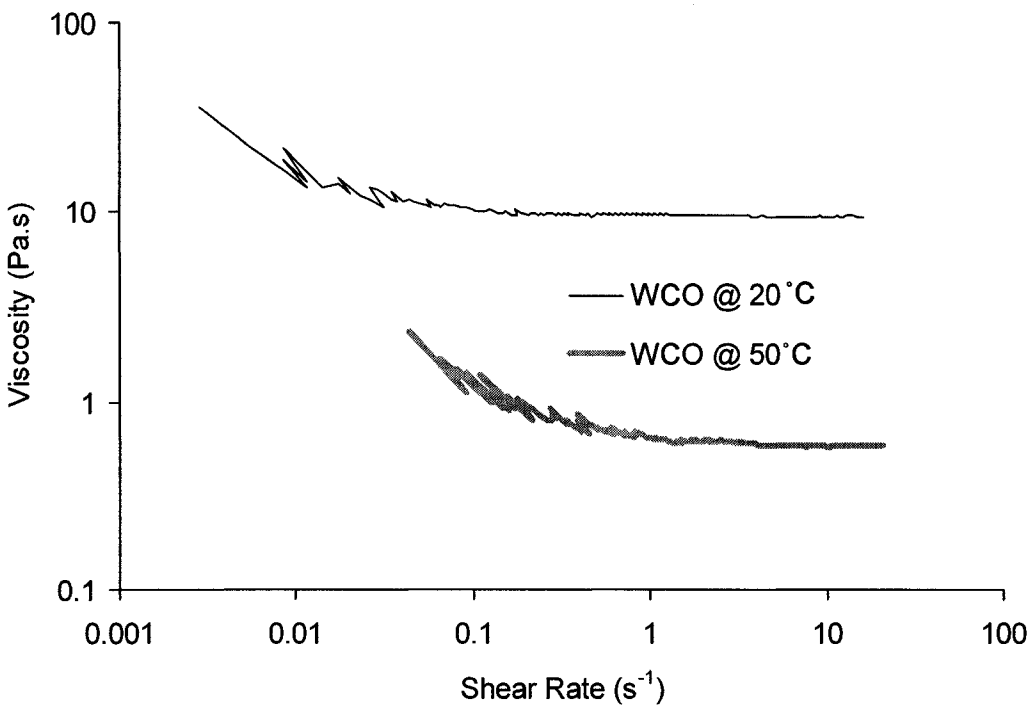

Figure 5.2 Viscosity of Western Canadian oil (WCO) at different temperatures

5.3 *Experimental Procedure*

The visual cell was packed with a mixture of fine, medium and coarse glass beads between 100 to 320 mesh, according to the procedure outlined in section 4.6.1. Table 5.1 lists the weight fractions of the glass beads size distribution constituting this medium.

Grain size (US Mesh)	Weight fraction (%)
d > 80	0.45
80-100	0.45
100-120	1.52
120-140	2.95
140-200	83.14
200-230	0.62
d < 230	10.87

Table 5.1 Weight fraction of the glass beads pack

The porous medium was saturated with distilled water, and its absolute permeability was determined at three different flow rates: 3, 6, and 9 cm^3/min. Depending on the size of glass beads used in packing the cell, each pack yielded differing permeabilities; all packed media had a porosity between 0.33 and 0.35. Even for a single porous medium pack, the local permeability varied slightly for each section of the cell. Therefore, the permeability was measured for the total length of the cell, its front and rear sections.

The desired emulsion was injected at a constant flow rate condition. The exit was opened to atmospheric pressure. Therefore, the injection pressure was measured by the absolute pressure transmitter and recorded as total differential pressure across the cell for assessing the reduction in the total permeability. Two differential pressure transmitters measured the pressure drop across different sections of the model during the experiment, to be used for assessing the front and rear sections' permeability reductions. Although the pump operated under a constant injection rate, the effluent was collected in a graduated cylinder in small time increments and the injection rate was reaffirmed. Meanwhile, the emulsion flow behavior through the porous medium was recorded and photographed continuously.

5.4 *General Observation on Emulsion Flow in Porous Media*

Mineral oil-in-water emulsion (M/W4) and Western Canadian oil-in-water emulsion (WC/W1) were injected into different glass bead packs. The purpose of this was to evaluate the flow behavior of these two emulsions from different perspectives. Each emulsion was made of two different oil types. The objective was to evaluate the frontal propagation rate, the corresponding pressure response and the permeability reduction for each type of emulsion. The reduction in permeability was assessed by water injection after the emulsion injection. Each experiment, which included the injection of M/W4 and WC/W1 emulsions separately, was conducted on the same packed porous medium. In addition, the injection rate was maintained constant at 3 cm^3/min for each of the experiments.

5.4.1 Frontal Advancement

The emulsion propagation rate was monitored during the injection in each set of experiments, using the same pack with sequences of injecting emulsion M/W4 first. Then the packed medium was cleaned by Isopropyl alcohol and five pore volumes of water. Injection of emulsion WC/W1 into the same pack was followed. Based on the observation made in Chapter 4, the mean droplet size was greater compared with the pore throat size for this porous medium.

At the moment the emulsion entered into the porous medium, some droplets, perhaps the larger ones, were filtered out of the continuous phase. These droplets distributed evenly across the flow path area and their accumulation resulted in a highly concentrated area. Other droplets being less in number, flowed ahead of this highly concentrated region. The emulsion front then proceeded into the porous medium in a way similar to that of a solid wall plane. Figures 5.3 and 5.4 depict the frontal advancement after the injection of 1.1 pore volumes of the emulsions M/W4 and WC/W1 into the porous medium.

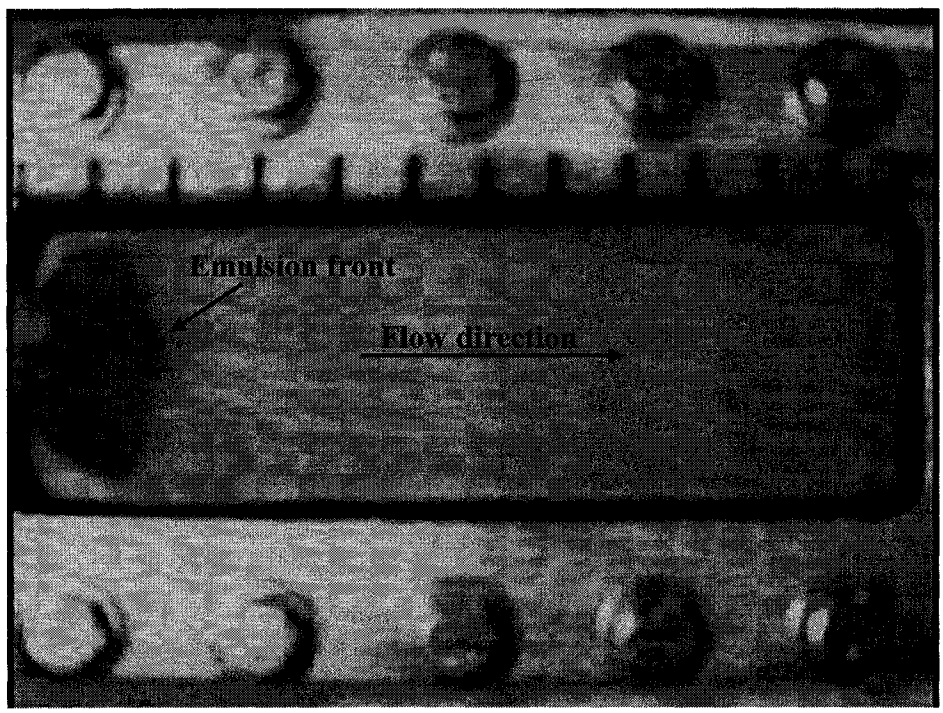

Figure 5.3 Front position after injection of 1.1 PV of emulsion M/W4

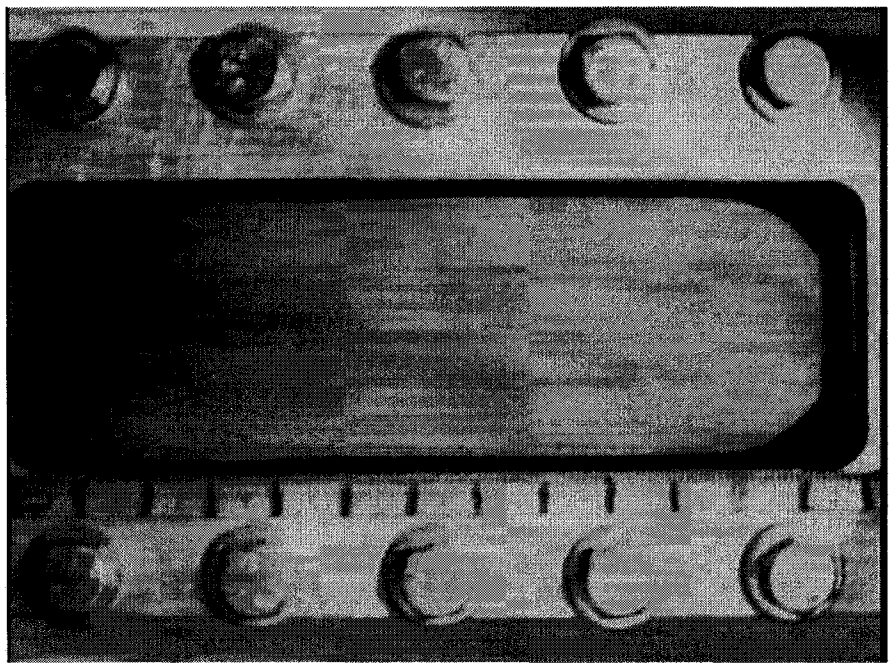

Figure 5.4 Front position after injection of 1.1 PV of emulsion WC/W1

Similarly, Figures 5.5 and 5.6 illustrate the frontal advancement after injection of 7.5 pore volumes of the emulsions M/W4 and WC/W1 into the porous medium.

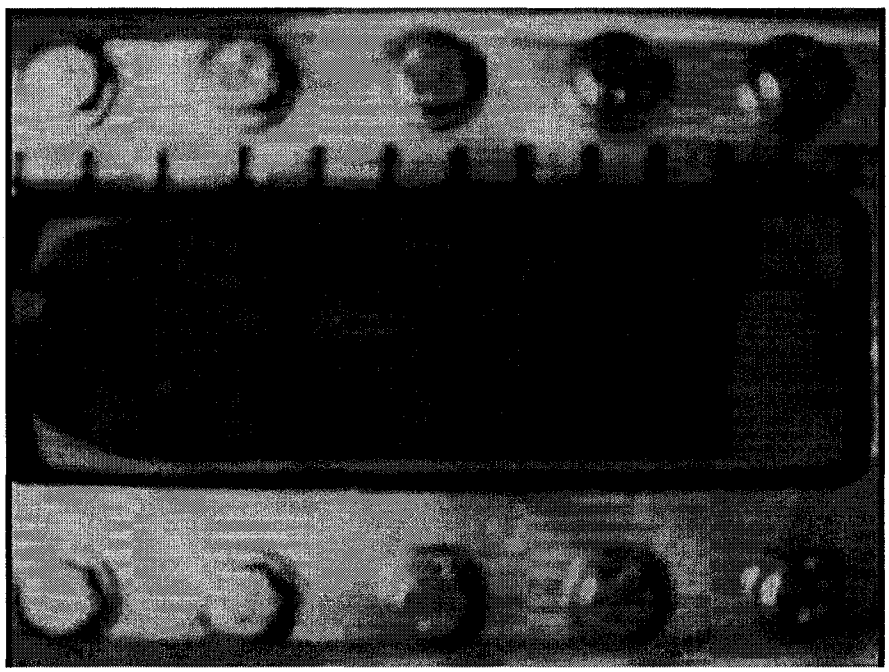

Figure 5.5 Front position after injection of 7.5 PV of emulsion M/W4

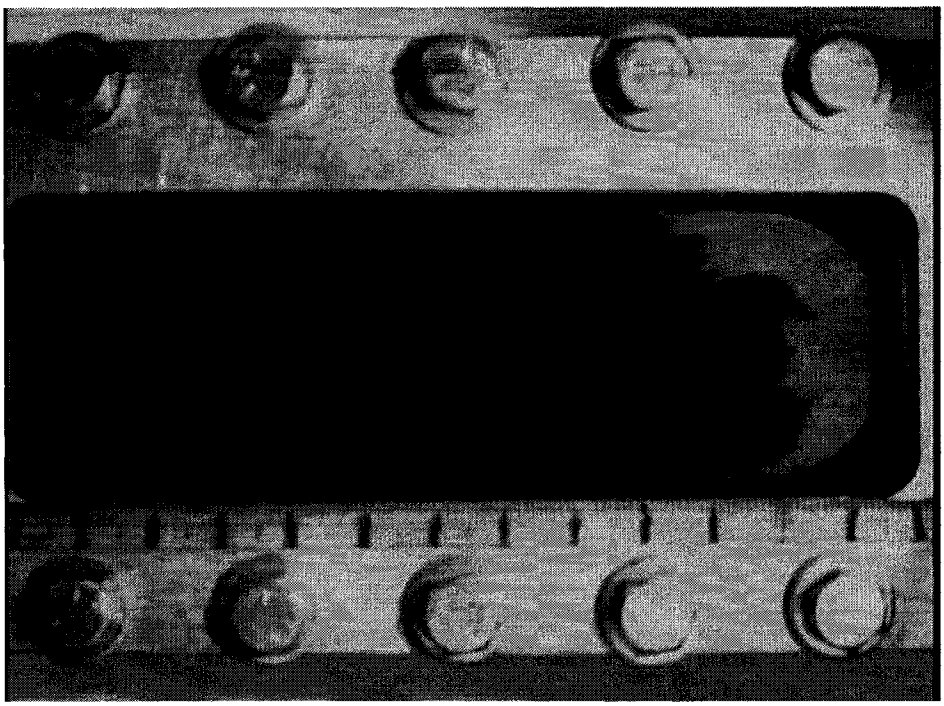

Figure 5.6 Front position after injection of 7.5 PV of emulsion WC/W1

The figures above indicate that the front position is identical regardless of the oil type for the injection of equal amounts of these two stable emulsions. Based on the above presented pictures and, also, by measuring the front position through video analysis (videos showing the emulsion propagation depth were recorded for each experiment) in different stages of the emulsion injection period, a general expression can be drawn with which to predict the frontal position of any stable emulsion that has a larger mean droplet size than the pore throat size:

$$L_F = L_T\,(PV)\,X \qquad (5.1)$$

where:

L_F = front position

L_T = total length

PV = pore volume of injected emulsion

X = emulsion quality

5.4.2 Effluent Droplets Size Distribution

The effluent droplet size distribution was measured for several of the experiments conducted in this part of the study. In the following, the results for the droplets size distribution measurement of emulsion M/W4 injected into a glass beads pack are presented. The porous medium was packed with fine beads less than 230 mesh. Figure 5.7 indicates the droplets size distribution for the injected emulsion M/W4. Almost 12 percent of the these droplets had a mean size of 26 μm.

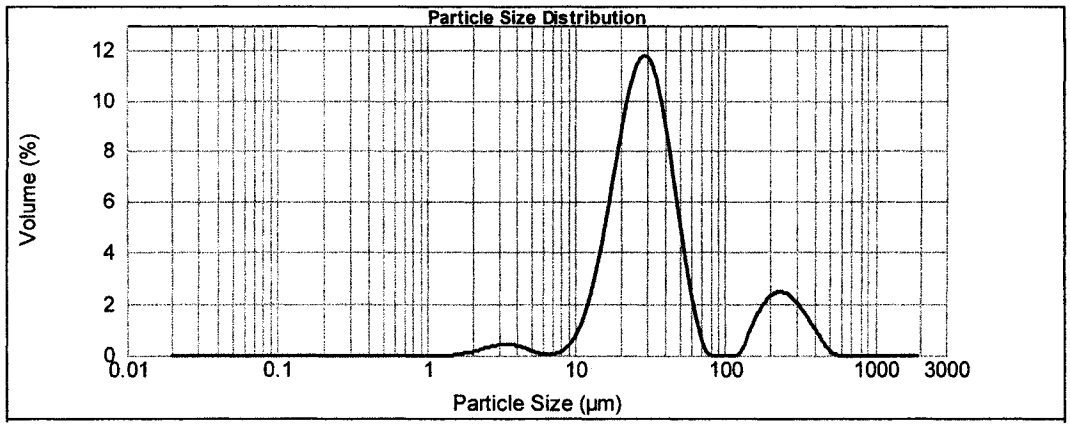

Figure 5.7 Droplet size distribution for the injected emulsion M/W4

When this emulsion was injected into the glass beads pack, almost all of the droplets were captured before the emulsion front reached the exit port of the cell. Figure 5.8 shows the measured effluent droplet size distribution just before the emulsion front exited the cell. By this time, almost nine pore volumes of the emulsion were injected. The graph indicates that only small droplets, between 4 and 20 μm, passed through the cell. Almost 19 percent (volume) of the droplets had an average size of 10 μm.

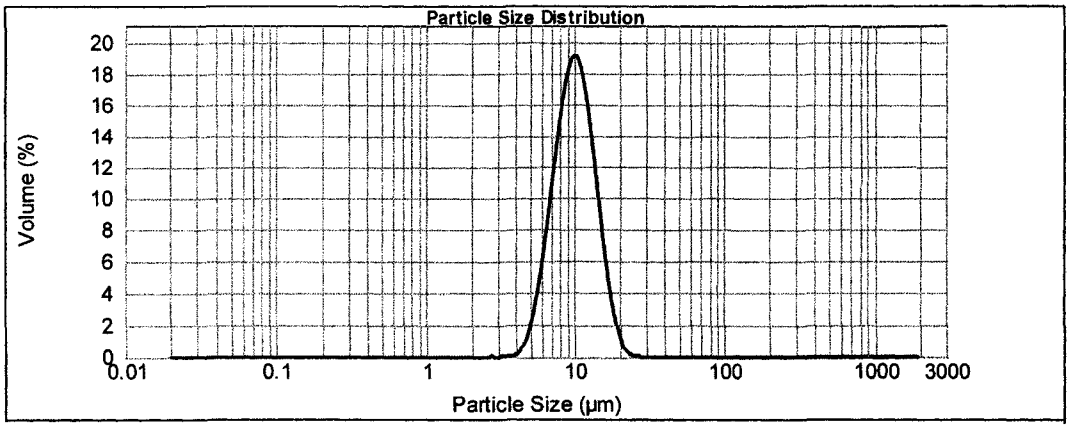

Figure 5.8 Effluent droplet size distribution after injection of 9 PV of emulsion M/W4

As the emulsion injection continued, another effluent sample was assessed. Figure 5.9 shows the measured effluent droplet size distribution after injection of 24 pore volumes of the emulsion M/W4. It indicates that the passing volume of small droplets decreased from 19 to 16 percent. The mean droplet size distribution, however, seemed to remain around 10 µm. Moreover, the figure demonstrates that at later stages of the injection, larger droplets passed through the porous medium (less than one percent of the droplets had an average size of 150 µm).

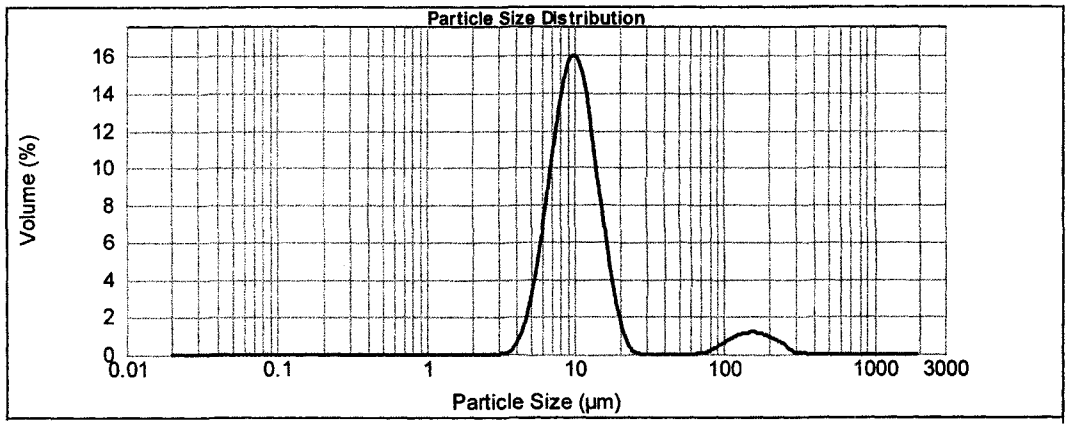

Figure 5.9 Effluent droplet size distribution after injection of 24 PV of emulsion M/W4

5.4.3 Pressure Gradient and Permeability Reduction

Emulsions M/W4 and WC/W1 were injected into two glass bead packs. The beads of these two packs were identical in size distributions (between 100 and 320 mesh). However, the method of packing the glass beads resulted in two porous media with different characteristics. In the first porous medium, the open gap between the two plates of the visual cell was packed with glass beads between 100 and 320 mesh. When the emulsions were injected into this porous medium, they touched the porous medium face at the injection point. This scenario was coined *"emulsion injection through restricted flow path"* based on the fact that the injection flow path area at the injection point (0.012 in^2 or 0.08 cm^2) was almost five times smaller than the actual flow path area (0.4 cm^2). In the second porous medium, the entrance section of the cell was packed with coarse glass beads between 100 and 120 mesh, to a length of 0.8 cm. The remainder of the open space between the two plates was packed with glass beads between 100 and 320 mesh. The coarse beads at the entrance section of the cell acted as a highly-porous distribution channel. Therefore, the injected emulsions touched the actual porous medium face after they took position across the entire flow path area. For this reason this scenario was called *"emulsion injection through unrestricted flow path"*. For each scenario, the corresponding pressure response for injection of these two emulsions is given below.

5.4.3.1 Emulsion injection through restricted flow path

Emulsions M/W4 and WC/W1 were injected into a glass bead pack with an absolute permeability of 2.1×10^{-12} m^2 (2.13 Darcy). Emulsion M/W4 was injected first. Then, the porous medium was flushed with a mixture of toluene and isopropyl alcohol, followed by injection of an excess amount of distilled water. This process was repeated until the porous medium restored its original permeability with a tolerance of three percent. Afterward, the injection of WC/W1 emulsion was initiated. Figure 5.11 indicates that the total pressure gradient (equal to the injection pressure) for both emulsions increased linearly with the injected emulsion pore volumes. The

trend continued until the emulsion front reached the exit of the cell, when it stabilized.

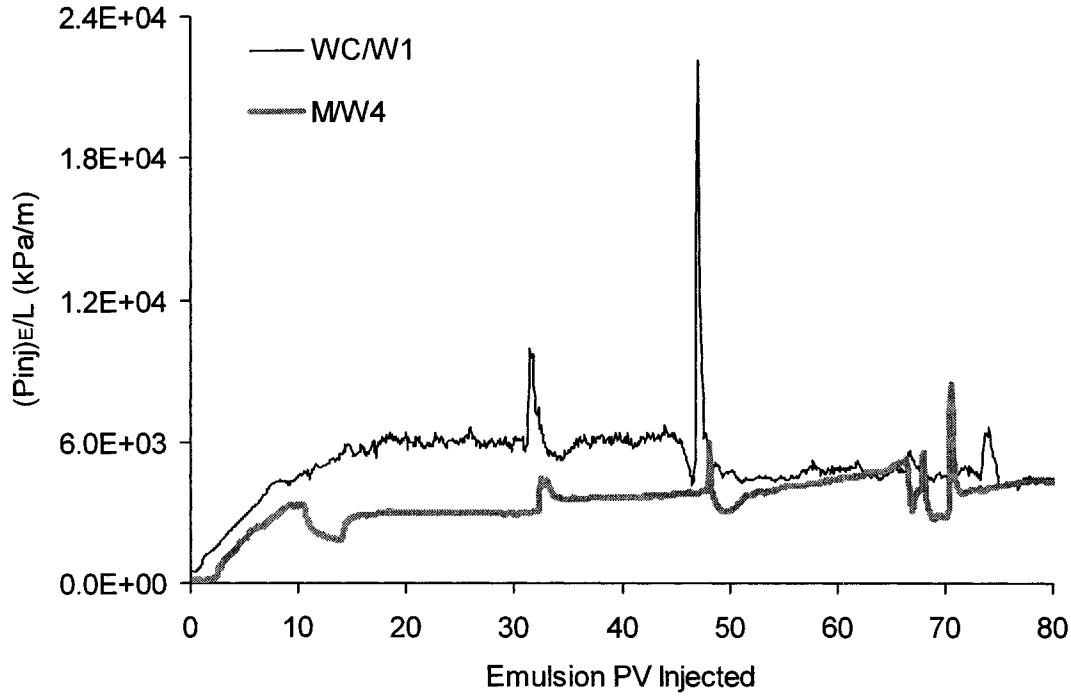

Figure 5.10 Overall pressure gradient profiles for injection of emulsions WC/W1 and M/W4

Figure 5.10 shows that the porous medium was blocked in different sequences while the experiments were conducted. This is evident from the pressure pulses that occurred during each experiment and the fact that each one was greater than the previous pulse. Perhaps, as time passed, each pore became occupied by strained droplets. The porous medium was then considered to be blocked, and pressure began to build up during that time. The pressure may have increased to two, three or even more times its original value before a small opening within the blocked region could be created. However, if an emulsion penetrated far enough into the porous medium, reopening may never have occurred even under high pressure. As shown in Figure 5.10, the pressure increased up to 22,000 kPa/m for an emulsion with relatively

viscous oil (WC/W1) and up to 8,500 kPa/m for an emulsion containing less viscous oil (M/W4). The reason for the increase in magnitude of pressure pulses is the increased droplet concentration within a pore each time a blockage occurred. Consequently, droplets coalesced when they were pushed too close to one another under increased pressure. Such coalescence resulted in larger droplets within the pores and, therefore, required a higher pressure for the subsequent blockage reopening.

Figure 5.11 is a summation of the front and rear sections of the visual cell pressure gradients for these two experiments. It illustrates that a sudden increase in pressure occurred at different stages of the injection, which explains the occurrence of blockage in different sections of the porous medium.

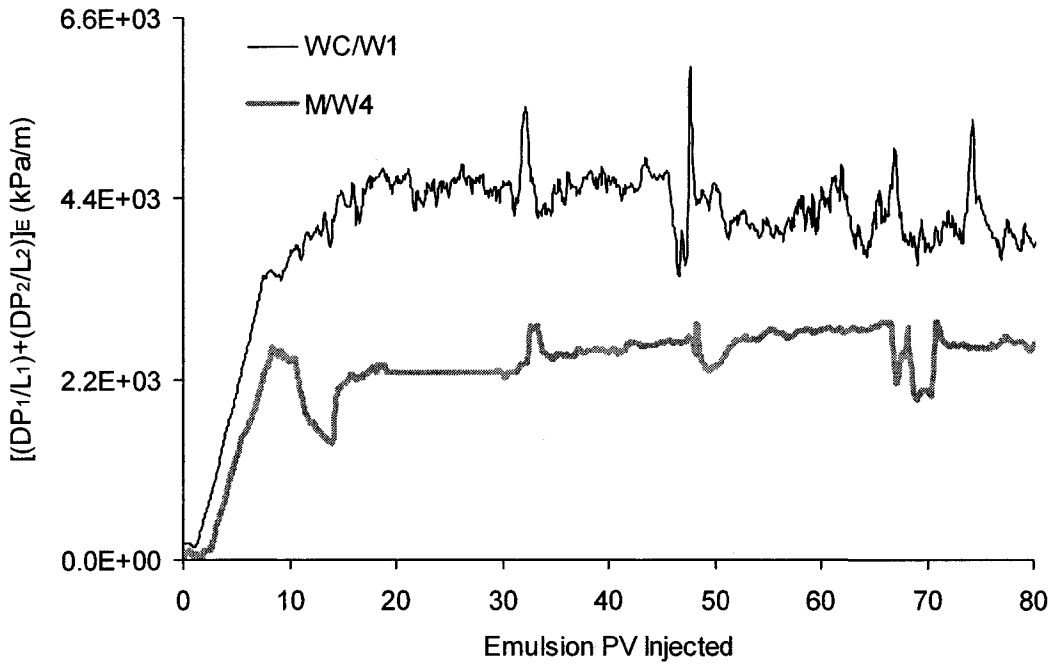

Figure 5.11 Summation of pressure gradients at front and rear sections for injection of emulsions WC/W1 and M/W4

The permeability reduction due to the injection of these two emulsions was calculated using Darcy's law. Figure 5.12 illustrates the permeability reduction for the injection of these two emulsions. In the figure, $k_{original}$ refers to the original absolute permeability when the flowing fluid was only water. The resulting permeability after emulsion injection is noted k. In the calculations, the viscosities of the flowing phases (water for $k_{original}$ and emulsion for k, respectively) were used. An average value was used for the emulsion viscosity as it varied during an experiment, as shown by the difference in average droplet size between the injected emulsion and the effluent (see Figures 5.7 and 5.8).

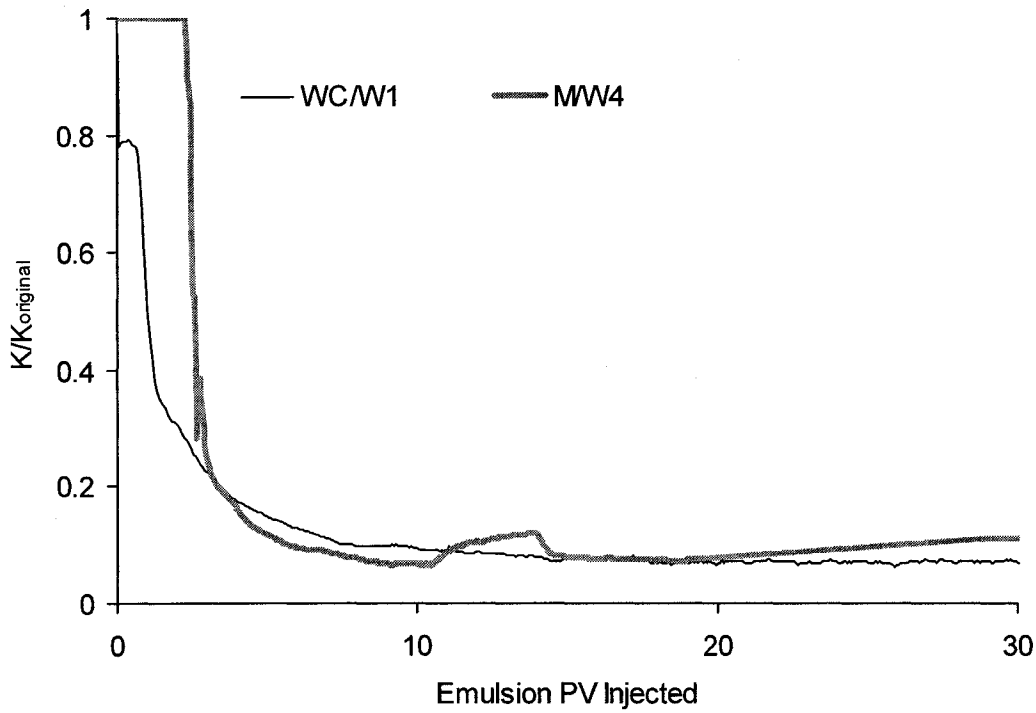

Figure 5.12 Overall permeability reductions for injection of emulsions WC/W1 and M/W4

Figure 5.12 illustrates that the original permeability was reduced by up to 93 percent of its original value with a greater reduction for the injection of an emulsion that was carrying more viscous oil (emulsion WC/W1). However, the final reduction in

permeability ratio ($k/k_{original}$) could be very close to 100 percent if the experiments were performed under lower flow rates.

5.4.3.2 Emulsion injection through unrestricted flow path

Emulsions M/W4 and WC/W1 were injected into a glass beads pack with an absolute permeability of 3.3×10^{-12} m^2 (3.38 Darcy). The experimental procedure was similar to one explained in the previous section (Section 5.4.3.1).

Figure 5.13 indicates that the total pressure gradient (equal to the injection pressure) for both emulsions increased linearly with the injected emulsion pore volumes. This trend continued until the emulsion front reached the end of the cell. The injection pressure for emulsion M/W4 stabilized soon after the front exited the cell. However, the injection pressure for emulsion WC/W1 continued to increase slowly over time.

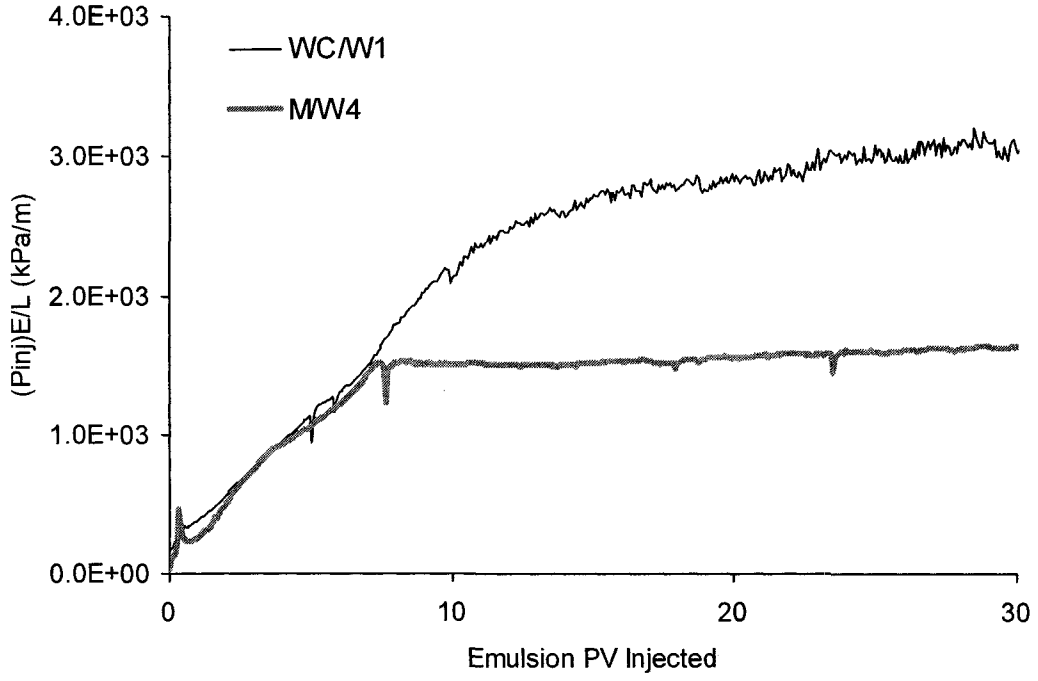

Figure 5.13 Overall pressure gradient profiles for injection of emulsions WC/W1 and M/W4

Figure 5.14 indicates similar trends of pressure gradients for these two emulsions at the front and rear sections. Careful investigation of this figure reveals an abrupt decrease in the pressure gradients for both emulsions at certain stages of the injection. This phenomenon can be more readily explained with the visual observations made during the experiments. During the experiments, a transient color change was observed in different sections of the blocked porous medium. As the injection pressure increased these regions became darker for emulsion WC/W1 and more red for emulsion M/W4. With further increases in the injection pressure, these blocked regions were swept out, causing a sharp decrease in injection pressure.

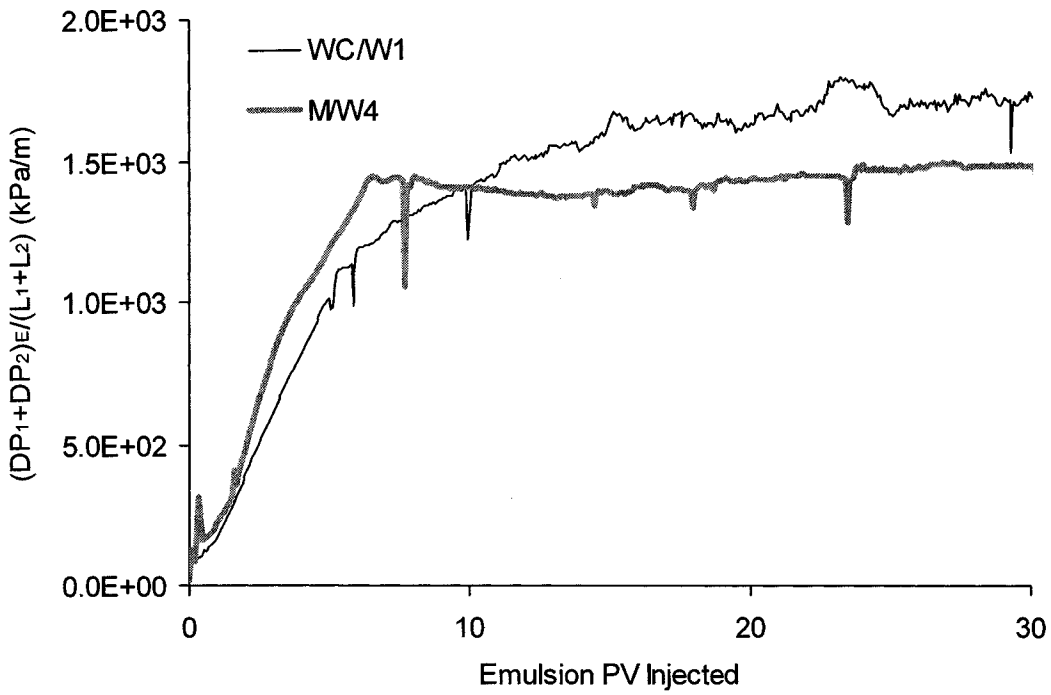

Figure 5.14 Pressure gradients across the middle section of the cell for injection emulsions WC/W1 and M/W4

Figure 5.15 illustrates the permeability reduction for emulsions M/W4 and WC/W1. The reduction in the original permeability was greater for injected emulsions that were carrying viscous oil (emulsion WC/W1). Comparisons between Figures 5.15 and 5.12 proved that the final reduction in permeability for emulsion M/W4 was less

in the case of an unrestricted flow path compared to a restricted flow path. Nevertheless, the final reduction in permeability is a result of many parameters, including the absolute permeability, and will be further explained in the later sections of this chapter.

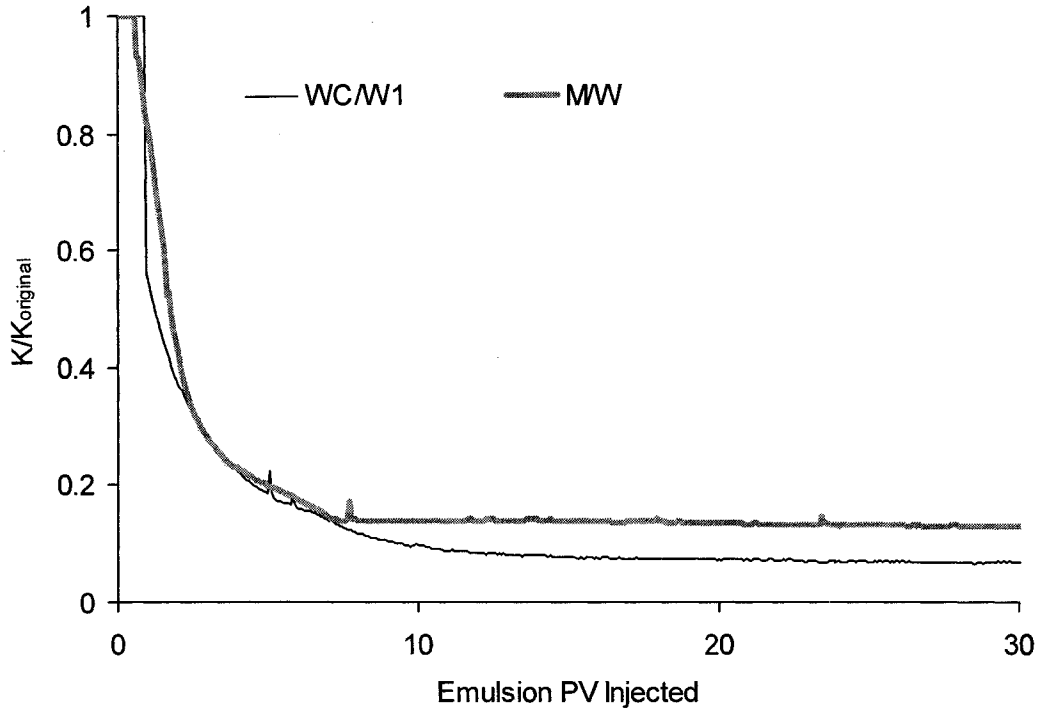

Figure 5.15 Overall permeability reductions for injection of emulsions WC/W1 and M/W4

5.4.4 Post-flush Water Injection

Almost 18 pore volumes of distilled water were injected into the pack following the injection of emulsions M/W4 and WC/W1. The water injection rate was equal to the emulsion injection rate (i.e. 3 cm^3/min). The frontal advancement, the reduced permeability, and the effluent droplet size distributions were studied for each post-treatment water injection experiment.

5.4.4.1 Frontal advancement

When many pore volumes of water were injected into the porous medium, the injected water spread across the entire flow path. The water then passed through the porous medium by removing the smaller droplets, rather than by fingering into the porous medium. In addition, the water did not sweep out the captured droplets. Instead, it reduced the number of total captured droplets in each capture site. Figures 5.16 and 5.17 display the thinning effect that the water created in the dispersed phase for emulsions M/W4 and WC/W1, respectively. Eventually, this caused the color in blocked region to fade.

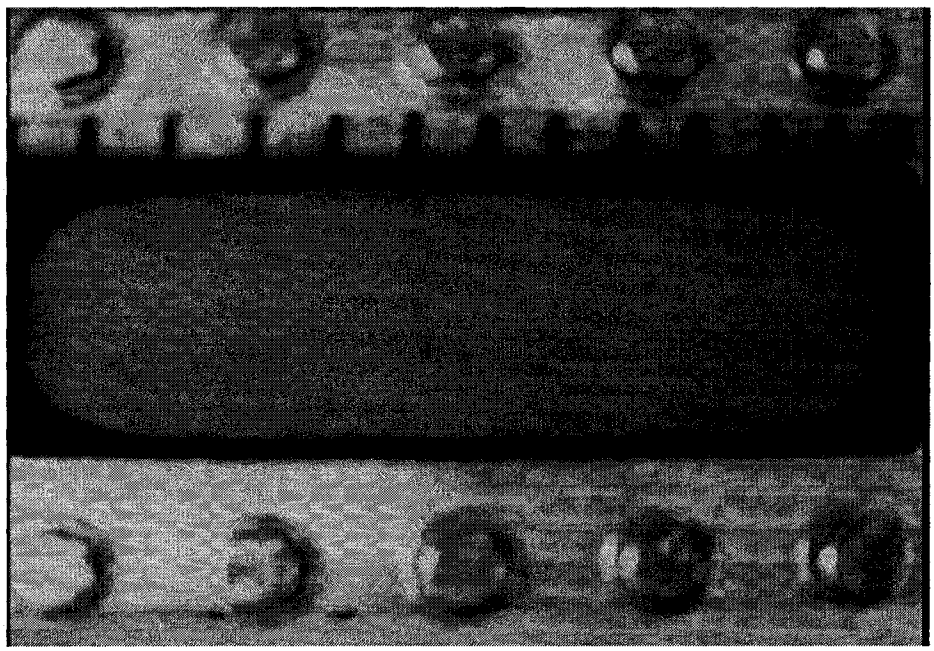

Figure 5.16 Reduced color intensity of emulsion M/W4 after water injection

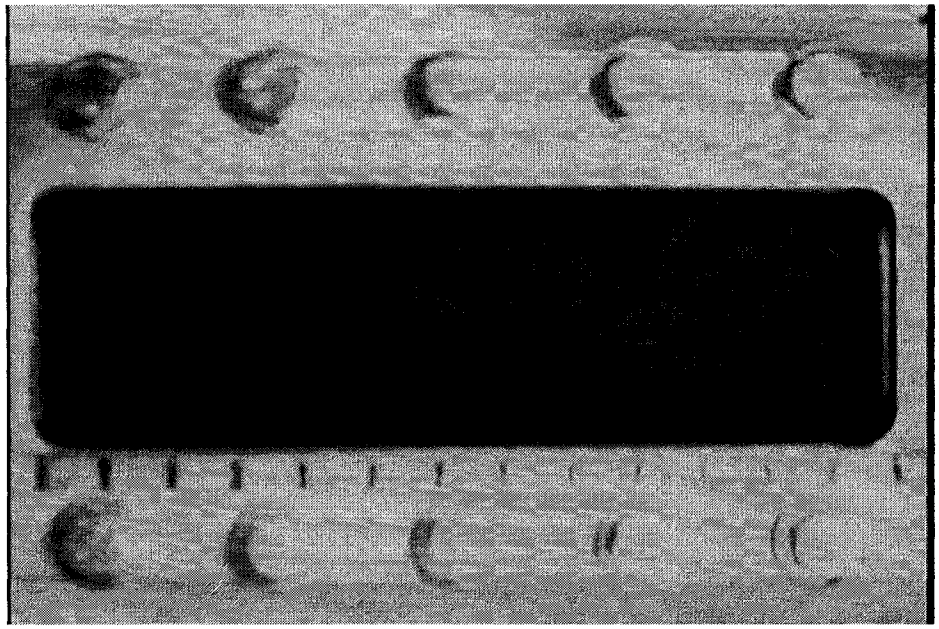

Figure 5.17 Reduced color intensity of emulsion WC/W1 after water injection

5.4.4.2 Permeability reduction

Assessment of the reduced permeability because of water revealed that the reduction was permanent. The assessment was tested for each different section of the visual cell: the overall permeability, the front section permeability, and the rear section permeability. Figure 5.18 shows that the permeability ratio for emulsion M/W4, with an absolute permeability of 2.1×10^{-12} m^2 (Section 5.4.3.1), remained constant even after injection of 18 pore volumes of water. Comparisons between Figures 5.18 and 5.12 demonstrate that the overall permeability ratios were equal at the end of both emulsion injections and post-flush water injection periods. As well, the rear section permeability decreased more than that of the front section. The difference in absolute permeabilities in each section could be the reason for such behavior.

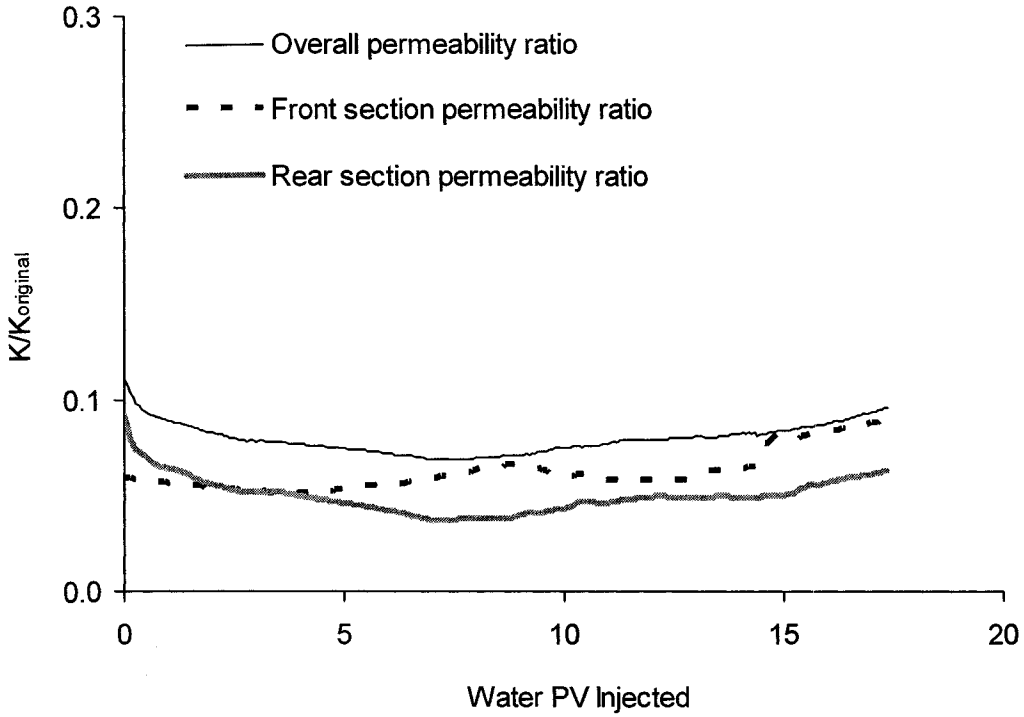

Figure 5.18 Permeability ratios after water injection, following the injection of emulsion M/W4

Figure 5.19 shows that the permeability ratio for injection of emulsion WC/W1 into the same porous medium (absolute permeability of 2.1×10^{-12} m^2 - Section 5.4.3.1) continued to be constant even after injecting numerous pore volumes of water. Similarly, comparisons between Figures 5.19 and 5.15 demonstrate that the overall permeability ratios were equal at the end of both emulsion injection and post-flush water injection periods. Contrary to the behavior observed with emulsion M/W4, the front section permeability decreased more than in the rear section for emulsion WC/W1.

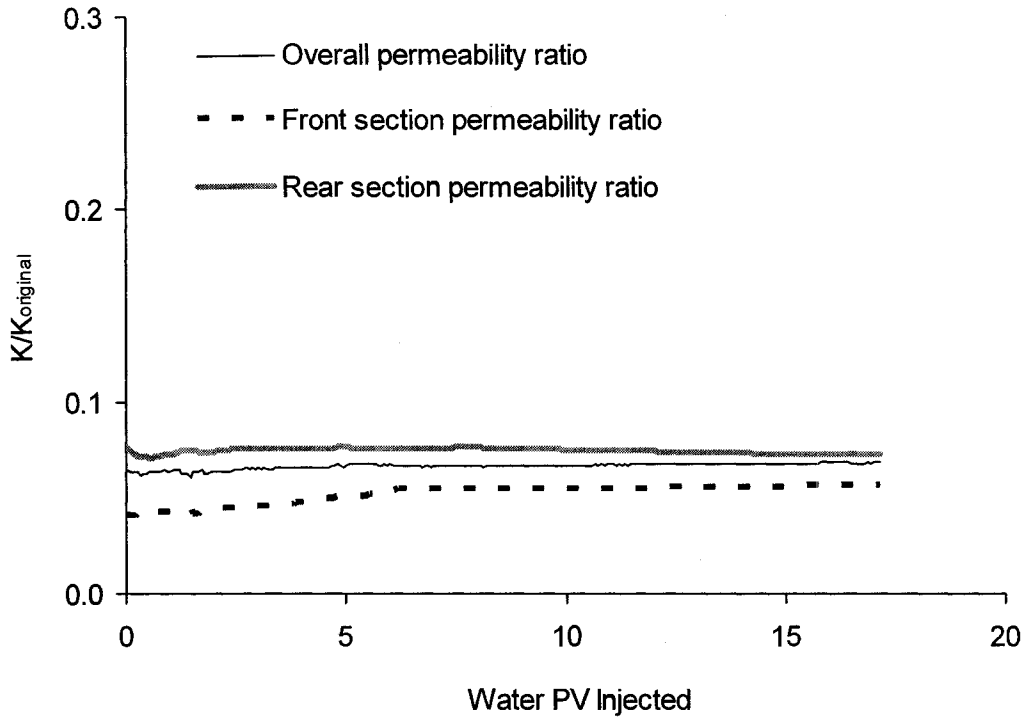

Figure 5.19 Permeability ratios after water injection, following the injection of emulsion WC/W1

5.4.4.3 Effluent droplet size distribution

The produced droplets were analyzed during the water injection period. The results were found to be similar to the observation made during the emulsion injection. Earlier observations (Section 5.4.2) indicate that smaller droplets were produced first at the early stage of the emulsion injection (Figure 5.8) and augmented later by larger droplets in late stages of the injection. Figure 5.20 illustrates a similar observation: that small droplets with a mean size of 10 μm were produced during the water injection, following the injection of emulsion M/W4. The primary difference is that the volume percentage of the produced small droplets during the water injection was almost 40 percent less than what was measured during the emulsion injection time. Also, smaller droplets with a volume percentage lower than two and mean size of one μm were observed in the produced effluent.

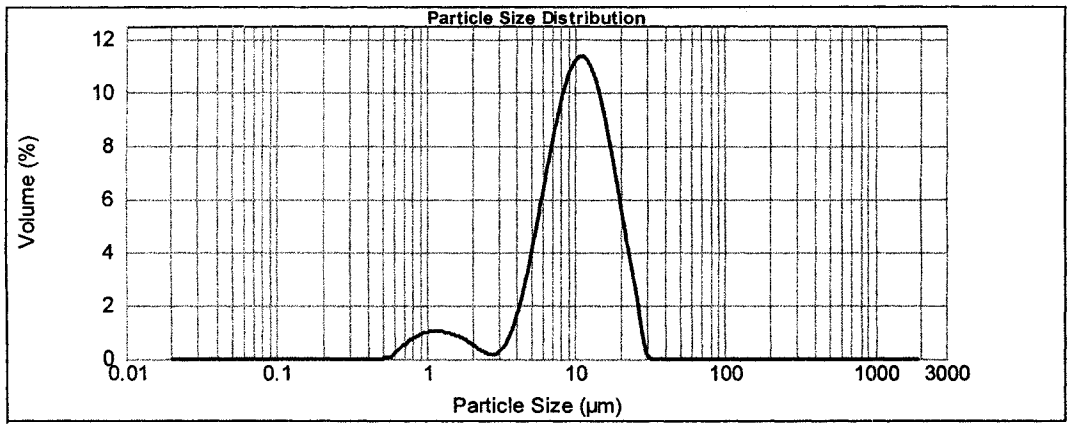

Figure 5.20 Effluent droplets size distribution for emulsion M/W4 during water injection

The effluent droplet size distribution was measured for emulsion WC/W1. Figure 5.21 shows the measured effluent droplet size distribution at the early stage of the water injection. It illustrates that only small droplets, between 4 and 20 μm, were pushed out of the cell by the injected water. Almost 19 percent (volume) of the droplets had an average size of 10 μm.

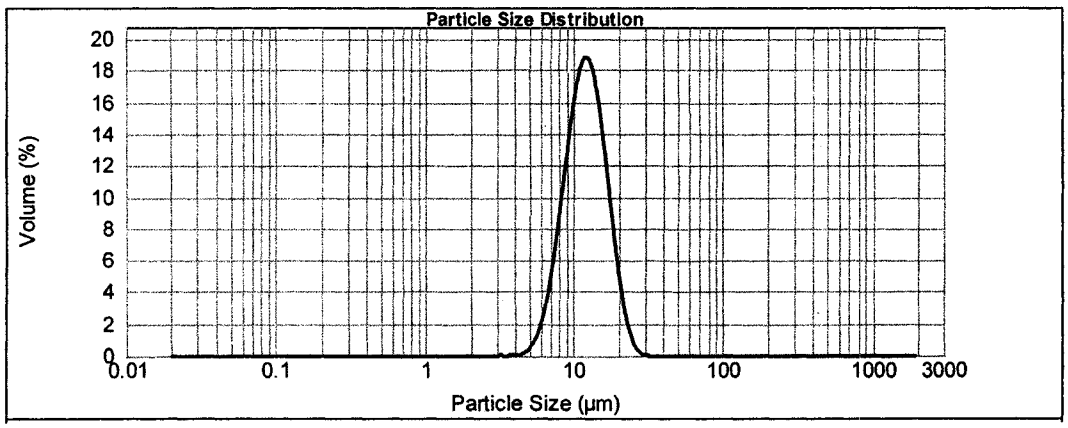

Figure 5.21 Effluent droplet size distribution for emulsion WC/W1 during early stage of water injection

As the water injection continued, another effluent sample was assessed. Figure 5.22 shows the measured effluent droplet size distribution after injection of 18 pore volumes of distilled water. It indicates that the volume percentage of smaller

droplets was decreased from 19 to 15 percent. The mean droplet size distribution, however, remained around 10 μm. Also, the figure indicates that at the later stages of the water injection, larger droplets were also pushed out of the porous medium. They had a volume percentage of approximately three percent with a mean size of 250 μm.

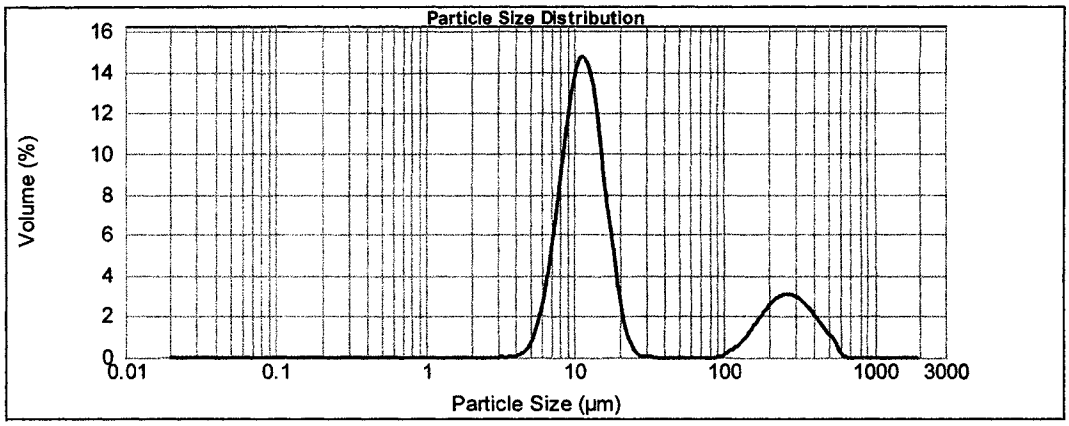

Figure 5.22 Effluent droplet size distribution for emulsion WC/W1 during late stage of water injection

5.5 *Effect of Droplet-to-pore Size Ratio*

The following section is a description of the experiments performed and the subsequent results. Droplet-to-pore size ratio greatly affects the local capillary pressure across a trapped non-wetting droplet. The magnitude of this local capillary pressure can be calculated using the Laplace equation if the droplet and pore throat sizes are known. In the following experiments, the droplet size distributions were measured for all of the used emulsions. However, it was impossible to measure the pore throat size distributions because of the lack of laboratory equipment. Instead, a qualitative representation of different pore throat size distributions was applied. For this purpose, the porous medium was packed with glass beads that had a narrow size distribution. It was assumed that using uniform-sized glass beads would result in a narrow pore throat size distribution. The measured permeability, which is directly

related to the pore throat size distribution of each porous medium, confirmed these assumptions.

5.5.1 Fixed Droplet Sizes – Variable Pore Throat Sizes

Two experiments were performed in this portion. Emulsion M/W4, which had a mean droplet size of 26.3 μm, was injected into two glass bead packs with different pore size distributions. The utilized emulsion (M/W4) was identical in both experiments; consequently, its droplet size distribution remained constant in both cases.

One porous medium was packed with glass beads between 120 and 140 mesh. Its absolute permeability was measured at 7.41×10^{-12} m^2 (7.18 Darcy). T he other porous medium was packed with glass beads between 200 and 230 mesh. Its absolute permeability was measured at 3.92×10^{-12} m^2 (2.79 Darcy). The entrance of the cell was packed with glass beads between 100 and 120 mesh in both experiments.

The emulsion was injected at a constant rate of 3 cm^3/min in both cases. Figure 5.23 indicates that the pressure gradient across a porous medium with a smaller pore throat size was nearly 2.3 times greater than the gradient in a medium with a larger throat size for the injection of the same emulsion and with the same flow rates. In addition, Figure 5.24 reveals that the reduced permeability at the end of the injection periods for the porous medium with smaller pore throat sizes (permeability ratio of eight percent) was less than the permeability of the porous medium with larger pore throat sizes (permeability ratio of ten percent).

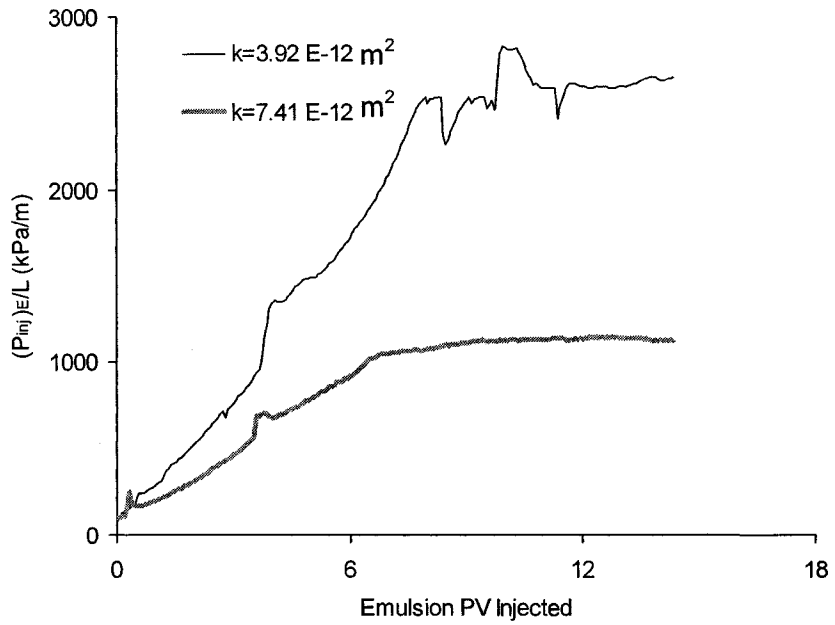

Figure 5.23 Pressure gradients for injection of identical emulsion into porous media with different pore throat sizes

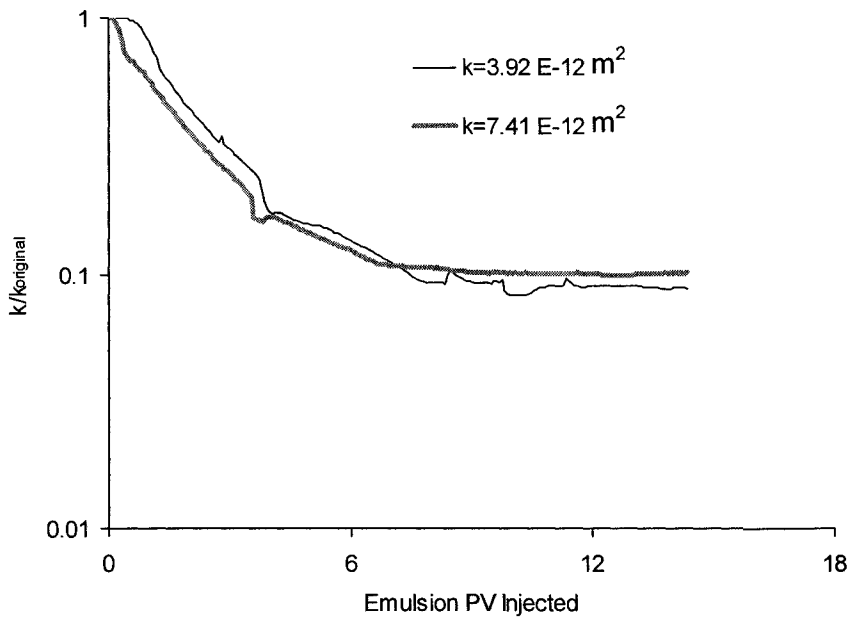

Figure 5.24 Permeability ratios for injection of identical emulsion into porous media with different pore throat sizes

5.5.2 Fixed Pore Throat Sizes – Variable Droplet Sizes

Two experiments were performed in this portion. The porous medium was identical in both experiments. The porous medium was packed with glass beads between 230 and 250 mesh. Its absolute permeability was measured at 2.31×10^{-12} m^2 (2.32 Darcy). The entrance of the cell was packed with glass beads between 100 and 120 mesh to facilitate flow.

Two mineral oil-in-water emulsions, with different droplet size distributions, were injected into the same glass beads pack. Both emulsions had similar characteristics: quality of 13% and surfactant concentration of 0.12% (volume/volume). The first emulsion was identical to emulsion M/W4 which had a mean droplet size of 26.3 μm. Emulsion M/W4 was produced at a shear mixing rate of 5000 rpm with the Brinkmann homogenizer.

The second emulsion, M/W6, was produced at a shear mixing rate of 5800 rpm. It displayed a mean droplet size of approximately 13.6 μm.

Emulsion M/W4 was injected first, at a constant rate of 3 cm^3/min. Then, the porous medium was cleaned with a mixture of toluene and isopropyl alcohol. Its original permeability was restored by flushing it with several pore volumes of distilled water. Then, emulsion M/W6 was injected at the same rate as emulsion M/W4 (3 cm^3/min).

Figure 5.25 indicates that the pressure gradient across the same porous medium for the injection of an emulsion with larger droplets (M/W4) was much greater than the gradient for the injection of an emulsion with smaller droplets (M/W6).

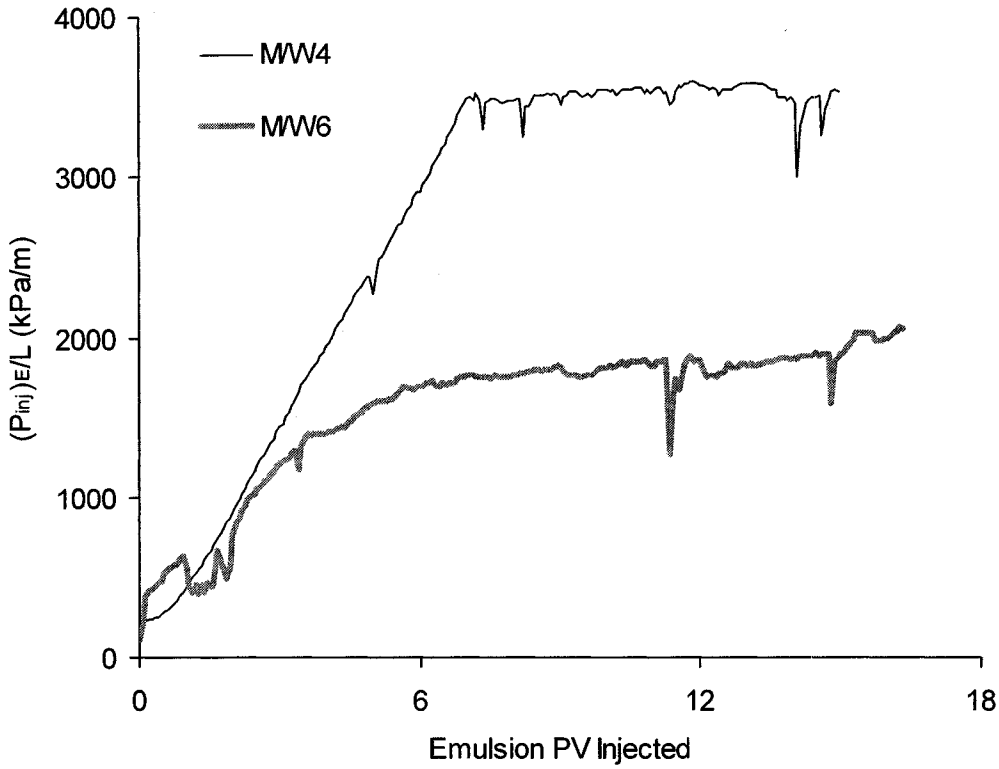

Figure 5.25 Pressure gradients for the injection of emulsions with different droplet size distributions into an identical porous medium

In addition, Figure 5.26 indicates that the reduced permeability at the end of the injection periods for the same porous medium is greater for the injection of larger droplets (permeability ratio of 10 percent) compared with injecting smaller droplets (permeability ratio of 15 percent).

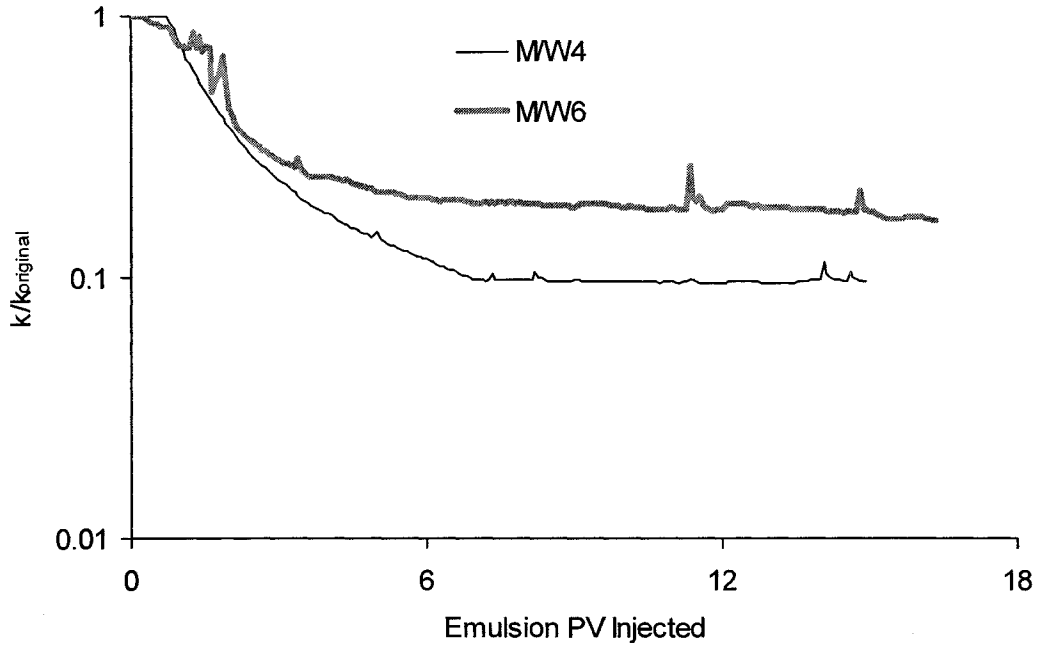

Figure 5.26 Permeability ratios for the injection of emulsions with different droplet size distributions into an identical porous medium

5.6 *Effect of Surfactant Pre-flush Solution*

The surfactant concentration in a solution has a pivotal effect on the flow behavior of an emulsion through a porous medium. It affects the stability of the injected emulsion and may alter the porous medium wettability if adsorbed onto the surface. In order to investigate the effect of surfactant concentration, emulsions M/W7 (mineral oil-in-water) and WC/W2 (Western Canadian oil-in-water) were used. The surfactant content in these emulsions was very close to that of the CMC (0.025%, volume/volume), and both emulsions had a 13% quality. These two emulsions lacked excess surfactant that could have acted as a wettability-altering agent. They were both tested on a porous medium that was initially saturated with water, and then, with a pre-flush solution. The pre-flush solution was a mixture of nonionic Triton X-100 surfactant and distilled water (0.12 % volume/volume or 0.13% weight/volume).

Each experiment was performed in three stages: emulsion injection without pre-flush, cleaning and restoration of the porous medium surface properties, and pre-flush injection followed by injection of the same emulsion. The order of each set of experiments was as follow:

- injection of water for saturation and determination of the absolute permeability of the porous medium,
- injection of the selected emulsion,
- injection of water to test the emulsion's ability to plug the porous medium,
- cleaning of the porous medium by flushing it with toluene and isopropyl alcohol,
- flushing of the porous medium with several pore volumes of water,
- flushing of the porous medium with five pore volumes of surfactant pre-flush solution,
- injection of the same emulsion,
- injection of water to test the emulsion's ability to plug the porous medium.

A mixture of fine and coarse glass beads porous medium ranging from 100 to 320 mesh was used for these experiments. Two types of investigations, restricted and unrestricted flow paths, were carried out for all of experiments. In a restricted flow path, the entire porous medium was packed with the same size of glass beads, while in an unrestricted flow path, the entrance of the porous medium was prepared with larger glass beads (100-120 mesh).

The emulsion front position is illustrated in Figures 5.27 and 5.28 after injection of 7.5 pore volumes of emulsion M/W7, with and without a pre-flush solution through a restricted injection flow path, respectively. Figures 5.29 and 5.30 show the frontal position after injection of 7.5 pore volumes of emulsion M/W7, with and without a surfactant pre-flush solution through an unrestricted injection flow path, respectively.

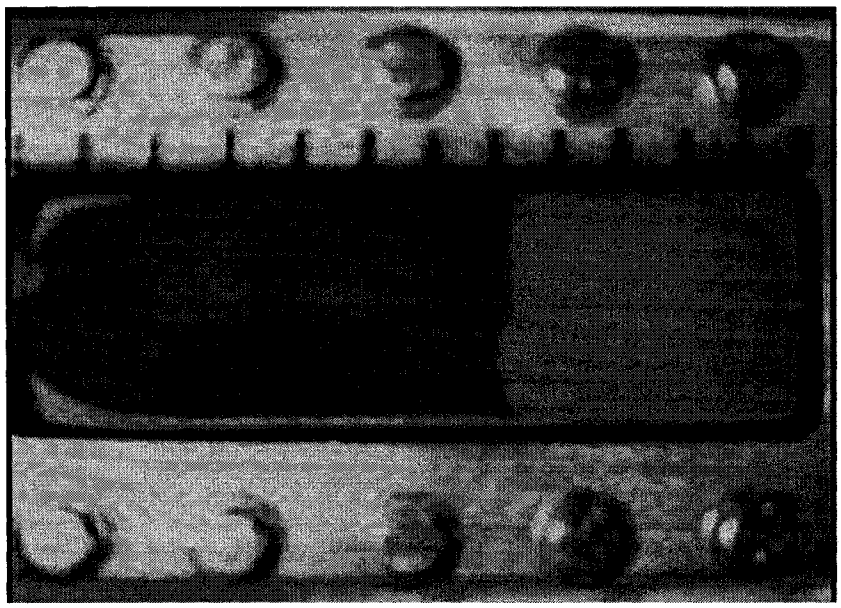

Figure 5.27 Front position after injection of 7.5 PV of emulsion M/W7 with surfactant pre-flush through a restricted flow path

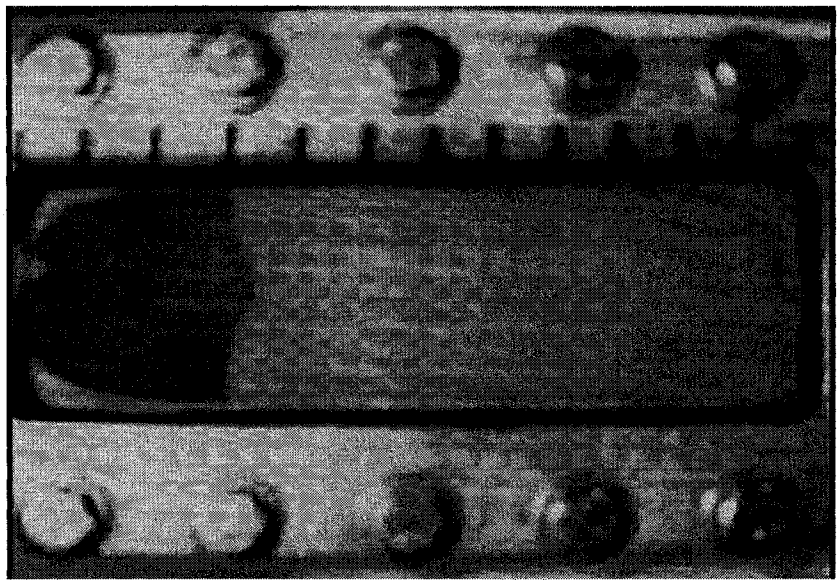

Figure 5.28 Front position after injection of 7.5 PV of emulsion M/W7 without surfactant pre-flush through a restricted flow path

These figures indicate that the application of a pre-flush surfactant solution improved the emulsion M/W7 penetration depth by almost 150% for the restricted

flow path glass bead pack. However, this penetration depth was only approximately 50% for the same emulsion through an unrestricted injection flow path (Figures 5.29 and 5.30).

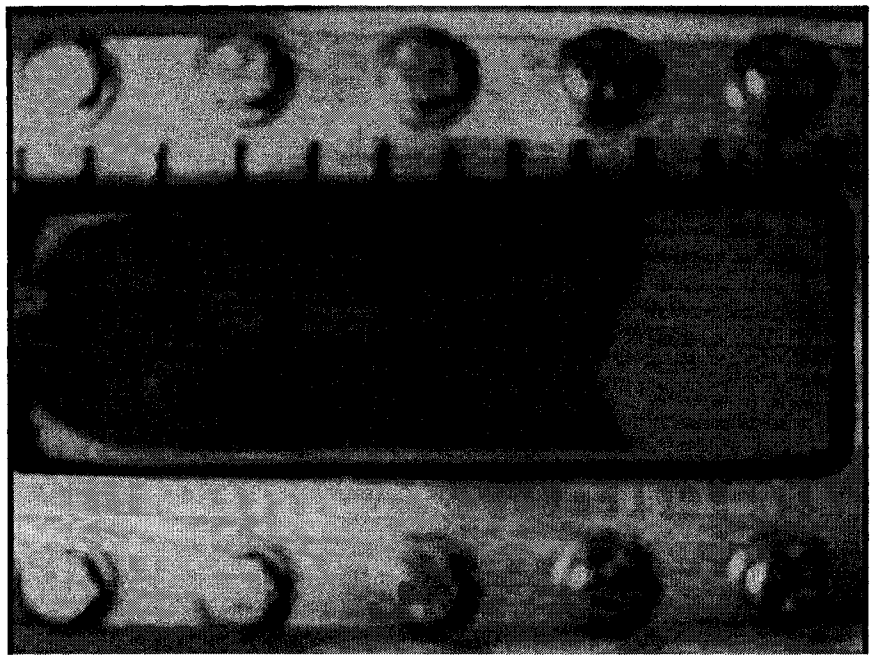

Figure 5.29 Front position after injection of 7.5 PV of emulsion M/W7 with surfactant pre-flush through an unrestricted flow path

Similarly, Figures 5.31 and 5.32 show the frontal position enhancement with the use of a surfactant pre-flush solution in one case, and without it in the next, prior to injecting five pore volumes of emulsion WC/W2 through an unrestricted flow path area.

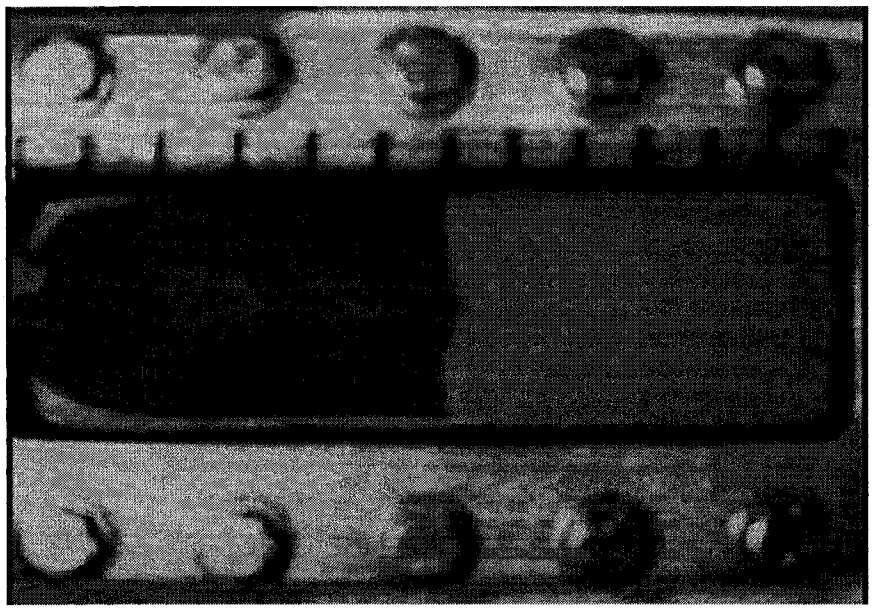

Figure 5.30 Front position after injection of 7.5 PV of emulsion M/W7 without surfactant pre-flush through an unrestricted flow path

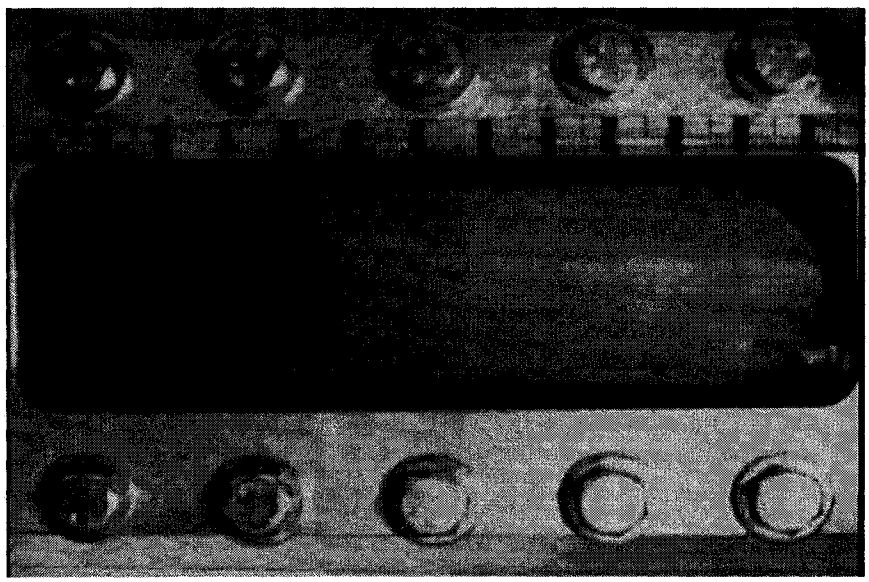

Figure 5.31 Front position after injection of 5 PV of emulsion WC/W2 with surfactant pre-flush through an unrestricted flow path

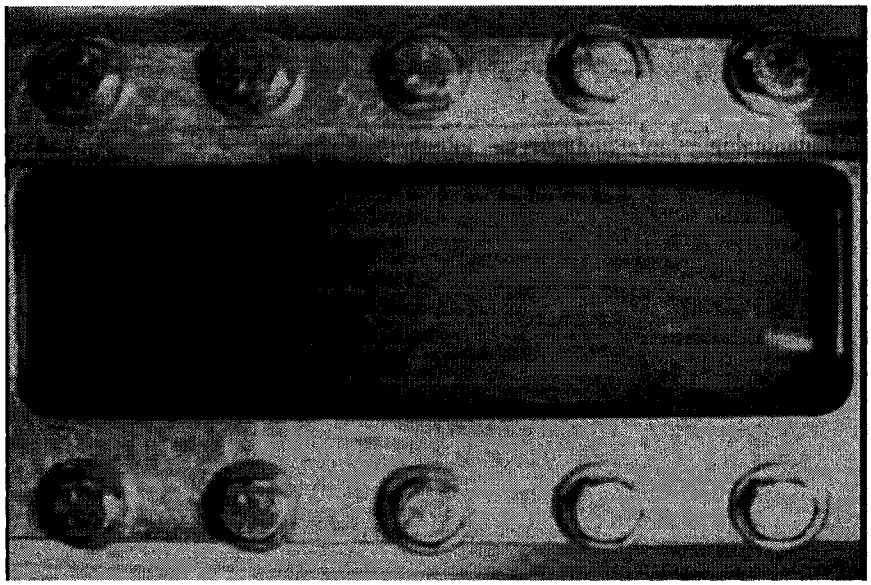

Figure 5.32 Front position after injection of 5 PV of emulsion WC/W2 without surfactant pre-flush through an unrestricted flow path

5.7 *Effect of Surfactant Content*

Six experiments were conducted in this portion. The emulsions were prepared with different oil types and each was injected into the same porous medium at a flow rate of 3 cm^3/min. The porous medium was packed with fine and coarse glass beads between 100 and 320 mesh. Its absolute permeability was measured at 2.19×10^{-12} m^2 (3.23 Darcy). The entrance of the cell was packed with larger glass beads for a better flow distribution. The following are the results obtained from two sets of experiments: the first consisting of mineral oil-in-water emulsions and the second with Western Canadian oil-in-water emulsions.

5.7.1 Mineral Oil-in-water Emulsions

Three mineral oil-in-water emulsions (M/W) with surfactant contents of 0.01% (M/W5), 0.025% (M/W7), and 0.12% (M/W4) (volume/volume) were prepared and injected into the same porous medium. In addition, another mineral oil-in-water emulsion (M/W8) with 0.06% surfactant concentration and 13% quality was prepared and injected into the same glass beads pack. The measured mean droplet

size for this emulsion was 27.7 μm. The droplet size distributions for these four emulsions are presented in Appendix C. The emulsions' viscosity was measured by using the Advanced Rheometer AR-2000. Figure 5.33 indicates the viscosity for each emulsion at different shear rates. All emulsions exhibited a non-Newtonian behavior. Emulsions containing 0.06% and 0.12% surfactant concentration followed a Binghom plastic model, while the other two emulsions displayed a non-Newtonian behavior that followed a Power law viscosity model.

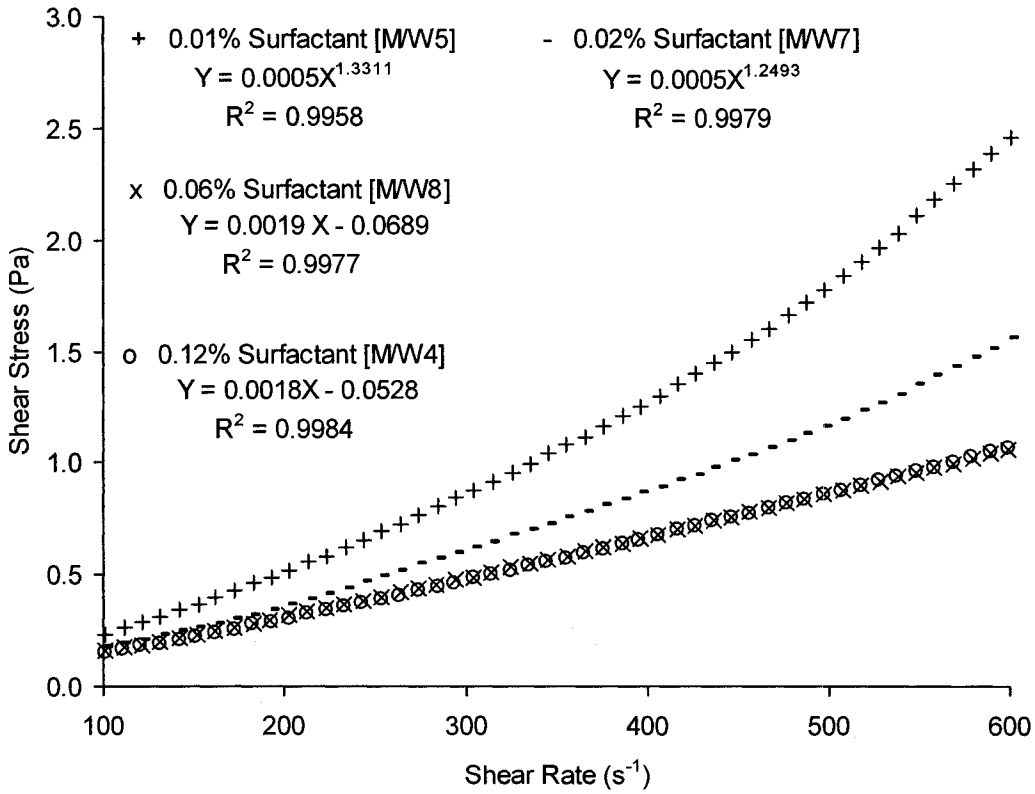

Figure 5.33 Viscosities for M/W emulsions with different surfactant concentrations

During the experiments, the overall pressure drop was recorded and the total permeability reduction was calculated. In Figure 5.34, the emulsion that contained less surfactant created a higher pressure gradient across the same porous medium. The pressure gradients were normalized with respect to the linear flow velocities.

Also, the figure illustrates that, as the surfactant content of the emulsions increased, the pressure drop decreased.

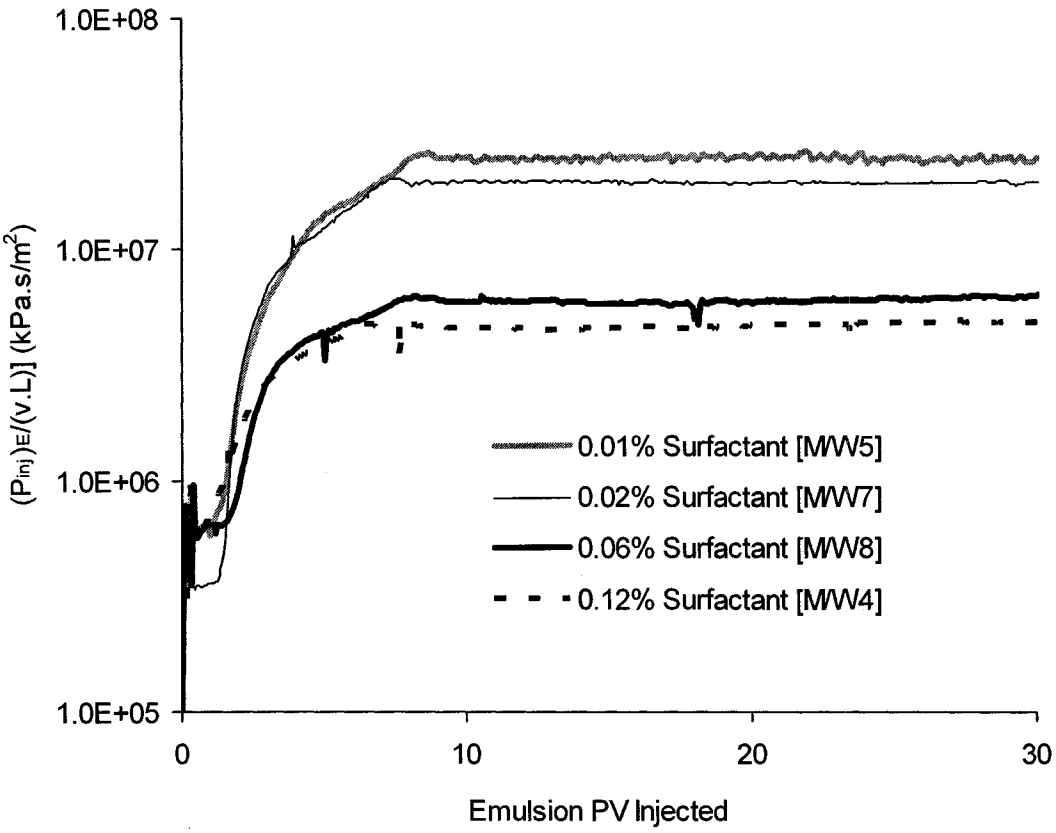

Figure 5.34 Normalized pressure gradients for the injection of M/W emulsions with different surfactant contents

In addition, as indicated in Figure 5.35, the highest reduction in permeability occurred when the emulsion with the lowest surfactant content was injected and vice versa. The results obtained from the emulsion droplet size distribution measurements, combined with the results in Figures 5.34 and 5.35, reveal that lower surfactant content resulted in a larger droplet size distribution, increased pressure drop across the porous medium and a greater permeability reduction.

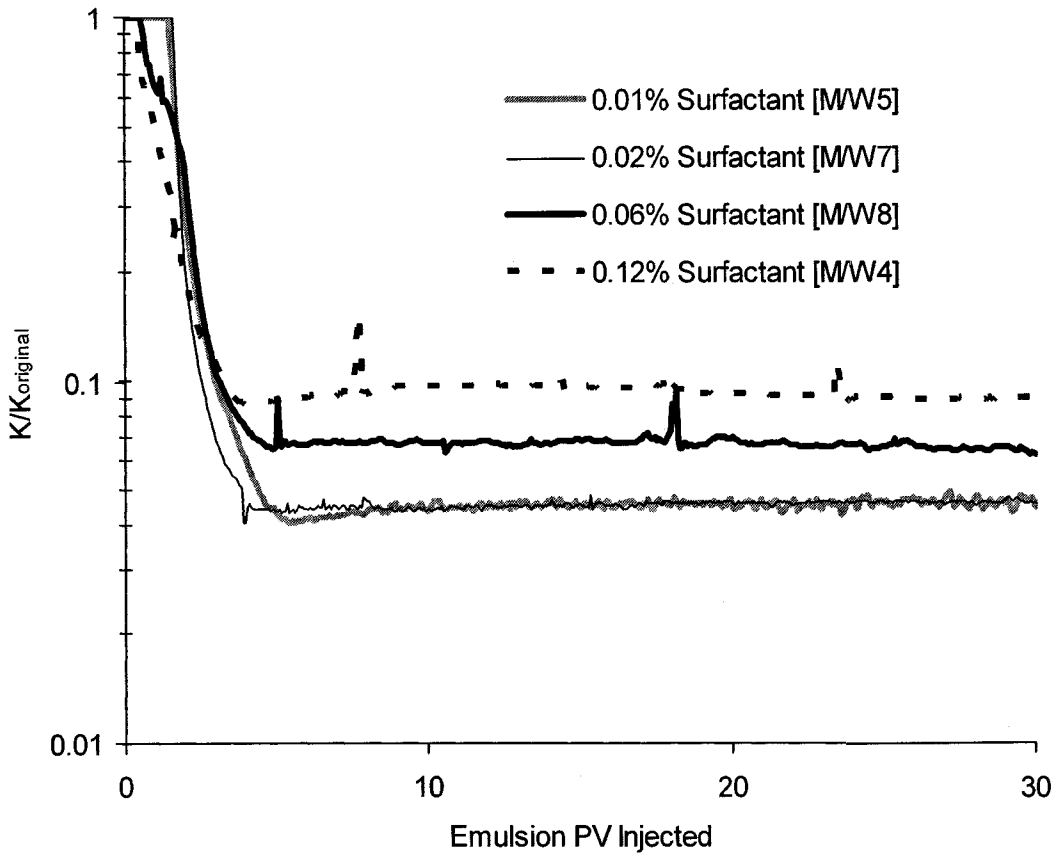

Figure 5.35 Permeability ratios for the injection of M/W emulsions with different surfactant contents

5.7.2 Western Canadian Oil-in-water Emulsions

Two experiments were conducted in this portion. Western Canadian oil-in-water emulsions (WC/W) with different surfactant contents were injected into the same pack. Emulsion WC/W1 (0.12% surfactant content, volume/volume) was injected first. In the other experiment, a newly prepared emulsion (WC/W3) was injected into the same pack. It had a 13% quality and 0.06% surfactant concentration (volume/volume). The measured mean droplet size for this emulsion was 59.3 μm, and the droplet size distribution for this emulsion is presented in Appendix C. The emulsion's viscosity was measured using the Advanced Rheometer AR-2000. Figure

5.36 illustrates the viscosity for these emulsions at different shear rates. Both emulsions displayed a Newtonian behavior over a wide range of shear rates.

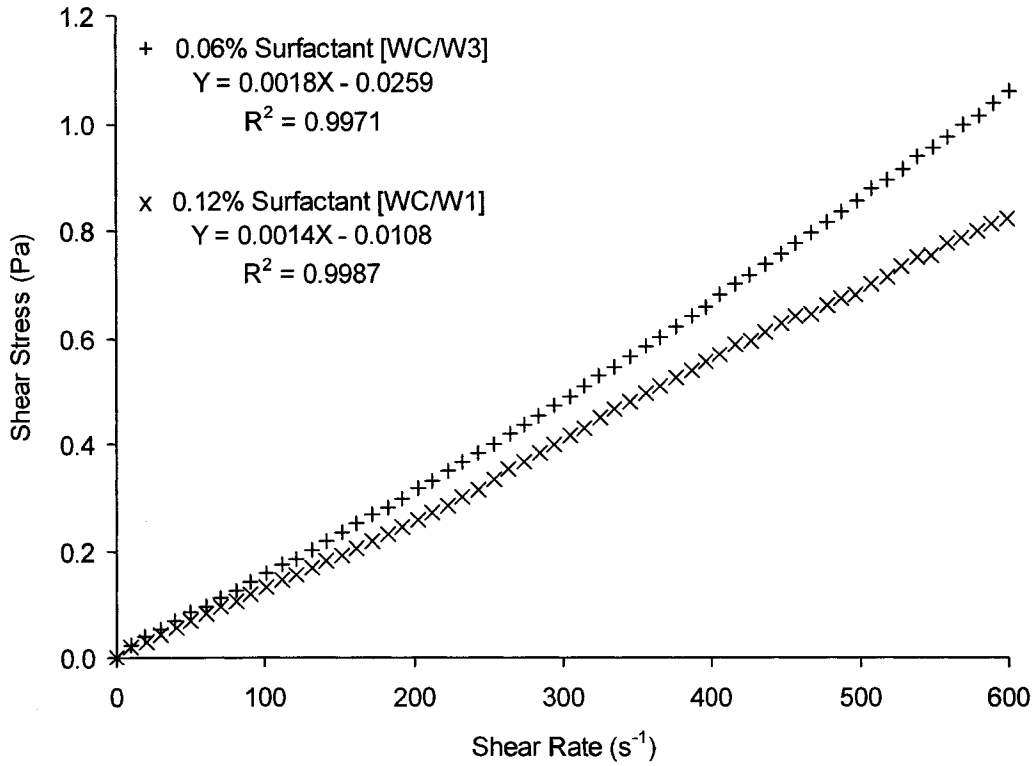

Figure 5.36 Viscosity of WC/W emulsions with different surfactant concentrations

Figures 5.37 and 5.38 illustrate the effect of surfactant content on the normalized pressure gradient and permeability reduction. These figures show that lower surfactant content resulted in greater pressure drop across the porous medium and a greater reduction in permeability. Comparison of the results presented in this part of the experiments with the results in the previous sections indicate that the emulsions carrying highly viscous oil experienced a greater pressure drop and permeability reduction compared to the ones containing less viscous oil.

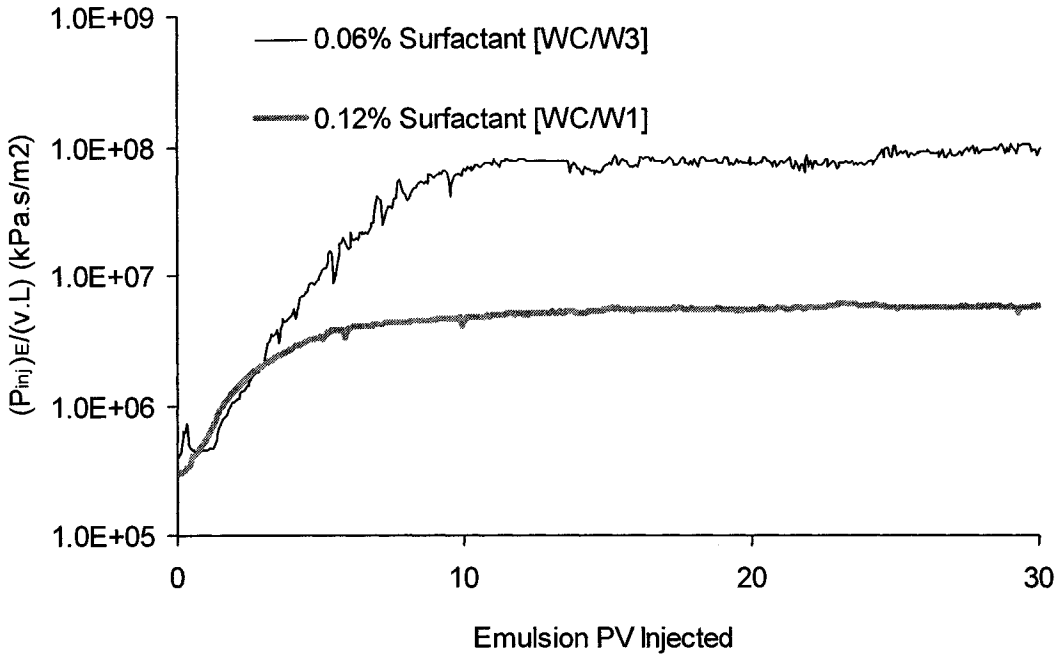

Figure 5.37 Pressure gradients for the injection WC/W emulsions with different surfactant contents

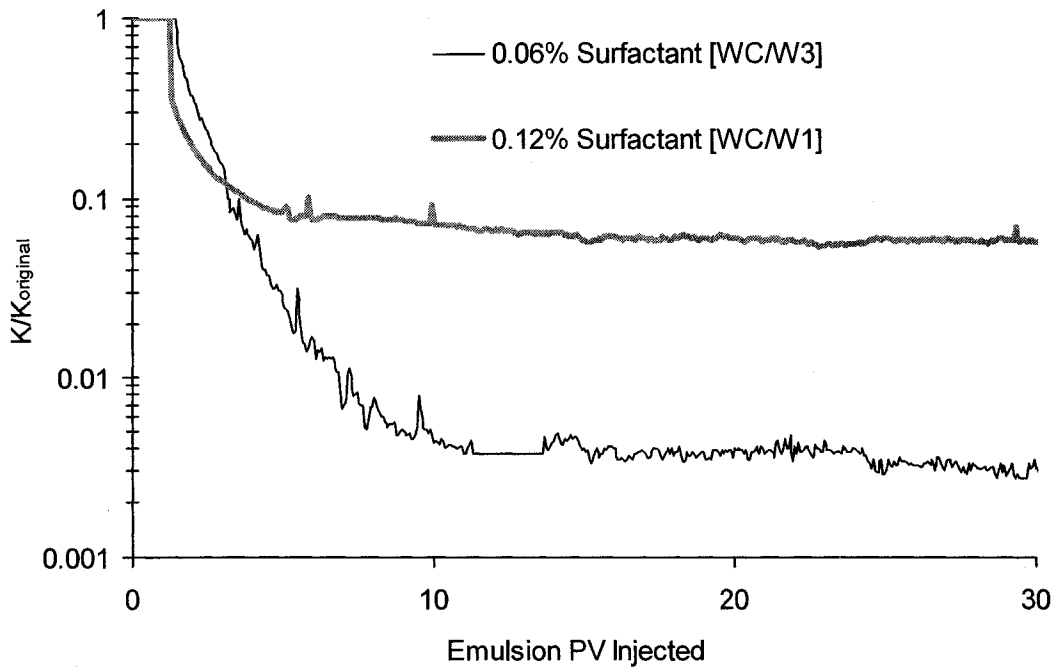

Figure 5.38 Permeability ratios for injection of WC/W emulsions with different surfactant contents

5.8 *Effect of Permeability and Injection Velocity*

Seven experiments were performed in this part of the study. They were conducted to quantify the effect of porous medium permeability and injection velocity on the overall pressure drop across a porous medium for emulsions prepared with different oil types. The mineral oil-in-water (M/W4) and Western Canadian oil-in-water (WC/W1) emulsions were injected into different glass bead packs with a wide range of permeabilities. Both emulsions had a 13% quality and a surfactant content of 0.12% (volume/volume). All experiments were performed at a constant injection rate of 3 cm^3/min.

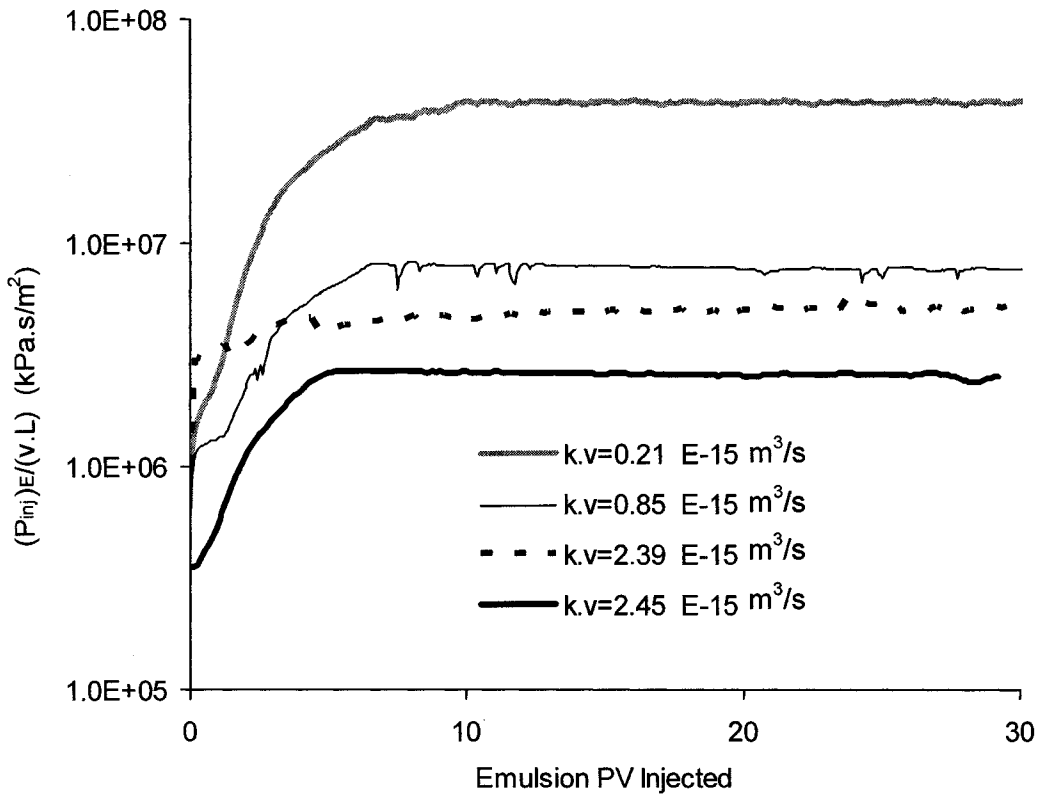

Figure 5.39 Pressure gradients for the injection of emulsion M/W4 with various velocities into different porous media

Figure 5.39 shows the overall normalized pressure gradient profiles for the experiments that used emulsion M/W4. It indicates that the overall pressure gradient

has a direct inverse relationship to the porous medium permeability times the injection velocity. Similarly, Figure 5.40 indicates that the overall pressure gradient has a direct inverse relationship to the porous medium permeability times the injection velocity for all of the experiments that used emulsion WC/W1.

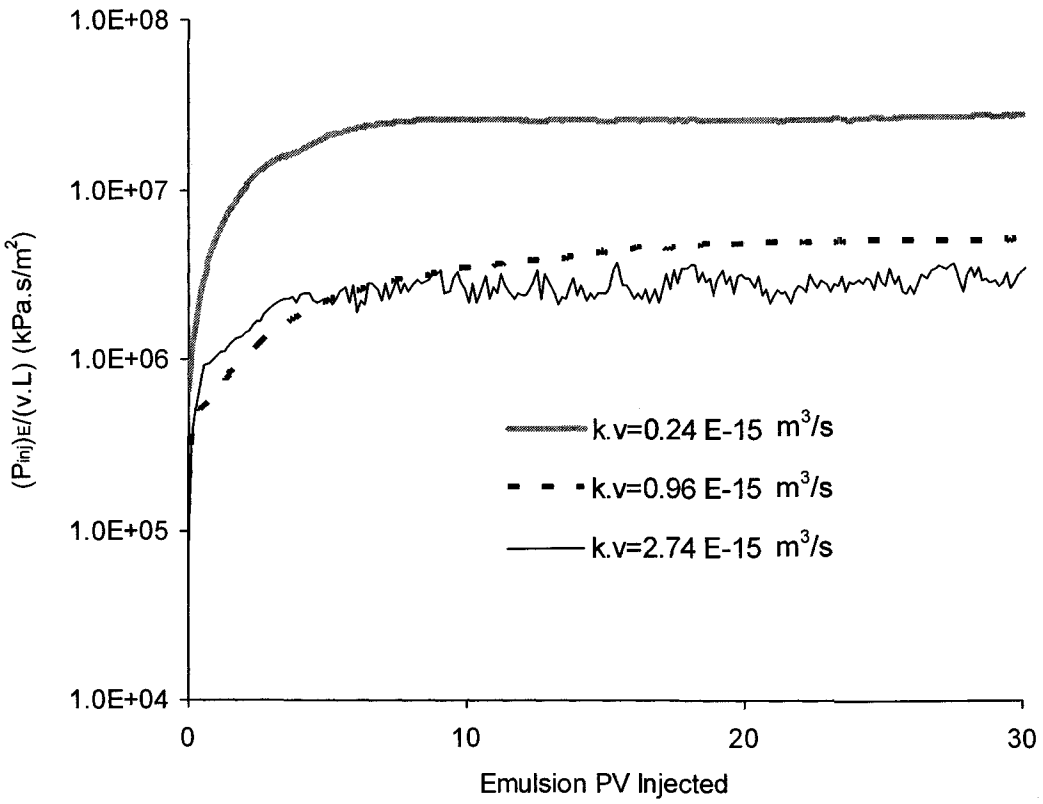

Figure 5.40 Pressure gradients for the injection emulsion WC/W1 with various velocities into different porous media

Chapter 6. Core Flood Experiments

In the previous two chapters, the emulsion blocking mechanism and factors that affected its penetration depth into a porous medium were studied in low pressure visual flow tests. In the field, however, high pressures are usually applied to inject emulsions into a formation. Therefore, core flood experiments were undertaken at high pressures to alleviate the limitations involved in the visual flow experiments. This allowed the preparation of low permeability packs, which are more representative of field conditions. The only drawback is that visualization was not possible in the steel core holders. The aim was to demonstrate the principle of placement and the fixing of a heavy oil-in-water emulsion in a porous medium. Experiments were conducted to ensure that the previously visualized mechanisms involved in the sealing process were applied to a natural porous medium. Additionally, parameters that affect the placement of the emulsion into the porous medium were studied. Placement involves injection, penetration, and propagation of the emulsion. This chapter describes the experimental setup, the characteristics of the emulsions used and the properties of the porous media. Next, the applicability and effectiveness of heavy oil-in-water emulsion in sealing a porous medium is presented. Finally, the elements of a heavy oil-in-water emulsion's effect on sealing efficiency and penetration depth are adjusted in order to block off a specific porous medium with a known permeability.

6.1 *Experimental Setup and Procedure*

Figure 6.1 is a schematic of the experimental setup. It consists of a piston-type constant rate ISCO pump, a stainless steel core holder with a total length of 29.2 cm and inner diameter of 1.9 cm, a pressure transducer, an HP data logger, and a computer for storing the pressure data. A transfer vessel was used to displace the desired emulsion by water, which was pumped by the ISCO pump. An injection

pressure relief system, which includes a pressure gauge and a relief valve, was used to offset the high pressure environment.

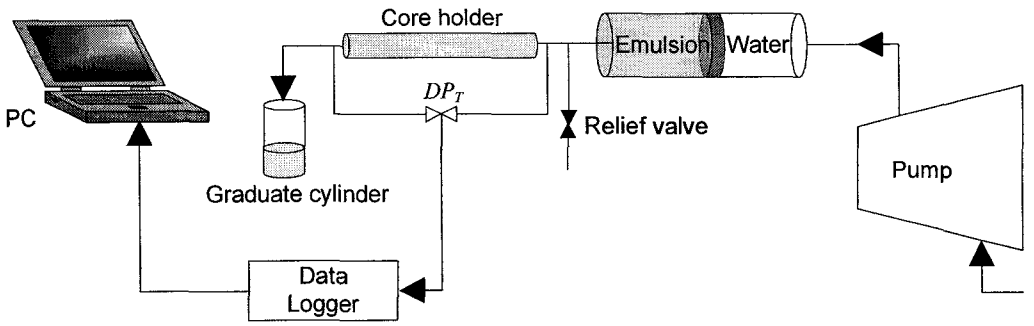

Figure 6.1 Schematic of the experimental setup for core flooding experiments

Figure 6.2 shows a photograph of this experimental setup. This is the setup that was used to determine the properties of a porous medium. The figure does not include two pieces of equipment: the transfer vessel and the pressure relief system. They were added to the setup before the initiation of emulsions injection tests.

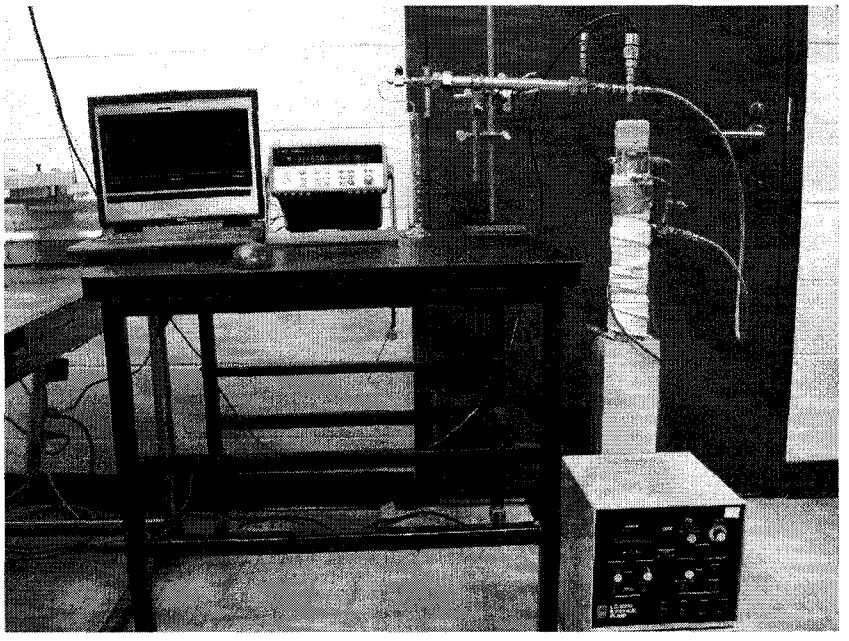

Figure 6.2 Photograph of the experimental setup for core flooding experiments

The procedure for conducting the experiments was identical to those that preceded it. Glass bead packs were dry packed into the core holder. Then, the dry-packed porous medium was degassed by saturating it in a vertical position and under capillary imbibition forces for twelve hours. The packed medium properties, including pore volume, porosity, and permeability, were then determined. Pore volume was measured using imbibition of distilled water; porosity was determined using the weight method; finally, permeability was calculated using Darcy's law at several flow rates. Once the properties were determined, the medium was saturated with distilled water and the emulsion injection tests began.

6.2 *Emulsion Types*

Heavy oil-in-water emulsions were used in the experiments. They were prepared by the agent-in-water method with a 13% quality by volume. The Lloydminster oil was mixed with a solution of water and Triton X-100 surfactant using the Brinkmann homogenizer. It was impossible to mix the oil into the distilled water at room temperature because of its high viscosity. Therefore, the oil was warmed up to 50°C and mixed with slightly preheated distilled water. The produced emulsions were characterized in terms of their stability and droplet size distributions. Table 6.1 summarizes the properties of the emulsions prepared for and used in the experiments.

Emulsion designation	Oil type	Quality (%)	Surfactant concentration (%)	Mean droplet size (μm)
LM/W2	Lloydminster oil	13	0.12	11
LM/W3	Lloydminster oil	13	0.48	6.7
LM/W4	Lloydminster oil	13	0.12	11.2
LM/W5	Lloydminster oil	13	0.24	10.3

Table 6.1 Properties of emulsions used in core flooding experiments

6.3 *Blockage Demonstration*

This section provides the results obtained in examining the ability of heavy oil-in-water emulsions to block a porous medium. For the purpose of field applications, cores with different permeabilities, ranging from hundreds to thousands of milli-Darcies, were tested. The emulsion LM/W2 was injected into these cores. This emulsion had a quality of 13%, surfactant content of 0.12% (volume/volume), a mean droplet size of 11 μm and was produced at a shear mixing rate of 5000 rpm.

6.3.1 Emulsion Injection in Low-permeability Core

In this experiment, the core holder was packed with very fine glass beads (less than 250 mesh), which yielded a permeability of 0.285×10^{-12} m^2 (0.289 Darcy). The emulsion LM/W2 was injected under a constant flow rate of 3 cm^3/min. The injection pressure increased consistently at the early stage of injection. Figure 6.3 shows that the glass beads pack plugged after injecting only 2.1 pore volumes of the emulsion. The maximum injection pressure was set at 12,400 kPa (1,800 psi); any injected fluid beyond this pressure was bled through the relief valve.

Examining the core after the experiment, we found that the oil droplets were captured within the first 20% (~ 6 cm) of the total length of the core. Considering the quality of the emulsion was 0.13 and the fact that most of the droplets were captured within the porous medium, we can expect that the emulsion front penetrated into the core up to 2.1 times 0.13, which is equal to 0.27 fraction (27%) of the total core length (7.8 cm). This difference could be the result of droplets that are captured and coalesce at the porous medium face, rather than inside the porous medium.

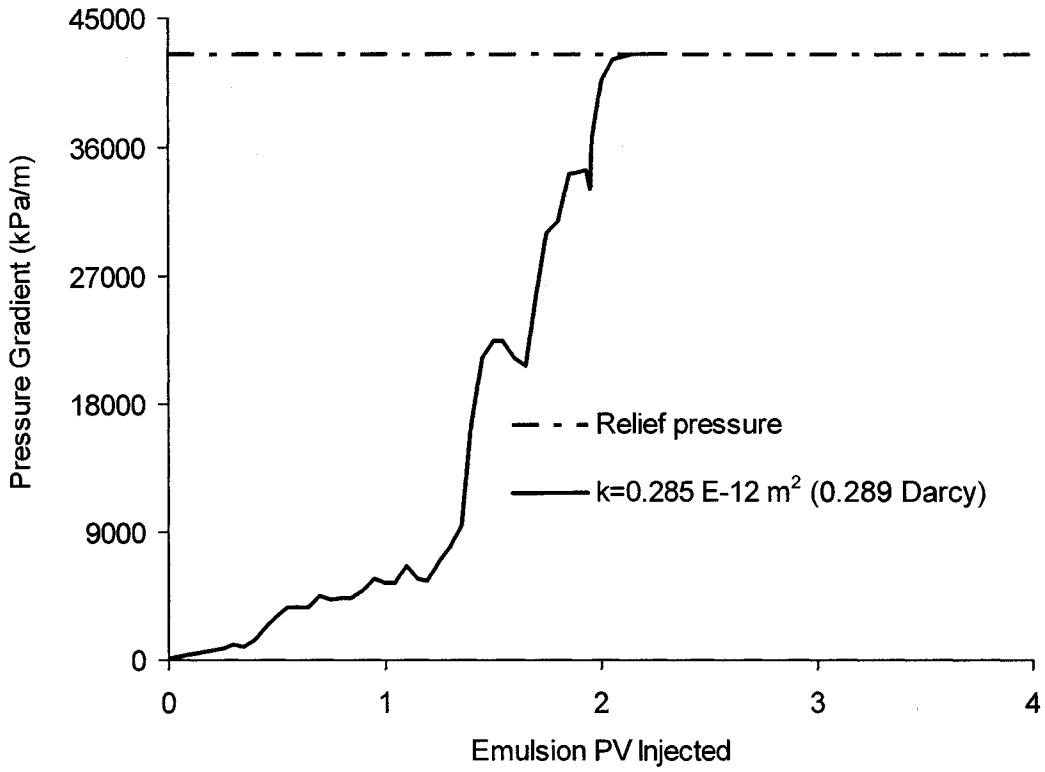

Figure 6.3 Pressure gradient for the injection of emulsion LM/W2 in low-permeability core

6.3.2 Emulsion Injection in Medium-permeability Core

In this experiment, the core holder was packed with relatively fine glass beads between 200 and 230 mesh, which yielded a permeability of 0.69×10^{-12} m^2 (0.70 Darcy). The emulsion LM/W2 was injected under a constant flow rate of 3 cm^3/min. Its front penetrated deeper into the core compared to the pervious experiment (i.e. low permeability core). As the emulsion injection continued, the injection pressure increased dramatically. After injecting 4.6 pore volumes of the emulsion, the pressure increased abruptly and a few minutes later the pressure became too high for further injection.

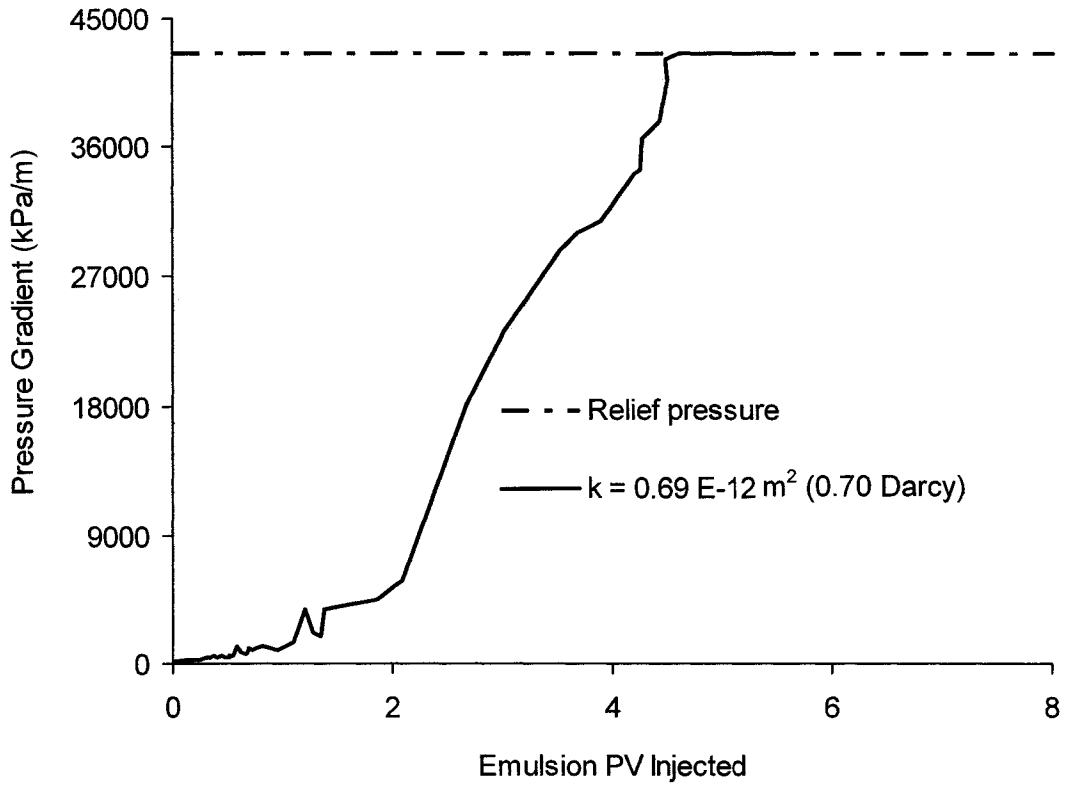

Figure 6.4 Pressure gradient for the injection of emulsion LM/W2 in medium-permeability core

Figure 6.4 illustrates the pressure gradient for this experiment. This figure also indicates that the core was plugged after injection of 4.6 pore volumes of emulsion. As in the previous experiment, the injected fluid was bled through the relief valve when the injection pressure exceeded 12,400 kPa (1,800 psi).

Examining the core after the experiment revealed that the emulsion front penetrated within the first 58% of the total length of the core (~ 16.9 cm). This was close to the prediction that the emulsion should have propagated into 60% of the total length of the core (4.6 times 0.13 = 0.60) before blocking it.

6.3.3 Emulsion Injection in High-permeability Core

In this experiment, the core holder was packed with a mixture of fine and coarse glass beads between 100 and 320 mesh, which yielded a permeability of 2.83×10^{-12} m^2 (2.87 Darcy).

Similar to the previous two experiments, the emulsion LM/W2 was injected at a constant flow rate of 3 cm^3/min. However, its front passed through the core before plugging the pack. The core was plugged after injection of nearly 9 pore volumes of emulsion. As in the previous experiments, the injected fluid was bled through the relief valve when the injection pressure exceeded 40,700 kPa (1,800 psi). Figure 6.5 shows the pressure gradient across the core in this experiment.

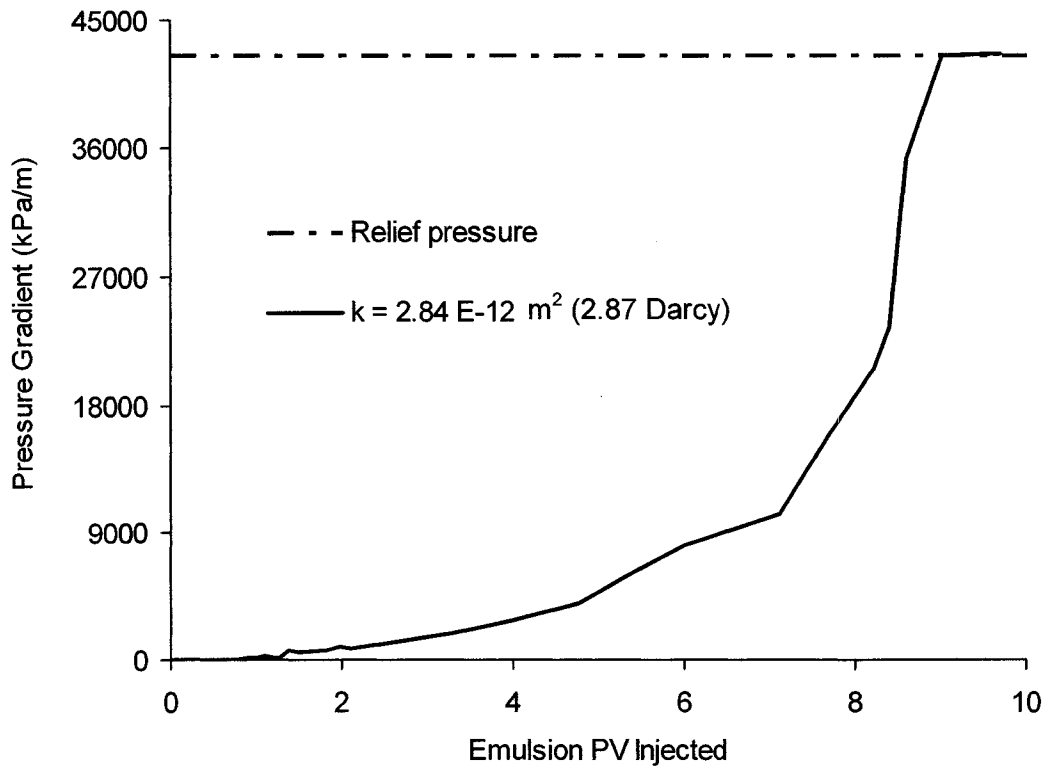

Figure 6.5 Pressure gradient for the injection emulsion LM/W2 in high-permeability core

6.4 *Formulation an Emulsion to Block a Porous Medium*

In this portion of the experiment, the mean droplet size and surfactant content of a Lloydminster oil-in-water emulsion were adjusted to block a porous medium with a given permeability. Ideally, the customized emulsion would penetrate as deeply as possible into the porous medium before blocking it. The core holder was packed with glass beads between 120 and 140 mesh. The reason for choosing a relatively narrow glass bead size was so that its mean pore throat size could be calculated mathematically. The mean pore throat size for this medium was 10.25 μm and the measured permeability was 3.55×10^{-12} m^2 (3.6 Darcy).

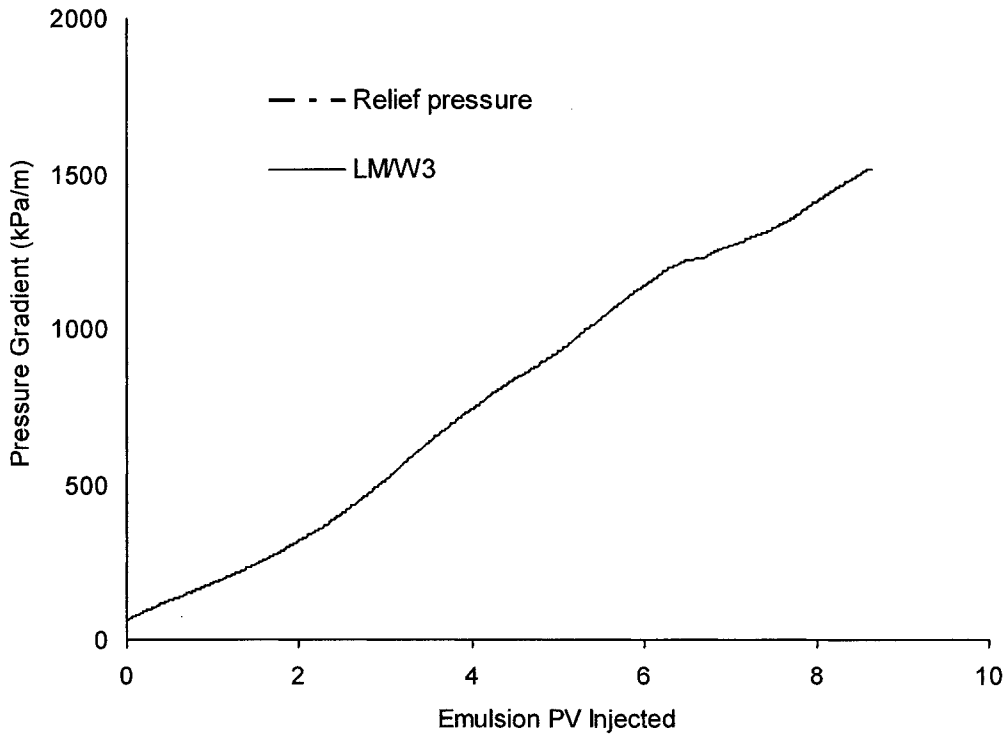

Figure 6.6 Pressure gradient for the injection of emulsion LM/W3

In the first step, the Lloydminster oil-in-water emulsion (denoted LM/W3) with a dispersed phase ratio of 13% and surfactant concentration of 0.48% (volume/volume) was prepared at a shear mixing rate of 6000 rpm. This emulsion had a mean droplet size of 6.7 μm. It was injected at a constant rate of 3 cm^3/min.

During the injection, most of the emulsion passed through the porous medium without blocking it, likely because the high surfactant content and low ratio of its droplet-to-pore throat sizes. Figure 6.6 illustrates the pressure gradient for the injection of this emulsion.

In the second step, the same porous medium was washed with toluene, IPA and an excess amount of water. Emulsion LM/W4 was prepared similar to emulsion LM/W3 except that the surfactants content differed (0.12% volume/volume) and the shearing mixing rate was lower (4900 rpm). The mean droplet size of this emulsion was 11.21 μm, and it was injected at a rate of 3 cm^3/min. Figure 6.7 indicates that the porous medium was blocked after the injection of only six pore volumes of this emulsion. The emulsion front penetrated up to 78% of the total core length (i.e. 6 pore volumes times 0.13 emulsion quality = 0.78 of the total core length) before it broke down and blocked the porous medium.

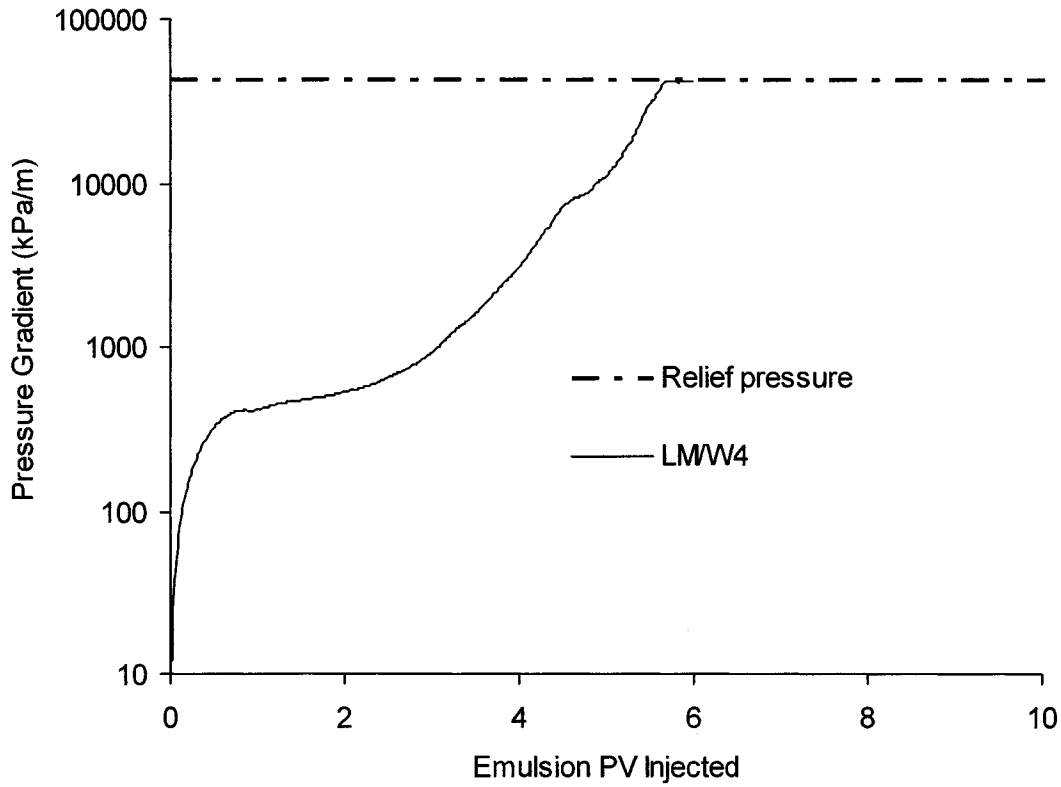

Figure 6.7 Pressure gradient for the injection of emulsion LM/W4

In the final step, the emulsion's penetration depth was maximized to the desired distance: the total core length in this experiment. Analysis of the previous two experiments indicated that the penetration depth could be improved with slightly smaller droplet sizes and higher surfactant content compared to LM/W4, but larger droplets and lower surfactant content than emulsion LM/W3. Therefore, emulsion LM/W5, which contained 0.24% (volume/volume) surfactant, was prepared at a shear mixing rate of 5100 rpm. It exhibited a mean droplet size of 10.3 μm. Figure 6.8 indicates the pressure gradient for the injection of the emulsion LM/W5 at 3 cm^3/min into the same core. It illustrates that the injection of the carefully formulated emulsion LM/W5 was successful in blocking the porous medium (after injection of 13 pore volumes of the emulsion). The desired penetration depth was achieved, and the blockage only occurred after the emulsion front exited the core.

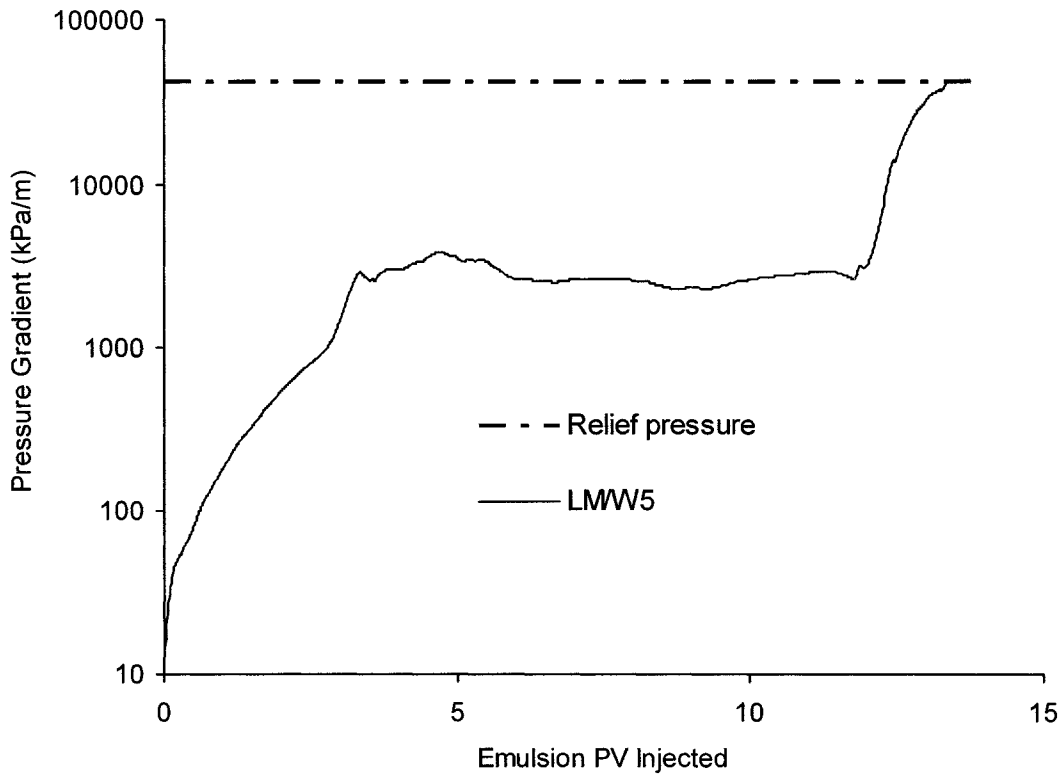

Figure 6.8 Pressure gradient for the injection of carefully formulated emulsion LM/W5 to block a porous medium with known permeability

Chapter 7. Discussion of Results

In this chapter, the results presented in the last three chapters are evaluated in greater detail and the effects of certain parameters are discussed. A general overview of the experimental repeatability and error analysis are presented. The results are then discussed and compared with works reported in the literature.

7.1 *Repeat of the Experiments and Error Analysis*

All of the experiments presented in Section 5.8 were repeated to ensure the reliability of the results and to calculate the error involved in repeating experiments. The knowledge that we have about each set of experiments is obtained from the experimental measurements. All laboratory measurements are subject to uncertainties. It is preferred to minimize the error.

The nature of each experiment and the complexity involved in conducting it dictate the number of repetitions. For example, in conducting the qualitative experiments presented in Chapter 4, an experiment may have been repeated more than 10 times until a good image of the droplets captured. The main problem was related to detecting the light oil (i.e. mineral oil) droplets under the microscope. Different dyes (black, blue, purple and red) were used in order to produce oil droplets with good contrasts. The red dye created the best contrast and therefore it was used in all the mineral oil-in-water emulsion experiments. Another issue was related to the visualization system. Droplets smaller than 40 μm were barely visible under the microscope. Stable emulsions with droplet sizes greater than 75 μm were produced only from mineral oil but the Lloydminster and Western Canadian oils did not produce coarse emulsion with mean droplet size of greater than 75 μm. This is the reason why mineral oil-in-water emulsion was used in most of the experiments conducted on the etched glass micro-model.

The uncertainty associated with the glass bead experiments presented in Chapter 5 is even greater. The main issue is related to the size distribution of the glass beads within the cell and also how closely these beads are packed. The size distribution of the glass beads is known before packing; however, it changes during the packing process. Most likely the coarser beads stay at the top and the smaller ones settle at the bottom of the cell. Also, the packs were affected by the procedure of assembling the micro-model. Table 7.1 shows the variation in the calculated average permeability of the front, rear, and the entire packed medium for the experiment that was presented in Section 5.8 (injection of emulsion M/W4, k.v = 2.45 m^3/s).

Water flow rate (cm^3/min)	Porous medium front section permeability (m^2)	Porous medium rear section permeability (m^2)	Porous medium overall permeability (m^2)
3	4.08 E-12	4.03 E-12	4.02 E-12
6	4.05 E-12	3.96 E-12	4.00 E-12
9	4.03 E-12	3.96 E-12	3.99 E-12
Average			**4.00 E-12**

Table 7.1 Variation of permeability at different sections of the packed two-parallel plate micro-model

Figure 7.1 shows the normalized pressure gradients for the main experiment (permeability times linear flow velocity = 2.45 m^3/s) and the experiment that was repeated (permeability times linear flow velocity = 2.44 m^3/s) under similar conditions. Both experiments included the injection of emulsion M/W4 at injection rates of 6 cm^3/min into same glass beads pack (original permeability of 4.0×E-12 m^2).

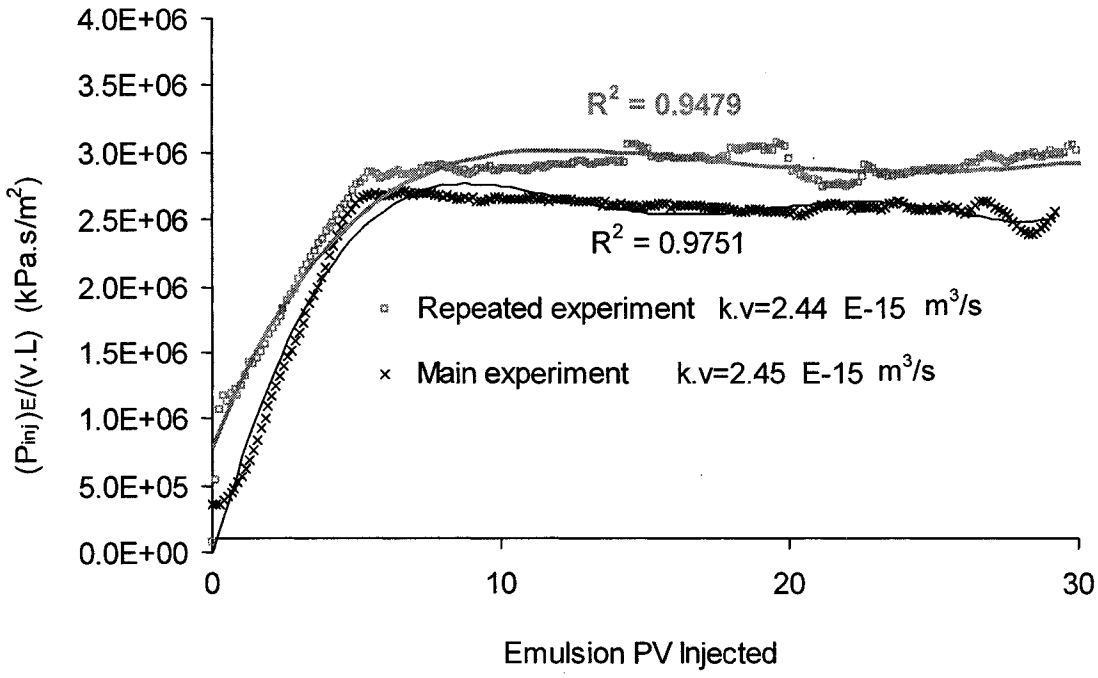

Figure 7.1 Error associated with the injection of emulsion M/W4 into identical glass bead packs (permeability of 4.0×10^{-15} m^2)

When analyzing the errors associated with conducting an experiment, two types of error analysis should be considered: systematic and random. The above discussion points out the main sources of systematic errors such as those related to equipment operation, calibration and their sensitivity or related to other variables such as the method of packing the glass beads, etc. Systematic errors tend to shift all measurements in a systematic way so their mean value is displaced.

The two graphs in Figure 7.1 show a systematic error in the range of 0.25×10^6 to 0.42×10^6 kPa.s/m^2 for the repeated experiment. At least one source of such error is related to the permeability that apparently was slightly disturbed (permeability times linear flow velocity of 2.44 m^3/s instead of 2.45 m^3/s). Many factors could have affected the permeability including those related to cleaning the packs with toluene and isopropyl alcohol.

In analyzing the random errors (errors which fluctuate from one measurement to the next) associated with these two experiments, Figure 7.1 shows that the Residual Sum of Square error is reasonable for both experiments (R^2 of greater than 0.94 for both experiments).

The error analysis of six more experiments is presented in Appendix D.

7.2 *Effect of Droplets Size on the Capture Mechanism*

Analysis of the qualitative experiments performed in Chapter 4 indicates that the droplet-to-pore size ratio had a significant impact on the capture mechanism. The observations were very similar to the mechanisms postulated by Cartmill,[16, 17] McAuliffe,[19] and Soo and Radke.[24, 25] The capture phenomenon was dominated by the droplets larger in size than the pore throat constrictions. The oil droplets flowed slower than the continuous water phase, because they encountered capillary resistance during their flow through smaller pore constrictions. Such mechanism was proposed earlier by McAuliffe,[19] and was implemented in Devereux's[38, 39] mathematical model. However, this was in contrary to the observation made by Soo and Radke,[24, 25] during their flow tests in visual micro-model. They argued that stable oil droplets did not flow in porous medium by being squeezed through pore constrictions.

Droplets captured by size exclusion created an incremental increase in the total pressure gradient. Figure 7.2 illustrates that, for the same emulsion under an equal injection velocity, the pressure gradient increased in the emulsion that carried larger droplets. The pressure gradient was directly related to the number of captured droplets per each site and the depths to which these droplets penetrated the porous medium. This is in accordance with the Young-Laplace equation that predicts the capillary forces across a trapped non-wetting (oil) droplet. As the number of trapped oil droplets increased, the summation of capillary forces and consequently the resultant pressure drop across the micro-model increased.

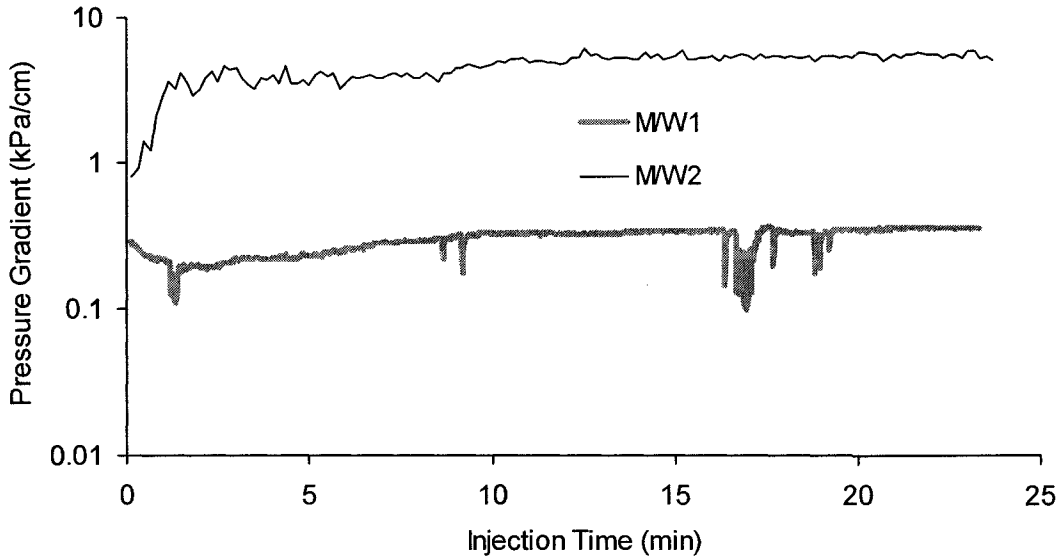

Figure 7.2 Emulsion carrying larger droplets (M/W2) resulted in a higher pressure gradient than the emulsion carrying smaller droplets (M/W1)

On the other hand, smaller droplets had little or no effect on the capture mechanism. They passed through the pore constrictions easily and were driven out of the porous medium under relatively medium to high shear forces. However, at low injection rates, in which the summation of drag, gravity and frictional forces overcame the local shear forces, small droplets could potentially deposit themselves inside pore cervices and at pore throat entrances (Figures 4.10 and 4.19).

Moreover, the number of captured droplets increased as more emulsion was injected. The droplets then accumulated on top of one another, but exhibited different stability behavior, which appeared to be oil-type related.

7.3 *Effect of Oil Type on the Capture of Droplets*

The effect of oil type on the emulsion blocking mechanism has been observed from three different perspectives: the effect of oil type on the release and capture of a

droplet, the droplets' coalescence, and the magnitude of pressure drop across the reduced permeability zone.

Emulsions carrying droplets made of three different oil types, ranging in viscosity, were evaluated. Based on the observations in Figures 4.13, 4.33, 4.36 and 4.39, the probability of capturing oil droplets under straining mechanism seemed unrelated to oil type. Almost all droplets, even of different oil types, that were larger than the pore throat restrictions were captured in the pore entrances. However, Figure 7.3 indicates that the associated pressure drop created by each droplet, and consequently the droplet's maximum resistance against the incoming flow, was higher in relatively viscous droplets. The observations are consistent with the viscosity measurements of different oil-in-water emulsions presented in Figures 5.33 and 5.36. Typically, as the number of retained oil droplets within a porous medium increases, the viscosity of the flowing emulsion increases too. Therefore, the pressure gradient across the porous medium increases because of the combined effects of viscosity and capillarity.

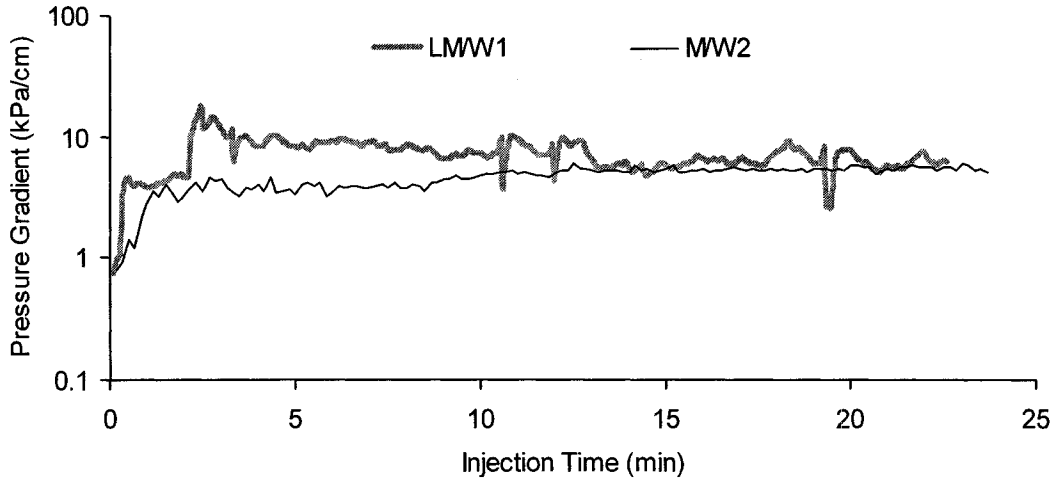

Figure 7.3 Emulsion carrying relatively viscous droplets (LM/W1) resulted in higher pressure gradient

On the other hand, the behavior of smaller droplets was completely different. Small droplets made of light oil (mineral oil) deposited in the pores by gravity and failed to coalesce (Figures 4.10 and 4.11). Their attachment to the pore surface was either nonexistent or so weak that it could not be detected using the visualization equipment. If such attachment of oil droplets to the pore's surface exists, then a more rigorous and sophisticated method of detection is required.

Contrary to the behavior of light oil droplets, the heavy droplets exhibited different behavior: they deposited themselves on the pore's surface (similar to what reported by Soo and Radke[24, 25]), accumulated on top of one another and eventually coalesced (Figures 4.19 and 4.20). As noted by Stanick[74], these heavy fine droplets attached to the pore surface either by gravity or because of higher shear forces that brought them close to the pore surface. The attraction forces between these heavy droplets and the pore surface resisted the local increase in shear forces. The local shear forces increased because of the rising injection rates or of the restricted flow path caused by the deposited droplets. It appeared that the composition of these heavy oil droplets imposed a greater influence on the attachment of smaller droplets to the pore surface. Another consideration is the wettability of the solid phase and the chemistry of the mobile phase that dictates the attachment of such oil droplets to a pore surface. It can be conclude that the heavy oil droplets are most likely to attach to the pore surface more readily than the light droplets, resulting in greater pressure drops.

Figure 7.4 combines the pressure gradient for the injection of the mineral-oil-water (M/W1) and Lloydminster oil-water (LM/W1) emulsions, both with mean droplet sizes smaller than the pore throat size. The figure indicates that a larger pressure gradient resulted for the heavier Lloydminster oil droplets at the same injection rate.

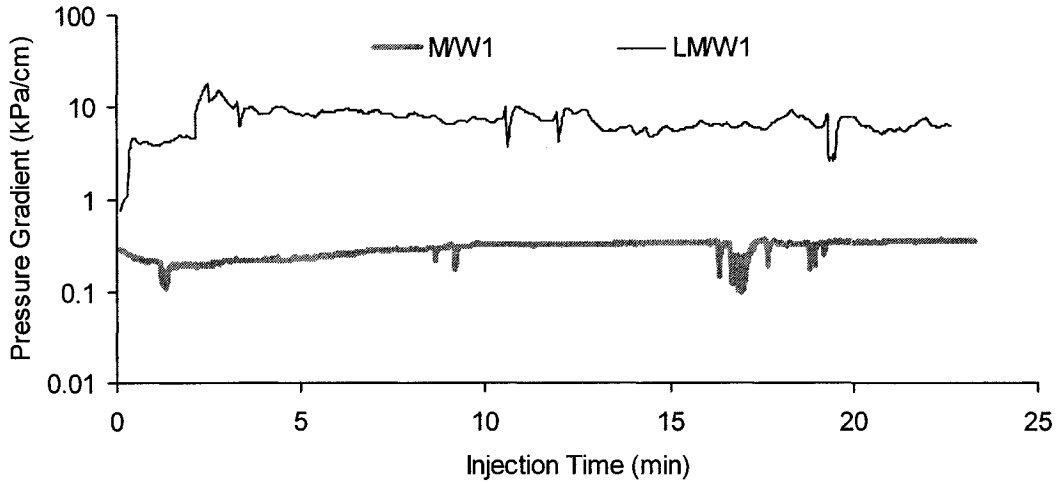

Figure 7.4 Emulsion carrying more viscous droplets (LM/W1) created higher pressure gradient (under the condition of same injection rate)

7.4 *Effect of Wettability Alteration on Capture of Droplets*

As discussed earlier (Section 2.3.2), the wettability of a porous medium affects the capture or release of a dispersed oil droplet and the local capillary pressure across a trapped oil droplet in a pore throat. In addition, it was mentioned that the wettability can be altered by surfactant adsorption on the pore surface or by altering the solution pH. The experiments performed in Section 4.5.2 investigated the effect of different pre-flush solutions on the porous medium wettability, which in turn affects the droplets' capture mechanism as well as the local capillary pressure. The experiments consisted of one base case injection of emulsion M/W3 and three focused on the injection of the same emulsion, each preceded by alkaline, acidic, or surfactant pre-flush.

The emulsion used consisted of large droplets compared to the pore throat sizes. Therefore, the droplets' propagation depth was highly constrained by the local capillary pressure. As anticipated, the wettability shifted to a water-wet system after the application of the surfactant and alkaline pre-flush solutions, facilitating the

passage of oil droplets through the pores, while the acidic pre-flush solution resulted in an oil-wet system. Figure 7.5 indicates the number of occupied pores per unit length of the micro-model in identical injection time intervals for all of the experiments.

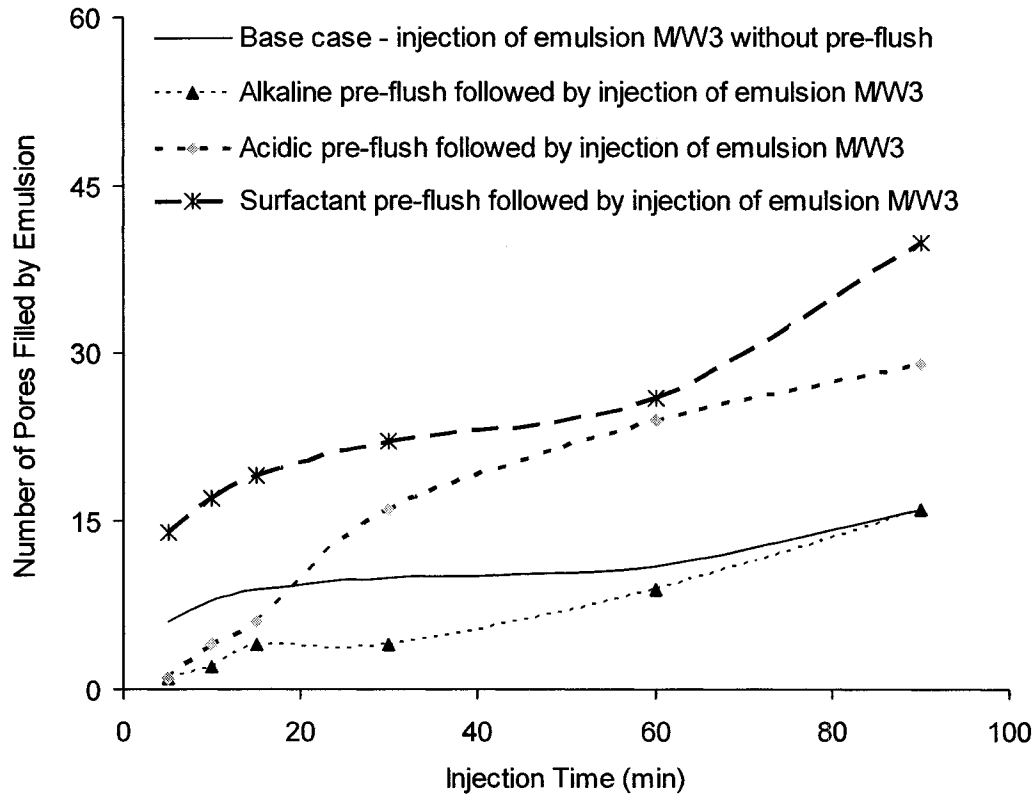

Figure 7.5 Emulsion front position (from etched glass micro-model experiments)

Although there was no established method with which to measure the wettability changes inside the etched glass micro-model, the alkaline pre-flush did not enhance the droplets' penetration depth. The number of occupied pores in series was equal in the base case emulsion injection and in the alkaline pre-flush solution case. However, the acidic pre-flush solution increased the droplets' penetration depth by 81% compared to the base case. Similarly, the surfactant pre-flush increased the penetration depth by 250% compared to the base case.

Clearly, the surfactant pre-flush enhanced the droplets' propagation rate drastically. However, the alkaline and acidic pre-flush solutions affected the droplet penetration depth contrary to original expectations. In general and as reported by Squires,[11] Uren and Fahmy,[13] Atkinson[14] and Cooke et al.,[20] it is expected that the wettability will shift to highly water-wet and oil-wet systems, by applying the alkaline and acidic pre-flush solutions respectively. Therefore, the passage of an oil droplet, with a comparable size to the pore throat constriction, is affected by the wettability of the system. Also, if the droplet is smaller than the pore throat constriction, its motion is constrained by the wettability of the pore surface when such droplet slides over the pore surface and passes from one pore to another. If the system is water-wet, the oil droplet may pass through the pore body easily, while the opposite will occur in an oil-wet system.

The droplet-to-pore size ratio is an important consideration in evaluating the effect of alkaline and acidic solutions on the wettability of the system. If the droplets are much larger than the pore throats, the capillary forces will dominate the capture phenomenon. In such circumstances, the interfacial forces become primary and the effect of wettability is minimized as a result. In the above experiments, the oil droplets were three times larger than the pore throat, so the wettability had a modest impact compared to that of the interfacial tension forces. This helps explain why the surfactant pre-flush improved the droplets' penetration depth by reducing the interfacial tension and altering the wettability. As expected, the surfactant pre-flush solutions increased droplet penetration since the interfacial tension forces dominated the oil droplets and pore structure system.

The inconsistent behavior of the pre-flush solutions is related to their effects on the mobile phase system. The pre-flush solutions affected not only the wettability, but also the stability of the interfacial film. It was well understood by Strassner[65] and Layrisse et al.[66] that an alkaline solution increases the stability of the interfacial film in an emulsion system. The results obtained in this study, also, suggesting that the stability of the droplets increased because of the application of alkaline pre-flush

solution. This increase in the stability of the oil droplets' interfacial film did not allow the droplets to deform and therefore hindered them from percolating further into the pore network. If the droplets were comparable in size with the pore throats, the wettability enhancement as a result of the alkaline pre-flush would be revealed in the form of greater droplet percolation depth. On the other hand, the acidic pre-flush solution caused the destruction of the interfacial film, and the breaking up and coalescence of the droplets. Moreover, this resulted in the production of oil ganglia, which squeezed through pore throats easier than the smaller parental droplets. Figure 7.6 illustrates the detailed effect of the pre-flush solution on the droplet capture and the corresponding pressure gradient in each experiment.

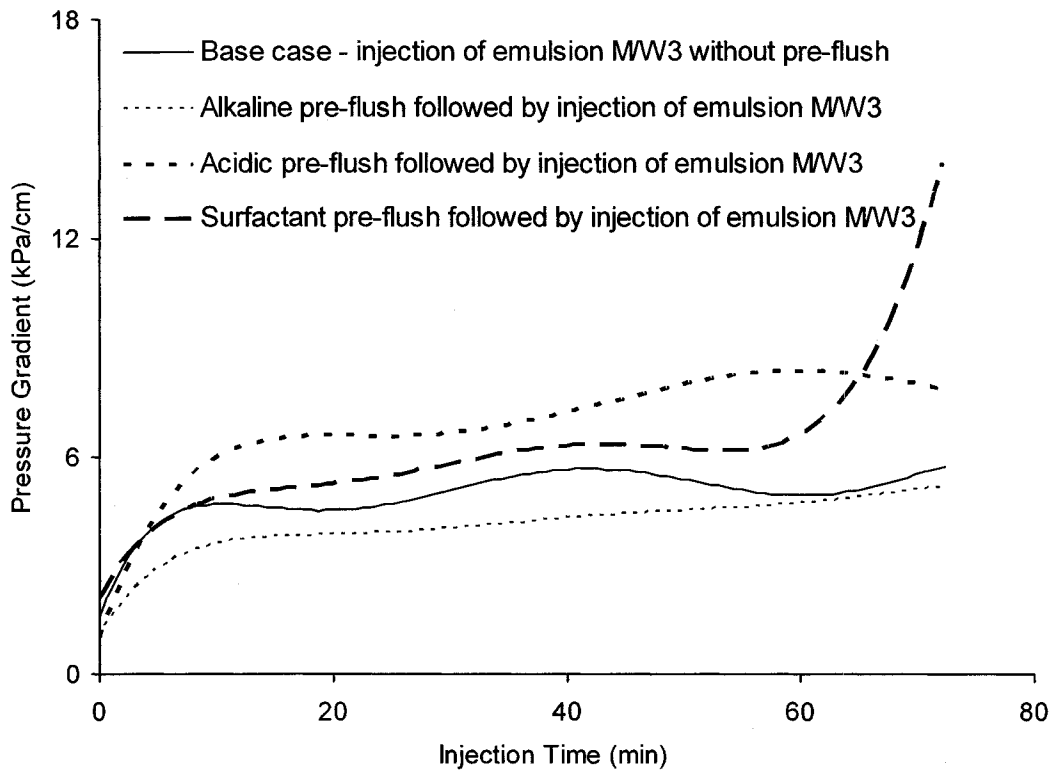

Figure 7.6 The effect of different pre-flush solutions on the pressure gradient

This figure indicates that pressure gradients were directly proportional to the number of captured droplets in each capture site and the depths to which they penetrated the porous medium. The pressure gradient is nearly tripled in the case of the surfactant

pre-flush relative to the base case. This increase in pressure drop was attributed to the droplets' greater penetration depth. Since the acidic pre-flush caused some droplets to coalesce and produce larger droplets, higher injection pressure was required to pass these large droplets through pore throats. Moreover, the alkaline pre-flush reduced the pressure drop more across the porous medium compared to the base case, because of its combined effect on wettability and interfacial tension forces.

7.5 *Effect of Surfactant Content on Droplet Capture*

Analysis of the results in Chapter 4, specifically S ection 4.6, revealed that the surfactant content within an emulsion is the most important factor affecting droplet capture. As the surfactant content of an emulsion increased, the size of the droplets decreased because of the further reduction in the oil droplets-to-water interfacial tension. The reverse case is valid for low surfactant content. Since the importance of droplet size in the capture mechanism has been emphasized, such capture mechanism is highly related to oil-to-water interfacial tension phenomenon.

If a sufficient amount of surfactant is present in the emulsion, the droplets will accumulate in the pore throats and within the pores, and squeeze through the pore throats under high injection pressures (Figures 4.14, 4.33 and 4.36). As proposed by Cartmill,[16, 17] the droplets may undergo deformation or, in some instances, break apart while squeezing through the pore constrictions (Figures 4.15 and 4.16). The pressure gradient created by these strained droplets increased linearly as more pore volumes of the emulsion were injected. Similar to the observations made by Soo and Radke[24, 25] and Woo et al.[33], the magnitude of this pressure gradient was controlled by the volume of retained droplets, and the droplets' ability to restrict flow. The pressure gradient then leveled off after each capture site was filled.

On the other hand, the results obtained from experiments conducted on low surfactant emulsions (Sections 4.6.3 and 4.6.5) reveal that the oil droplets are most

likely to coalesce at some point during the injection. The droplets' coalescence results in the production of highly viscous oil ganglia (if the droplets were made of highly viscous oil) that demand high pressure to be mobilized within the porous medium.

7.6 *Effect of Surfactant Content on Emulsion Flow Behavior*

The experiments presented in Section 5.7 reveal that the surfactant content within an emulsion has a critical effect on the emulsion flow behavior. All of the experiments presented in Section 5.7 were combined: the pressure drop behavior of each is shown in Figure 7.7. This figure illustrates the flow behavior of emulsions comprised of two oil types: mineral oil and Western Canadian oil. Each emulsion had a different surfactant concentration.

This figure indicates that the emulsion with the least surfactant content created a higher pressure drop when it was comprised of the same oil type and injected into an identical porous medium under equivalent injection rates. For mineral oil-in-water emulsions (M/W), emulsion M/W5 resulted in a higher pressure drop relative to M/W4. Similarly, the pressure drop across the porous medium was greater with emulsion WC/W3 compared to WC/W1.

For the emulsions that contained equivalent amounts of surfactant, but were comprised of different oil types, the emulsion carrying highly-viscous oil droplets experienced the most dramatic pressure drop. For example, Western Canadian oil-in-water emulsion with 0.06% surfactant content (emulsion WC/W3) created a higher pressure drop than the mineral oil-in-water emulsion with the same surfactant content (emulsion M/W8).

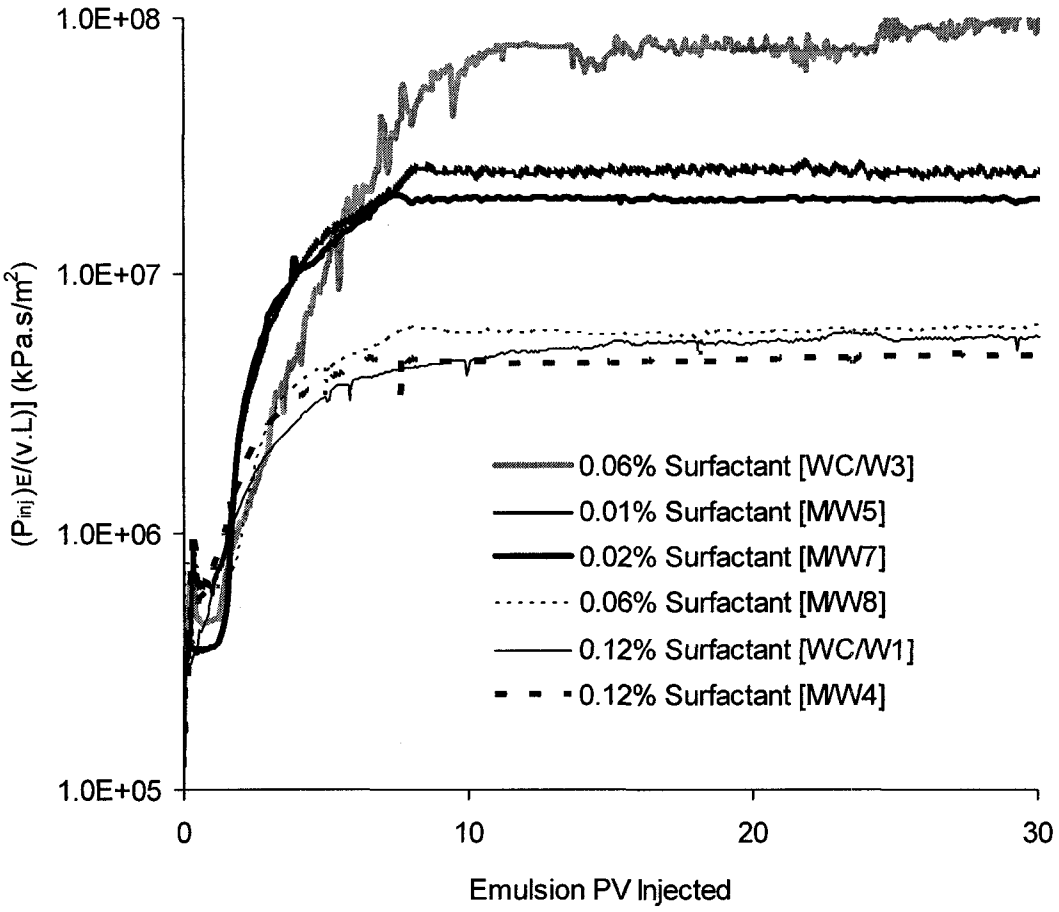

Figure 7.7 Effect of surfactant concentration on the flow behavior of different emulsions

The permeability of the porous medium decreased as the surfactant content within an emulsion decreased for the same oil type (Figure 7.8). For example, emulsion M/W5 and WC/W3 reduced the permeability of the porous medium more than emulsions M/W4 and WC/W1, respectively. In addition, the emulsion that was comprised of highly-viscous oil and contained low surfactant content caused the highest reduction in the permeability of the porous medium.

The overall trend of permeability reduction was very similar to those reported in the literature by Cartmill,[16, 17] McAuliffe,[19] Soo and Radke,[24, 25] French et al.[27] and Yeung and Farouq Ali.[29] The permeability ratio was decreased as the emulsion front

propagated into a porous medium. However, the continuous reduction in permeability was in contrary to the Mendez's[32] results, who showed that the permeability reduced in two stages.

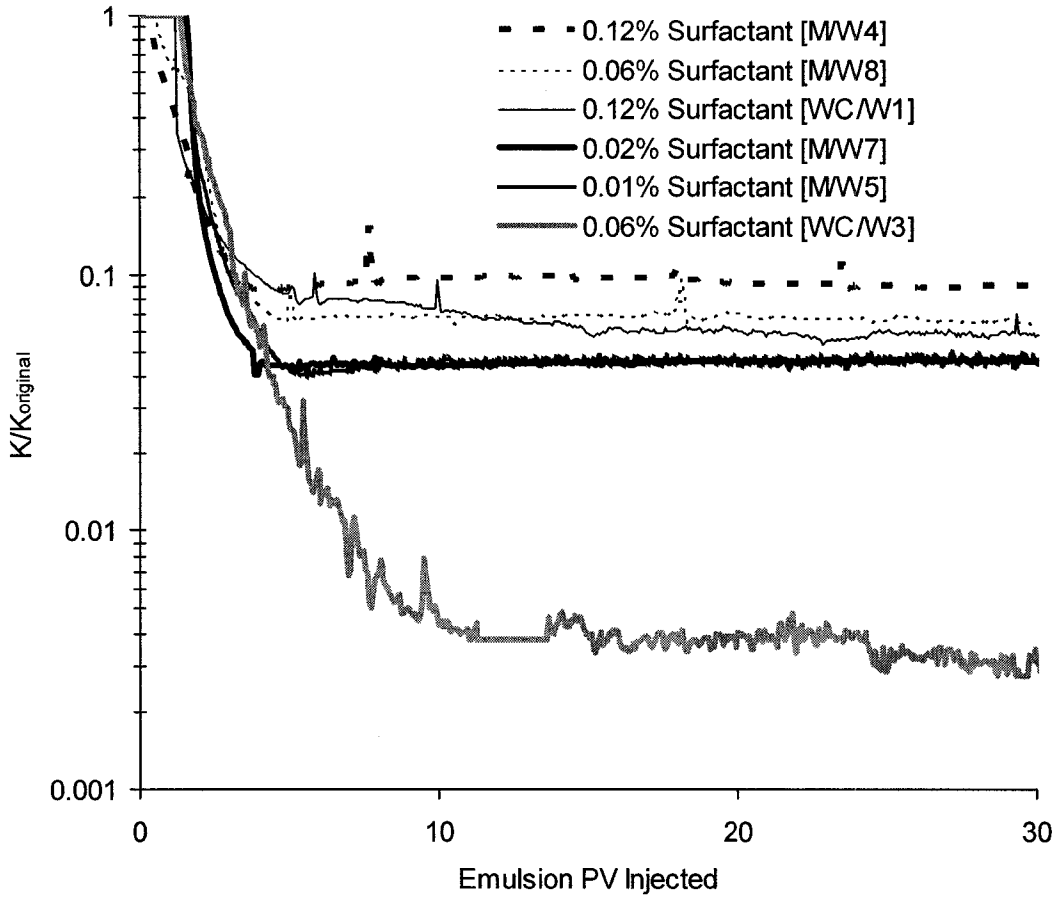

Figure 7.8 Effect of surfactant content and emulsion type on permeability ratios

7.7 *Effect of Droplet-to-Pore Size Ratio on Emulsion Flow*

As discussed in Section 7.2, the droplet size has a significant effect on the capture phenomenon. Similarly, the flow behavior of an emulsion through a porous medium is highly affected by the droplet-to-pore size ratio. Section 5.1 presents the results of experiments that were designed to evaluate this effect. Figure 5.24 illustrates that a high pressure drop is expected in a porous medium with small pore throat sizes

when an identical emulsion is injected under identical conditions in two porous media with different pore throat distributions. Similarly, Figure 5.26 indicates that a high pressure drop occurred by injecting an emulsion with large droplet sizes into identical porous media. Figure 7.9 combines the effects of injecting an identical emulsion (M/W4) under similar injection constraints into two porous media. One medium was packed with fine glass beads while the other was packed with a mixture of fine and coarse glass beads. This illustrates that a high pressure drop and reduction in permeability occurred in a porous medium with smaller pore throat openings (i.e. fine glass beads).

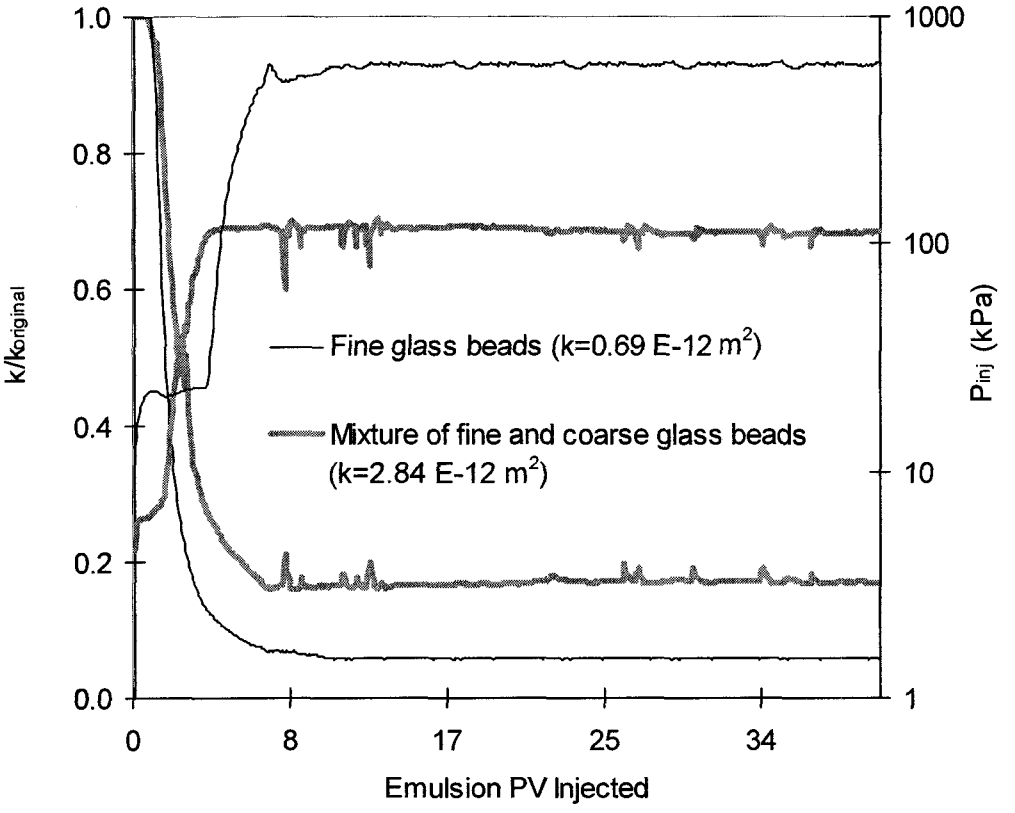

Figure 7.9 Injecting identical emulsions into two glass bead packs with different pore throat sizes

7.8 *Effect of Oil Type, Injection Velocity and Permeability on Emulsion Flow*

The following is a discussion of the results of the seven experiments presented in Section 5.8. These experiments included the injection of different emulsions prepared of different oil types into synthesized porous media with a wide range of permeabilities. The most important factors affecting flow behavior are the porous medium properties (permeability and wettability), and the properties of the emulsion including emulsion quality and oil type, surfactant type and concentration. In the following discussion, the effect of oil type, permeability and injection velocity will be considered assuming constant emulsion quality, surfactant content and emulsion droplet size. The results show that, for a specific emulsion injected into two porous media with different characteristics and under equivalent injection velocity, higher pressure drops resulted for a porous medium with the smaller permeability.

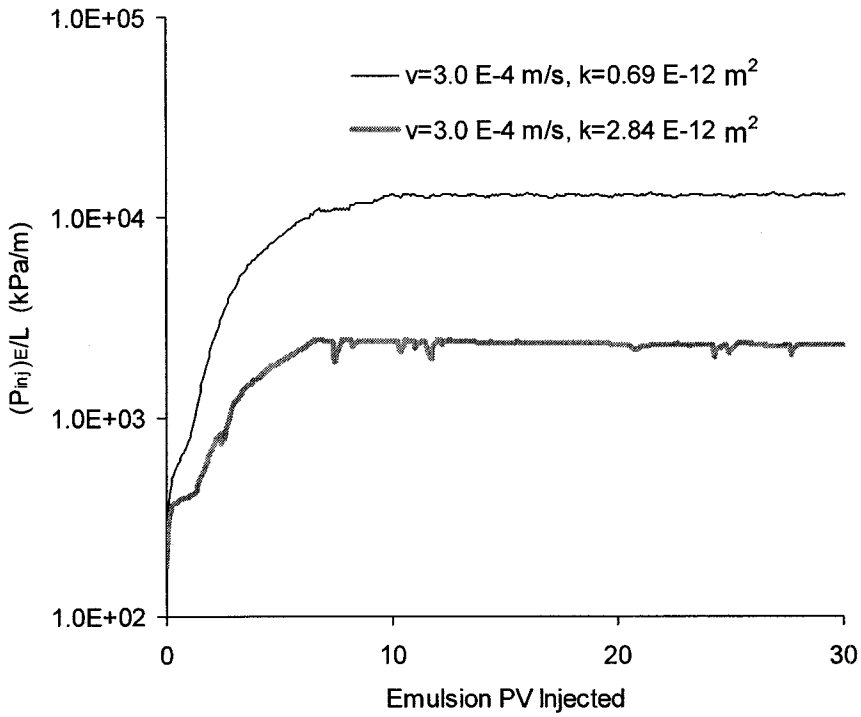

Figure 7.10 Pressure gradient for the injection of emulsion M/W4 in two porous media with different permeabilities

Figure 7.10 displays the pressure gradient for the injection of emulsion M/W4 into two glass bead packs with different permeabilities. However, the droplet size distribution affected the pressure gradient dramatically. Similarly, injection of emulsion WC/W1 in two porous media with different permeabilities resulted in a higher pressure gradient for the porous medium with a lower permeability (Figure 7.11).

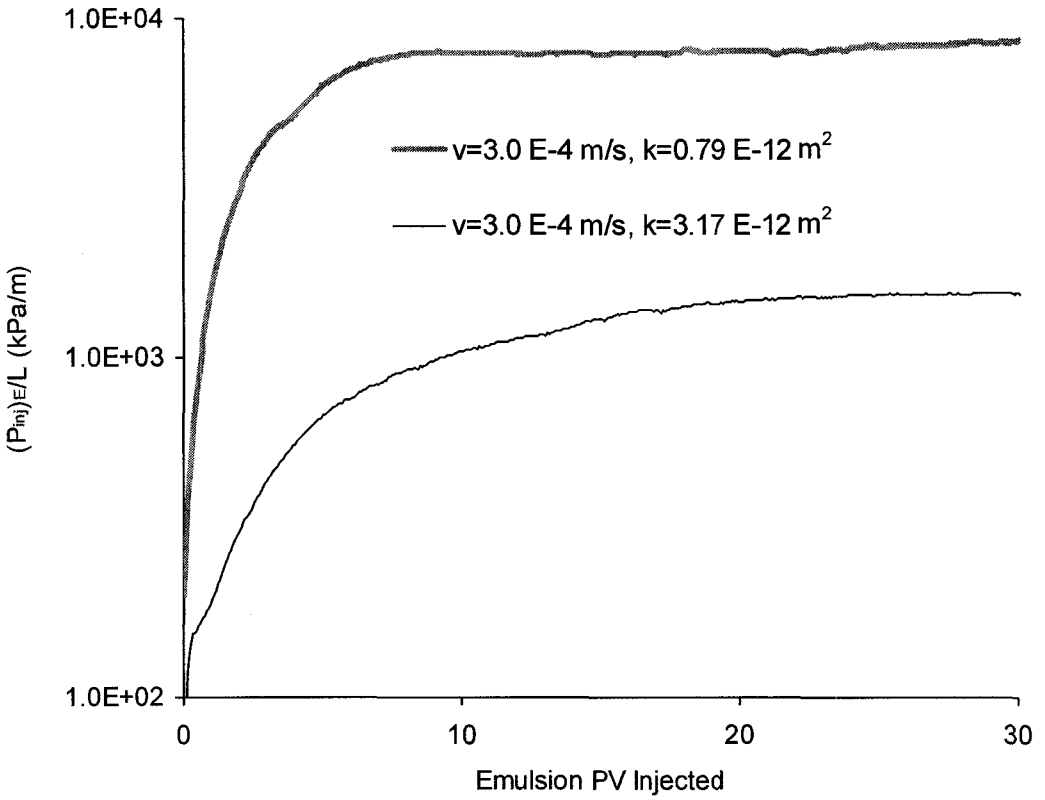

Figure 7.11 Pressure gradient for the injection of emulsion WC/W1 in two porous media with different permeabilities

Comparison between Figures 7.10 and 7.11 reveal that the emulsion comprised of heavier oil droplets resisted an increased pressure drop for a given porous medium permeability and injection velocity. Clearly, the emulsions normalized pressure gradient has a direct inverse relationship to the porous medium permeability times the injection velocity as illustrated in Figure 7.12.

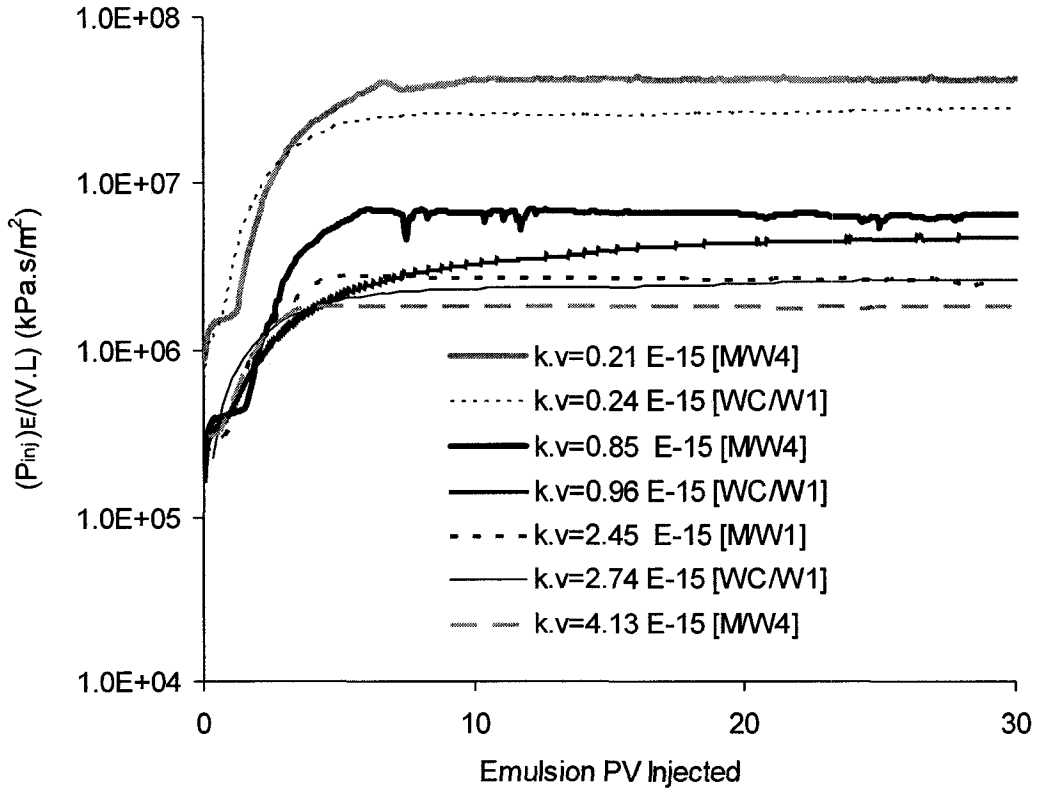

Figure 7.12 Effects of oil type, injection velocity and permeability on pressure gradient for the injection of different emulsions

The overall emulsion flow in porous media was found to be similar to the filtration process proposed by Soo and Radke.[24, 25] A correlation (Equation 5.1) was proposed that predicts the front position of any stable oil-in-water emulsion in porous media. This equation was extracted based on the emulsion front that was monitored during the injection of different emulsions in a variety of porous media. It predicts accurately enough the front position of a stable oil-in-water emulsion that carries oil droplets with a mean size of greater than the pore throat diameter.

7.9 *Effect of Emulsion Type in Sealing a Porous Medium*

The experimental results presented in Chapter 6 indicate that emulsion characteristics, specifically oil type, mean droplet size and emulsion viscosity,

determine its ability to block a porous medium. As investigated by Romero et al.[35] in attempt to seal a highly permeable fractured zones, it was found that the use of properly produced viscous oil-in-water emulsion may result in the sealing of a porous medium that can resist high pressures. Although Romero et al. were not able to plug a porous medium completely, this work proved that applying the Lloydminster oil-in-water emulsion (LM/W2) blocked porous media with differing permeabilities (Figure 7.13). However, the depth to which the emulsion penetrated before it broke down was less in the lower permeability porous media. In the other words, all porous media were sealed, but the desired penetration depth was not achieved simply by injecting a randomly produced emulsion. Therefore, the emulsion must be customized to be delivered to a certain depth before it plugs a porous medium.

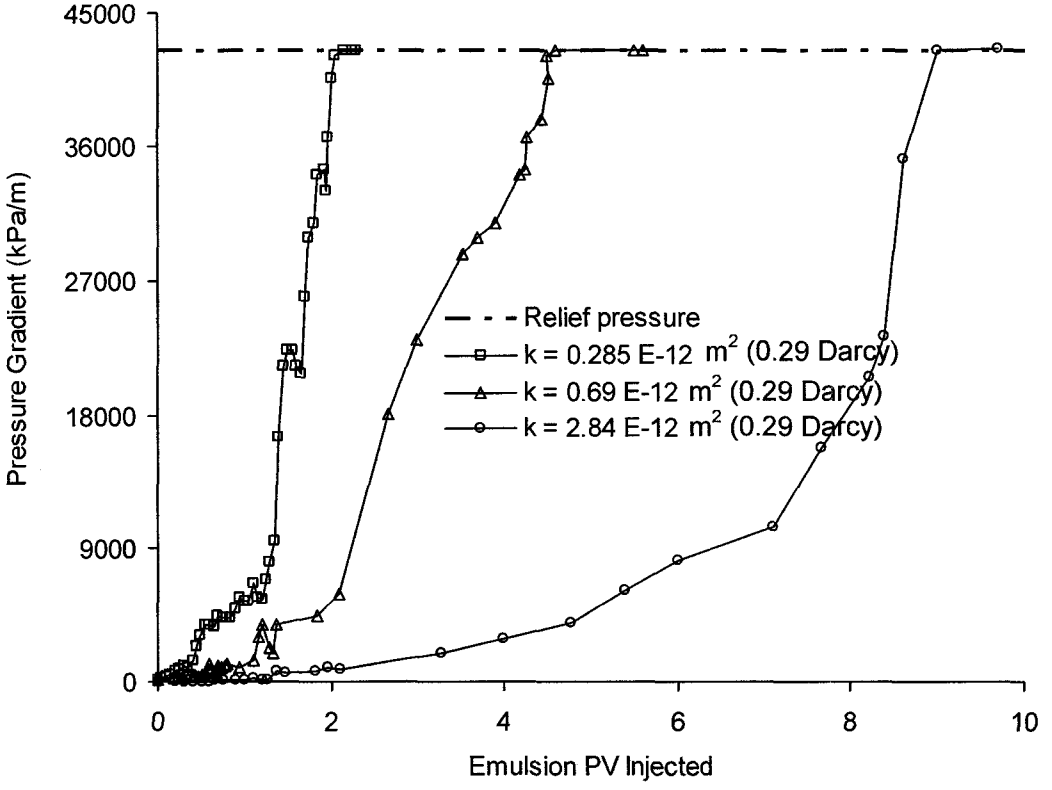

Figure 7.13 Heavy oil-in-water emulsion blocking porous media with different permeabilities

In addition, core flooding revealed the importance of adjusting droplet size and surfactant content of an emulsion in order to maximize its propagation depth and successfully plugging the medium. Figure 7.14 illustrates the results for the injection of three Lloydminster oil-in-water emulsions into the same glass beads pack. It indicates that while emulsion LM/W3, which had smaller mean droplet size compared to the mean pore throat size, did not block the porous medium, LM/W4 plugged the medium without complete penetration. More importantly, by adjusting the emulsion (LM/W5) droplet size (by varying the input shear mixing rate) and its surfactant content, two main objectives were achieved: the emulsion penetrated the full length of the core and also plugged it.

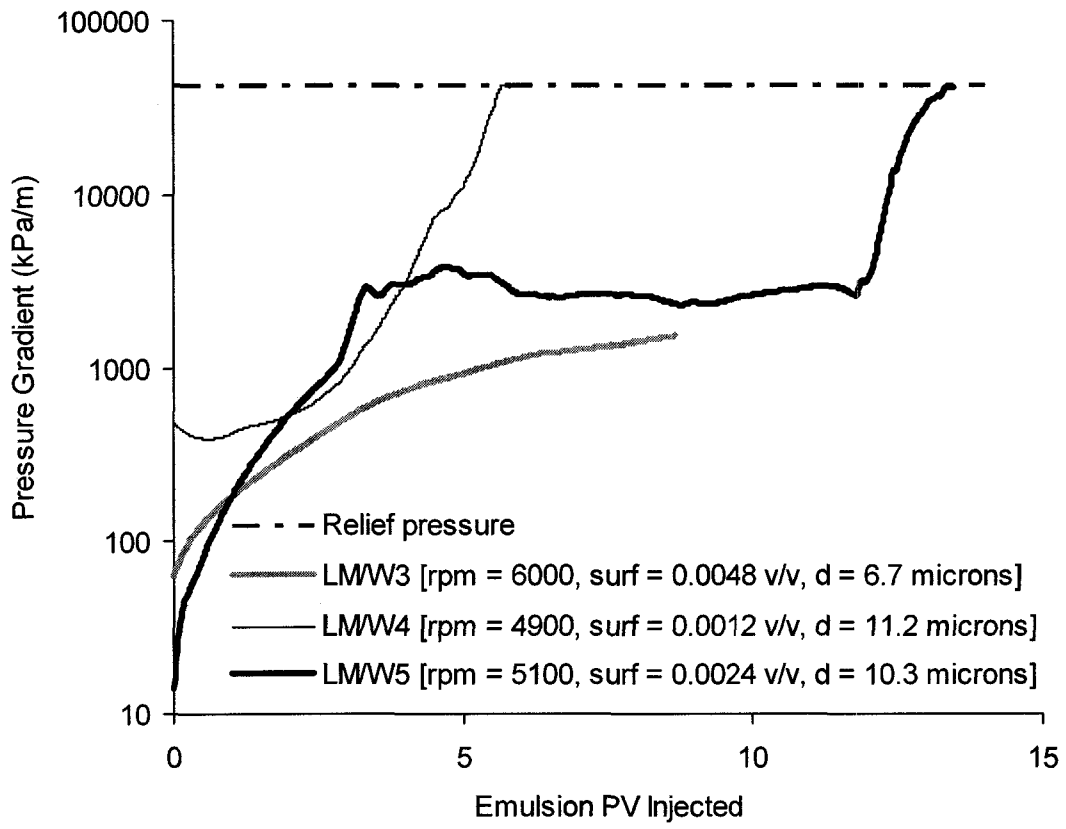

Figure 7.14 Penetration depth of Lloydminster heavy oil-in-water (LM/W) emulsions into the same core

Chapter 8. Conclusions and Recommendations

8.1 *Conclusions*

This study investigated the emulsion flow and blocking mechanism through porous media. The emulsion droplet capture mechanism was examined rigorously through micro-visualization experiments. Following this, the emulsion flow behavior and factors affecting its frontal advancement were studied. Finally, for the purpose of field applications, the blockage phenomenon was demonstrated through high-pressure sand packs experiments and methods of customizing the properties of a heavy oil-in-water emulsion in order to a block a porous medium with a given permeability were presented.

The main conclusions drawn from this study are as follows:

1. The application and effectiveness of a heavy oil-in-water emulsion to block a porous medium was demonstrated as a variety of porous media were sealed and the sealed porous media withstood pressures as high as 42,500 kPa/m (i.e. 1,800 psi for a 29.2 cm of porous medium).

2. The emulsion penetration depth was a function of surfactant concentration and the ratio of droplet-to-pore throat size. Low shear mixing rate and/or less surfactant content resulted in larger droplet size, higher emulsion viscosity, and insufficient plugging penetration depth. However, if the surfactant concentration exceeded its optimum amount, plugging may never have occurred. Therefore, depending on the type of porous medium and its pore throat size distribution, an emulsion property would need to be adjusted in terms of its surfactant type and

concentration, as well as its droplet size distribution, in order to achieve plugging with a maximum penetration depth.

3. A porous medium may be completely blocked after the injection of 10 pore volumes of a low concentration emulsion. The blockage might be extensive in the first few pore volumes of injection if more concentrated emulsions are utilized. A smaller amount of emulsion is required to block a finer, less permeable porous medium compared to a coarser, more permeable one if injecting the same emulsion. Emulsions carrying viscous oils may withstand higher pressure compared to those with less viscous oils due to the combined effect of capillarity and viscosity, acting therefore as better plugging agents.

4. Droplets' capture mechanism, during the emulsion flow through porous media, was distinguished by the capture of larger droplets at the pore throats due to size exclusion. The captured droplets can resist pressure without jumping to the next pore as long as the total shear forces exerted on the droplet do not exceed local capillary forces.

5. The mechanism of droplet capture was dominated by the ratio of droplet-to-pore throat size. Droplets may coalesce and produce a larger droplet due to an insufficient surfactant concentration and/or higher local shear rate. Larger droplets may resist higher pressures and their injection may result in more durable plugging.

6. Use of surfactant pre-flush solution dramatically enhanced the depth to which an emulsion penetrated into a porous medium. Generally, water-wet wettability is preferred for an oil-in-water emulsion to penetrate deeper into a porous medium. Therefore, solutions with a sufficient surfactant concentration may alter a porous medium's wettability if the surfactant is adsorbed onto the porous medium, thereby enhancing the emulsion propagation rate. However, application of equal amounts of surfactant in solution was more effective than

its use as a pre-flush, in terms of transporting the emulsion deeper into the porous medium.

7. Pre-flush solutions effectively facilitated the delivery of an emulsion deeper into a porous medium where the injection flow path would be restricted, compared to the unrestricted flow path. This is an important parameter to consider for injecting an emulsion through the casing and the perforations into the reservoir sand face.

8. Generally, the overall flow behavior of an emulsion through a porous medium indicated a dependency on surfactant type and concentration, porous medium permeability, and emulsion linear flow velocity. As an emulsion injection into a porous medium continued, the normalized pressure drop across the blocked region showed a direct inverse relationship to the porous medium permeability times the linear flow velocity.

8.2 *Recommendations for Field Application and Future Research*

The results obtained in this research study are encouraging for future field application of a heavy oil-in-water emulsion as a novel sealant in the near wellbore region. They are general guidelines; a basis of understanding of the sealing mechanism. However, a more systematic approach to the sealing process in the field demands a more accurate prediction of the sealant properties that can be applied to reservoir rocks with different properties. The following suggestions are important in elevating the current suggested process to a successful commercial stage. In addition, the following recommendations are imperative to the mathematical modeling of emulsion flow through porous media that can be extended to a variety of systems.

1. This study examined the effectiveness of a novel sealant (a heavy oil-in-water emulsion) in sealing a variety of porous media against water flow. A potential application of the novel sealant would be to use this novel sealant for eliminating the gas leakage in abandoned gas wells, eliminating the CO_2 leakage to the surface in CO_2 storage reservoirs and/or hindering the contaminant migration near oil refineries. For such applications, laboratory tests are needed to investigate the resistance of the novel sealant against the gas back flow. Moreover, the solubility of the gas into the entrapped oil droplets and its effects on the viscosity of the oil droplets as well as the change in the pH of the continuous water phase should be investigated.

2. Field applications of the novel sealant demand an accurate prediction of the porous rock properties and its compatibility with the novel sealant. In this work, the experiments were performed on glass bead packs that were strongly water-wet. The packs also were relatively homogenous since the well-rounded beads were distributed evenly within the packs. However, the properties of the underground porous rocks could be completely different: they are made of irregular sand grains that are tightly compacted; they are often not homogeneous and they may have a water-wet, oil-wet, or mixed wettability. If the porous rocks are oil-wet then the novel sealant may not be suitable because of the preference of heavy oil droplets in attaching to the pore surface. Under such circumstances the heavy oil-in-water emulsion will not be compatible with the porous rocks and the emulsion may breaks down right at the sand face.

   Another obstacle in regards to the underground porous media is their pore geometry and pore structure as well as the properties of their composite materials. A natural porous medium may have a wide range of pore throat distribution. Customizing a heavy oil-in-water emulsion to seal such a porous medium seems to be a challenging task. Moreover, the presence of fine particles and their reaction with the novel sealant is another issue. For example, if clay particles presents inside a porous medium, an emulsion penetration depth into

the medium may reduce dramatically as the water phase absorbed by the clay and causes its swelling. All above mentioned concerns leads us to the point that for the field applications, the best practice would be to examine the effectiveness and compatibility of the novel sealant on a natural core samples taken from the field.

3. It is recommended that viscous heavy oil-in-water emulsions with an average droplet size of 1.3 to 1.5 times the mean pore throat size, be applied. The estimation of mean pore throat size is not possible without a laboratory measurement of capillary pressure for the given porous medium with a specific permeability. It is possible to use the Karmen-Kozeny equation, which relates the porous medium permeability with the grain size and is based on the calculated average grain size, to estimate the average pore throat constriction through mathematical averaging. This procedure seems to be inaccurate and inapplicable to a system that is highly dependent on the accurate estimation of mean pore throat sizes. Therefore, it is necessary to develop a relationship between the porous medium permeability and the mean pore throat size.

4. The proposed sealing process revealed a high dependency on the droplet coalescence. However, it was impossible to predict the onset of droplet coalescence during the experiments because it depends on several factors, including the composition of oil droplets, applied local shear rates, surfactant type and concentration, and the chemistry of the continuous water phase. After selecting the components constituting the sealant, a separate study should be conducted to predict the onset of droplet coalescence. It would be ideal if the coalescence could be predicted as a function of applied pressure and surfactant concentration along with other important variables involved in the process. If such a prediction was possible, the breaking of the emulsion and, consequently, its propagation depth within the porous medium, can be predicted.

5. A stable emulsion may be used during the sealing process if there is a high level of uncertainty involved in predicting the emulsion breakup within the reservoir. After ensuring that the optimum penetration depth has been achieved, the injected emulsion may be fixed within the porous medium by injecting small quantities of low pH solutions or concentrated saline water.

6. The more concentrated emulsions, under higher injection rates, break easier compared to those that are less concentrated with lower injection rates, assuming that both emulsions have an equal amount of surfactant. Thus, if the emulsion must be delivered deeper into the reservoir, less concentrated emulsions and lower injection rates may be applied. This is also true for the injection of an emulsion through the casing perforations that reduce the flow path significantly. In such circumstances, employing a surfactant pre-flush should facilitate the passage of droplets inside the reservoir rocks and result in greater penetration depth of the emulsion.

7. During the experiments, it was impossible to measure the effects of pre-flush solutions on porous medium wettability and the amount of surfactant adsorption on the sand grains. It would be worthwhile to measure such effects and as a result, predict their contribution to the overall blockage mechanism.

8. The experiments were conducted at room temperature, which is considered almost equal to the downhole temperature of intervals no deeper than 1500 meters in Western Canadian reservoirs. The sealant properties need to be re-evaluated if the process is considered for application in deeper formations with higher temperatures.

9. The emulsions prepared for the experiments were stabilized by a nonionic surfactant (DOWFAX Triton X-100). The surfactant pre-flush solution also was made of the same surfactant. It is recommended to examine the effects of other

types of surfactant, such as anionic and cationic surfactants, on the stability and droplet size distributions of heavy oil-in-water emulsions.

References

1. King, R. W.; *"Heavy Oil Emulsion Rheology,"* M.Sc. Thesis, University of Alberta, Alberta, Canada, 1985

2. Bahadori, A. and Zeidani, K.; *"Analysis of Crude Oil Electrostatic Desalters Performance,"* 56th Annual Petroleum Society CIM Technical Meeting Proceedings 2005, Calgary, Alberta, 7-9 June 2005

3. Janssen, P. H., van den Broek, W. M. G. T., and Harris, C. K.; *"Laboratory Study Investigating Emulsion Formation in the Near-Wellbore Region of a High Water-Cut Oil Well,"* SPE Journal, Vol. 6, No. 1, PP. 71-79, 2001

4. Kokal, S.; *"Crude-Oil Emulsions: A State-of-the-Art Review,"* SPE Production & Facilities, Vol. 20, No. 1, PP. 5-13, 2005

5. Kokal, S. L., Maini, B. B., and Woo, R.; *"Flow of Emulsions in Porous-Media,"* Advances in Chemistry Series, Vol. 231, PP. 219-262, 1992

6. Marsden, S. S. and Raghavan, R.; *"System for Producing and Transporting Crude Oil as an Oil-Water Emulsion,"* Journal of the Institute of the Petroleum, Vol. 59, PP. 273-278, 1973

7. Podolsak, A. K., Tiu, C., and Fang, T. N.; *"Flow of Non-Newtonian Fluids Through Tubes With Abrupt Expansions and Contractions (Square Wave Tubes),"* Journal of Non-Newtonian Fluid Mechanics, Vol. 71, No. 1-2, PP. 25-39, 1997

8. Sarbar, M. A. and Wingrove, M. D.; *"Physical and Chemical Characterization of Saudi Arabian Crude Oil Emulsions,"* 72nd Annual SPE Technical Conference, San Antonio, TX, pp. 675-685, 5-8 October 1997

9. Bibic, O.; *"Laboratory Testing of Novel Sealant for Leaky Wells,"* M.Sc. Thesis, University of Alberta, Alberta, Canada, 2005

10. Mollet, H. and Grubenmann, A.; *"Formulation Technology: Emulsions, Suspensions, Solid Forms,"* WILEY-VCH, Weinheim, Germany, 2001

11. Squires, F.; *"Method of Recovering Oil and Gas,"* US Patent No. 1238355, 1917

12. Beckstrom, R. C. and Van Tuyl, F. M.; *"The Effect of Flooding Oil Sands with Alkaline Solutions,"* AAPG Bulletin, Vol. 11, PP. 223-227, 1927

13. Uren, L. C. and Fahmy, E. H.; *"Factors Influencing Recovery of Petroleum from Unconsolidated Sands by Waterflooding,"* Trans. AIME, Vol. 77, PP. 318-335, 1927

14. Atkinson, H.; *"Recovery of Petroleum from Oil Bearing Sands,"* US Patent No. 1651311, 1927

15. Haines, W. B.; *"Studies in the Physical Properties of Soil, V, The Hysteresis Effect in Capillary Properties, and the Modes of Moisture Distribution Associated therewith,"* Journal of Agricultural Science, Vol. 20, PP. 97-116, 1930

16. Cartmill, J. C. and Dickey, P. A.; *"Flow of a Disperse Emulsion of Crude Oil in Water,"* 44th Annual Fall Meeting of SPE of AIME, Denver, CO, 28 September-01 October 1969

17. Cartmill, J. C. and Dickey, P. A.; *"Flow of a Disperse Emulsion of Crude Oil in Water through Porous Media,"* The American Association of Petroleum Geologists Bulletin, Vol. 54, No. 12, PP. 2438-43, 1970

18. Marsden, S. S. J. and Uzoigwe, A. C.; *"Emulsion Rheology and Flow through Unconsolidated Synthetic Porous Media,"* 45th Annual Fall Meeting of SPE of AIME, Houston, Texas, 4-7 October 1970

19. McAuliffe, C. D.; *"Crude-Oil-in-Water Emulsions to Improve Fluid Flow in an Oil Reservoir,"* Journal of Petroleum Technology, Vol. 25, PP. 721-726, 1973

20. Cooke, C. E. J., Williams, R. E., and Kolodzie, P. A.; *"Oil Recovery by Alkaline Waterflooding,"* Improved Oil Recovery Symposium, Tulsa, OK, United States, pp. 51-62, 22-24 April 1974

21. Johnson, C. E. J.; *"Status of Caustic and Emulsion Methods,"* Journal of Petroleum Technology, Vol. 28, PP. 85-92, 1976

22. Radke, C. J. and Somerton, W. H.; *"Enhanced Recovery with Mobility and Reactive Tension Agents,"* 5th Annual DOE Symposium on Enhanced Oil and Gas Recovery, Tulsa, OK, Vol. 1, pp. 1-23, 22-24 August 1979

23. Foster, W. R.; *"Low-Tension Waterflooding Process,"* Journal of Petroleum Technology, Vol. 25, No. FEB, PP. 205-210, 1973

24. Soo, H. and Radke, C. J.; *"Flow of Dilute, Stable Liquid and Solid Dispersions in Underground Porous Media,"* AICHE Journal, Vol. 31, No. 1, PP. 1926-1928, 1985

25. Soo, H. and Radke, C. J.; *"Velocity Effects in Emulsion Flow through Porous Media,"* Journal of Colloid and Interface Science, Vol. 102, PP. 462-476, 1984

26. Schmidt, D. P., Soo, H., and Radke, C. J.; *"Linear Oil Displacement by the Emulsion Entrapment Process,"* Society of Petroleum Engineers Journal, Vol. 24, PP. 351-360, 1984

27. French, T. R., Broz, J. S., Lorenz, P. B., and Bertus, K. M.; *"Use of Emulsions for Mobility Control During Steamflooding."* 56th Annual California Regional Meeting, Society of Petroleum Engineers, Oakland, CA, United States, Vol. 1, pp. 43-54, 2-4 April 1986

28. Yeung, K.; *"Mobility Control by Emulsions under Bottom Water Conditions,"* M.Sc. Thesis, University of Alberta, Alberta, Canada, 1991

29. Yeung, K. and Ali, S. M. F.; *"Waterflooding Reservoirs with a Water Leg using the Dynamic Blocking-Process,"* Journal of Canadian Petroleum Technology, Vol. 34, No. 7, PP. 50-57, 1995

30. Fiori, M. and Farouq Ali, S. M.; *"Optimal Emulsion Design for the Recovery of a Saskatchewan Crude,"* Journal of Canadian Petroleum Technology, Vol. 30, No. 2, PP. 123-132, 1991

31. Khambharatana, F., Thomas, S., and Farouq Ali, S. M.; *"Macroemulsion Rheology and Drop Capture Mechanism during Flow,"* 6th SPE Oil & Gas International Conference in China, Beijing, China, Vol. 1, pp. 657-665, 2-6 November 1998

32. Mendez, Z. d. C.; *"Flow of Dilute Oil-in-Water Emulsions in Porous Media,"* Ph.D. Thesis, University of Texas at Austin, Texas, United States, 1999

33. Woo, R., Jackson, C. and Maini, B. B.; *"Evaluation of the Effect of Stability on Emulsion Flow in Porous Media,"* SSC File No. XSG94-00146-(608), 1996

34. Collins, I. R., Jordan, M. M., and Taylor, S. E.; *"The Development and Application of a Novel Scale Inhibitor Deployment System,"* SPE Production & Facilities, Vol. 17, No. 4, PP. 221-228, 2002

35. Romero, L., Ziritt, J. L., Marin, A., Rojas, F., Mogollon, J. L., Manrique, E., and Paz, F.; *"Plugging of High Permeability-Fractured Zones using Emulsions,"* SPE/DOE 10th Symposium on Improved Oil Recovery, Tulsa, OK, Vol. 2, pp. 611-621, 21-24 April 1996

36. Wang, F. Q., Qu, Z. H., and Kong, L. R.; *"Experimental Study on the Mechanism of Emulsion Flooding with Micromodels,"* Shiyou Kantan Yu Kaifa/Petroleum Exploration and Development, Vol. 33, PP. 221-224, 2006

37. Dullien, F. A. L.; *"Porous Media: Fluid Transport and Pore Structure,"* 2nd Edition, ASME, New York, NY, USA, 1995

38. Devereux, O. F.; *"Emulsions Flow in Porous Solids I. A Flow Model,"* Chemical Engineering Journal and the Biochemical Engineering Journal, Vol. 7, PP. 121-128, 1974

39. Devereux, O. F.; *"Emulsion Flow in Porous Solids II. Experiments with a Crude Oil-in-Water Emulsion in Porous Sandstone,"* Chemical Engineering Journal and the Biochemical Engineering Journal, Vol. 7, PP. 129-136, 1974

40. Alvarado, D. A. and Marsden, S. S. J.; *"Flow of Oil-in-Water Emulsions through Tubes and Porous Media,"* Society of Petroleum Engineers of AIME Journal, Vol. 19, PP. 369-377, 1979

41. McAuliffe, C. D.; *"Oil-in-Water Emulsions and Their Flow Properties in Porous Media,"* Journal of Petroleum Technology, Vol. 25, PP. 727-733, 1973

42. Soo, H. and Radke, C. J.; *"Filtration Model for the Flow of Dilute, Stable Emulsions in Porous Media - I. Theory,"* Chemical Engineering Science, Vol. 41, PP. 263-272, 1986

43. Soo, H., Williams, M. C., and Radke, C. J.; *"Filtration Model for the Flow of Dilute, Stable Emulsions in Porous Media - II. Parameter Evaluation and Estimation,"* Chemical Engineering Science, Vol. 41, PP. 273-281, 1986

44. Soo, H. and Radke, C. J.; *"Flow Mechanism of Dilute, Stable Emulsions in Porous Media,"* Industrial & Engineering Chemistry, Fundamentals, Vol. 23, PP. 343-347, 1984

45. Sahimi, M. and Imdakm, A. O.; *"Hydrodynamics of Particulate Motion in Porous-Media,"* Physical Review Letters, Vol. 66, No. 9, PP. 1169-1172, 1991

46. Abou-Kassem, J. H. and Farouq Ali, S. M.; *"Modelling of Emulsion Flow in Porous Media,"* Journal of Canadian Petroleum Technology, Vol. 34, PP. 30-38, 1995

47. Lopez-Montilla, J. C.; *"Spontaneous Emulsification: Mechanisms, Physicochemical Aspects and Applications,"* Ph.D. Thesis, University of Florida, Florida, United States, 2003

48. Ryoo, W. S.; *"Emulsions and Microemulsions of Water and Carbon Dioxide: Novel Surfactants and Stabilization Mechanisms,"* Ph.D. Thesis, University of Texas at Austin, Texas, United States, 2005

49. Soma, J. and Papadopoulos, K. D.; *"Flow of Dilute, Submicron Emulsions in Granular Porous-Media - Effects of pH and Ionic-Strength,"* Colloids and Surfaces A-Physicochemical and Engineering Aspects, Vol. 101, No. 1, PP. 51-61, 1995

50. Soma, J. and Papadopoulos, K. D.; *"Deposition of Oil-in-Water Emulsions in Sand Beds in the Presence of Cetyltrimethylammonium Bromide,"* Environmental Science & Technology, Vol. 31, No. 4, PP. 1040-1045, 1997

51. Pena, A. A.; *"Dynamic Aspects of Emulsion Stability,"* Ph.D. Thesis, Rice University, Texas, United States, 2004

52. Zhao, X.; *"Drop Breakup in Dilute Newtonian Emulsions under Steady Shear,"* Ph.D. Thesis, Rice University, Texas, United States, 2004

53. Laroche, I., Wu, X., Masliyah, J. H., and Czarnecki, J.; *"Dynamic and static interactions between bitumen droplets in water,"* Journal of colloid and interface science, Vol. 250, No. 2, PP. 316-326, 2002

54. Li, J. Q. and Gu, Y. G.; *"Coalescence of Oil-in-Water Emulsions in Fibrous and Granular Beds,"* Separation and Purification Technology, Vol. 42, No. 1, PP. 1-13, 2005

55. Qu, G.; *"Effect of Chemical Additives on Stability of Water-in-Diluted Bitumen Emulsions,"* M. Sc. Thesis, University of Alberta, Alberta, Canada, 2006

56. Tsamantakis, C.; *"Properties of Water-Bitumen Interface,"* M.Sc. Thesis, University of Alberta, Alberta, Canada, 2003

57. Masliyah, J. H.; *"Electrokinetic Transport Phenomena,"* Alberta Oil Sands Technology and Research Authority, Alberta, Canada, 1994

58. Liu, J., Zhou, Z., Xu, Z., and Masliyah, J.; *"Bitumen-clay interactions in aqueous media studied by zeta potential distribution measurement,"* Journal of Colloid and Interface Science, Vol. 252, No. 2, PP. 409-418, 2002

59. Shaw, D. J.; *"Introduction to Colloid and Surface Chemistry,"* 4th Edition, Elsevier Butterworth-Heinemann, MA, United States, 1992

60. Sharma, R.; *"Surfactant Adsorption and Surface Solubilization,"* American Chemical Society, Washington, DC, 1994

61. Sharma, R.; *"Small-molecule surfactant adsorption, polymer surfactant adsorption, and surface solubilization: An overview,"* Surfactant Adsorption and Surface Solubilization, Vol. 615, PP. 1-20, 1995

62. Dong, J.; *"Study of the Surfactant Nanostructures at the Solid/Liquid Interface,"* Ph.D. Thesis, Wayne State University, Michigan, United States, 2003

63. Zhou, W.; *"Effects of Surfactant Adsorption and Distribution on Enhanced Heavy Oil Recovery by Alkaline/Surfactant Flooding,"* M.A.Sc. Thesis, University of Regina, Saskatchewan, Canada, 2005

64. Lawson, L. M. B.; *"Water-in-Oil-in-Water Double Emulsions: Exploring Stability, Release, and Targeted Delivery,"* Ph.D. Thesis, Tulane University, Louisiana, United States, 2005

65. Strassner, J. E.; *"Effect of pH on Interfacial Films and Stability of Crude Oil-Water Emulsions,"* Journal of Petroleum Technology, Vol. 20, PP. 303-312, 1968

66. Layrisse, I., Rivas, H., and Acevedo, S.; *"Isolation and Characterization of Natural Surfactants Present in Extra Heavy Crude Oils,"* Journal of Dispersion Science and Technology, Vol. 5, PP. 1-18, 1984

67. Gillberg, G. and Eriksson, L.; *"pH Sensitive Microemulsions."* Industrial & Engineering Chemistry, Product Research and Development, Vol. 19, PP. 304-309, 1980

68. Levius, H. P. and Drommond, F. G.; *"Elevated Temperature as an Artificial Breakdown Stress in the Evaluation of Emulsion Stability,"* Journal of Pharmacy and Pharmacology, Vol. 5, No. 10, PP. 743-756, 1953

69. Harusawa, F., Machida, Y., Mitsui, T., and Nakamura, S.; *"Changes in the Interfacial Tension with Temperature and their Effects on the Particle Size and Stability of Emulsions,"* Kolloid Z Z Polymere, Vol. 250, No. 3, PP. 227-230, 1972

70. Saito, H. and Shinoda, K.; *"Stability of W/O Type Emulsions as a Function of Temperature and of the Hydrophilic Chain Length of the Emulsifier,"* Journal of Colloid and Interface Science, Vol. 32, No. 4, PP. 647-651, 1970

71. Rosen, M. J.; *"Surfactants and Interfacial Phenomena,"* 3rd Edition, Wiley, Toronto, Canada, 2004

72. Yang, C., Dabros, T., Li, D. Q., Czarnecki, J., and Masliyah, J. H.; *"Visualizing method for study of micron bubble attachment onto a solid surface under varying physicochemical conditions,"* Industrial and Engineering Chemistry Research, Vol. 39, No. 12, PP. 4949-4955, 2000

73. Taylor, S. D.; *"Colloidal Interactions in Water-in-Diluted-Bitumen Emulsions,"* Ph.D. Thesis, University of Alberta, Alberta, Canada, 2002

74. Stancik, E. J.; *"Colloids at Fluid Interfaces: Structure, Dynamics, and Droplet Stability,"* Ph.D. Thesis, Stanford University, California, United States, 2004

APPENDIX A: Etched Glass Micro-model Cell Window Preparation

The procedure received from Alberta Microelectronic Centre: Temco Dual Depth Micro-model Process (two-level Process) [A1, A2]:

1. Substrate preparation

   Inspection: visual inspection for defects on the glass substrates.

   Clean: glass substrates cleaned in H_2SO_4/H_2O_2 (3:1) for 10 minutes.

2. Metal deposition

   The glass substrates were deposited with 3 metals, as the masks for the glass etching steps, as shown.

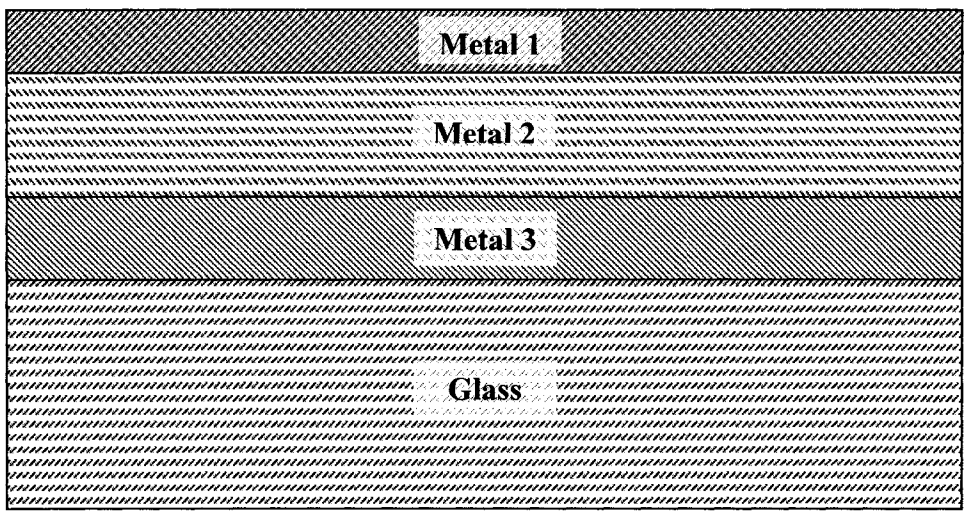

Figure A.0.1 Metal deposition scheme for glass etching

3. Metal 1 scheme (for shallow etch: 15 μm)

   The throat patterns transferred onto the photo resist coated substrates and the metal layer removed using metal etchant.

4. Metal 2 scheme (for deep etch: 60 μm)

The pore patterns transferred onto the photo resist coated substrates and the 3 metals removed using metal etchant.

5. Glass etch 1 (deep etch: 60 μm)

   The pores in the substrates etched to about 60 μm using HF based glass etchant.

6. Metal 2 remove (remove the metal 2 and metal 3)

   Removed the metal 2 and metal 3, using metal etchant.

7. Glass etch 2 (shallow etch: 15 μm)

   The throats in the substrates etched to about 15 μm and the pores also etched to about 75 μm, using HF base glass etchant.

References:

A1. Lillico, D. A., Jossy, W. E., *"Visualisation of Bubbles of Foamy Oil within a Dual Depth Micromodel,"* AACI Report # 9697-8, Alberta Research Council, Edmonton, Alberta, Canada, September 1996

A2. Lillico, D. A., Jossy, W. E., *"Visualization of Bubbles of Foamy Oil within Hele-Shaw Cells: APPENDIX,"* AACI Report #9697-4A, Alberta Research Council, Edmonton, Alberta, Canada, July 1996

APPENDIX B: Two-Parallel Plate Micro-model Design Details

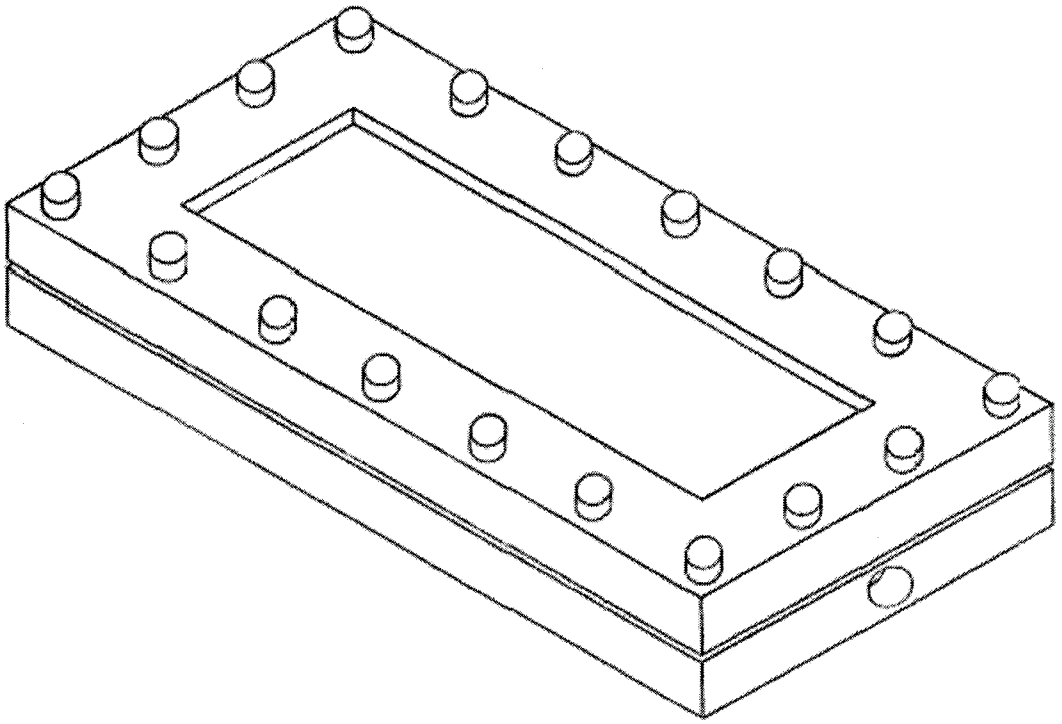

Figure B. 1 Two-parallel plate micro-model 3-D view

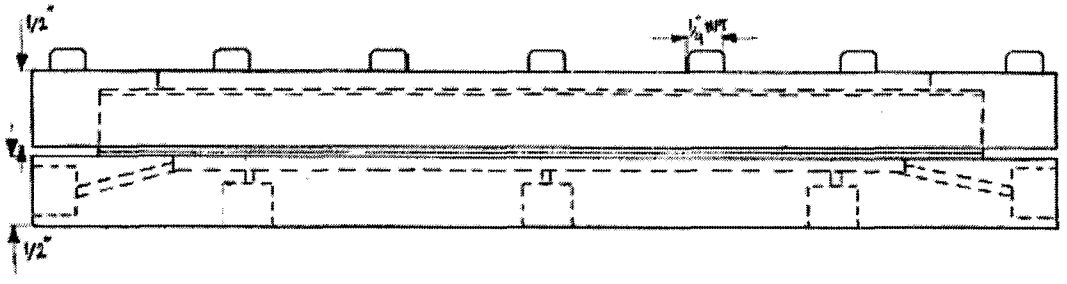

Figure B. 2 Two-parallel plate micro-model front view

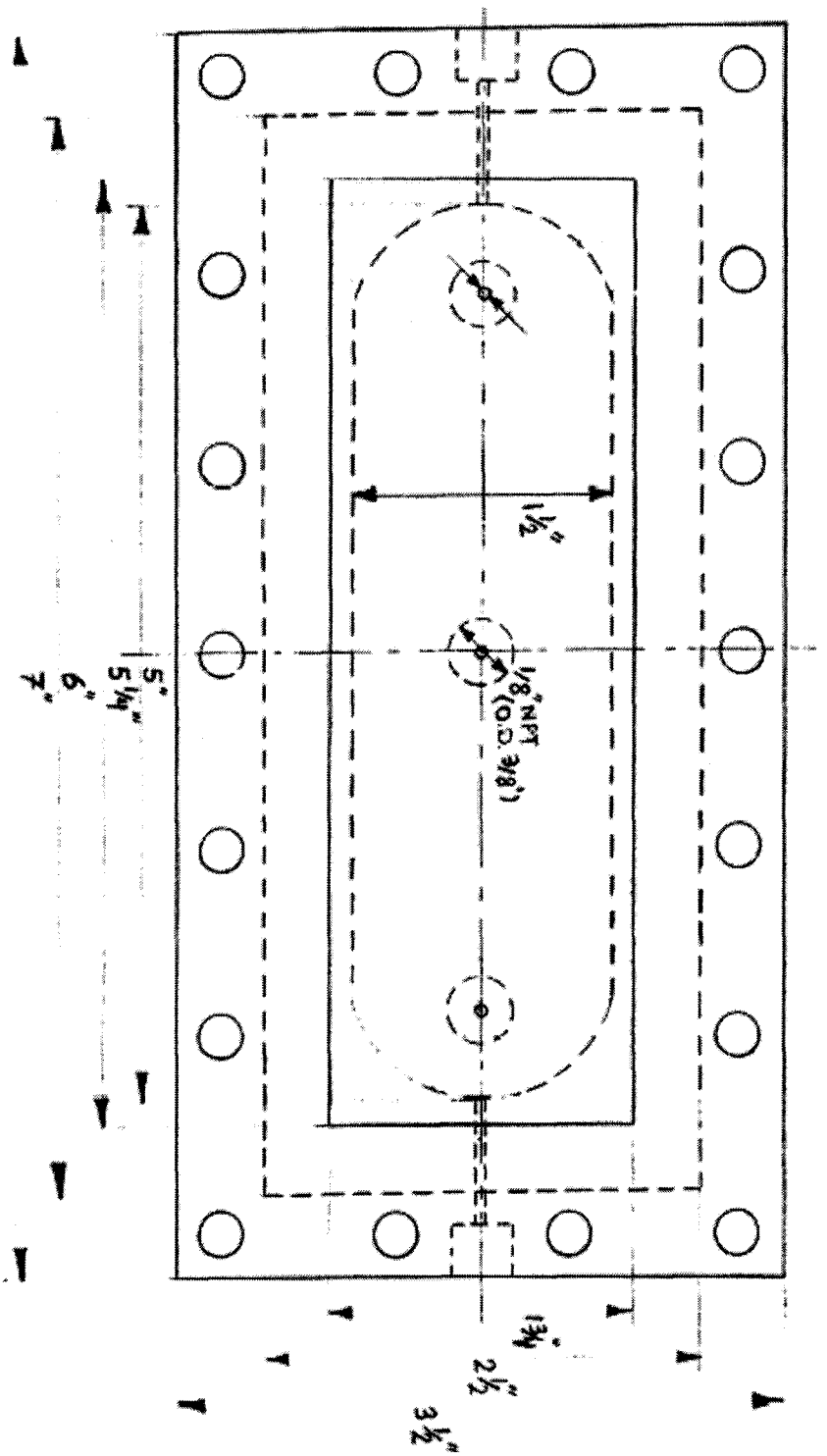

Figure B. 3 Two-parallel plate micro-model top view

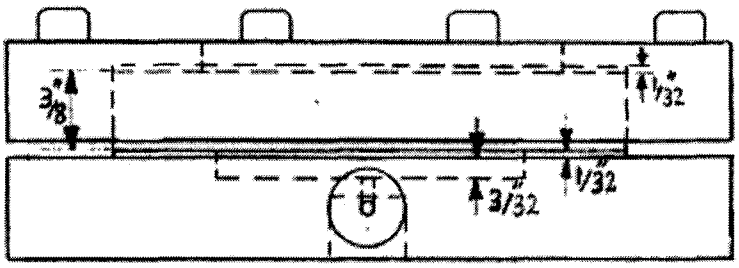

Figure B. 4 Two-parallel plate micro-model side view

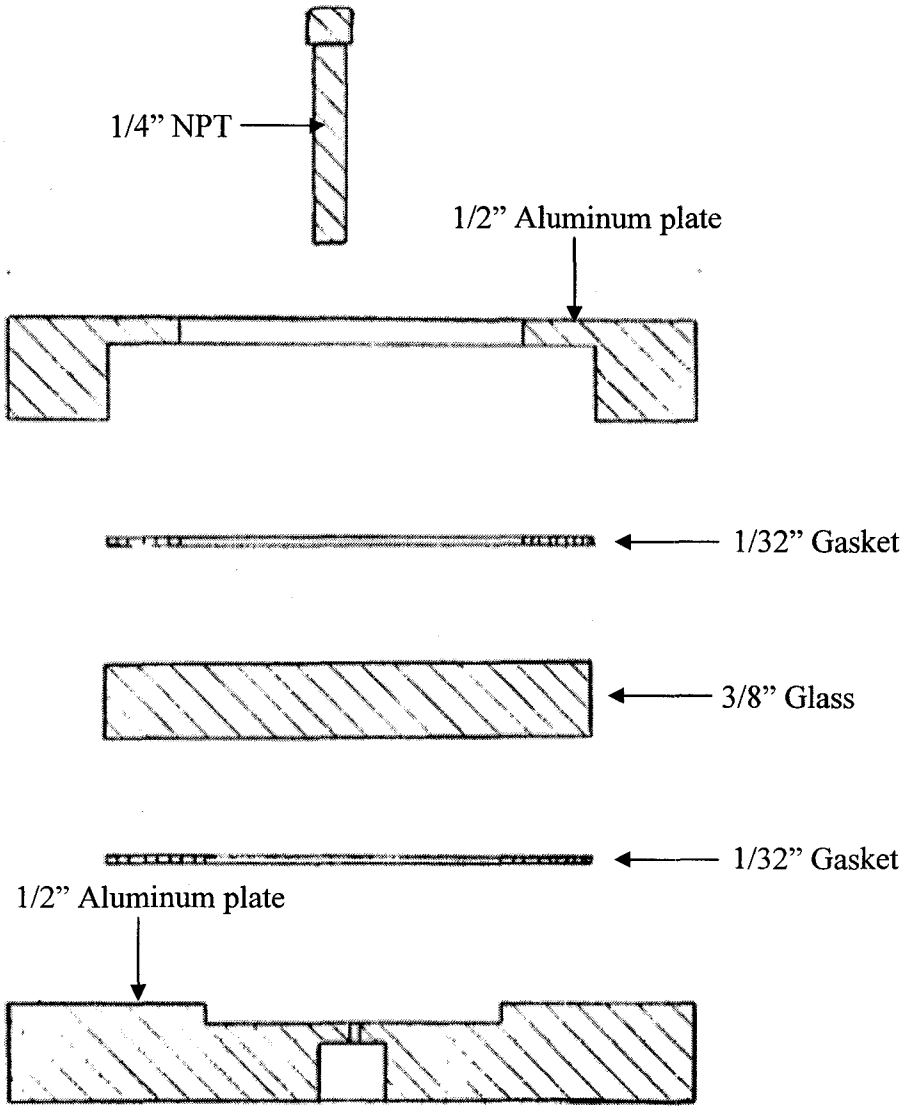

Figure B. 5 Two-parallel plate micro-model side-cut and the order of materials (top to bottom)

APPENDIX C: Emulsion Specifications

C.1 *Emulsion LM/W1 Specifications*

Emulsion designation	LM/W1
Emulsion type	Oil-in-water
Emulsion quality (%)	5
Oil type	Lloydminster oil
Surfactant type	Triton X-100
Surfactant concentration (v/v) (%)	0.12
Phases mixing method	Brinkmann homogenizer
Shear mixing rate (rpm)	4500
d(0.1) (μm)	6.2
d(0.5) (μm)	21
d(0.1) (μm)	449.8

Table C. 1 Emulsion LM/W1 characteristics

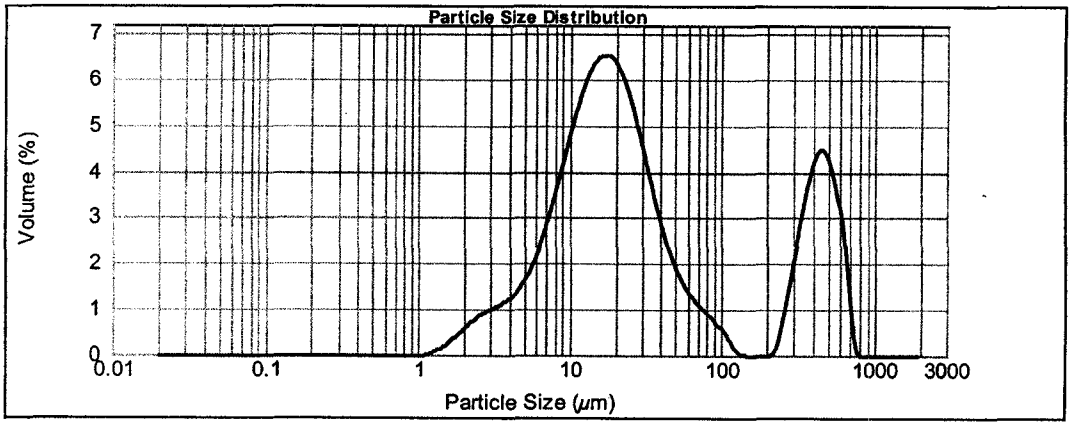

Figure C. 1 Emulsion LM/W1 droplet size distribution

C.2 *Emulsion LM/W2 Specifications*

Emulsion designation	LM/W2
Emulsion type	Oil-in-water
Emulsion quality (%)	13
Oil type	Lloydminster oil
Surfactant type	Triton X-100
Surfactant concentration (v/v) (%)	0.12
Phases mixing method	Brinkmann homogenizer
Shear mixing rate (rpm)	5000
d(0.1) (μm)	3.8
d(0.5) (μm)	11
d(0.1) (μm)	35.1

Table C. 2 Emulsion LM/W2 characteristics

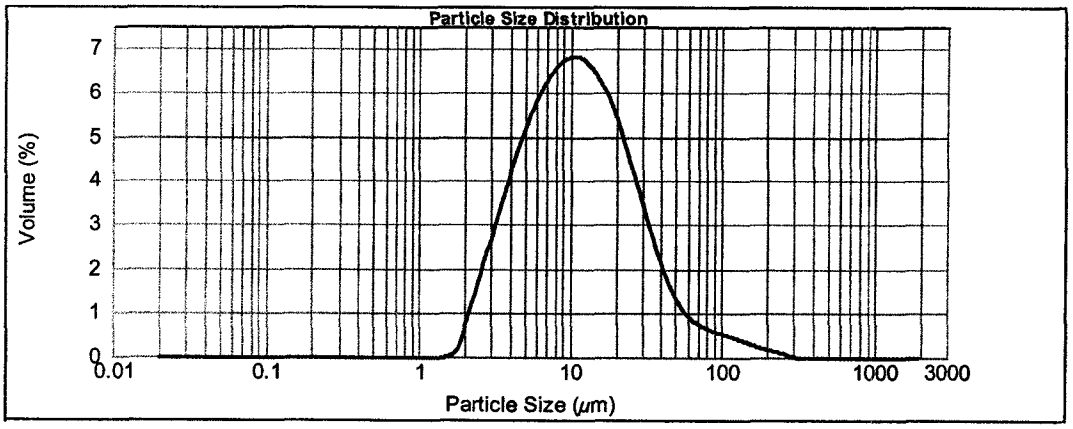

Figure C. 2 Emulsion LM/W2 droplet size distribution

C.3 *Emulsion LM/W3 Specifications*

Emulsion designation	LM/W3
Emulsion type	Oil-in-water
Emulsion quality (%)	13
Oil type	Lloydminster oil
Surfactant type	Triton X-100
Surfactant concentration (v/v) (%)	0.48
Phases mixing method	Brinkmann homogenizer
Shear mixing rate (rpm)	6000
d(0.1) (μm)	3.3
d(0.5) (μm)	6.7
d(0.1) (μm)	18.3

Table C. 3 Emulsion LM/W3 characteristics

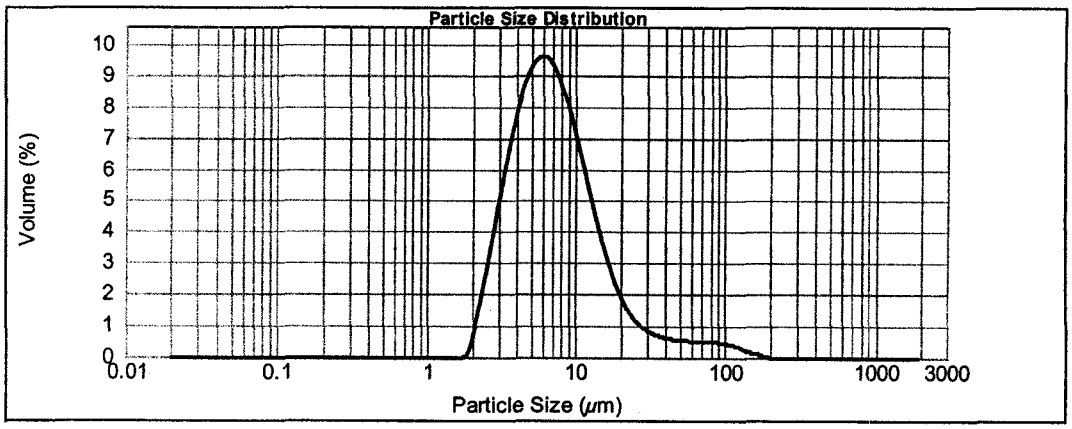

Figure C. 3 Emulsion LM/W3 droplet size distribution

C.4 *Emulsion LM/W4 Specifications*

Emulsion designation	LM/W4
Emulsion type	Oil-in-water
Emulsion quality (%)	13
Oil type	Lloydminster oil
Surfactant type	Triton X-100
Surfactant concentration (v/v) (%)	0.12
Phases mixing method	Brinkmann homogenizer
Shear mixing rate (rpm)	4900
d(0.1) (μm)	3.9
d(0.5) (μm)	11.2
d(0.1) (μm)	36.4

Table C. 4 Emulsion LM/W4 characteristics

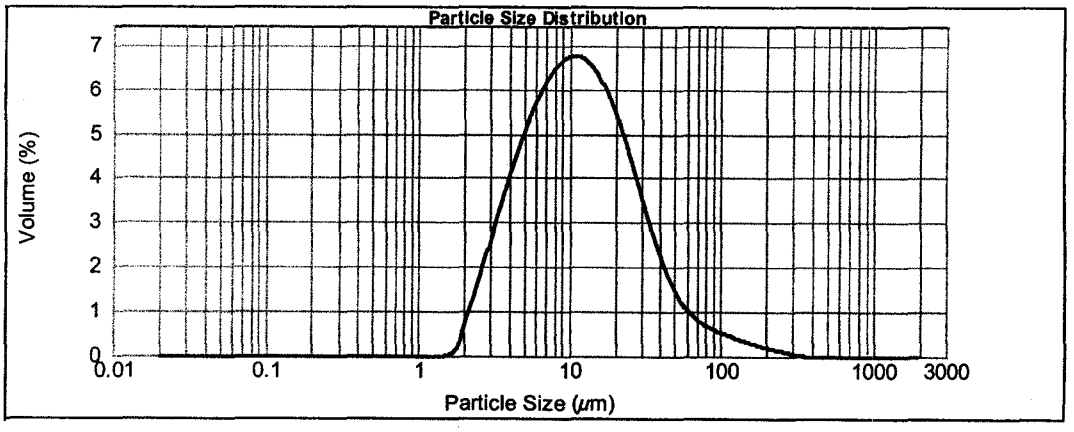

Figure C. 4 Emulsion LM/W4 droplet size distribution

C.5 *Emulsion LM/W5 Specifications*

Emulsion designation	LM/W5
Emulsion type	Oil-in-water
Emulsion quality (%)	13
Oil type	Lloydminster oil
Surfactant type	Triton X-100
Surfactant concentration (v/v) (%)	0.24
Phases mixing method	Brinkmann homogenizer
Shear mixing rate (rpm)	5100
d(0.1) (μm)	3.6
d(0.5) (μm)	10.3
d(0.1) (μm)	57.9

Table C. 5 Emulsion LM/W5 characteristics

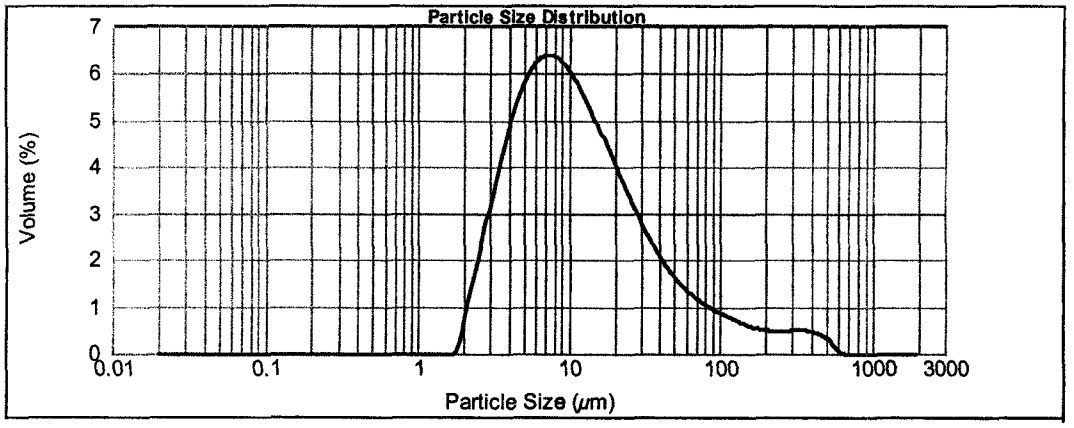

Figure C. 5 Emulsion LM/W5 droplet size distribution

C.6 *Emulsion M/W1 Specifications*

Emulsion designation	M/W1
Emulsion type	Oil-in-water
Emulsion quality (%)	5
Oil type	Mineral oil
Surfactant type	Triton X-100
Surfactant concentration (v/v) (%)	0.12
Phases mixing method	Brinkmann homogenizer
Shear mixing rate (rpm)	5000
d(0.1) (μm)	2.4
d(0.5) (μm)	5.4
d(0.1) (μm)	9.8

Table C. 6 Emulsion M/W1 characteristics

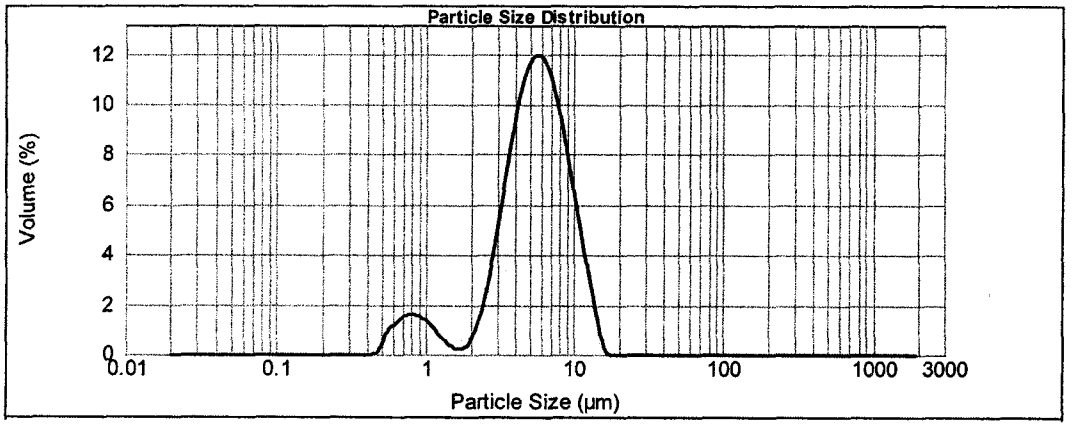

Figure C. 6 Emulsion M/W1 droplet size distribution

C.7 *Emulsion M/W2 Specifications*

Emulsion designation	M/W2
Emulsion type	Oil-in-water
Emulsion quality (%)	13
Oil type	Mineral oil
Surfactant type	Triton X-100
Surfactant concentration (v/v) (%)	0.12
Phases mixing method	Manual shaking
Shear mixing rate (rpm)	NA
d(0.1) (μm)	117
d(0.5) (μm)	198
d(0.1) (μm)	328

Table C. 7 Emulsion M/W2 characteristics

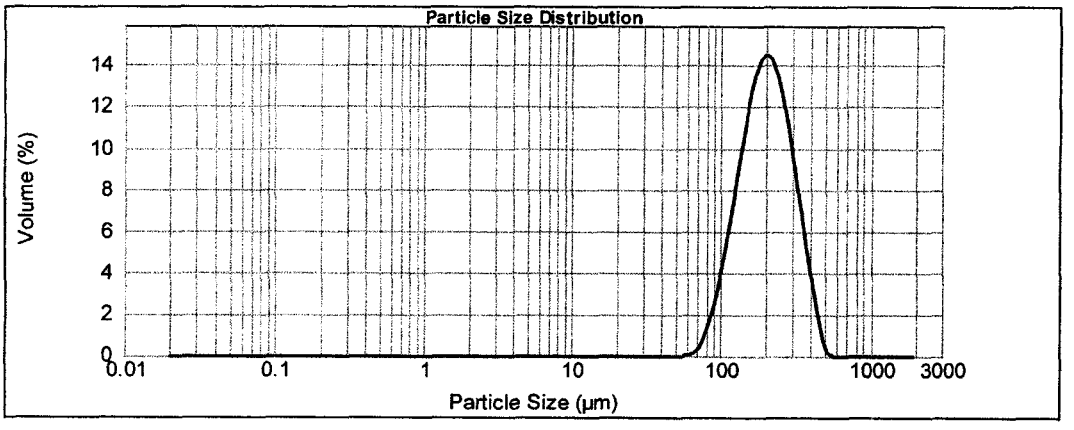

Figure C. 7 Emulsion M/W2 droplet size distribution

C.8 *Emulsion M/W3 Specifications*

Emulsion designation	M/W3
Emulsion type	Oil-in-water
Emulsion quality (%)	13
Oil type	Mineral oil
Surfactant type	Triton X-100
Surfactant concentration (v/v) (%)	0.12
Phases mixing method	Manual shaking
Shear mixing rate (rpm)	NA
d(0.1) (μm)	80
d(0.5) (μm)	225
d(0.1) (μm)	475

Table C. 8 Emulsion M/W3 characteristics

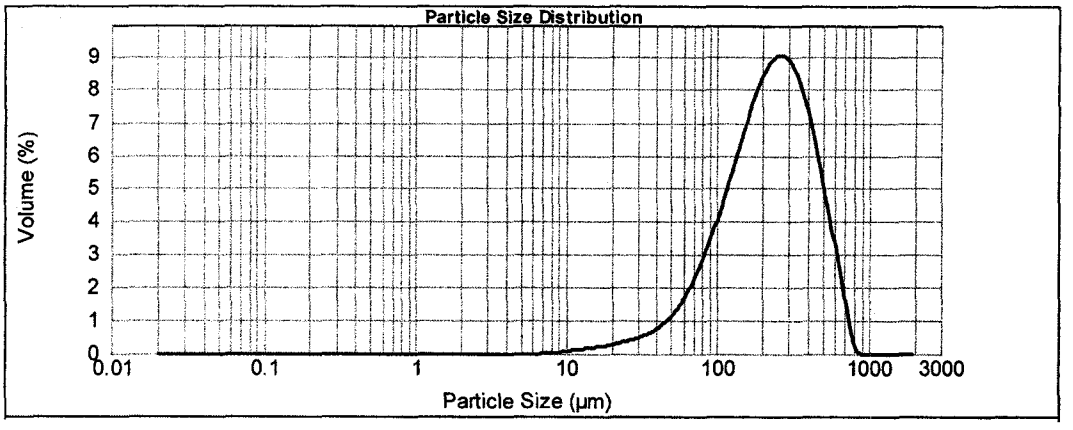

Figure C. 8 Emulsion M/W3 droplet size distribution

C.9 *Emulsion M/W4 Specifications*

Emulsion designation	M/W4
Emulsion type	Oil-in-water
Emulsion quality (%)	13
Oil type	Mineral oil
Surfactant type	Triton X-100
Surfactant concentration (v/v) (%)	0.12
Phases mixing method	Brinkmann homogenizer
Shear mixing rate (rpm)	5000
d(0.1) (μm)	10.1
d(0.5) (μm)	26.3
d(0.1) (μm)	48

Table C. 9 Emulsion M/W4 characteristics

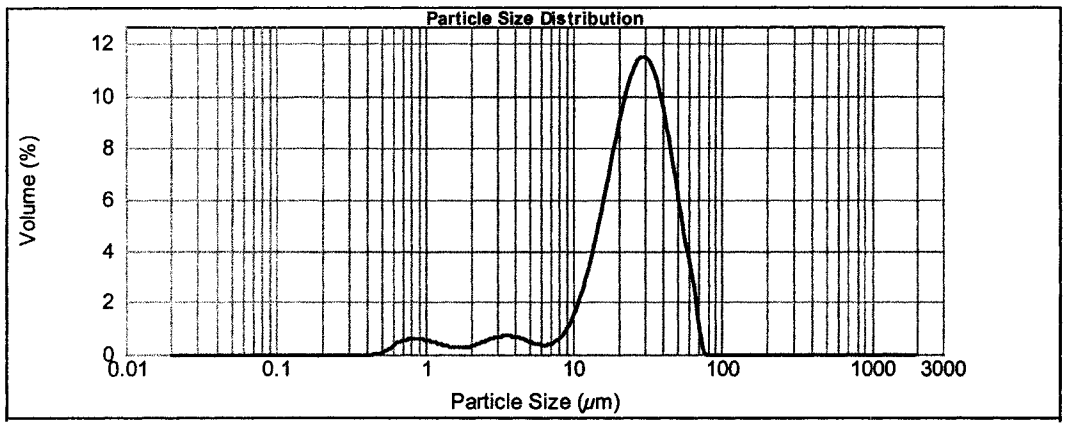

Figure C. 9 Emulsion M/W4 droplet size distribution

C.10 *Emulsion M/W5 Specifications*

Emulsion designation	M/W5
Emulsion type	Oil-in-water
Emulsion quality (%)	13
Oil type	Mineral oil
Surfactant type	Triton X-100
Surfactant concentration (v/v) (%)	0.01
Phases mixing method	Brinkmann homogenizer
Shear mixing rate (rpm)	5000
d(0.1) (μm)	18.9
d(0.5) (μm)	72.2
d(0.1) (μm)	172.9

Table C. 10 Emulsion M/W5 characteristics

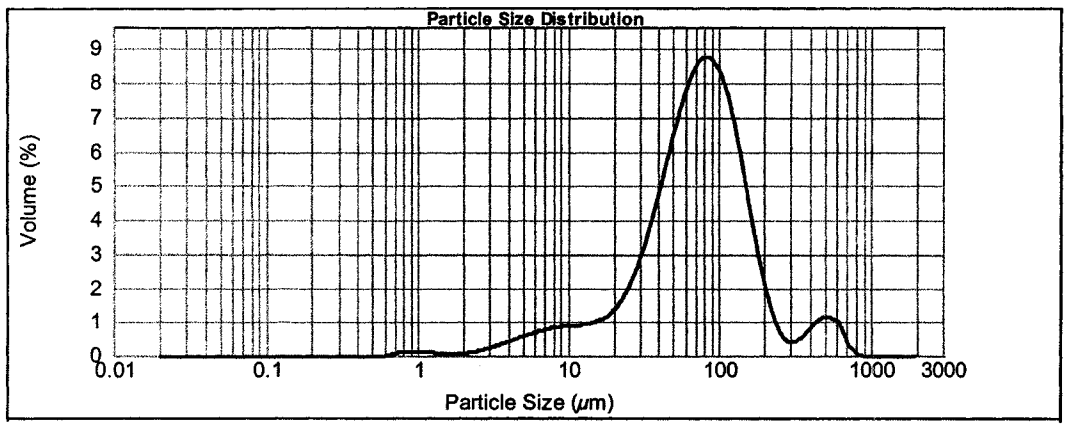

Figure C. 10 Emulsion M/W5 droplet size distribution

C.11 *Emulsion M/W6 Specifications*

Emulsion designation	M/W6
Emulsion type	Oil-in-water
Emulsion quality (%)	13
Oil type	Mineral oil
Surfactant type	Triton X-100
Surfactant concentration (v/v) (%)	0.12
Phases mixing method	Brinkmann homogenizer
Shear mixing rate (rpm)	5800
d(0.1) (μm)	2.4
d(0.5) (μm)	13.6
d(0.1) (μm)	667

Table C. 11 Emulsion M/W6 characteristics

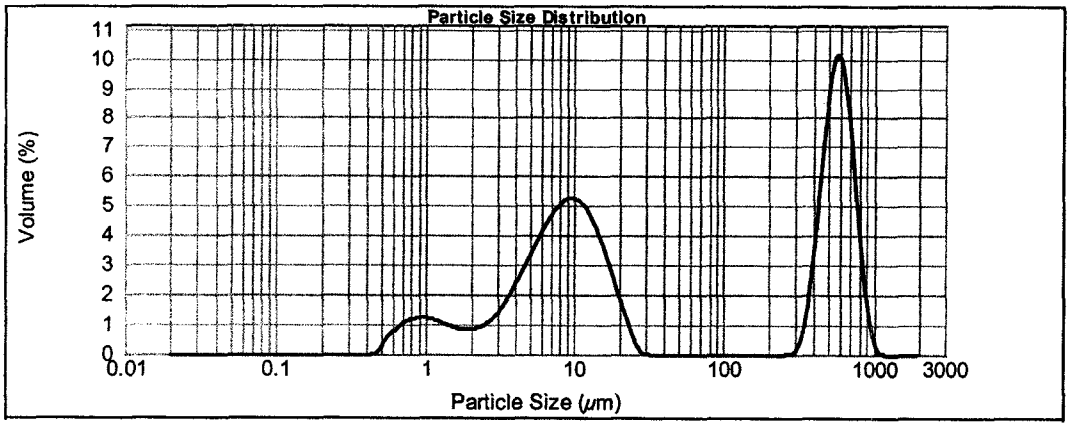

Figure C. 11 Emulsion M/W6 droplet size distribution

C.12 *Emulsion M/W7 Specifications*

Emulsion designation	M/W7
Emulsion type	Oil-in-water
Emulsion quality (%)	13
Oil type	Mineral oil
Surfactant type	Triton X-100
Surfactant concentration (v/v) (%)	0.025
Phases mixing method	Brinkmann homogenizer
Shear mixing rate (rpm)	5000
d(0.1) (μm)	14.5
d(0.5) (μm)	39.2
d(0.1) (μm)	104

Table C. 12 Emulsion M/W7 characteristics

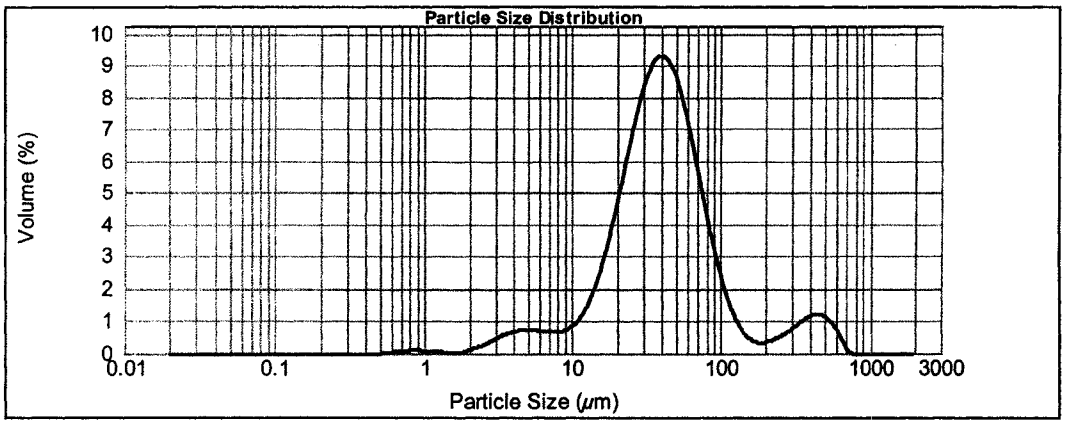

Figure C. 12 Emulsion M/W7 droplet size distribution

C.13 *Emulsion M/W8 Specifications*

Emulsion designation	M/W8
Emulsion type	Oil-in-water
Emulsion quality (%)	13
Oil type	Mineral oil
Surfactant type	Triton X-100
Surfactant concentration (v/v) (%)	0.06
Phases mixing method	Brinkmann homogenizer
Shear mixing rate (rpm)	5000
d(0.1) (μm)	10.3
d(0.5) (μm)	27.7
d(0.1) (μm)	51.2

Table C. 13 Emulsion M/W8 characteristics

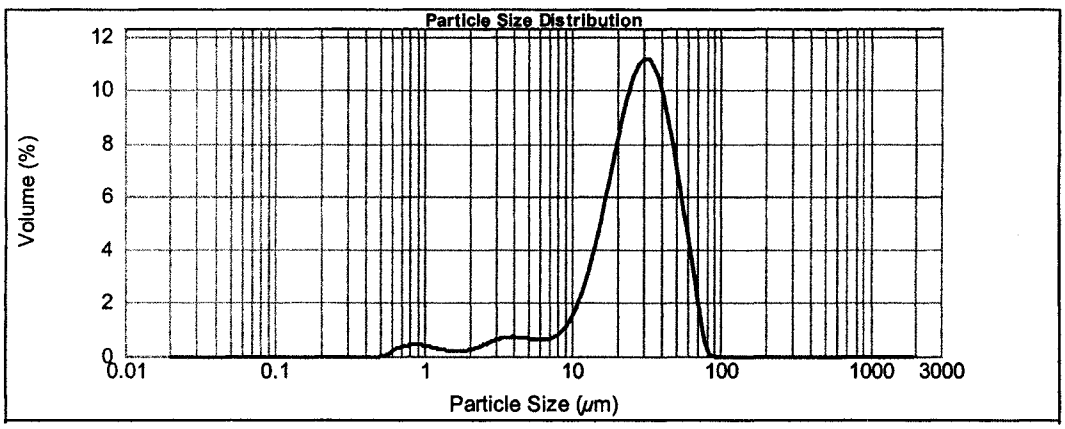

Figure C. 13 Emulsion M/W8 droplet size distribution

C.14 *Emulsion WC/W1 Specifications*

Emulsion designation	WC/W1
Emulsion type	Oil-in-water
Emulsion quality (%)	13
Oil type	Western Canadian oil
Surfactant type	Triton X-100
Surfactant concentration (v/v) (%)	0.12
Phases mixing method	Brinkmann homogenizer
Shear mixing rate (rpm)	5000
d(0.1) (μm)	5.6
d(0.5) (μm)	15.9
d(0.1) (μm)	40.8

Table C. 14 Emulsion WC/W1 characteristics

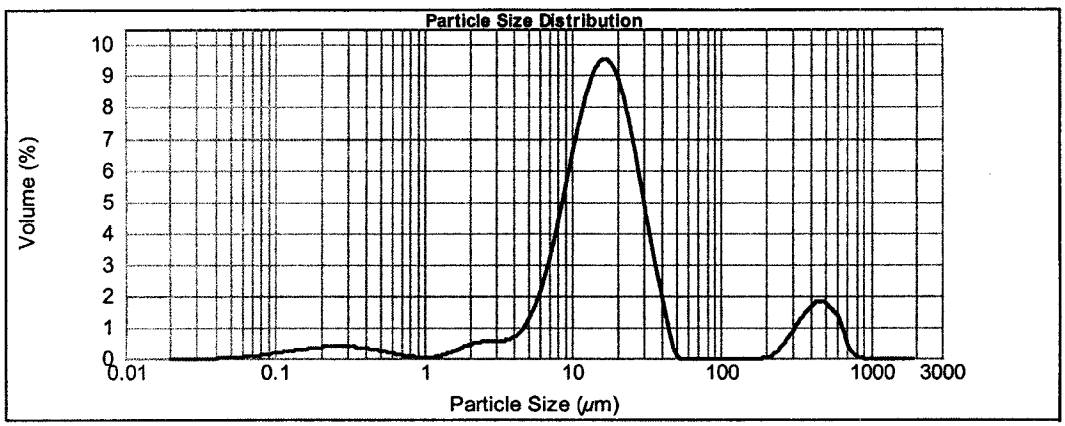

Figure C. 14 Emulsion WC/W1 droplet size distribution

C.15 *Emulsion WC/W3 Specifications*

Emulsion designation	WC/W3
Emulsion type	Oil-in-water
Emulsion quality (%)	13
Oil type	Mineral oil
Surfactant type	Triton X-100
Surfactant concentration (v/v) (%)	0.06
Phases mixing method	Brinkmann homogenizer
Shear mixing rate (rpm)	5000
d(0.1) (μm)	9.8
d(0.5) (μm)	59.3
d(0.1) (μm)	270.9

Table C. 15 Emulsion WC/W3 characteristics

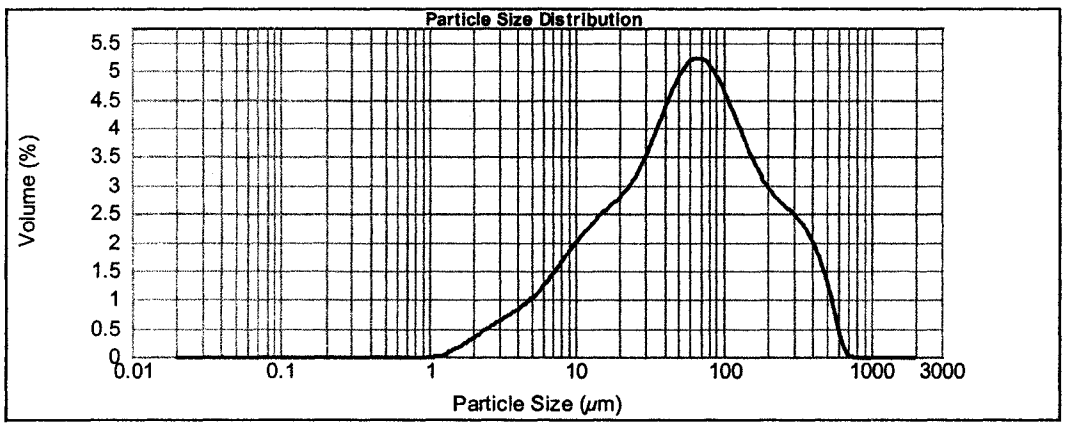

Figure C. 15 Emulsion WC/W3 droplet size distribution

APPENDIX D: Error Analysis of the Experiments

Seven experiments presented in Section 5.8 were repeated and the random error associated with repeating each experiment was estimated through curve fitting. The main discussion of experimental error analysis, and the results for one experiment were presented in Section 7.1. Figures D.1 through D.6 are the results of random error analysis of six more experiments that were performed on two-parallel plate visual model packed with glass beads. Figures D.1, D.3, D.4 and D.5 show that the error (systematic and random) associated with repeating each experiment was within acceptable range. Figures D.2 and D.6 show a noticeable error. The cause of this error could be higher injection rates.

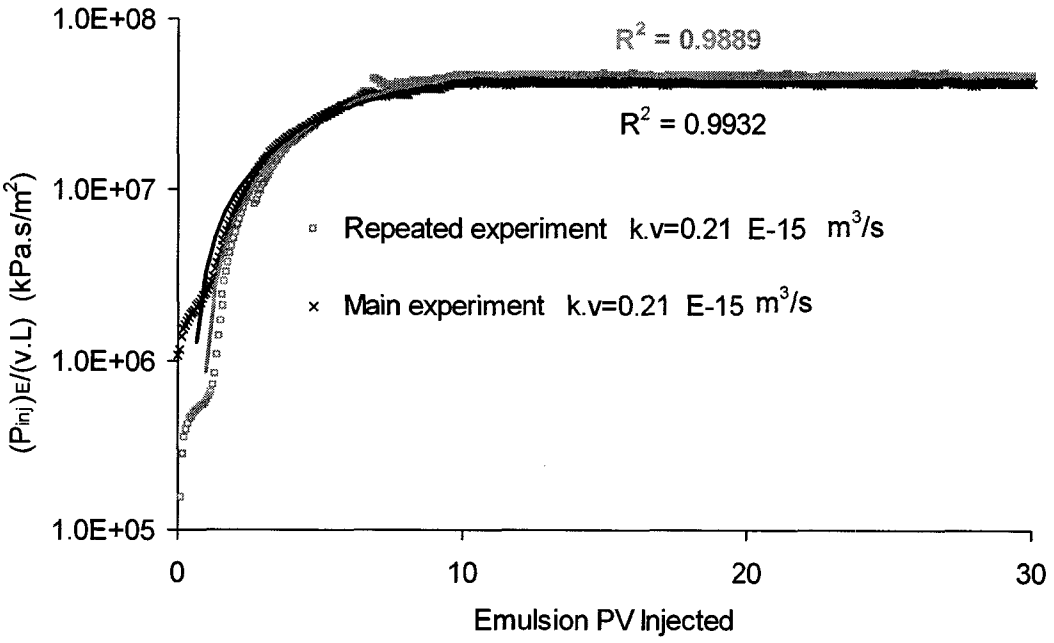

Figure D. 1 Error associated with the injection of emulsion M/W4 into identical glass bead packs (linear flow velocity of 3.0×10^{-4} m/s)

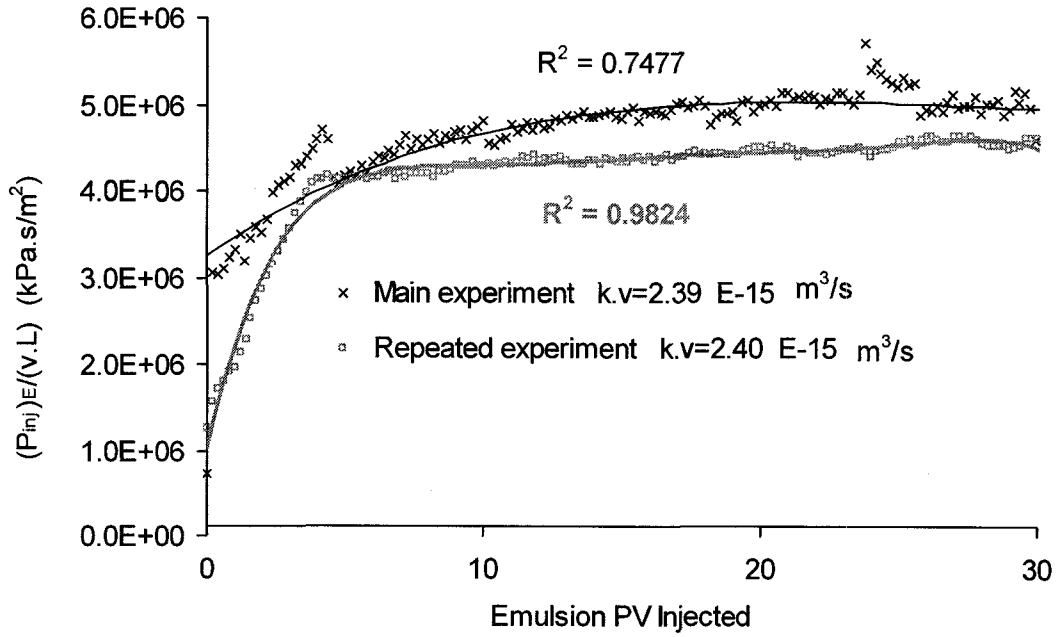

Figure D. 2 Error associated with the injection of emulsion M/W4 into identical glass bead packs (linear flow velocity of 9.4×10^{-4} m/s)

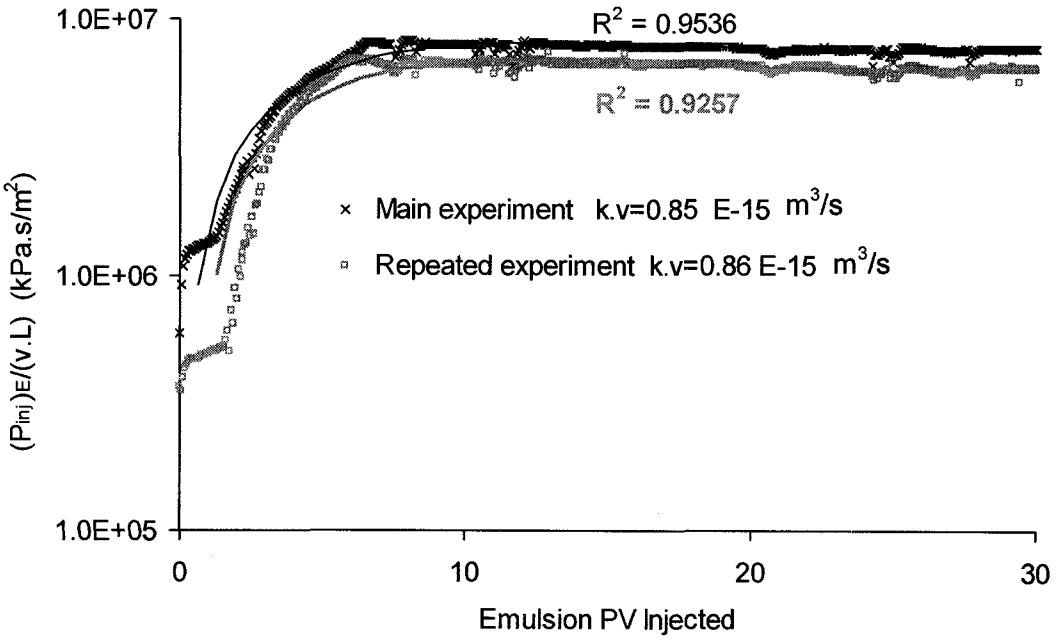

Figure D. 3 Error associated with the injection of emulsion M/W4 into identical glass bead packs (linear flow velocity of 3.0×10^{-4} m/s)

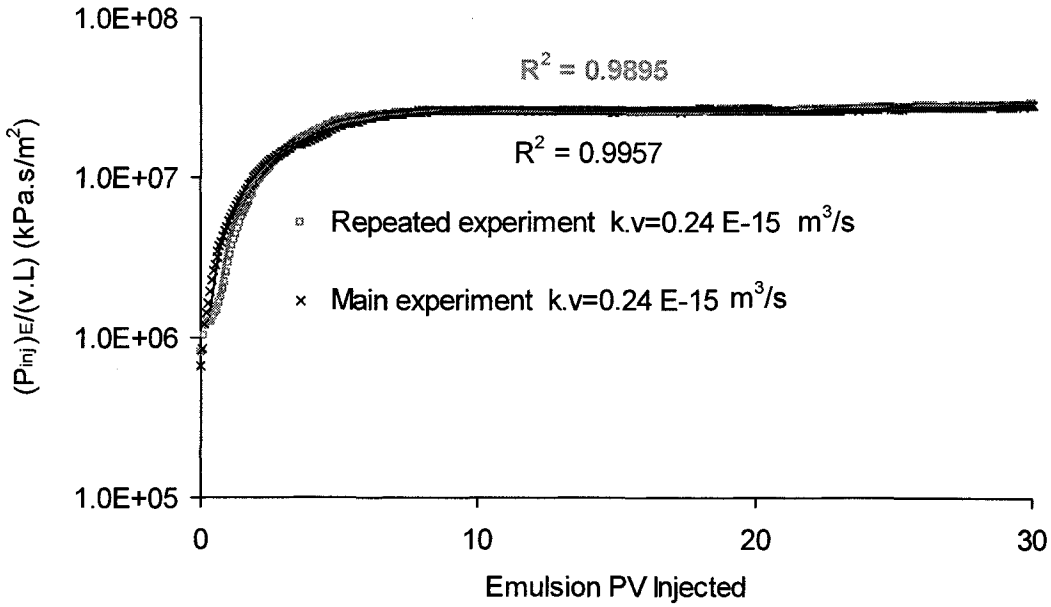

Figure D. 4 Error associated with the injection of emulsion WC/W1 into identical glass bead packs (linear flow velocity of 3.0×10^{-4} m/s)

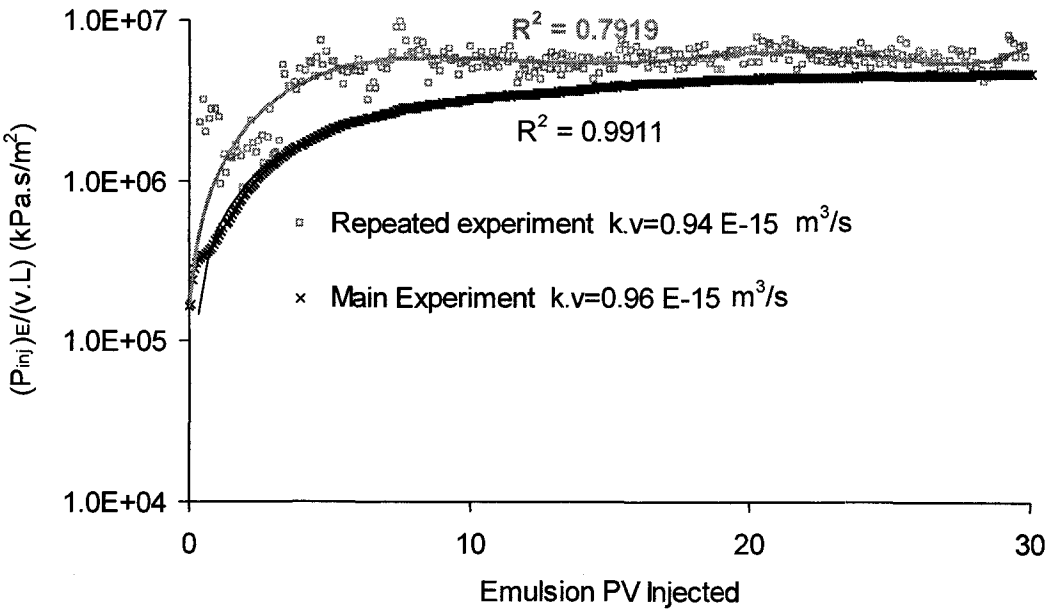

Figure D. 5 Error associated with the injection of emulsion WC/W1 into identical glass bead packs (linear flow velocity of 3.0×10^{-4} m/s)

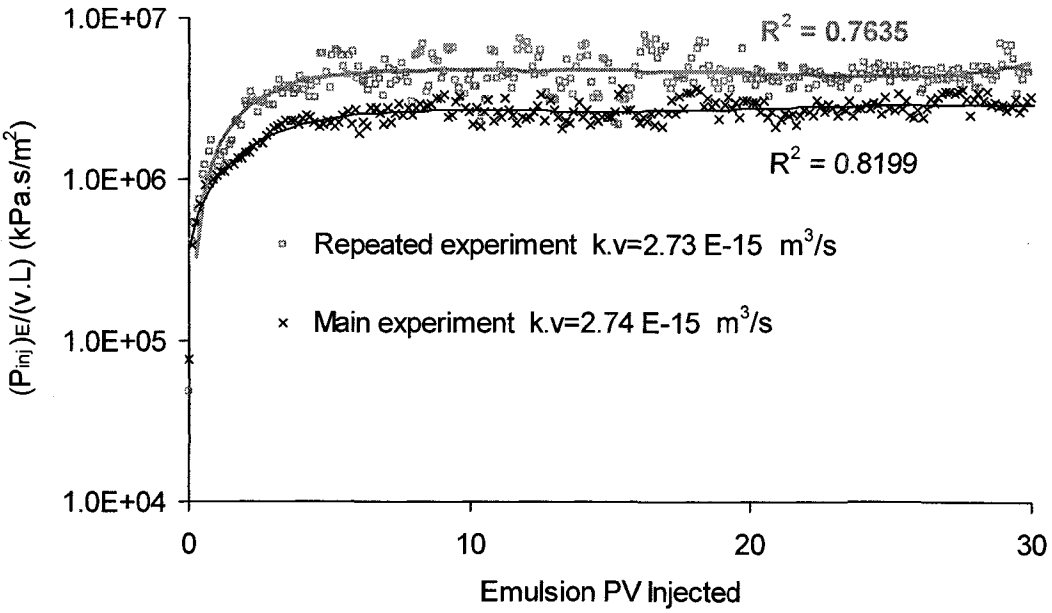

Figure D. 6 Error associated with the injection of emulsion WC/W1 into identical glass bead packs (linear flow velocity of 6.75×10^{-4} m/s)